Identification of glioma specific targets using aptamers

by

Mohit Arora

A thesis submitted in partial fulfilment for the requirements for the degree of Doctor of Philosophy, Master of Philosophy at the University of Central Lancashire

February 2020

STUDENT DECLARATION FORM

1. Concurrent registration for two or more academic awards

*I declare that while registered as a candidate for the research degree, I have not been a registered candidate or enrolled student for another award of the University or other academic or professional institution

_____

2. Material submitted for another award

***I** declare that no material contained in the thesis has been used in any other submission for an academic award and is solely my own work

_____

(state award and awarding body and list the material below):

_____

3. Collaboration

Where a candidate's research programme is part of a collaborative project, the thesis must indicate in addition clearly the candidate's individual contribution and the extent of the collaboration. Please state below:

_____

4. Use of a Proof-reader

No proof-reading service was used in the compilation of this thesis.

Signature of Candidate _____ _____

Print name: _____**Mohit Arora**_____

Type of Award_____**PhD**_____

School **School of pharmacy**_____

Abstract

Gliomas are primary brain tumours. Glioblastoma multiforme is a grade IV tumour and is the most aggressive type of tumour with a poor prognosis (overall survival approx. 12 months post diagnosis). Advances in diagnosis and treatment have been hindered by numerous factors including identification of novel target biomarkers and the ability of therapeutics to cross the blood brain barrier (BBB).

Aptamers could advance the identification of novel drug targets because their properties allow them to act as both a targeting ligand and a drug delivery moiety. Aptamers are small and highly structured single-stranded oligonucleotides that bind with high affinity (within the low nano molar range) to a target molecule. Aptamers used in this study, SA43 and SA44 were generated by cell-SELEX and shortened, which showed selective binding to glioma cells. The target ligand was unknown.

The aim of this project was to develop an aptamer precipitation or aptoprecipitation (AP) protocol to identify the target ligand of novel aptamers generated against different glioma cells. Commercially available glioma cell lines U87MG, 1321N1, and SVGP12 and short term patient derived cultures BTNW911, BTNW914, BTNW370, IN1528, IN1612, W2045 and W859 were first characterised using conventional staining methods. These cells were then assessed for binding with SA43 and SA44 aptamers and 7 novel aptamers (TDM aptamers 2,3,7,9,10 and SAneg1 and SAneg2) using confocal microscopy and protein extraction methods. Confocal microscopy confirmed the binding of biotinylated aptamers to glioma cell lines and patient tissue derived short term cultures. Protein extraction from cells was optimised and AP of the targets was performed. LC-MS/MS analysis showed that 8 of the novel aptamers identified Ku70/80 heterodimer as the target in glioma cells. Ku70/80 was further confirmed as the target ligand for the aptamers by Western blot in glioma cells and siRNA knockdown in U87MG cells.

This research will help in detecting new biomarkers for glioma and possibly other cell lines. It has helped in establishing a method for aptamer target detection. It can also help in developing targeted therapy and patient specific therapy.

Table of Figures

List of tables

ABBREVIATIONS

5- ALA	5- aminolevulinic acid
A	Adenine
AA	Anaplastic Astrocytoma
ABC	Avidin-biotin complex
AP	Aptoprecipitation
APS	Ammonium persulphate
ATCC	American Type Culture Collection
ATRX	Alpha-thalassemia/mental retardation
BBB	Blood brain barrier
BCNU	bis-chloroethlynitrosourea
BRCA1/2	Breast cancer 1
BTNW	Brain Tumour North West
C	Cytosine
CNS	Central nervous system
CRUK	Cancer Research UK
CSCs	Cancer stem cells
CSF	Cerebrospinal fluid
CT	Computed tomography
DAB	3,3-Diaminobenzidine
DAPI	4', 6-diamidino-2-phenylindole

DMEM	Dulbecco's modified eagle medium
DNA	Deoxyribonucleic acid
DNAPKs	DNA protein kinases
ECACC	European Collection of Cell Cultures
EGFR	Epidermal growth factor receptor
ELISA	Enzyme-linked immunosorbent assay
EMEM	Eagle's minimum essential medium
EORTC	European organisation for research and treatment of cancer
EpCAM	Epithelial cell adhesion molecule
EPR	Enhanced permeability and retention effect
ER	Estrogen receptor
FBS	Fetal bovine serum
FDA	Food and Drug administration
G	Guanine
GBM	Glioblastoma multiforme
GFAP	Glial fibrilliary acidic protein
GSCs	Glioma stem-like cells
HC	Histochemistry
HIV	Human immunodeficiency virus
HLA	Human leukocyte antigen
HPLC	High performance liquid chromatography
HSP	Heat shock protein

IDA	Information Dependent Acquisition
IDH	Isocitrate dehydrogenase
IHC	Immunohistochemistry
IP	Immunoprecipitation
kDa	kilo Dalton
Ku70	X-ray cross complementing protein 6
Ku80	X-ray cross complementing protein 5
LS-MS/MS	Liquid chromatography and mass spectrometry
LSM	Laser scanning microscopy
MFI	Mean fluorescence intensity
MGMT	O6-methylguanine-DNA methyltransferase
mRNA	Micro-RNAs
MRI	Magnetic resonance imaging
MS	Mass-spectrometry
NEAA	Non-essential amino acid
NHA	Normal human astrocytes
NHEJ	Non-homologous end joining
NICE	National Institute of Clinical health Excellence
NOS	Not otherwise specified
OS	Overall survival
OPARATIC	Olaparib with temozolamide for glioblastoma that has come back

PA	Pilocytic Astrocytoma
PARADIGM	Olapraib and radiotherapy for people with glioblastoma trial
PARP	Poly ADP-ribose polymerase
PBS	Phosphate buffer saline
PCD	Paraneoplastic cerebellar degeneration
PDGFR	Platelet derived growth factor receptor
PEG	Polyethylene glycol
PET	Positron emission tomography
PFA	Paraformaldehyde
PFS	Progression free survival
PI	Propydium iodide
PKC	Protein kinase C
PNS	Peripheral nervous system
PSMA	Prostrate specific membrane antigen
PTEN	Phosphate and tensin homolog
QALY	Quality adjusted life years
REGOMA	Regorafenib in relapsed glioma
RNA	Ribonucleic acid
SA	Shortened aptamer
SDS	Sodium dodecyle sulphate
SELEX	Systemic Evolution of Ligands by Exponential enrichment
SLS	Scientific laboratory supplies

SPECT	Single photon emission computed tomography
T	Thymine
T-ALL	T-cell acute lymphoblastic leukaemia
TCA	Tri-carboxylic cycle
TEMED	Tetramethylethylenediamine
TERT	Telomerase reverse transcriptase
TP53	Tumour protein p53
TTF	Tumour treating field
U	Uracil
Uclan	University of Central lancashire
UK NEQAS	United Kingdom National External Quality Assessment Service
VA RNA	Virus associated RNA
VEGF	Vascular endothelial growth factor
VEGFR	Vascular growth factor receptor
WHO	World Health Organisation
XRCC5	Ku80
XRCC6	Ku70

Contents

Chapter 1

1 Introduction

1.1 Brain Tumours

Brain tumours are neoplasms in the brain which can arise either from the brain, termed as primary brain tumours or as 'metastasis' from other parts of the body (Ellenbogen, 2012; Rotta et al., 2018). Like every neoplasm, primary brain tumours can be further divided into benign or malignant brain tumours (Ellenbogen, 2012; Greenberg, 2014). Benign brain tumours are tumours which do not recur or are very slow to recur. Malignant tumours are those which can recur at the primary site after treatment or can metastasise elsewhere (Bernstein and Woodard, 1995; Ellenbogen, 2012). Malignant brain tumours rarely metastasise outside the brain (Bernstein and Woodard, 1995; Mourad et al., 2005; Chang et al., 2018) (Figure 1.1).

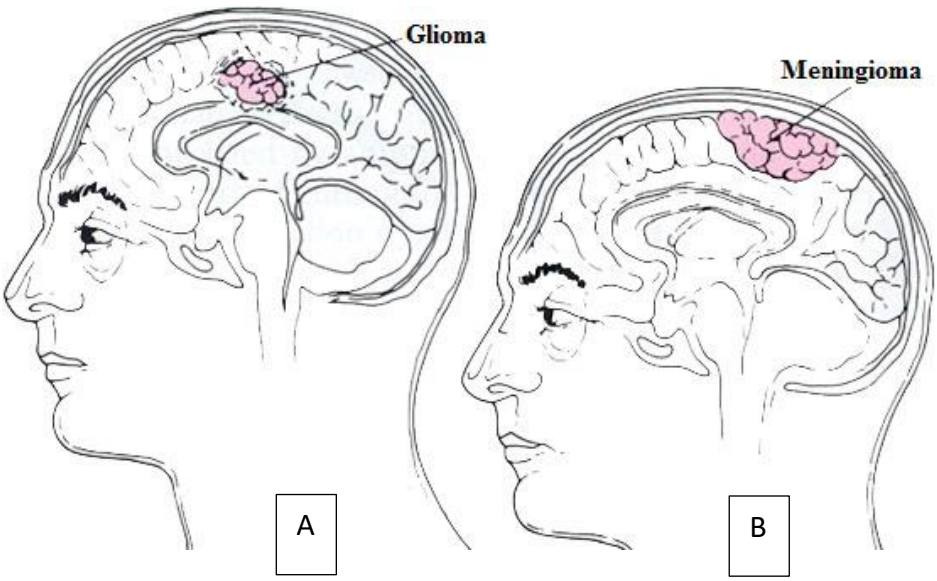

Figure 1.1 Diagram showing two broad types of brain tumours.

A) Glioma, primary tumour arising from glial tissue, B) Meningioma, tumour arising from brain meninges and pressing on brain tissue, taken from neuros.net (Neuros.net, 2014).

Around 9000 new brain tumours are diagnosed in the UK every year (CRUK, 2011) and their incidence has grown to 11,432 in 2015 (CRUK, 2019). There was 50% incidence in males to females in 2011 (CRUK, 2011) and about 48% to 52% male to female ratio in 2015. There is now greater incidence of primary brain tumour in the elderly population over 80 in the UK (CRUK, 2019), accounting for nearly a quarter of new cases every year. Astrocytoma (Park et al., 2019) remain to have the highest incidence in the group of primary brain tumours at 34% (CRUK, 2019) in both children and adults. This incidence is closely followed by meningiomas at 21% and other intracranial tumour incidence. The burden of metastasis to the brain is now greater than primary tumours (Jenkinson M, 2017; CRUK, 2018) at about 16000 per year compared to 9000 new cases of primary brain tumours.

1.2 Glioma

The term 'glioma' is used to refer to all the tumours of glial origin. Gliomas have been historically classified according to the World Health organisation (WHO) from Grade I to IV (Louis et al., 2007) based on histopathological features. A newer classification system has come into practise since 2016 after review of molecular developments made in glioma diagnosis (Louis et al., 2016; Wesseling and Capper, 2018). Historically, prior to 2016, Grade I and II tumours were classified as low grade tumours whereas Grade III and IV were considered as high grade. Patients with high grade tumours on histopathological diagnosis have had the poorest survival prognosis. The prognosis is still poor but molecular diagnosis has helped to further diversify the tumour types and provide appropriate treatment modality.

Addressing the previously known classification of gliomas first, Glioblastoma Multiforme or GBM is the most malignant brain tumour of glial origin (Holland, 2000; Behin et al.,

2003). It refers to grade IV glioma and is classified due to the appearance of histological characteristics of vascular proliferation, mitoses, pleomorphism and central necrosis (Louis et al., 2007; Agnihotri et al., 2013; Greenberg, 2014). Glioblastoma multiforme is now a historical term since the advent of the 2016 WHO classification of brain tumours (Louis et al., 2016). Glial brain tumours arise from a common progenitor and subsequently differentiate to give rise to various grade of glioma (Huse and Holland, 2010; Agnihotri et al., 2013) (Figure 1.2). They may develop *de novo* (primary glioblastoma) or by progression from low grade glioma (Ohgaki and Kleihues, 2007; Bready and Placantonakis, 2019).

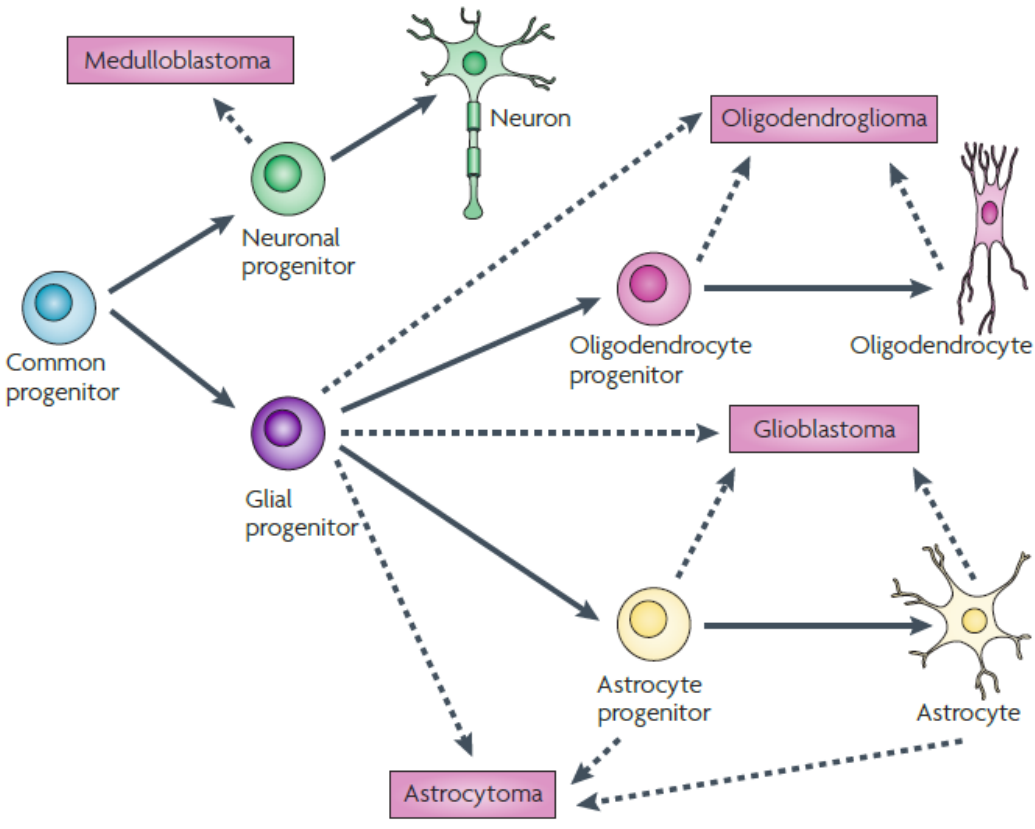

Figure 1.2 Flow diagram showing the origin of various glial tumours, taken from Holland, 2010 (Huse and Holland, 2010)

1.2.1 Current outcomes in glioma and targeted therapy

Patients diagnosed with grade IV glioma have an overall poor prognosis (Sanai and Berger, 2008). Based on the extent of initial resection of tumour, the prognosis is better with concurrent chemotherapy and radiotherapy. Studies have shown increase in the survival rates of patients with grade IV glioma to a median of 12 months (Krex et al., 2007). Recent advances have improved median survival upto 21 months (Fabian et al., 2019b). Around 4,300 benign cancers of the brain (McKinney, 2004) are also diagnosed every year, making brain cancer the 16th commonest cancer in the UK. Seven people out of a 100,000 will have a newly diagnosed Brain tumour UK (McKinney, 2004). Glioma accounts for two percent of newly diagnosed cancers in adults in the population in the UK every year (McKinney, 2004).

Despite the advances in treatment of other cancers, treatment for brain tumours is still far from providing cure. Improved outcomes in primary cancers of the breast, lung, melanoma and renal are a testament to the advances in treatment and awareness of these tumours.

Brain tumour treatment is also hampered by the bioavailability of the drugs across the blood brain barrier (Deeken and Löscher, 2007). Tight junctions in the brain along with adherens proteins prevent paracellular diffusion (Warren, 2018), thus affecting the bioavailability of systemically administered drugs. This remains controversial for treatment of metastasis and high grade tumour where blood brain barrier is disrupted. Tumour enhancement in metastasis is also due to blood brain barrier disruption (Fortin, 2012). Grade IV gliomas do alter blood brain barrier but it is sufficiently intact to prevent drug distribution to the tumour cells (Da Ros et al., 2018).

There also remains the need to be selective in targeting tumour cells as it is difficult to recognise the true margins of the primary brain tumour. Recent advances in glioma surgery have been helped with 5-aminolevulinic acid (5-ALA) use (Stummer et al., 2008; Stummer et al., 2011; Hadjipanayis et al., 2015) including surgery for other brain tumours as hemangioblastoma (Utsuki et al., 2011). Current treatment plans for brain tumours are based on surgical debulking, concurrent chemotherapy and radiotherapy (NICE.org.uk, 2018).

Recent advance in targeting cell growth has resulted in reduction of cell mitosis and reducing the growth of grade IV glioma by application of magnetic field (Omar, 2014; Fabian et al., 2019a; Korshoej et al., 2019). Tumour treating fields (TTF) are low intensity and intermediate frequency electric field that disrupts cell division and hence reducing tumour growth (Hottinger et al., 2016). This has resulted in improved median progression free survival with TMZ to 20 months from 16 months with TMZ and DXT alone (Hottinger et al., 2016) in grade IV glioma. Despite a break through, the treatment is not mainstream due to the high cost of the equipment needed for treatment. It is not approved by NICE since it does not meet the QALY (Quality adjusted life years) threshold (NICE, 2019).

1.2.2 World Health Organisation (WHO) Classification of glioma 2007

The WHO 2007 system of classification of glioma was based on the morphology of tissue and immunohistochemical features of the tumour sample (Louis et al., 2007). The first WHO classification of brain tumours was defined by Zulch in 1979 (Zulch and Mennel, 1977; Zulch, 1980, 1981). This was based on Rudolf Virchow's first reported brain tumour classification from 1863 and was based on tissue and cell morphology. Features such as mitosis, hyper cellularity, microvascular proliferation and necrosis were included. The newer WHO 2016 classification supersedes and adds molecular staining with IDH, ATRX, MGMT and 1p/19q co-deletion for further classification to the earlier WHO 2007 morphological diagnosis of glioma.

Due to the use short term cultures in this project from patient biopsies was based on the 2007 WHO classification of gliomas, this section is integral to the presentation of the results. Historically, based on the morphological characteristics, the primary brain tumour can be divided into multiple grades (Table 1.1 and Table 1.2). The classification takes into account the cell lineage and proliferation with presence of mitosis and proliferation markers used in standard immunohistochemistry techniques(Louis et al., 2007). Presence of two types of cell in the tumour gave the terms "oligoastrocytic" tumours which is now not used as per the recent WHO 2016 classification(Louis et al., 2016; Banan and Hartmann, 2017).

Table 1-1 Types of neuroepithelial tumours

	Classification	Tumour
1	Astrocytic tumours	Infiltrating astrocytoma Pilocytic astrcytoma Pleomorphic xanthoastrocytoma Subependymal giant cell astrocytoma
2	Oligodendroglial tumours	Oligodendroglioma
3	Ependymal tumours	Ependymoma
4	Mixed glioma	Oligoastrocytoma
5	Choroid plexus tumours	Papilloma
6	Neuronal and mixed neuro-glial tumours	Gangliocytoma Glangliоglioma Dysembryonic neuroepithelial tumour (DNET)
7	Pineal tumours	Pineocytoma Pineoblastoma
8	Embryonal tumours	Neuroblastoma Retinoblastoma Primitive neuroectodermal tumour (PNET)

Table 1-2 Histological classification of diffuse gliomas and their median survival (Louis et al., 2007)

Cell lineage	WHO grading	Histological subtype	% Incidence
Astrocytic tumours	Grade I	Pilocytic astrocytoma	5-6%
		Subependymal giant cell astrocytoma	<1
	Grade II	Diffuse astrocytoma, pleomorphic astrocytoma	10-15%
	Grade III	Anaplastic astrocytoma	10-15%
	Grade IV	Glioblastoma multiforme, Gliosarcoma	12-15%
Oligodendroglial tumours	Grade II	Oligodendroglioma	2.5%
	Grade III	Anaplastic oligodendroglioma	1.2%
Oligoastrocytic tumours	Grade II	Oligoastrocytoma	1.8%
	Grade III	Anaplastic oligoastrocytoma	1.2%

1.2.3 Pilocytic Astrocytoma

Pilocytic Astrocytoma (PA) is a slow growing, WHO grade I astrocytoma, most commonly affecting patients in the second decade of life (Ellenbogen, 2012). They can differ histologically from diffuse to fibrillary astrocytoma (a tumour matrix rich with neuroglial fibrils which give the tumour its name and firm consistency). They have a benign course due to lack of invasion and malignant tendency. PA are usually resectable and rarely recur or undergo malignant transformation (Ellenbogen, 2012; Nelson et al., 2019). Primary surgical debulking with chemotherapy is effective in children with pilocytic astrocytoma (Goodden et al., 2014) and good resection predicts reduced risk of progression (Nelson et al., 2019).

1.2.4 Astrocytoma

The 2007 WHO classification describes astrocytoma as Grade II, 'low grade' tumours (Louis et al., 2007). These usually occur in the fifth decade of life, with a median age of 35 years (Whittle, 2004)and account for around 15-25 % of gliomas in most series of cases published (Ellenbogen, 2012; Lanese et al., 2018). Astrocytoma are slow growing and the usual presentation is with a seizure (Whittle, 2004). Magnetic resonance imaging or MRI is the gold standard for non-invasive imaging for low grade gliomas (Ellenbogen, 2012). Pathologically, they are less cellular show no calcification and have no mitoses (Ellenbogen, 2012; Forst et al., 2014) (Figure 1.3). Treatment remains surgical resection, with 80 % 5 year survival rate for gross resection, 50 % for partial resection and 45 % for biopsies (Ellenbogen, 2012). EORTC or European organisation for research and treatment of cancer have conducted trials for low grade tumours, EORTC 22844 and EORC 22845 (Forst et al., 2014). They identified poor prognostic indicators relating to

tumour size greater than 6 cm, age over 40 at presentation, midline shift and presence of neurologic deficit at diagnosis.

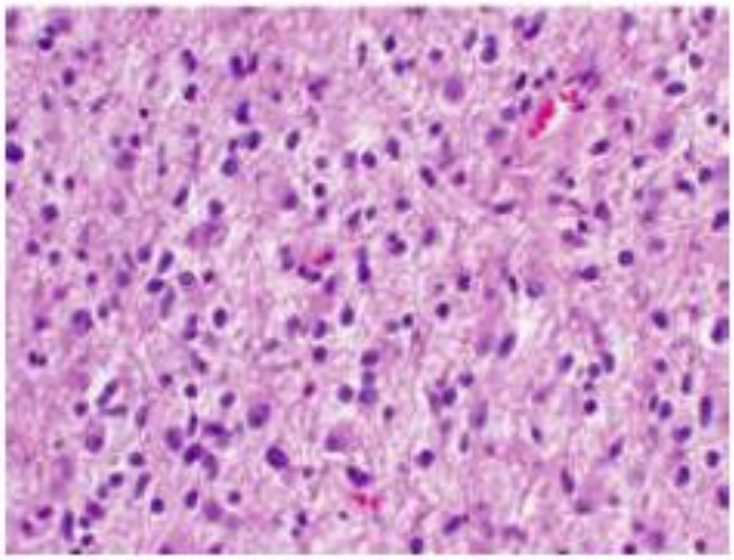

Figure 1.3 A micrograph showing astrocytoma, taken from Holland, 2010 (Huse and Holland, 2010).

1.2.5 Anaplastic Astrocytoma

Anaplastic astrocytoma (AA) is usually seen from the second to the fifth decade of life and AA can be either malignant transformation or as primary presentation (Ellenbogen, 2012; Forst et al., 2014). WHO 2007 classifies them as grade III tumours and they represent 10-15% of gliomas (Ellenbogen, 2012). Patients can present with various symptoms like seizures, confusion, headache and focal neurological deficits and sometimes being completely asymptomatic. They show contrast enhancement on CT scans and also have mass effect and oedema (Ellenbogen, 2012). MRI imaging is also likely to show heterogenous enhancement. Pathologically, AA show mitotic activity, increased cellularity and anaplasia (Figure 1.4). Treatment comprises of surgical resection followed by radiotherapy (Ellenbogen, 2012). Recent recommendation from NICE advice on 4-6 cycles of PCV concomitant with radiotherapy. After completion, a

further 12 cycles of temozolamide is recommended to patients with IDH wildtype, without 19/19q codeletion (NICE, 2019).

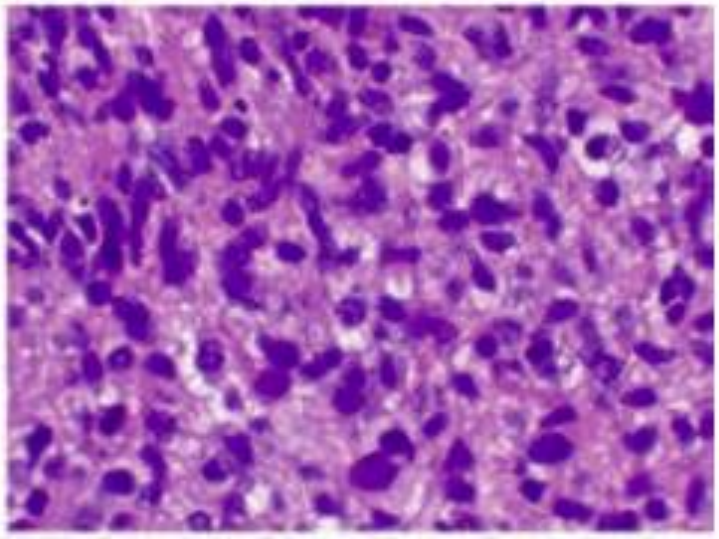

Figure 1.4 A micrograph showing anaplastic astrocytoma, taken from Holland, 2010 (Huse and Holland, 2010).

1.2.6 Glioblastoma multiforme

Glioblastoma multiforme or GBM is the most malignant brain tumour of glial origin (Behin et al., 2003) (Figure 1.5).

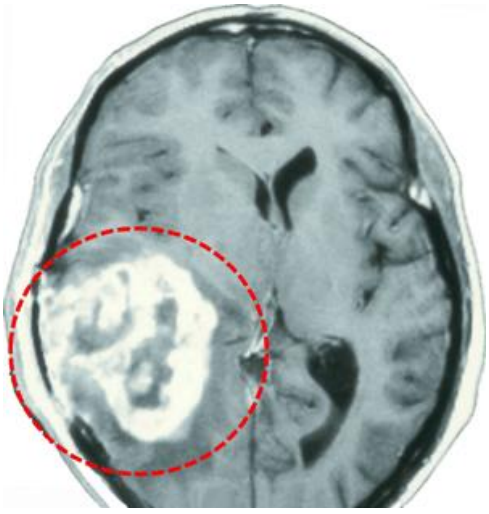

Figure 1.5 Post contrast axial MRI section showing glioma or Glioblastoma Multiforme (Neuros.net, 2014)

The term ‘glioblastoma’ was defined by Virchow (1863) as a tumour of glial origin. In 1926, Bailey and Cushing (1926) used the name ‘Glioblastoma Multiforme’ for the first time due to the variate, polymorphic features of the tumour on histology. As the term ‘multiforme or polymorphic’ implies, the most salient feature is the diversity of tissue patterns and cell forms encountered including anaplastic astrocytes, gemistocytic, fibrillary or pilocytic areas; and the presence of astroblastic, oligodendroglial, and dedifferentiated cells. Río Hortega (1932) and Polak (1966) described the 'isomorphic glioblastoma’ as a tumour constitute of little round glial cells which is distinct from a glioblastoma multiforme (Ellenbogen, 2012) (Figure 1.6).

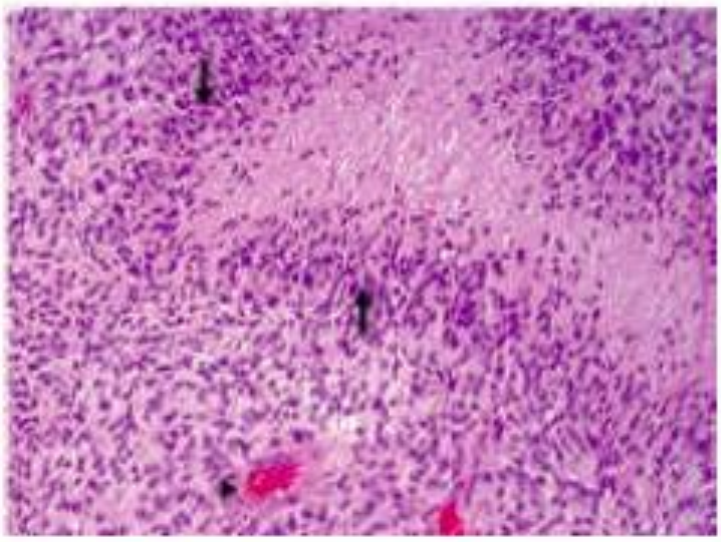

Figure 1.6 A micrograph showing Glioblastoma multiforme, taken from Holland, 2010 (Huse and Holland, 2010).

Patients usually present with headaches, personality changes and focal deficits and usually are very progressive in symptoms. GBM are the most frequent and aggressive primary brain tumours found in adults (Holland, 2000) arising from the glia, which is the precursor of the central nervous system. Glia or glial cells are supportive cells in the nervous system (Purves D, 2001.).They are supportive cells which help in the function of

neurones and outnumber them 3 to 1 (Purves D, 2001.). GBM occur mostly in either the sixth or the seventh decade of life but increasing incidence is being seen earlier in life. GBMs account for around 5000 new cases of brain cancer (malignant) diagnosed every year in the UK (McKinney, 2004).

GBM is the most common primary, intra-parenchymal, brain tumour and accounts for 30% of brain tumours and 50% in series representation (of documented cases) (Ellenbogen, 2012). GBM are characterised by heterogeneous enhancement on CT and MRI imaging (Ellenbogen, 2012).

1.3 WHO 2016 classification of glioma

Since the last revision in 2007 of the WHO grading system, a need for further stratification was needed due to molecular advancement techniques. The WHO 2016 classification takes into account molecular developments in glioma, but also creates room to grade without the molecular results, to allow diagnosis in regions where such tests are either inaccessible (Banan and Hartmann, 2017; Wesseling and Capper, 2018). A layered system of reporting was replicated from haematological reporting (Banan and Hartmann, 2017), incorporating molecular results. A three layered approach to results was adapted, with the top layer being the 'integrated results of lower layers' (Banan and Hartmann, 2017). Layer 2 is the histological diagnosis, layer 3 the grading and a layer 4 of molecular characteristics (Banan and Hartmann, 2017).

An important component in layer 4 is the application of two rules. Firstly, molecular results beats histology, as that is likely to define change in management. Secondly, the term 'not otherwise specified' or NOS was added in layer 4 for geographic regions where molecular testing is not available or the tissue sample is degraded and untestable (Banan

and Hartmann, 2017). IDH (isocitrate dehydrogenase), ATRX (alpha-thalassemia/mental retardation) and TERT (telomerase reverse transcriptase) are tested and help to diagnose tumour samples (Banan and Hartmann, 2017). It has also helped to remove the terms glioblastoma with oligodendroglial features and oligoastrocytomas from diagnosis with the help of 1p/19q deletion diagnosis being incorporated (Banan and Hartmann, 2017).

1.4 Current Treatment modalities for Glioma

Histological diagnosis is of paramount importance prior to further treatment in glioma (Ellenbogen, 2012) and confirmation with molecular state (Banan and Hartmann, 2017). The molecular analysis since WHO 2016 adds to the diagnosis and aids in directing treatment. Surgery, followed by radiotherapy and chemotherapy though still remains the mainstay of treatment for GBM. Radiotherapy and chemotherapy can be used together or individually as suited to the patient's tumour. Surgery is usually followed by concomitant radio-chemotherapy for six weeks with temozolamide (Stupp et al., 2005; Greenberg, 2014; NICE, 2019). Further, adjuvant chemotherapy is given for six months and continued longer depending on radiological stability and the patient's general condition. Due to the aggressive nature of the tumour, the median survival rate is around fourteen months. Two year survival is 27 % and five year survival rate is 5 % (Ellenbogen, 2012; Hottinger et al., 2016).

1.4.1 Surgical excision of glioma

Primary brain tumours still remain incurable and the aim of the treatment lies in alleviating the symptoms and prolongation of meaningful life. Surgery helps in reducing the tumour size and bulk (Figure 1.7). Surgery also provides the vital histological diagnosis for further treatment by chemo-radiotherapy and can act as an access for

delivery of local chemotherapy where needed (Rampling et al., 2004). Maximal, safe tumour resection followed by concomitant chemo-radiotherapy is the guidance as provided by NICE (NICE, 2019).

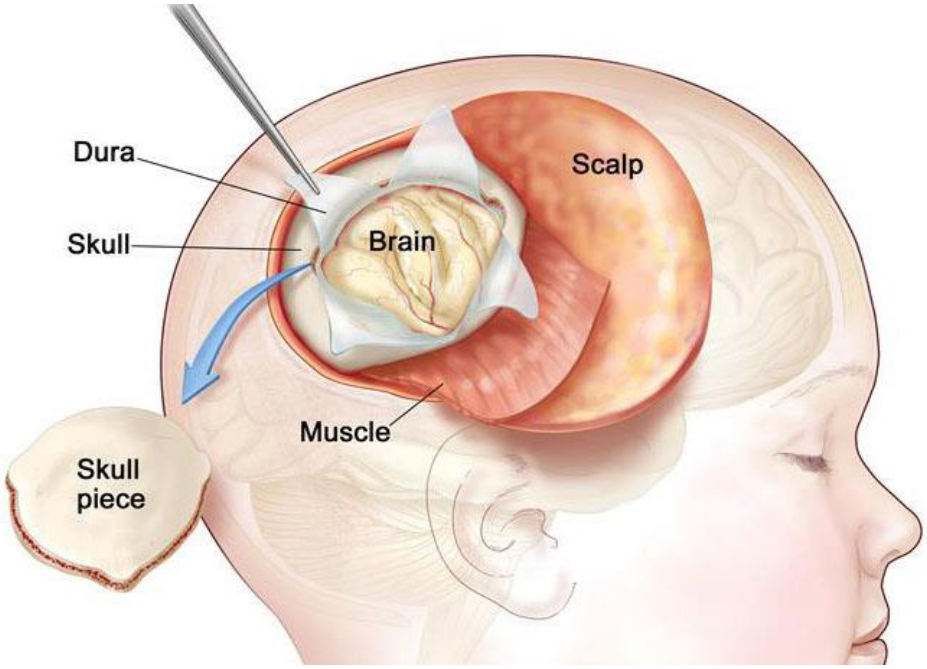

Figure 1.7 Diagram showing craniotomy for excision of tumour, taken from neuros.net (Neuros.net, 2014)

1.4.2 Tumour debulking and *in situ* chemotherapy

It is already known that maximal excision of tumour results in better outcome for the patient (Hentschel and Sawaya, 2003; Stummer et al., 2008; Stummer et al., 2011; Duffau, 2018). Adequate and safe tumour excision has been shown to reduce the morbidity involved with such surgeries and the mortality. The extent of tumour excision depends on the eloquence of the brain region it involves. Advances in imaging techniques like functional magnetic resonance imaging (fMRI) and surgery using brain mapping has vastly improved the surgical resections achievable today (Ellenbogen, 2012).

Based on the histological diagnosis, *in situ* chemotherapy can be instituted at the time of surgery. This has been shown to be beneficial as the direct delivery of the chemotherapy is within the blood brain barrier, an area of "constant barricade" of systemic chemotherapy agents. 'Carmustine' wafer chemotherapy when given to grade IV glioma patients results in statistically significant improvement in meaningful survival (Stupp et al., 2005; McGirt et al., 2009) (Figure 1.8).

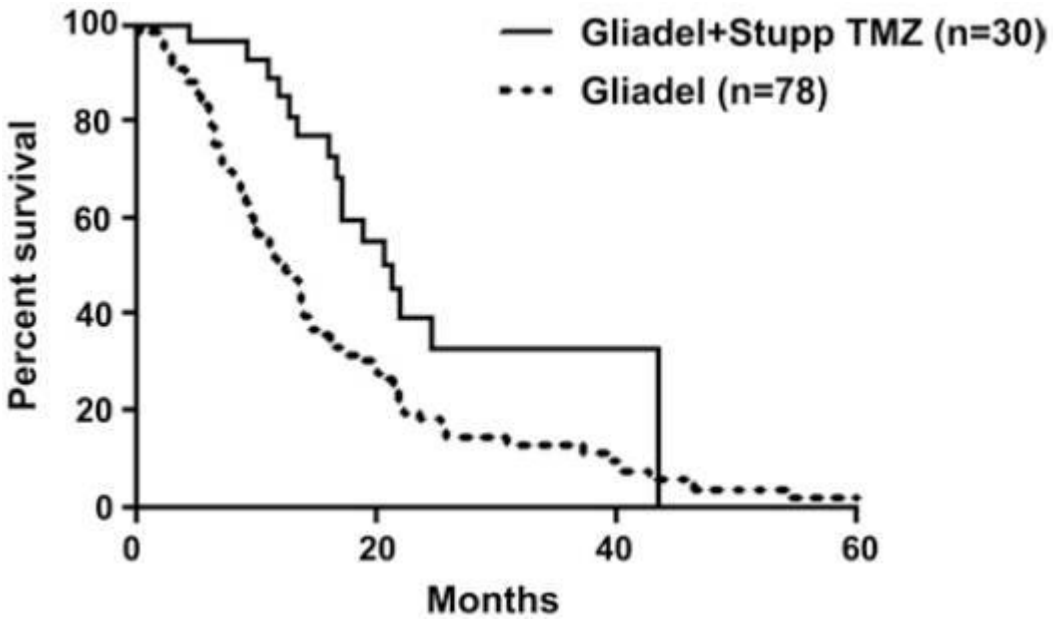

Figure 1.8 Kaplan-Meier survival plots after primary resection of GBM and fractionated radiotherapy in patients ≤ 70 years old.

Patients receiving concomitant TMZ according to the Stupp protocol in addition to Gliadel wafer implantation (30 patients) demonstrated improved survival compared with patients receiving Gliadel wafers and XRT alone (78 patients); median survival, 21.3 versus 12.4 months, respectively (p = 0.005) (McGirt et al., 2009).

Carmustine wafers have to be used only in cases of 90 % resection and only within specialized centers (NICE.org.uk, 2018). Their use is said to affect overall survival but there is increased incidence of surgical site infection as an adverse event (Chowdhary et al., 2015).

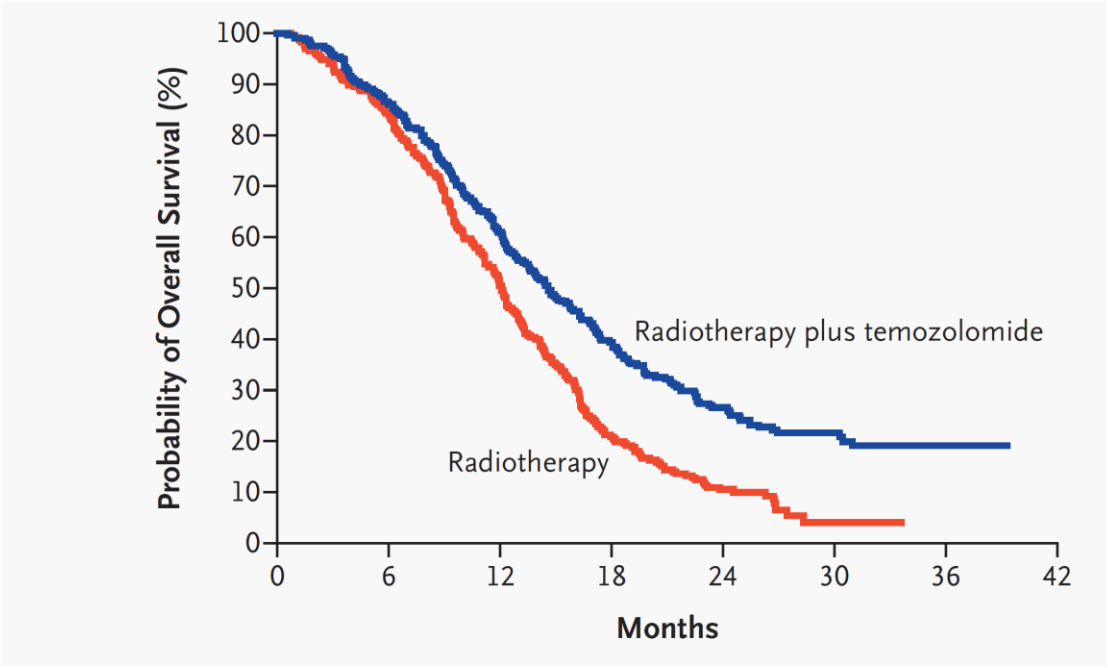

Figure 1.9 Kaplan-Meier curve of overall survival in patients receiving radiotherapy alone versus radiotherapy and temozolamide (Stupp et al., 2005).

NICE guidance on grade IV glioma management is based on the Stupp protocol for six weeks of concomitant chemotherapy and radiotherapy with temozolamide followed by 12 months of adjuvant temozolamide (Stupp et al., 2005; NICE, 2019). The above survival graph (Stupp et al., 2005) shows the increased survival with temozolamide and radiotherapy together.

1.5 Grade IV glioma and recent trials

Glioblastoma Multiforme, now a historical term as per the WHO 2016 classification (Louis et al., 2016), still rings the death knell for the patient. Since the Stupp protocol (Stupp et al., 2005) in 2005, multiple drug trials and therapies have been researched in grade IV glioma with varying success. Carmustine wafers or gliadel (Westphal et al., 2003) have been used for grade four glioma and is approved to be used by NICE in select patients who meet the criteria (McGirt et al., 2009; NICE, 2019). Overall adaptation varies and it does come with its own set of risks and complications (McGirt et al., 2009).

Antiangiogenic drugs have been researched for use in glioma (Lombardi et al., 2017), since grade IV glioma have neovascularization and over expression of VEGF (Vascular endothelial growth factor). Cilengitide is one of the anti-angiogenic agents used which is an integrin receptor inhibitor. Integrins are widely expressed in grade IV glioma and help in tumour migration (Lombardi et al., 2017). Cilengitide only showed a modest benefit in OS (Nabors et al., 2015) and ended after phase 2 study. Avastin or bevacizumab did not show any benefit in primary grade IV glioma (Iwamoto and Fine, 2010). Bevacizumab is an anti-VEGF antibody and the rationale for use was due to the overexpression of VEGF in glioma. It has shown some benefit in recurrent grade IV glioma (Wenger et al., 2017) with PFS of 5.4 months in responders compared to 1.9 months in non-responders. It is not currently approved by NICE for recurrent grade IV glioma (NICE, 2019).

REGOMA (regorafenib in relapsed glioma) is a trial which has looked at use of regorafenib in relapsed grade IV glioma after the Stupp trial (Lombardi et al., 2018). Regorafinib is an oral multi-kinase inhibitor which targets angiogenic and oncogenic receptor tyrosine kinase (Krishnamoorthy et al., 2015). It has concluded its phase 2 with improved OS (overall survival) and PFS and a phase 3 trial is being planned. Checkmate 143 is a trial which has looked at the use of Nivolumab, an anti-programmed cell death-1 antibody (Filley et al., 2017). Nivolumab has shown promise in other cancers (Guo et al., 2017) but it has not shown a prolongation in the OS in recurrent grade IV glioma patients. Further research is likely to continue as a small subgroup of 8% patients did show a favourable response (Filley et al., 2017).

PARADIGM 2 (Olapraib and radiotherapy for people with glioblastoma trial) (Fulton et al., 2017) is an ongoing study looking at targeting PARP (Poly ADP-ribose polymerase)

which is overexpressed in cell repair and in other cancers such as breast and peritoneal cancer. It is an ongoing research and does hold promise for future therapies (Morales et al., 2014). Novo TTF (Omar, 2014; Hottinger et al., 2016; Benson, 2018) which uses the application of magnetic fields to the dividing tumour cells to arrest growth has shown promise of increased OS to 20 months.

Despite the widespread research, progress in improving survival in grade IV glioma is slow. There lies a role in genetic targeting and using bio-active agents, which are directed at molecular targets in the cell (Chamberlain, 2011). Recent advances in the last decade since WHO 2007 to the WHO 2016 classification of glioma, molecular advances have been recognised and therapy is modulated according to known IDH, ATRX and MGMT status (Louis et al., 2016; NICE, 2019).

Tumour specific antibody targeting has been suggested in the literature towards brain tumours (Sampson et al., 2000). There is a shift from systemic to site specific tumour therapy using targeted interleukin-2 (Schrama, 2004) and antibody-directed enzyme prodrug therapy or ADEPT (Sharma et al., 2005). Antibodies were initially termed as the 'magic bullet' for targeted cancer therapy (Chester, 2004) in the early 1990s. Further developments in technology have brought antibodies for clinical applications, with predicted effects in animal models and cancer patients (Chester, 2004). There still remains a fundamental challenge in differentiating between normal and abnormal cells in cancer biology (Phillips et al., 2008) when using antibodies. Systematic Evolution of Ligands through Exponential enrichment or SELEX (Ellington and Szostak, 1990) is a technique specifically suited to developing biomarker probes (Stoltenburg et al., 2007; Phillips et al., 2008). The products of SELEX are termed as aptamer (Ellington and

Szostak, 1990; Tuerk and Gold, 1990). Aptamers have been researched on in grade IV glioma and may help some future treatments towards glioma (Cerchia et al., 2002)

1.6 Aptamers

Aptamers are small, single-stranded oligonucleotides, which contort to form various two dimensional structures and tertiary three dimensional structures due to hydrogen bonding (Tuerk and Gold, 1990) (Figure 1.9).

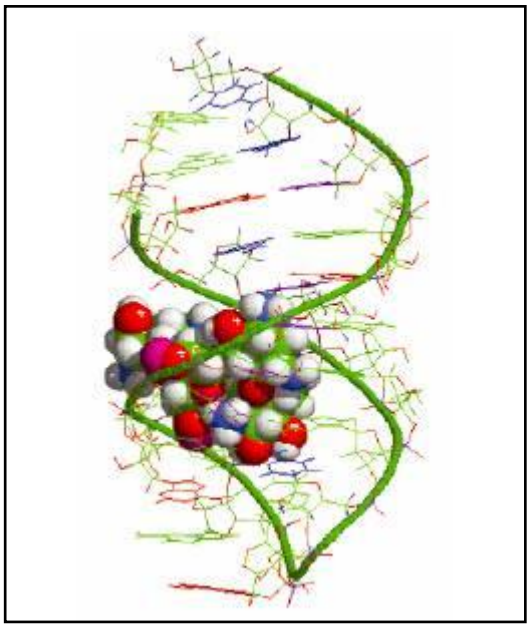

Figure 1.10 Diagram showing an aptamer molecule nestled on its target (Srisawat, 2014)

They bind with high affinity (within the low nano molar range) to a target molecule by providing a limited number of specific contact points embedded in a larger, defined three-dimensional structure (Mayer, 2009). Aptamer discovery is attributed to findings of virus associated RNA (VA RNA) during studies on human immunodeficiency virus (HIV) (Cullen and Greene, 1989; Marciniak et al., 1990). Further studies led to the significance of this functionalised RNA to be used as a therapy and coined the term 'aptamer'(Ellington and Szostak, 1990; Tuerk and Gold, 1990), 'aptus' – to fit and 'meros' – part. Production of aptamers using SELEX (Systemic Evolution of Ligands by

Exponential enrichment) could generate highly specific aptamers to the target molecule. The two groups produced similar conclusions but with different approaches. Tuerk and Gold (1990) targeted a molecule with known functionalised RNA interaction while Ellington and Szoztak (1990) produced novel functionalised RNA towards new targets. Hence, by exposing targets to a random library of DNA and RNA sequences, high affinity structures could be obtained with diagnostic and pharmaceutical value was proved.

1.6.1 Aptamers as drug targeting agents

Traditional SELEX works by a positive selection towards a known target and a negative selection against a non-target (Yan and Levy, 2009) (figure 1.10).

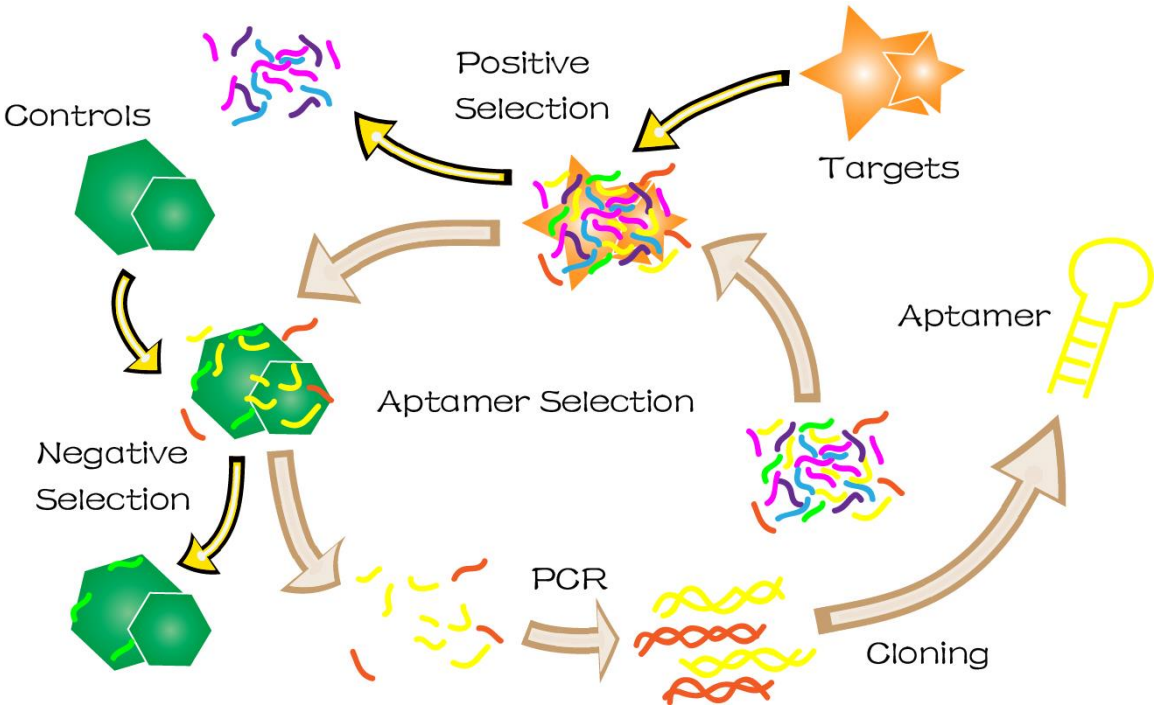

Figure 1.11 SELEX – Systematic Evolution of Ligands by exponential enrichment

Image describing the process of SELEX, the starting point being the reaction of aptamer library with the targets. Positive aptamer sequences are then reacted with negative controls to remove common binding targets and then PCR the left over aptamers, thus generating aptamers positive to the target and negative to the control.

SELEX can be modified by doing a negative selection against an unwanted target (Cerchia et al., 2005; Pestourie et al., 2006). Negative selection especially helps when positive selection is done against an unknown target but an undesirable target is used for negative selection. (Sampson, 2003). 10-15 cycles of SELEX is likely to deliver an aptamer with high affinity and specificity to its target (Shigdar, 2010).

Aptamers have been shown to distinguish between protein kinase C (PKC) isozymes which are 96% identical (Osborne et al., 1997). The final binding of an aptamer is highly specific due to its conformational tertiary and quaternary (Baird and Ferre-D'Amare, 2013) state it contorts into (Cerchia et al., 2009; Cibiel et al., 2012). The final tertiary or quaternary structure of the aptamer binds due to hydrogen bonds, Van der Waals forces and base pairing (Shigdar, 2010) (figure 1.11).

A disadvantage of the SELEX process is the uncertainty of success of the process (Mayer, 2009). Proteins which are positively charged under physiological conditions are excellent target and are 'aptamerogenic' (Mayer, 2009).

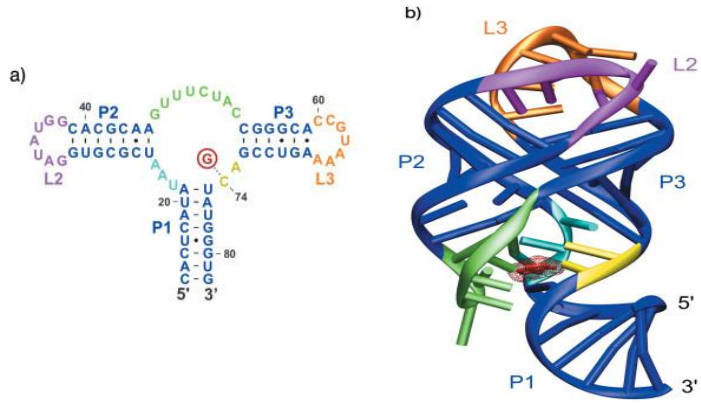

Figure 1.12 Secondary and tertiary structure of aptamer

a) Secondary structure of aptamer with straight components with base pairing and 'hair pin' 'free' ends available for binding. b) The tertiary structure of aptamer with free ends available for binding to targets (Klussman, 2005). The tertiary structure is formed by various binding forces and determines the final target binding.

1.6.2 Review of current aptamers for therapy

Aptamers (Ellington and Szostak, 1990; Tuerk and Gold, 1990) have been compared to antibodies (Jayasena, 1999) and projected as the future for diagnosis and treatment as a replacement for antibodies. In vitro SELEX can generate aptamer towards nearly most targets (Schüling et al., 2018). Applications of aptamers as therapeutics depends on their affinity to the target molecule (Brody and Gold, 2000). This has been demonstrated from NX1838, an aptamer towards the 165 isoform of vascular endothelial growth factor or VEGF (Ruckman et al., 1998; Brody and Gold, 2000). VEGF is implicated in pathological growth of blood vessels in proliferative conditions like age-related macular degeneration. Pegaptanib or 'macugen' is the first anti-VEGF aptamer approved by the United States Food and Drug Administration (USFDA) for use as intra-ocular injection for combating age related macular degeneration in 2005 (Ng et al., 2006). It is administered via an intra-ocular injection and has US FDA approval since 2005 (Bouchard et al., 2010). VEGF resistant molecules have been described to be effective for controlling angiogenesis in highly vascular tumours like glioblastoma. The PDGF-B blockade DNA aptamer, AX102, leads to the reduction of pericytes in Lewis Lung Carcinoma (Sennino, 2010; Takano, 2012). These are evidences of current aptamer research and the potential of using aptamers for further applications in therapy.

Similar to antibodies, aptamers can also be used as diagnostic agents (Brody and Gold, 2000) and for analytic applications (Tombelli et al., 2005; Tombelli et al., 2007). They can be used as target validation tools (Blank and Blind, 2005) and as sensors for platelet-derived growth factor (PDGF) which is an important protein regulating cell growth and division (Degefa and Kwak, 2008).

Aptamers have also been used as fluorescent beacon for measuring water hardness (Lerga and O'Sullivan, 2008), an electrochemical sensor for detecting adenosine (Feng et al., 2008; Chakraborty et al., 2009; Wang et al., 2009) using methylene blue as the indicator. Surface enhanced Raman scattering (SERS) has been demonstrated to detect adenosine (Chen et al., 2008) using aptamer signalling, thus demonstrating a method for adenosine assay. Adenosine is an important substrate in biological reactions (Huizenga and Szostak, 1995) and it is also a powerful vasodilator of blood vessels and a biological cofactor. Aptamers for coronary artery disease (NU172), von Willebrand's disease (ARC1779), haemophilia (ARC19499) and diabetes mellitus (NOX-E36) are currently in clinical trials (Gold et al., 2012; Sundaram et al., 2013). NOX-E36 trial concluded in 2014 and showed safety and efficacy of aptamer drug delivery by intravenous and subcuticular routes for patients with diabetes mellitus type 2 and albuminuria. The drug showed disease modifying characteristics by improving albumin to creatine ratio and also reducing glycated haemoglobin (HbA1c) in blood (NOXXON, 2015). The ARC19499 aptamer study showed correction in bleeding times and thrombin generation in phase 1 but was terminated due to inconsistency of results (Hartmann and Croteau, 2016).

Aptamers have been conjugated with nanomaterials (Yang et al., 2011) like gold, silica and carbon nanotubes for a variety of applications. Gold nano particles conjugated with aptamers have been used as sensing platform for thrombin (Li et al., 2008) which is an important component for thrombosis and haemostasis (Bock et al., 1992). Metal nanotubes, using gold and silver, were utilised for detection of vasopressin using aptamer-based assay and SERS (Huh and Erickson, 2010). Similar detection was performed for mercuric ion Hg_2^+ using silver nano particles (Wang and Chen, 2009).

Aptamers have been shown to work as molecular probes to detect cancer (Phillips et al., 2008) and in some cases to inhibit biological function of such molecule (Cerchia et al., 2002) as PDGF-B. Aptamers in central nervous system (Yang et al., 2007) have been used by developing against prions of transmissible spongiform encephalopathy (Weiss et al., 1997). This can help in developing diagnostic application towards transmissible spongiform encephalopathy diagnosis. Tenascin-C is a molecule overexpressed in wound healing and tumour growth (Yang et al., 2007). Anti-Tenascin-C aptamers have been isolated towards tenascin-C expressing glioblastoma cells (Hicke et al., 2001; Hicke et al., 2006) and can be used for tumour targeting, for delivery of chemical agents or radioisotopes.

Importantly, aptamers are not problematic with bacterial or viral contamination (Schüling et al., 2018). Despite bacterial or viral contamination, they can still be used in the lab. Though if the final use is therapeutic, that might not be the case. They can be stored at room temperature in an non-constituted state (Yan and Levy, 2009; Bunka et al., 2010).They are also a lot less expensive than antibodies (Yan and Levy, 2009). They can easily be produced and more economical to produce (Jayasena, 1999). The aptamer sequence can be emailed to anyone in the world and can be locally produced by the manufacturer. They are much smaller in size and is non-immunogenic due to being DNA or RNA only.

1.6.3 Disadvantages of aptamers and likely solutions

RNA and DNA are present in all living forms and are unstable in serum. Chemical modification can though make them more stable and resistant to enzymes (Osborne et al., 1997). The stability of modified anti-bFGF (basic fibroblast growth factor) aptamer was increased 1000 fold compared to anti-VEGF (vascular endothelial growth factor)

aptamer by addition of pyrimidines (Jellinek et al., 1995). Hence it is likely that aptamers will be confined to intra-venous administration in near future and not for oral consumption. Disulphide bonds in secondary structure provides thermal stability to the aptamer (Osborne et al., 1996; Lu et al., 2008). Phosphorothioate linkages to the 5' and 3' end provides stabilisation against exonuclease degradation (Green et al., 1995). Aptamers are also prone to nuclease degradation when compared to antibodies (Schüling et al., 2018).

1.6.4 Review of Current Aptamers in Glioma

In-vitro experiments performed by certain researchers have laid claim to certain DNA and RNA sequences of aptamers to be glial specific (Cerchia et al., 2009). The aim of the research was to generate tumour specific aptamers using SELEX against glioma cell lines. They performed initial 14 rounds of SELEX against U87MG cell line after which they came up with 71 aptamer sequences which could be categorised under 10 families. Further screening isolated the number to eight sequences which are thought to be glial specific and tested against other cancer cell lines and mouse fibroblasts. A-172 glioblastoma cell line has also been used to find glioma specific aptamers and their affinity tested using flow cytometry and binding analysis (Bayrac et al., 2011). TTA1, an aptamer to the extracellular matrix protein tenascin-C has been found to be taken up by breast, glioma, lung and colon tumours and it shows potential to be used as targeted chemotherapy (Hicke et al., 2006). Techniques for targeting tumour cells with aptamers have been described in literature, enabling to identify and detect specific aptamers (Cerchia and de Franciscis, 2010).

1.6.5 Future directions for glioma targeting aptamers

Techniques for cancer cell detection have recently been described using aptamers which would improve control over diagnosis and therapeutics (Pu et al., 2010). ChiP or chromatin immunoprecipitation is a technique which describes its use as a tool for studying transcription factor binding. ChIP can help in isolating the cellular structures responsible for binding of the aptamers (Spencer et al., 2003); (Viens et al., 2004). The technique combines chromatin immunoprecipitation and DNA microarray analysis to identify protein-DNA interactions that occur in living cells. Protein-DNA interactions are captured *in vitro* by chemical crosslinking (Aparicio et al., 2004), followed by cell lysis and immunoaffinity purification of the desired protein. Immnoaffinity purification will co-purify DNA fragments that are associated with the protein (Lee et al., 2006) and help in identification of relevant targets. Micro ChiP protocols have been described showing that they are much quicker (one day procedure) and moreover, they require a lesser number of cells in comparison to standard protocols (Dahl and Collas, 2008). Due to micro ChIP techniques, it is possible to use tiny amounts of frozen tissue sections. Micro ChIP can be particularly helpful when tissue is small in quantity. This can be of potential in patient targeted therapeutics where sample load is small, like an image guided biopsy (Brehar et al., 2012).

AptaBid (Aptamer-facilitated Biomarker Discovery) is another technique described for biomarker discovery. It has been described from the nascent stage of generating DNA aptamers to target molecules using SELEX and they are used to isolate biomarkers from the cells. The isolated biomarkers are identified by means of mass spectrometry and it has been termed, aptamer-facilitated biomarker discovery (AptaBiD) (Berezovski et al., 2008).

Currently, there is no documented method for performing biomarker discovery except AptaBiD, which was performed using dendritic mouse cells (Berezovski et al., 2008). There is no previously published work for aptamer associated biomarker discovery in glioma except the outcome paper from this thesis (Aptekar et al., 2015) as published in 2015. There remains a potential for developing a pull-down protocol to recognise potential biomarkers in glioma and establishing a working methodology.

1.7 Rationale of the project

The aim of this project was to develop a novel pull-down assay to identify the target ligands of aptamers generated against different glioma cell lines. Current treatment protocols for GBM is based on suitable surgical excision followed by chemo and radiotherapy. GBM is incurable and current treatment helps to increase meaningful survival (NICE, 2019). Patients with GBM still continue to have poor prognosis and long term outcomes (Krex et al., 2007). Despite multiple chemotherapeutic agents in the last decade being used in various trials, GBM survival has increased to 14 months. By being able to develop an assay to identify the target ligands, new patient specific targeted therapy could be developed. Aptamer selection against unknown targets is already established but no specific assay exists which can help identify the target molecule.

1.7.1 Aim of the Project

The main aim of this study was to develop a protocol for aptamer assisted precipitation. This will help for identifying target proteins, which are responsible for attachment with ‘aptamers’. These are likely to be glial specific. Furthermore, the study was designed to extract, isolate and characterize these target cell proteins and validate the novel ‘pull-down method’ based on microchip. To confirm the methodology for universal application.

1.7.2 Specific Aims

- To test glial specific aptamers already published in literature and to assess specificity towards various cell lines
- To use tissue culture techniques of fluorescent microscopy and immunostaining and assess binding of such aptamers for primary cell culture using confocal microscopy and biotin tagged aptamers.
- To develop an aptamer-assisted precipitation protocol and to extract the cell complex binding to the aptamers using cell lysis and Modified Chromatin Immunoprecipitation (ChIP)
- To identify the cellular complexes isolated using mass spectroscopy
- To analyse the data and to confirm target pull-down using Western blotting and staining with specific antibodies
- To confirm the validity of the protocol and expanded application to other aptamer-cell complexes.
- To analyse the data and conclude the project

Chapter 2

2 Materials and methods

2.1 Introduction

The experiments were carried out using different grades of immortalised human glioma cell lines; U87MG (grade IV glioblastoma), 1321N1 (grade II astrocytoma) and non-cancerous foetal astrocytes SVGp12. The cell lines were obtained from the European Collection of Cell Cultures (ECACC), UK and American Type Culture Collection (ATCC). Normal human astrocyte short term cultures were used during later parts of the experiments. Short term cultures from patient biopsies obtained from the Brain Tumour North-West (BTNW) consortium tissue bank

2.2 Media and supplements

The media and supplements were used for specific cell lines according to recommended guidelines of ECACC and ATCC. Media for the short-term cultures was used as per established protocols from BTNW guidelines (Appendix 2). The preparations were carried out under aseptic conditions. All cell lines were grown in 75 cm^2 or 25 cm^2 tissue culture flasks (Thermo Scientific, UK) and maintained in a 37°C humidified incubator, with 5% CO_2. For the experiments in the study, the cell lines were harvested at 70-80% confluence and used between passages 5-25. Short term cultures were used between passages 3-13. All plasticware was obtained from Fisher scientific, Leicestershire, UK, media and supplements from scientific laboratory supplies (SLS), Lonza, Nottingham, UK and reagents from Sigma-Aldrich Ltd, Butterworth, UK.

2.3 Cell culture with commercial cell lines

2.3.1 Commercial cell lines

Monolayer of cells at 70-80% confluency were subcultured. The U87MG and SVGp12 cell lines were grown in Essential Minimum Eagle Medium (EMEM) supplemented with 10% (v/v) FBS, 2 mM L-glutamine, 1 mM sodium pyruvate and 1 % (v/v) non-essential amino acids (NEAA), while the 1321N1 cell line was maintained in Dulbeccos's Modified Eagle's Medium (DMEM) supplemented with 10% (v/v) foetal bovine serum (FBS) and 2 mM L-glutamine. The media was aspirated and the cells were washed with 0.1 M phosphate buffered saline (PBS) (pH 7.41), twice, to remove any traces of serum from the cells. The cells were detached by incubation with 0.25% trypsin for 2 minutes at 37°C humidified incubator, with 5% CO_2. The flask was then tapped gently and viewed under the inverted light microscope to ensure the detachment of cells. Complete medium was then added to neutralise the reaction and mixed gently but well, to obtain a homogenous and evenly distributed cell suspension. The cells were seeded at the ratio of 1:4 to each fresh flask. These cell cultures were observed regularly and sub-cultured at 70-80% confluency.

2.3.2 Freezing cultures for storage

Cell flasks with confluent cultures were passaged as above. After trypsinising cells, complete medium was then added to neutralise the reaction and mixed gently but well, to obtain a homogenous and evenly distributed cell suspension. This suspension was centrifuged at 200 x g for 5 minutes to get a cell pellet. The supernatant was aspirated and the cell pellet suspended in 10ml of media. Cell count was performed using coulter counter (Beckman coulter Z1, serial AK03015). The cell count enables dividing cells optimally for storage at a million per vial. The appropriate cell dilution is achieved and

suspended in 1ml of freezing solution, made from 750µl of FBS and 250µl of DMSO (dimethyl sulfoxide). The cell suspension was then put in a freezing container, Mr Frosty™ (Thermoscientific, UK) and put in -80^{o}C. The container has isopropyl alcoholwhich enables cooling the cells at -1^{o}C per minute and keeping them viable. The cells were left for 24 hrs and then transferred to liquid nitrogen for longer storage.

2.4 Short term culture

Fresh tissue from the surgical biopsy was collected from the neurosurgical theatres at the Royal Preston Hospital in transport media (2 mM penicillin and streptomycin combined at 0.5% and amphotericin at 0.5% in DMEM (Dulbeco's Modified Eagle's Medium)). The specimens were processed immediately in most cases, the rest being store at 4^{0}C in the fridge for processing the following day. The tissues were processed in a class III ventilation hood (Holten HA243 BS and Jouan MSC 9) and transferred into a petri dish. The tissue was weighed in the primary culture lab and segregated into like for like sections using sterile scalpel blades and forceps. Ample tissue for diagnosis was taken and the residual tissue weighed again prior to being divided for culture and frozen sample. A final research tissue weight was recorded. Tissue for culture was diced and cut into small parts and washed with culture media, F10 Ham containing FBS. Penicillin and streptomycin combined (2 mM) and amphotericin (2 mM), both at final dilution at 0.5% was added to the initial culture media wash. The wash was performed to remove the dead and necrotic tissue accompanying the tissue sample and repeated three times with centrifugation for 30 seconds at 200 x *g*.

The tissue sample at the end of washes was either disaggregated using 50 U/ ml collagenase in 9ml volume of tissue suspension. This was done in a T25 flask at 37^{0}C with regular shaking to enable good disaggregation for 4-5 hours. The disaggregate at the

end was gently pipetted a few times and then centrifuged at 200 *g* for 5 minutes before removing the supernatant and putting into culture with fresh culture media at 37^0C in a new T25 flask. Fresh media was added to the disaggregation T25 flask as well and put at 37^0C. In cases of small amounts of tissue being available for culture, the tissue was washed and placed as an 'explant' (Freshney, 2006) into T25 flasks in fresh media for culture at 37^0C. After 24-48 hours, the media and non-adherent cells were removed and put into another T25 flask with fresh media to enable further culture growth. The media flask with primary disaggregation and explant would then have fresh media added and checked every 3-4 days. Media was changed at varying intervals when the colour of the original media in the flask faded and corresponded with growth in cultures. Half media change was performed at these times to ensure the media was not completely devoid of both endogenous and exogenous growth factors.

Table 2-1 Short term cultures and their source

Cell Line	Source	Glioma Grade
BTNW911	BTNW	GBM
BTNW914	BTNW	GBM
BTNW370	BTNW	Gliosarcoma
IN1528	Wolverhampton	GBM
IN1612	Wolverhampton	GBM
W2045	Wolverhampton	GBM
W857	Wolverhampton	GBM

2.5 Immunochemistry characterisation of short-term cell cultures

Immunostaining for short term cultures was performed using antibodies, GFAP (glial fibrillary acidic protein), EMA (epithelial membrane antigen) and CD34 (cluster of differentiation 34 protein) (Fina et al., 1990) as detailed in Table 2.2.

Table 2-2 List of antibodies and dilutions for characterisation of short-term cultures

Antibody/target	Dilution	Manufacturer	Type
GFAP	1:400	Abcam, UK	Rabbit polyclonal
EMA	1:350	Dako, UK	Rabbit polyclonal
CD34	1:300	Dako, UK	Rabbit polyclonal
Biotinylated secondary Antibody	1:500	Abcam, UK	Rabbit polyclonal

This was to confirm neural or glial tissue in origin (GFAP), absence of meningothelial cells (EMA) and absence of endothelial cells in origin (CD34). Immunostaining was performed using Vectastain® ABC kit (Vector Labs, USA) and immunocytochemistry protocol. Cells were grown in chambered slides and seeded at 10,000 cells per well. Cells were grown for 48 hrs and checked under a microscope for confluency. Excess media was removed and the slide washed with 10 mM tris-phoshate buffer saline (TBS) three times for 5 minutes each. The cells were then fixed with acetone methanol solution at 1:1 dilution, pre-chilled to -20^{0}C and kept at -20^{0}C for 10 minutes. Excess fixative was removed and cells were air dried and rehydrated with TBS. The cells were blocked with horse serum for 20 minutes and washed with TBS three times. Antibodies at manufacturer specified dilution was then added to the respective slide wells and incubated for 30 minutes at room temperature (except GFAP, incubated overnight at 4^{o}C). The excess antibody was

washed away and the slides washed with TBS three times. The secondary antibody from vectastain® kit was added to the chambers and incubated at room temperature for 30 minutes. The secondary antibody was then washed off and 200 uμ of Strep AB Complex, premixed and standing for 30 minutes was added to the chambers for 30 minutes. At the end of 30 minutes, ABC complex was removed and cells washed three times with PBS/TBS. Fresh DAB solution at dilution of 50 μL to 1ml of buffer was added to the chambers for 5-10 minutes. This was then washed off and cells were counter stained with haematoxylin for 20 seconds. This was washed in running water bath and then sequentially quenched with graded alcohol. The chamber was then removed using the special tool provided and slide rinsed finally in xylene and mounted with DPX (Thermoscientific, UK), a synthetic mounting resin and a large coverslip. DPX is a mixture of polystyrene, plasticizer and xylene.

2.6 Characterisation of cell lines

Cell cultures of U87MG, 1321N1and SVGP12 were grown in six well plates on standard cover slips to 80% confluence prior to characterisation. The coverslips were washed three times with PBS. The cells were then fixed using 4% paraformaldehyde (PFA) for 15-20 minutes. After fixation, the cells were washed three times with 0.1 M PBS (pH 7.4) for 5 minutes each and then blocked using 10% goat or donkey serum for 1 hour. Cells were again washed three times with PBS and the respective antibodies added to each coverslip after placing in separate wells as per manufacturer guidelines and incubated at room temperature for 30 minutes (Table 2.3). The excess antibody was washed away and the slides washed with PBS thrice. The secondary antibody was added to the coverslips and incubated at room temperature for 30 minutes, in the dark. The excess antibody was removed and the coverslips mounted on slides and sealed with nail

varnish. Images were taken on Zeiss LSM 510 laser scanning confocal microscope (excitation at 488 nm; emission at 543nm laser).

Table 2-3 List of antibodies and dilutions for characterisation of cell lines

Antibody/target	Dilution	Manufacturer	Type
GFAP	1:300	Abcam, UK	Rabbit polyclonal
HLA	1:250	Abcam, UK	Rabbit polyclonal
VEGF	1:200	Abcam, UK	Rabbit polyclonal
Isotype control	1:100	Santacruz, UK	Rabbit polyclonal
Alexa Fluor 488 2^{o} ab	1:1000	Life technologies, UK	Goat, anti rabbit

2.7 Binding of fluorescent tagged aptamer to cell lines

2.7.1 Live cell incubation with Cy3 tagged aptamer.

To evaluate the binding of fluorescent Cy3 tagged aptamers, SA44 DNA (Aptekar et al., 2015), SA43 DNA and SA56 RNA (IDT, UK) (table 2.4 and novel TDM aptamers table 2.5); cell cultures of U87MG, 1321N1 as glioma cell lines and SVGP12 as control were used.

Table 2-4 Aptamer sequences for SA aptamers

Aptamer	Sequence 5' to 3'	Sugar	5' label	Reference
SA44	ACG TTA CTC TTG CAA CAC CCA AAC TTT AAT AGC CTC TTA TAG TTC	Deoxy ribose	Cy3/ Biotin	Cerchia *et al.*, 2009
SA43	ACG TTA CTC TTG CAA CAC AAA CTT TAA TAG CCT CTT ATA GTT C	Deoxy ribose	Cy3/ Biotin	Cerchia *et al.*, 2009
SA56	TGA TTT TGC AGC ACT TCT TGT TAT CTT AAC GAA CTG TTG ATG A	Ribose	Cy3	Cerchia *et al.*, 2009
SANeg1	GGA AAA TTA TAC CCT CCA TTA AAT CCA CCA TTA CCA CAC CCT TTA	Deoxy ribose	Cy3/ Biotin	In-house
SANeg2	CCG TTA ATT AGG CCC TTA AAT GGC ATA AAA TTT GAA AGG GAA T	Deoxy ribose	Cy3/ Biotin	In-house

Table 2-5 Novel TDM aptamer sequences

Aptamer	Sequence 5' to 3'	Sugar	5' label	Reference
TDM2	CACTCCAAAACTCACCTGAACTGTAATAGG GGATGTGTGCTACACTATCG	Deoxy ribose	Biotin	In-house
TDM3	GGCACATTCCGACACGGGTTGGCGGTTTGG GATTGATGAACTGGCAGTTG	Deoxy ribose	Biotin	In-house
TDM7	GCGGCAGCTGTGCCCGTGCTGCGTCTAGAC TCGTGATGAGAAGGAGGGCT	Deoxy ribose	Biotin	In-house
TDM9	CGCTCATTCGTGGATGATTAATGCGGAGCG TGGTGGGAAGCGGGCAGCGG	Deoxy ribose	Biotin	In-house
TDM10	CCGCTAGTGGGCGGACGATGCGTGGGATAG GGGGGCGAATTGGGGGATTT	Deoxy ribose	Biotin	In-house

The cells were grown in six well plates on standard cover slips. The cells were grown to 80% confluence prior to treatment with the aptamer then washed with PBS at 37^0C. The aptamers were diluted with respective media to achieve a final concentration of 100nM in 1 ml. The cells were incubated with the aptamer in dark for 90 minutes followed by removal of the media and sequentially washed three times with PBS for 5 minutes each. The cells were then fixed using 4% PFA for 15-20 minutes. This was followed by another three washes with PBS for 5 minutes each. The coverslips were then mounted on glass slides with 10 µl of DAPI (4',6-diamidino-2-phenylindole) upside down and the edges sealed with nail varnish to prevent drying of the cells and DAPI. The slides were imaged under confocal microscope (Zeiss LSM 510 laser scanning confocal microscope) at 20x and at 40x using the oil based lens (excitation at 543 nm; emission at 560-615nm laser) once the coverslips were immobile.

2.7.2 Fixed cell incubation with Cy3 tagged aptamer.

The cells were grown (see section 3.2 for details) and were fixed with 4% PFA prior to aptamer treatment. After fixation, the cells were washed three times with PBS for 5 minutes each and then blocked using 10% goat or donkey serum for 1 hour. This was

then again washed three times with PBS and the aptamer incubated for 90 minutes. The cells were then washed three times with PBS and then mounted on slides using DAPI in the dark and visualised using confocal microscopy, using the same settings as Section 2.7.1.

2.8 Aptamer chemistry with biotinylated aptamer

Aptamer binding was determined using biotinylated aptamers to commercially available cells lines and patient derived short-term cultures. Biotinylated aptamers were utilised to establish binding affinity of aptamers seen with fluorescent tagged aptamer, as the biotin tag would be utilised in the aptamer assisted precipitation of target molecule. Commercial cell lines were used to develop the protocol and then the protocol was applied to short-term cultures. Fixed and live cells were both used to evaluate binding with biotin conjugated aptamers.

2.8.1 Biotinylated aptamer binding to live cells

Commercial cell lines U87MG and SVGP12, were grown in chambered slides (Falcon™ chambered slides, Fisher scientific, UK) to 80% confluence. The chambers were seeded with 30-40,000 cells and utilised for aptamer binding the following day. The media was removed and fresh media with aptamer at dilution of 100nM was added to the slide and incubated at 37^0C for 90 minutes. Excess media was removed, and the slide washed with 0.1 M PBS or Trisphoshate buffer (TBS) three times for 5 minutes each. The cells were then fixed with acetone methanol solution at 1:1 dilution, pre-chilled to -20^0C and kept at -20^0C for 10 minutes. Excess fixative was removed, cells were air dried and then rehydrated with PBS/TBS. The cells were blocked with 10% horse serum for 20 minutes and washed with TBS three times. Approximately 200µL of Strep AB Complex from the Vectastain™ kit, premixed and standing for 30 minutes was then added to the chambers

for 30 minutes. At the end of 30 minutes, ABC complex was removed and cells washed three times with PBS/TBS. Fresh DAB (diaminobenzidine) solution at dilution of 50µL to 1ml of Buffer was added to the chambers for 5-10 minutes. Diaminobenzidine works by amplification of the signal by multiplying the avidin-biotin (Viens et al., 2004) to achieve a brown stain. This was then washed off and cells were counter stained with haematoxylin for 20 seconds. This was washed in running water bath and then sequentially quenched with graded alcohol. The chamber was then removed using the special tool provided and slide rinsed finally in xylene and mounted with DPX and large coverslip.

2.8.2 Biotinylated aptamer binding to fixed cells

The above protocol as in section 2.8.1 was followed for cell culture and aptamer incubation. After media removal, the cells were washed with PBS and fixed with paraformaldehyde solution (PFA) at 4 % dilution at room temperature for 10 minutes. Excess fixative was aspirated and the slides washed with PBS. The cells were then incubated with 0.1% triton X100 to permeabilise the cells for 5 minutes at room temperature. Excess fluid was then aspirated and washed again with PBS three times. The cells were blocked with 10% horse serum for 20 minutes and washed with TBS three times. The aptamer at 100nM dilution in PBS was then added for 60 minutes at room temperature. The rest of steps for ABC and DAB staining were followed as in section 2.8.1. The slides were then quenched with alcohol and mounted using DPX as in section 2.8.1.

2.8.3 Changes to staining methodology with AB Complex and DAB

ABC staining method was altered to assess if better visualisation could be achieved. ABC staining works by amplification of the signal by multiplying the avidin-biotin complexes

(Spencer et al., 2003; Viens et al., 2004), which undergo a reaction with diaminobenzidine to generate a brown stain. One avidin molecule has the capacity to bind to four biotin molecules, hence resulting in the amplification (Livnah et al., 1993). Due to the primary target in the experiment being biotin (biotinylated aptamer), premixing AB complex could result in slightly less availability of avidin for binding. Hence, the experiment was altered from the protocol described in Section 8.1 at the ABC stage. Avidin complex was first incubated with the cells after fixation, instead of premixing avidin and biotin (A and B). After reacting the avidin for 15 minutes, the excess was aspirated and the slide washed with PBS. Biotin was then incubated with the slide at room temperature for 15 minutes. Fresh DAB solution was also diluted to 50µl to 1.5ml dilution. The rest of the protocol was as in section 2.8.1.

2.8.4 Biotinylated aptamer on fixed commercial cell lines and short-term cultures

Cell lines were cultured as in section 2.8.1. At 80% confluence, the cells were fixed with 4% PFA at room temperature for 10 minutes. Excess fixative was aspirated and the slides washed with PBS. The cells were then incubated with 0.5% triton X100 to permeabilise the cells for 5 minutes at room temperature. The cells were blocked with 10% horse serum for 20 minutes and washed with PBS three times The cells were washed again with PBS three times and then incubated with aptamer at 100nM dilution in PBS at room temperature. After incubation, the cells were washed with PBS three time and proceeded for ABC staining as in section 2.8.1.

2.9 Methods of Protein extraction

2.9.1 Protein extraction techniques for fixed cells with RIPA buffer

Cells were cultured in T75 flasks to 80 % confluence followed by washing with PBS and fixed with 4% PFA at room temperature for 20 mins. The cells were then washed with PBS three times and scraped from the flasks in the presence of RIPA (radioimmunoprecipitation) lysis buffer (pH 8.0). A total volume of 1ml of the cells and RIPA was put in an eppendorf and kept for lysis at 4^0C for 30-45 minutes. At the end, the eppendorf was centrifuged at 4472 x g for 20 minutes at 4^0C. The supernatant aspirated was assessed for protein concentration using Bradford assay (Bradford, 1976).

Protein extraction was also performed using the above technique until the cells were scraped into RIPA lysis buffer. RIPA has the lowest concentration of SDS at 0.1% and is least denaturing (Zhang et al., 2015). It also has least interference with the proteomic assessment in bradford assay. The following variations for protein extractions were attempted:

a) Freeze and thaw of cell suspension using liquid nitrogen and water bath at 37^0C for eight cycles for optimisation of protein extraction
b) Heat the cell suspension at 100^0C for 20 minutes followed by 60^0C for 2 hours
c) Pass the cell suspension through a 27 gauge needle attached to a syringe for six passes
d) Water bath sonication of the cell suspension for cycles of 30 seconds, interspaced with rest period of 1 minute for 15 cycles
e) Probe sonication of the cell suspension at 20 hertz for 30 seconds on ice, with rest periods of 1 minute for 6 cycles

The above lysates were then centrifuged at 4472 x g for 20 minutes at 4^0C and the supernatant was assessed using Bradford assay.

2.9.2 Protein extraction using various lysis buffers on fixed cells

Protein extraction was further optimised by using other lysis buffers on fixed cells. The following lysis buffers were made

a) RIPA, containing 2% SDS (pH 8.0)
b) 2% SDS in PBS lysis buffer (pH 8.0)
c) 1% SDS in PBS lysis buffer (pH 8.0)
d) Native lysis buffer (pH 8.0)

The above lysis buffers were used for fixed cell lysis using the techniques mentioned in section 2.9.1 and analysed using Bradford assay for protein dilution.

2.9.3 Protein extraction on unfixed cells

Cells were trypsinised and complete medium was then added to neutralise the reaction and mixed gently but well, to obtain a homogenous and evenly distributed cell suspension. This suspension was centrifuged at 200 *x g* for 5 minutes to get a cell pellet. This cell pellet could be used immediately or stored at -80°C for future use. The cell pellet was then resuspended with RIPA buffer to a 1ml volume. The cells were lysed in this solution for 45 minutes at 4^0C on a rotating platform at 2.236 *x g* (200 rpm). The lysate was then centrifuged at 4^0C for 10 minutes at 4472 *x g* and the supernatant was assessed using Bradford assay, section 2.10.

Extraction was finalised for pull-down using triton X100 at 0.1% dilution to avoid denaturation of proteins with RIPA and SDS. Using triton X100, maintains the proteins

in a native state and enable specific pulldown. Triton X100 also has less interference with Bradford reagent and hence gave a more accurate protein estimation.

2.10 Bradford Assay

Bradford assay is a method for protein estimation involving the reaction of Coomassie brilliant blue G-250 dye to the proteins in the sample (Bradford, 1976). Protein standards, made from bovine serum albumin (BSA) were made. They had a dilution of 0.2 to 2 mg/mL and were used as a reference. Samples and standards were diluted in Bradford reagent (Sigma, Poole, UK) (1 in 50 dilutions or 5µl sample to 250µl of Bradford reagent). The plate was incubated for 10 minutes on ice to prevent protein degradation. The plate was then read using absorbance values, at wavelengths from 590 to 612 nm using a plate reader, Enspire by PerkinElmer (Massachusetts, US). Three consecutive readings were taken of all the samples. The absorbance of BSA samples was plotted against the dilution and a linear standard plot was determined. Cell extract proteins were then calculated by respective dilution factors.

2.11 Method development of aptamer assisted protein pulldown

2.11.1 Aptamer precipitation using Aptsci kit

Anti-EGFR aptamer kit (Amsbio/ Aptamer sciences Inc, UK) was used as per protocol but supplemented with SA aptamers.

Aptamer was added to ultrapure water to make a 100nM solution. Cells were washed with ice cold PBS twice in a cell pellet and 1X APB (apto-precipitation buffer, custom, contents unknown) containing protease inhibitor on ice for 10 minutes. The stock solution was stored at -20 to 4ºC. 1µl of stock is added to 20µl of 1X APB and heated for 5 minutes at 95 ^{0}C and allowed to cool at room temp for 20 mins prior to use. Add the

above to 1 ml volume of cell lysate (0.95ml lysate and 0.05ml of 20X S1 solution (custom buffer, contents unknown)). S1 solution is meant for minimising non-specific binding. The contents are then incubated at 4 ^{0}C for 2 hours while rotating at 2.236 *x g*.

Included beads (custom, specifics unknown) were prepared by washing twice with 0.5ml of 1X WB (washing buffer, custom solution, contents unknown) and collect the beads with a magnetic stand and remove the supernatant. The reaction mixture was then added to the beads and mixed for 10 mins at 4 ^{0}C at 2.236 *x g*. The eppendorfs were then placed on a magnetic stand and supernatant discarded. The beads are washed with 1X WB for 1 minute gently by inverting and collect the beads on the magnetic stand. Beads were washed three more times and supernatants discarded. Elution was done using 30µl 1X EB (custom buffer for elution, contents unknown) to the tube and mix for 15 minutes at room temp while mixing at 37 ^{0}C. Place tube on magnetic stand and transfer supernatant to new tube. The elutent was then run on 10% SDS PAGE gels and protein was visualised with Coomassie blue, section 2.12.3

2.11.2 Aptamer precipitation using magnetic beads

Cells cultured in T75 flask were trypsinised and centrifuged in a 1.5mL eppendorf for 5 minutes at 200 *x g* to form a cell pellet. The supernatant was discarded and the cell pellet was mixed with 1 ml of PBS and put into an eppendorf tube for washing and centrifuged for 5 minutes at 200 *x g*. Cell pellets can be used immediately or stored at -80°C for future use. The cell pellet was then mixed with 0.1% Triton X100 in cold PBS solution of 1ml volume and protease inhibitors. The cells were lysed in this solution for 45 minutes at 4^{0}C on a rotating platform at 2.236 *x g*. The lysate was then centrifuged at 4^{0}C for 10 minutes at 4472 *x g*. The supernatant was taken for aptamer assisted precipitation and cell debris discarded. Magnetic trial streptavidin beads, dyna beads (Thermo fischer, UK)

were used for incubating with aptamer and cell lysate. Two approaches were taken; the magnetic beads were first incubated with the aptamer, with the aim of conjugating the aptamer to the beads, and then the aptamer-bead conjugate was incubated with the cell lysate. The second approach was to incubate the cell lysate with the aptamer followed by incubation with the beads for 45 minutes at 4^0C. At the end of the reaction, the beads were washed with cold PBS three times and separated on a magnetic separator. The beads at the end of the final wash were boiled in 5x SDS sample buffer for 5 minutes at 95^0C. 15µl of the boiled AP (aptamer pulled precipitate) and Input (whole cell lysate) were then run on 10% SDS PAGE gels and protein was visualised with Coomassie blue, section 2.12.3

2.11.3 Aptamer precipitation using streptavidin agarose beads

Aptamer precipitation protocol was changed to use streptavidin agarose beads. Aptamer was added to the cell lysate and incubated for 45 minutes at 4^0C. Streptavidin agarose beads were taken and prepared by washing with cold PBS three times, lasting for 5 minutes each at 4^0C and centrifuged. These beads were then blocked with BSA for 2 hours while rotating on a shaker at 200 rpm at 4^0C. Following the blocking, the beads were then washed with cold PBS thrice, lasting for 5 minutes each at 4^0C. The beads were centrifuged and then incubated with aptamer-lysate for 30 minutes at 4^0C on a shaker at 200 rpm. The beads were then centrifuged and washed four times with cold PBS on a shaker for 5 minutes each. The beads at the end of the final wash were boiled in 5x SDS sample buffer for 5 minutes at 95^0C. The input sample was prepared by taking 50µl from the cell lysate and boiled with 50µl of SDS sample buffer for 5 minutes at 95^0C. 15µl of the boiled AP and Input were then run on 10% SDS PAGE gels and visualised using Coomassie blue, section 2.12.3

2.11.4 Aptamer assisted precipitation technique

The cell pellet was mixed with 0.1% triton X100 in cold PBS solution of 1ml volume. The cells were lysed in this solution for 45 minutes at 4^0C on a rotating platform at 2.236 *x g.* The lysate was then centrifuged at 4^0C for 10 minutes at 4472 *x g*. The supernatant was taken for aptamer assisted precipitation and cell debris discarded. An aliquot was taken from the supernatant of the eppendorf for Bradford assay and protease inhibitors at 1:200 dilution in PBS, was added to the residual lysate. Aptamer was added to the cell lysate and incubated for 45 minutes at 4^0C. Streptavidin agarose beads were taken and prepared by washing with cold PBS three times for 5 minutes each at 4^0C and centrifuged at 200 *x g*. These beads were then blocked with BSA for 2 hours while rotating on a shaker at 2.236 *x g* at 4^0C. The beads were then washed with cold PBS three times for 5 minutes each at 4^0C. Sedimentation of beads was performed to remove BSA by leaving on an eppendorf rack for 5 minutes. This was performed to reduce non-specific precipitation and reduce errors. At the end of the aptamer incubation, the aptamer-lysate mix was added to the prepared streptavidin agarose beads and incubated for 30 minutes at 4^0C on a shaker at 2.236 *x g*. At the end of the incubation with the beads, they were kept on ice for sedimentation of the beads for 5 minutes and the supernatant was removed and kept separately. The beads were then washed with cold PBS three times at 4^0C on a shaker for 5 minutes. At the end of each wash, the beads were allowed to settle by sedimentation. The beads at the end of the final wash were boiled in 5x SDS sample buffer for 5 minutes at 95^0C. The input sample was prepared by taking 50µl from the cell lysate and boiled with 50µl of SDS sample buffer for 5 minutes at 95^0C. 15µl of the boiled AP and Input were then run on 10% SDS PAGE gels and visualised with Coomassie blue (section 5.2).

2.12 Western blot for target confirmation

Western blotting technique was developed for protein separation on gel blocks for mass spectrometry analysis and for antigen identification. The initial part of Western blotting involves separation of protein according to molecular weight. The latter part is transfer of the proteins from gel to nitrocellulose membrane for antigen identification using antibodies. In the scope of this thesis, the technique was also modified for aptamer binding.

2.12.1 Sample preparation

Protein concentration of input samples was determined using a BSA standard curve from 0.1 mg/ml to 2mg/ml after determining the absorbance using the Bradford assay testing. Twenty-five µl of input protein sample at 2mg/ml was mixed with 5x laemmli buffer (Sigma, Dorset, UK) (containing 4% SDS, 20% glycerol, 10% 2-mercaptoethanol, 0.004% bromphenol blue and 0.125 M Tris HCl, pH approx. 6). at a ratio of 1:1. The eppendorfs were heated in a heat block at 95^{o}C for 5 minutes, after which, the sample was ready for loading into pre-cast or cast 10% polyacrylamide gels (section 2.12.2) for separation of proteins prior to mass spectrometry analysis.

Sample preparation from aptamer assisted precipitation was done using the final aliquot eluted from streptavidin beads. After the final wash from aptamer precipitation, 50µl of 5x laemmli buffer was added to the beads to facilitate detachment of biotin and streptavidin. The eppendorfs containing the beads and laemmli buffer were heated in a heat block at 95^{o}C for 5 minutes after which the sample was ready for loading. 15µl to 25µl sample was loaded into each of the wells. Exact protein concentration of the final extract could not be estimated due to the small size of the elute and interference of SDS in the laemmli buffer in Bradford assay.

2.12.2 Gel electrophoresis

The top loading part of the gel was made of 4% polyacrylamide stacking gel and bottom separation or resolving with 10% polyacrylamide gel. An electric current was applied across the gel which enabled separation of proteins according to their molecular weight and measured against a pre-set ladder with specific molecular weights. The stacking gel was poured into the setup and allowed to polymerise with tetramethylethylenediamine (TEMED, 10 µL in 10% and 6 µL in 4% gel) and ammonium persulphate (APS, 100 µL in 10% and 60 µL in 4% gel). TEMED initiates a polymerising and APS act as a catalyst for the chain reaction. Air contact has to be obliterated for this and hence the stack was covered with water. After the resolving gel had polymerised, the water seal was removed and stacking gel was poured. A well comb was inserted and set in the stacking gel to enable creation of sample loading sites. The gels were then placed in an electrophoresis tank, filled with 1.5 M tris glycine buffer, at pH 7.4 and the wells were loaded with 25µl protein lyste:laemmeli buffer. The gels were run for 90 minutes at 120V before being removed for either staining or transfer.

2.12.3 Gel staining

The gels were stained with Coomassie blue (Coomassie Blue R-250 0.1% w/v, deionised water 50%, methanol 40%, acetic acid 10%) at room temperature for one hour on a rotating platform at 0.559 *x g*. At the end of the staining, the gel was destained using destaining solution (deionised water 50%, methanol 40%, acetic acid 10%), changed at 20-minute intervals. Destaining was stopped when clear stained bands could be visualised by the naked eye and background staining removed. The gels were then imaged using Geldoc™ imager (Bio-rad Laboratories Inc., Watford, UK) ™ imager (Bio-

rad Laboratories Inc., Watford, UK) (Biorad, UK), white light, transwhite setting (302 nm excitation).

2.13 Mass spectrometry analysis

The protein samples from aptamer assisted precipitation that had been separated by gel electrophoresis were cut into bands and chunks. They were appropriately labelled and sent to St. Andrews university for mass spectrometry analysis. This was a commercial purchase of service and the protocol followed for the analysis is given in Section 2.13.1.

2.13.1 nLCESI-MSMS (Nano-scale liquid chromatographic tandem mass spectrometry) analysis

The peptides were concentrated, if necessary, using a SpeedVac (ThermoSavant). They were then separated on an Acclaim PepMap 100 C18 trap and an Acclaim PepMap RSLC C18 column (ThermoFisher Scientific), using a nanoLC Ultra 2D plus loading pump and nanoLC as-2 autosampler (Eskigent). The peptides were eluted with a gradient of increasing acetonitrile, containing 0.1 % formic acid (5-40% acetonitrile in 5 min, 40-95% in a further 1 min, followed by 95% acetonitrile to clean the column, before re-equilibration to 5% acetonitrile). The eluent was sprayed into a TripleTOF 5600 electrospray tandem mass spectrometer (ABSciex) and analysed in Information Dependent Acquisition (IDA) mode, performing 250 msec of MS followed by 100 msec MS/MS analyses on the 20 most intense peaks seen by MS. The MS/MS data file generated was analysed using the Mascot algorithm (Matrix Science) against the NCBInr database Aug 2013 with no species restriction, trypsin as the cleavage enzyme, carbamidomethyl as a fixed modification of cysteines and methionine oxidation and deamidation of glutamines and asparagines as variable modifications. Peptides for

proteomic analysis were identified above 95% confidence level and with at least two hits were analysed. The proteins identified by LC-MS/MS were uploaded onto PANTHER (protein annotation through evolutionary relationship) classification system (http://www.pantherdb.org/) to enable analysis of functional and pathway classification of the proteins. These categories were then represented in pie charts.

2.14 Protein Transfer

Gels that were not used for mass spectrometry analysis were transferred to a nitrocellulose membrane. A sandwich of Whatmann filter paper and sponges with a 0.2 µm nitrocellulose membrane (BioRad, UK) in the middle, was put in transfer buffer (1.5 M tris glycine buffer, pH 7.4). Transfer was performed for at least 1 h at 90 V in an ice bath. The gel needs to be on the negative polarity and the nitrocellulose paper on the positive polarity to enable transfer of proteins.

2.14.1 Antibody probing

TBS or Tris buffer saline was made using 1mM tris buffer saline with 0.1% tween 20 and used for further western blotting experiments. The protein transferred membrane was washed with distilled water and incubated with blocking buffered solution, made of TBST with 5% milk, for 1 h at room temperature. Blocking reduces non-specific binding of proteins and ligands. After 1 h, the blot was washed with TBST three times, for 10 minutes each at room temperature. After washing, the appropriate primary antibody was incubated, suspended in TBS with 5% milk solution, overnight at 4^{o}C (Table 2.6). The blot was washed with TBS three times for 10 min each at room temperature, the following day. Washing removes the unbound primary antibody and then was incubated with secondary antibody for 1 h at room temperature, before washing again with TBS. The blot was then reacted with ECL plus kit (GE healthcare, UK) as per manufacturer

instructions and imaged using Geldoc™ imager (Bio-rad Laboratories Inc., Watford, UK) ™ imager (Bio-rad Laboratories Inc., Watford, UK) (Biorad, UK), colorimetric with epi-white at 302 nm excitation.

Table 2-6 List of antibodies and dilutions for Western blotting for Ku proteins

Antibody/target	Dilution	Manufacturer	Type
Ku70	1:5000	Abcam, UK	Rabbit polyclonal
Ku80	1:3000	Abcam, UK	Rabbit polyclonal
Secondary Antibody	1:10000	Abcam, UK	Donkey polyclonal secondary antibody to rabbit IgG/ mouse IgG

2.14.2 Dot blot analysis

Protein samples made after lysis and aptamer precipitation were used for dot blot analysis. 5µl samples containing 2mg/ml of protein were pipetted on the nitrocellulose membrane and air dried for 15 minutes. The same samples were repeated with 5µl of twice to increase the protein content for detection. After air drying, the membrane was washed with distilled water and incubated with blocking buffered solution, made of TBST with 5% milk, for 1h at room temperature. After 1 h, the blot was washed with TBS three times, for 10 minutes each at room temperature. After washing, the appropriate primary antibody was incubated, suspended in TBS with 5% milk solution, overnight at 4^{o}C. The blot was washed with TBS three times for 10 min each at room temperature after the incubation period. It was then incubated with secondary antibody for 1 h at room temperature, before washing again with TBS. The blot was then reacted with ECL plus kit (GE healthcare, UK) as per manufacturer instructions, and imaged using Geldoc™

imager (Bio-rad Laboratories Inc., Watford, UK) ™ imager (Bio-rad Laboratories Inc., Watford, UK) (Biorad, UK), colorimetric with epi-white at 302 nm excitation.

2.14.3 Dot blot and probing with aptamer

The above protocol for protein transfer and dot blot was followed until pre-antibody incubation. For aptamer incubation, the aptamer was suspended in TBS with 5% milk and incubated for 90 minutes. The blot was washed with TBS three times for 10 min each at room temperature after the incubation period. AB complex staining was performed as per immunochemistry and incubated for 30 minutes. The membrane was then washed with TBS three times and incubated with DAB solution for 5 minutes. The membrane was then finally washed with TBS and visualised on Geldoc™ imager (Bio-rad Laboratories Inc., Watford, UK) ™ imager (Bio-rad Laboratories Inc., Watford, UK) (Biorad, UK).

2.15 Ku70 and Ku80 knockdown and immunostaining

2.15.1 Ku70 and Ku80 knockdown

Ku70 and Ku80 knockdown was performed by Farjana Begum Rowther at the University of Wolverhampton. Short interfering (si) RNA transfections were facilitated using DharmaFECT-1 transfection reagent in a serum containing media and the transfection efficiency was assessed using positive control Cyclophilin-B siRNA (Thermo Scientific, UK). ON-TARGETplus SMARTpool siRNA targeting human *XRCC5* or *XRCC6* at 25 nm was employed (Dharmacon, GE; UK). In addition, these cultures were transfected in parallel with ON-TARGETplus non-targeting siRNA pool at the same concentration (Dharmacon, GE; UK). In experiments where combined knockdown of *XRCC5* and *XRCC6* was performed, siRNA at 25nM of both were treated for the specified time as individually.

Non-targeting siRNA are abbreviated as siNT. Cells were seeded at 40-50% confluence and incubated for 48 hours before commencing transfection to assess the success of the transfection.

For detection analysis, Q-PCR was carried out using TaqMan Q-PCR assay with FAM reporter [Thermo Scientific, UK] on an ABI 7500 Sequence Detection System [Applied Biosystems]. 2µl of cDNA was amplified in a 20µl reaction volume using 1X TaqMan qPCR master mix with low ROX [Thermo Scientific, UK] and amplifications were performed in triplicate. The *XRCC5/6* detection levels were normalised to *GAPDH*, and the relative detection was determined using the $2^{-\Delta\Delta CT}$ method relative to control treatments (siNT). Cells were investigated for aptamer binding according to section 2.8.2.

Chapter 3

3 Glioma Cell line culture and patient tissue derived short-term culture

3.1 Introduction

Commercially available cell lines, U87MG, 1321N1 and SVGp12 and short term cultures from patient tissue (BTNW 370, BTNW 914, BTNW 911 and IN1077) were used for the research. Characterisation and establishment of growth curves is essential to cell culture experiments as a pre-requisite (Dang C, 2003; Wadsworth, 2007). During cell culture, cross contamination is a major concern for the researcher (Markovic and Markovic, 1998) and establishment of proper protocol for culture and characterisation of the cell lines is important. In terms of commercially available lines, we established that the cell lines are glial in origin (GFAP)(Goyal et al., 2015), Human (HLA)(Bergström et al., 1998) and show tumour activity (VEGF)(McMahon, 2000). Short term cultures, since grown from patient tissue, are characterised by being glial in origin (GFAP)(Goyal et al., 2015), are not meningothelial cells (EMA)(Ng et al., 1987) and not endothelial in origin (CD34)(Lin et al., 1995; Sidney et al., 2014). Growth curves of the cell lines help in establishing the phases of cell growth namely, lag phase, exponential phase and plateau phase (Dang C, 2003). This enables one to identify the appropriate cell density for plating cells for downstream experiments.

The aim of the chapter was to characterise the cell lines and the short term cultures and establish growth curves to provide information on the growth characteristics of the cells. This confirms the appropriate cell density for each cell line and short term culture for further experiments.

3.2 Growth curves of commercial cell lines

Growth curves were performed to establish the various phases of cell growth for individual cell lines (Figure 3.1). The 1321N1 (human brain astrocytoma), U87MG (human brain glioblastoma) and SVGp12 (human foetal astrocyte) were seeded at day 0 at a density of 2 x 10^4 cells in T25 flask. Cancerous cell lines U87MG and 1321N1 showed exponential growth from day 2 to day 7, giving adequate and optimum cell count from day 6 onwards (Figure 3.1A and B). SVGp12 foetal astrocyte derived cell line also showed an exponential growth from day 2 to day 6 (Figure 3.1C). There was a reduction in cell growth in all cell lines between day 7-8 and likely linked to iatrogenic cause. It could be because of a population of cells dying and being replaced by the proliferating subculture. Cell growth reached a plateau after day 6 in all cell lines and declined subsequently due to over confluence of the flask (Figure 3.1).

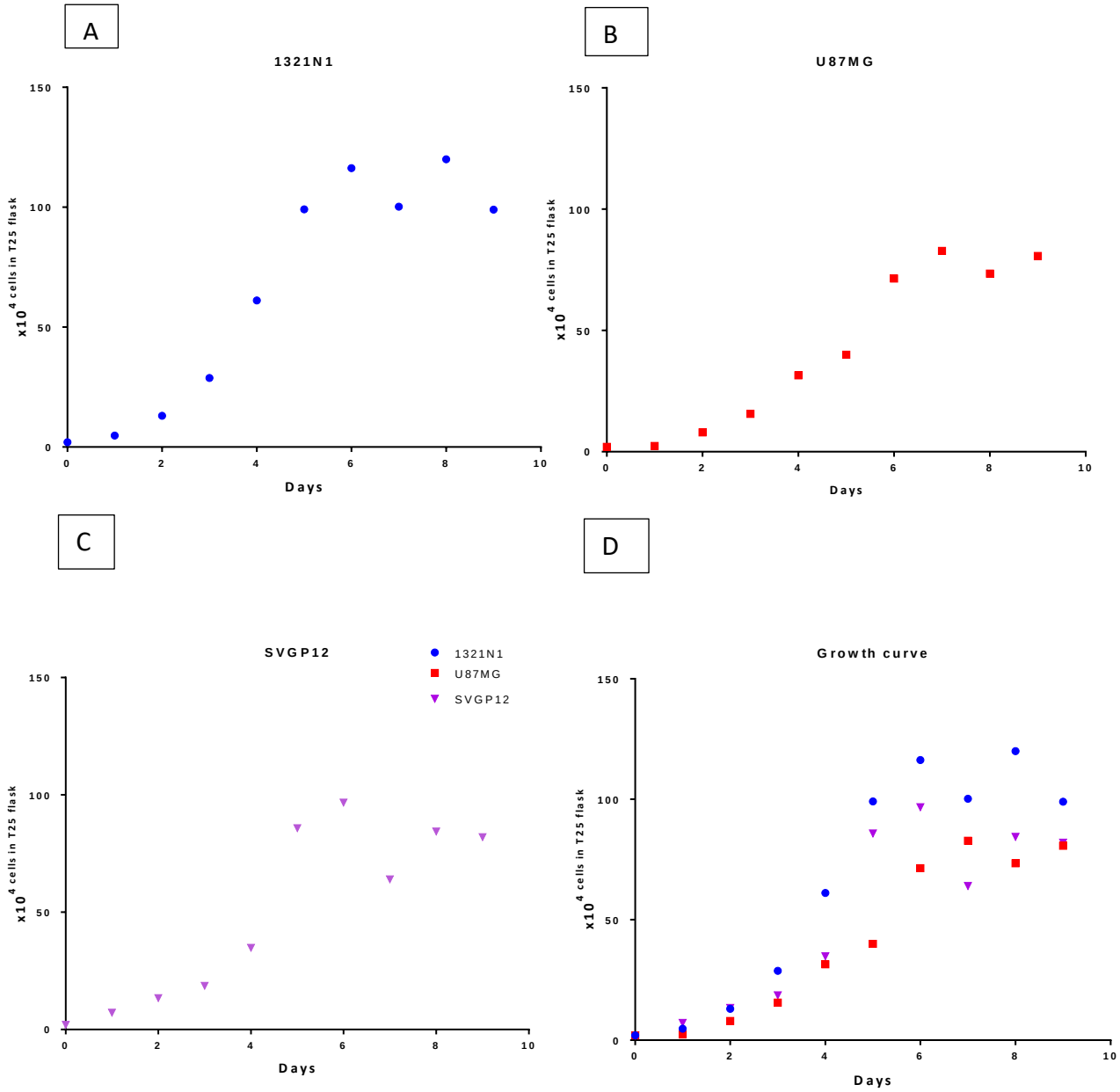

Figure 3.1 Growth characteristics of U87MG, 1321N1 and SVGp12 cell lines.

The cell counts were calculated using the trypan blue exclusion assay and counted on a haemocytometer from day 0 to day 9. The data points are representative of three replicates (n=3) and are presented as mean cell density ± standard error (SE). The growth curve showed a lag phase growth from day 0 to day 3 and in exponential phase from day 4 to day 7 in U87MG (A), 1321N1 (B) and SVGp12 (C). A reduction in cell density occurred on day 7 in U87MG cells (A) and SVGp12 cells (C) and day 8 in 1321N1 cells. D shows all cell lines plotted on the same axes (red squares=U87MG, purple triangles=SVGp12, blue squares=1321N1). U87MG cells showed the fastest proliferation rate compared to 1321N1 and SVGp12 cells.

3.3 Growth curve of short-term cultures

Short term cultures are derived from tissue donated by the patients. The cells were grown in tissue culture flasks after disaggregation of tissue (using collagenase) and provided with appropriate physiological conditions to sustain growth. Since tissue is heterogeneous, it will need to undergo separation . Cell density of cultures was low (Furneaux et al., 2008). Further passaging and subculture was needed to grow short term cultures. Forty-two tissue samples were obtained from patients at the Royal Preston hospital and put into culture. Very few of the cell cultures were generated and utilised for experiments. An example of short term culture growth curve is shown below (Figure 3.2).

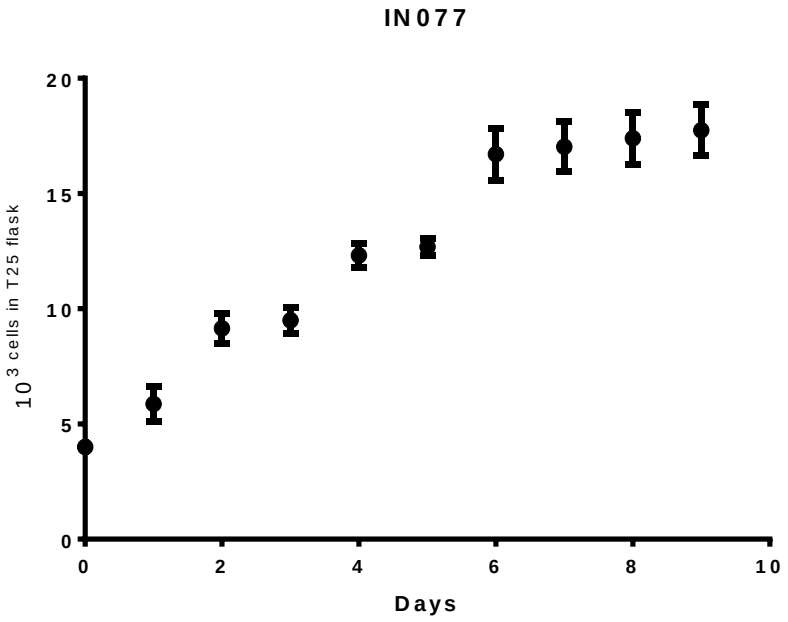

Figure 3.2 Growth curve of IN077, a short-term culture from a grade IV glioma.

Cell counts were obtained using a coulter counter from day 0 to day 9. The data points are mean cell counts (±SEM) from n=3 replicates. The growth curve shows growth from day 0 to day 4 and in a plateau phase from day 6 onwards. This is different from commercial cell lines where a clear exponential phase is evident.

IN077 cells were previously stored from a tissue sample and a growth analysis was done to guide protein extraction and experimental timing from short term cultures. Further attempts from other short term cultures totalling five in number (BTNW 911, BTNW 913, BTNW 914, BTNW 915, BTNW 370) and normal human astrocytes (NHA) was made but growth was slow.

3.4 Characterisation of commercial cell lines

Cell lines were characterised by evaluating GFAP, HLA and VEGF detection by immunofluorescence. This is done to ensure that in the process of repeated passages, no cross contamination has occurred. In terms of commercially available lines, we established that the cell lines are glial in origin (GFAP), Human (HLA) and show tumour activity (VEGF) (Figure 3.3). An isotype antibody was used as a negative control for the experiments.

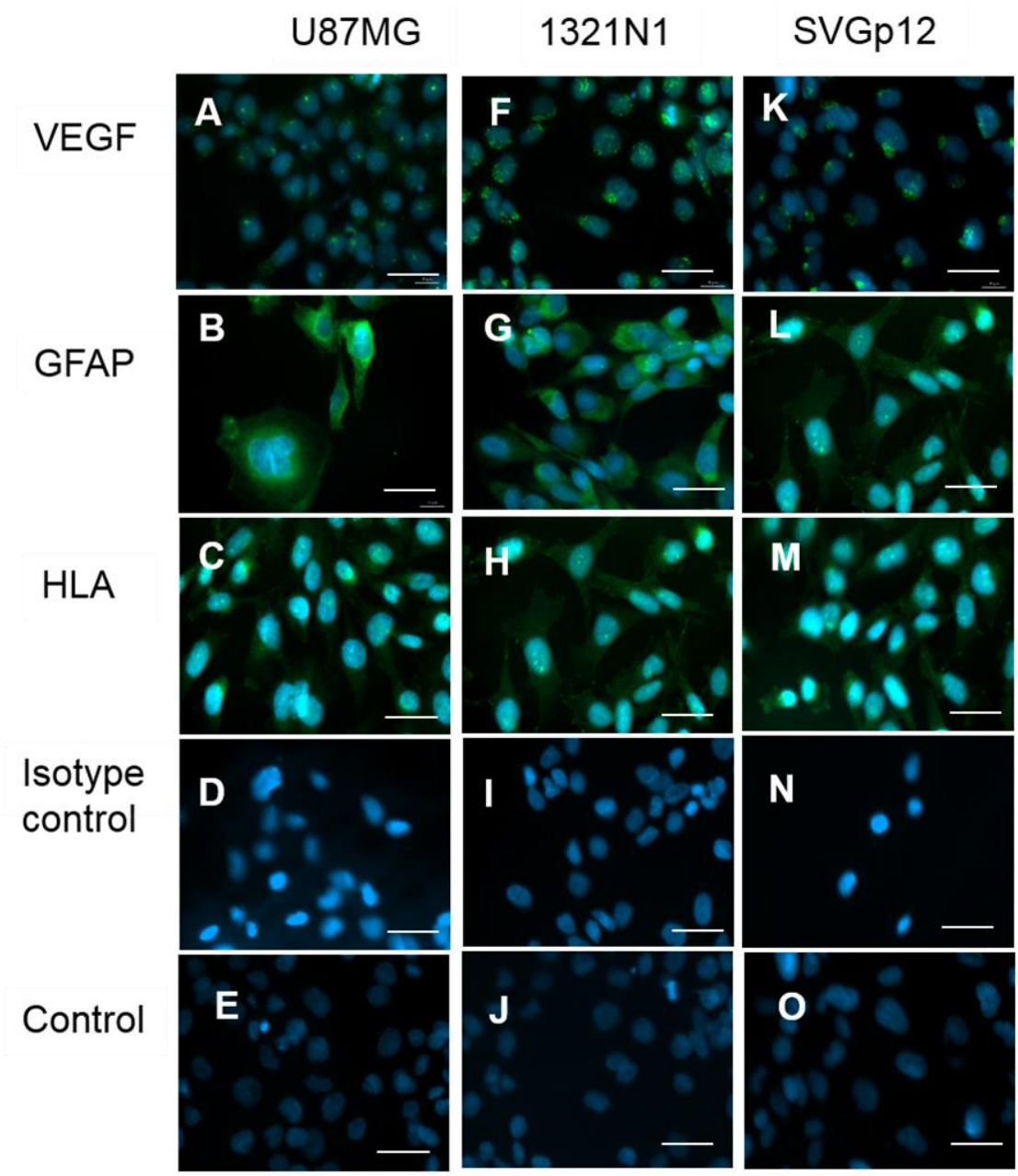

Figure 3.3 Detection of HLA-I, GFAP and VEGF antigens (green) in cultured 1321N1, U87MG and SVGP12 cells.

A, B, and C represent detection of HLA-I, GFAP and VEGF counterstained with DAPI (nuclear stain) respectively, in U87MG cells. D and E represent isotype control and control, counterstained with DAPI (nuclear stain) respectively, in U87MG cells. F, G and H represent detection of HLA-I, GFAP and VEGF counterstained with DAPI respectively, in 1321N1 cells. I and J represent isotype control and control, counterstained with DAPI respectively, in 1321N1 cells. K, L and M represent detection of HLA-I, GFAP and VEGF counterstained with DAPI respectively, in SVGp12 cells. N and O show isotype control and control, counterstained with DAPI respectively, in SVGp12 cells. Scale bar = 20 µm.

3.5 Characterisation of short-term cultures

Short term cultures established from patient glial tissue were characterised to confirm the cell type. Patient derived short term cultures were categorised as early passage up to P3, mid-passage up to P7 and late passage up to P12. GFAP was used to confirm for glial cells, epithelial membrane antigen (EMA) as a marker for meningothelial cells and CD34 for endothelial cells. Due to the high possibility and ease of growing endothelial cells, CD34 was used to exclude cultures that exhibited a high proportion of endothelial cells.

The BTNW914 culture at early passage 3 showed a heterogeneous cell population and expressed both GFAP and CD34 (Figure 3.4, A-E). At mid passage 7, the cells showed strong staining for GFAP, indicating a continued detection for GFAP and faint brown stain for CD34 (Figure 3.4, F-J). At passage 12, the cells showed faint staining for GFAP and no staining for CD34 (Figure 3.4, K-O). EMA did not show any significant staining at any stage, thus excluding presence of meningothelial cells. The cells did not show any staining in the isotype or negative control at any of the passages.

The BTNW370 at passage 3 showed detection of GFAP, and for CD44, but no staining for EMA. (Figure 3.5, A-E). At passage 7 the cells staining for GFAP and no staining for CD44 or EMA (Figure 3.5, F-J). At passage 12, GFAP was still positive with absence of CD34 and EMA (Figure 3.5, K-O).

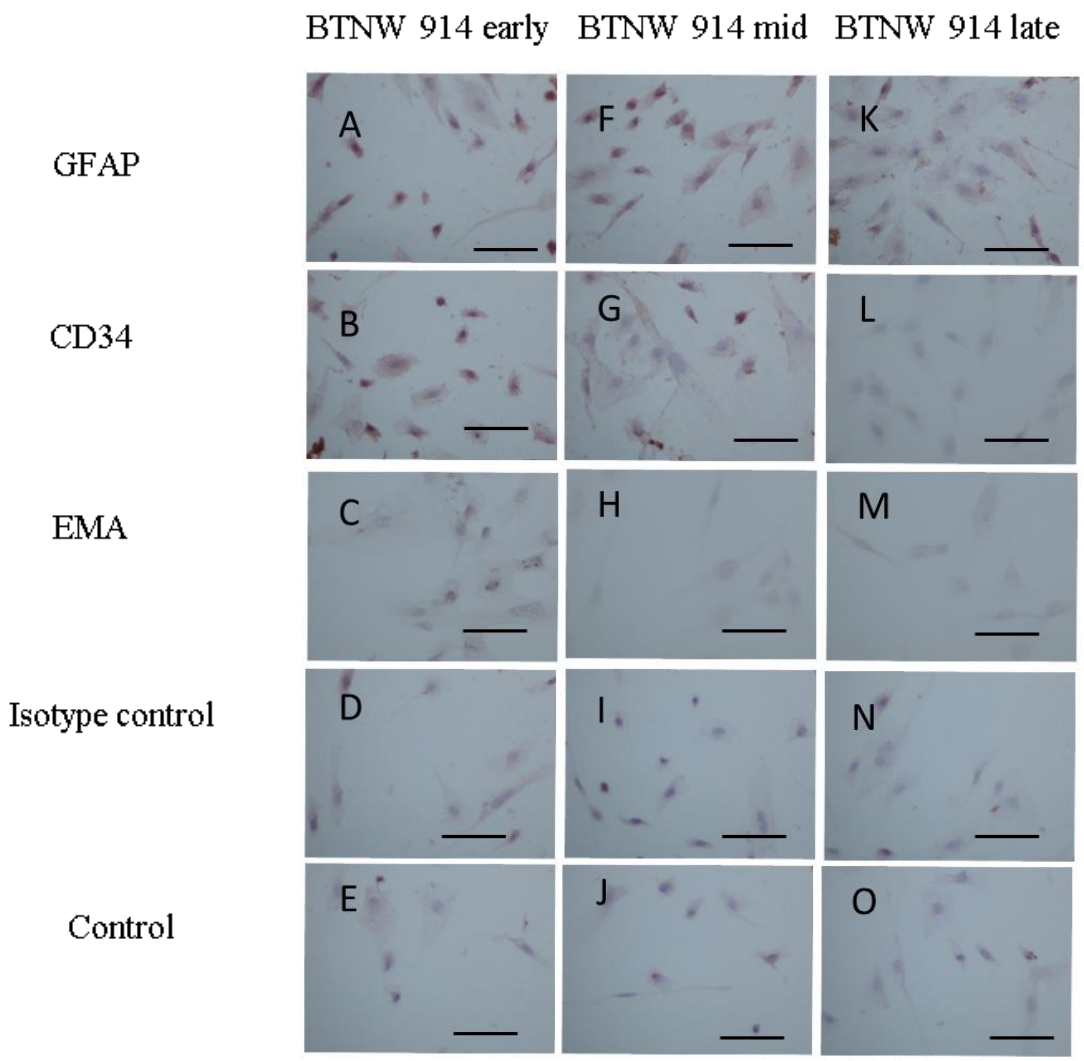

Figure 3.4 Detection of GFAP, CD34 and EMA in patient derived short term cultures at various stages of passage in BTNW 914

Cells stained with GFAP, EMA and CD44 at early passage (P3) (A-E), mid passage (P7) (F to J) and late passage (P12) (K to O). Cells were counterstained with haematoxylin. The isotype control was a rabbit IgG primary antibody (D, I, and N) and control was no primary antibody (E, J and O). All cells were counterstained with haematoxylin. The detection of GFAP (A, F & K) decreased with increase in passage number (A). The cells showed reduced detection of CD44 (B, G) and EMA (C) in later passages representing the mixed nature of cultures in early passage for CD34 (L) and EMA (H & M). Scale bar =50 µm.

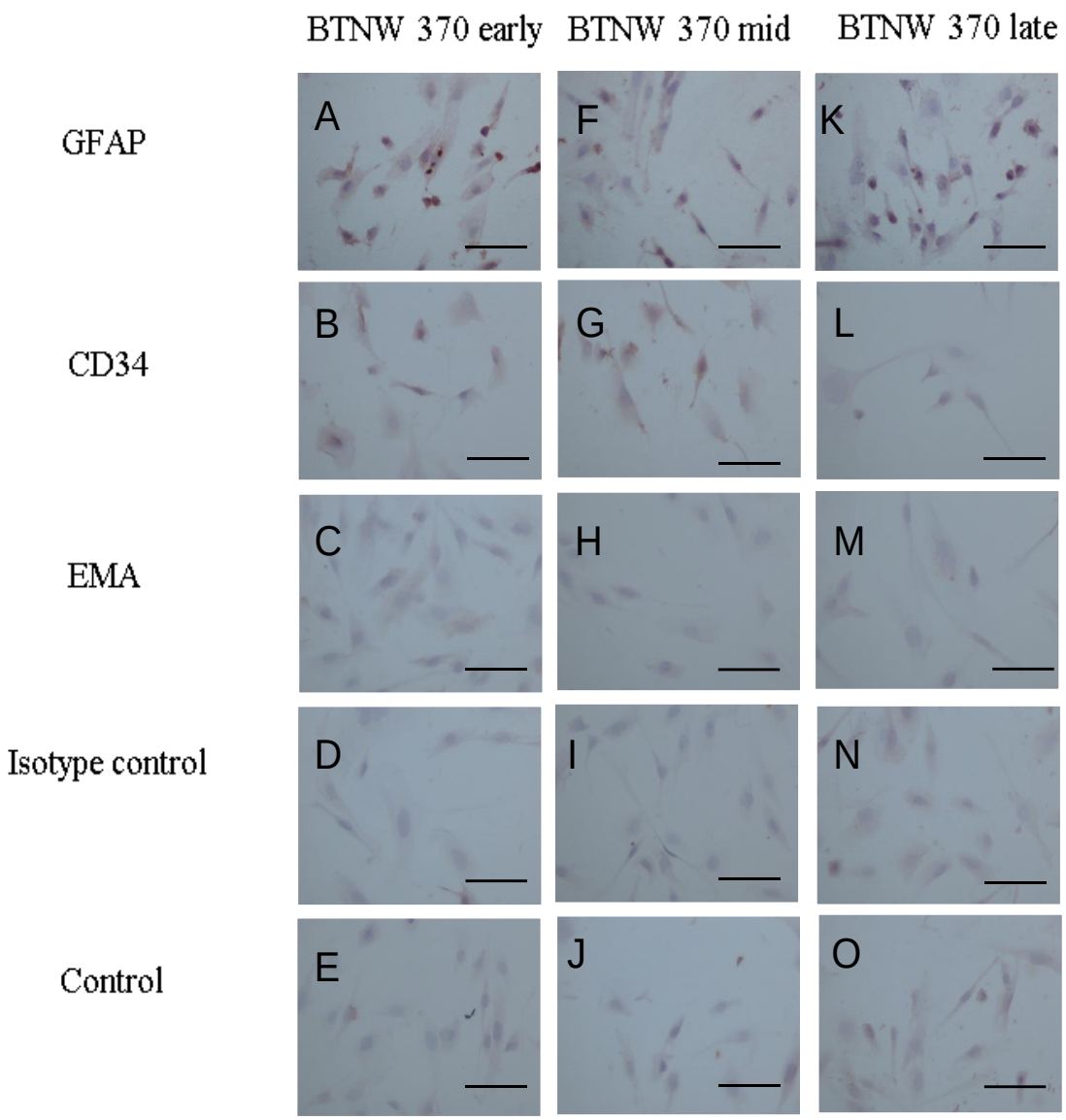

Figure 3.5 Detection of GFAP, CD34 and EMA in patient derived short term cultures at various stages of passage in BTNW 370

C*ells stained with GFAP, EMA and CD44 at early passage (P 3) (A-E), mid passage (P7) (F to J) and late passage number (P12) (K to O). The cells were counterstained with haematoxylin. The isotype control was a rabbit IgG primary antibody (D, I, and N) and control was no primary antibody (E, J and O). All cells were counterstained with haematoxylin. The detection of GFAP (A, F & K) decreased with increase in passage number (A). The cells showed reduced detection of CD44 (B, G) representing the mixed nature of cultures in early passage for CD34 (L). There was no detection of EMA seen in any passage (C, H and M). Scale bar=50 µm.*

3.6 Discussion

Growth characteristics show that U87MG and 1321N1 cell lines exhibit exponential phase from day 2 to 7 (Eyvazzadeh et al., 2015) and SVGP12 showed exponential phase from day 2 to 6. As expected, the U87MG and 1321N1 cell lines exhibited an epithelial morphology (Machado et al., 2005) while the non-cancerous SVGp12 cell line showed fibroblastic morphology (Baba et al., 2007). Further characterisation determined the commercial cell lines were human in origin, of glial origin and U87MG and 1321N1 were cancerous.

Growth curves in short term cultures are difficult to be standardised due to the indeterminate nature of cell growth and apoptosis (Mitra et al., 2013). Short term cultures are also difficult to grow and maintain due to variable nature of cell type (Freshney, 2006; Kaur and Dufour, 2012). The growth curve in short term cultures is not consistent between passages and hence an example growth curve of IN077 was performed during the initial stages of the project. Short term cultures, characterised with GFAP, CD34 and EMA showed that the cells grown from patient tissue were of glial tumour origin. This was confirmed by DAB staining, evident with brown staining pertaining to antigen-antibody reaction. The lack of positive staining in the isotype control showed that the antigen-antibody staining was specific.

Characterisation is essential prior to commencing work on cell biomarker discovery due to various reasons. It is important to ensure the various phases of cell growth namely, growth phase and lag phase (Dang C, 2003). Cells in lag or plateau phase may lack the functional isotope of interest and can generate negative or false positive results. Gos *et al* (2005) showed upregulation of *Wnt6, uPar, Tdag51, Egr1, Ini1a* and *Mor1* in confluent C3H10T1/2 cells and Cancela *et al* (1997) showed that matrix proteins were significantly

altered during different growth phases of normal rat kidney cells. Growth curves established the optimal incubation time for the aptamers to be added to the cell cultures. Commercial cells were harvested in their exponential growth phase from day 3 to 6 for all further experiments in the thesis.

Short term cultures are used after establishing experimental protocol with cell lines to validate the results. Cell lines over the years of use can be contaminated or lose certain genetic characteristics (Nardone, 2007; Capes-Davis et al., 2010; Allen et al., 2016). To counter false results and failure of further research, it becomes important to validate results with patient derived cultures.

Cell lines have the advantage of being readily available, cost effective and easy to maintain with mostly known growth pattern (Kaur and Dufour, 2012). There also exists plenty of information to corroborate the data and thus help in setting up research in less time (Gazdar et al., 2010). They also give consistent results. However, the cell lines do not reflect actual tumour physiology (Kaur and Dufour, 2012) and treatment response is not representative of in vitro conditions. Cell lines also tend to form a distinct group, which is different than their respective tissue (Lukk et al., 2010) Short term cultures represent, in early stages, a heterogeneous population of cells, close to the original parent tumour tissue (Gazdar et al., 2010). After initial passages, they too develop into subcultures of cell population but still carry a better representation of tumour cells. There is also the elimination of using a contaminated cell line (Capes-Davis et al., 2010) but user handling is also a factor. In vitro cancer models are needed to support the research (Gillet et al., 2011) and hence best supported by short term cultures.

Chapter 4

4 Confirmation of aptamer binding to glioma cells

4.1 Introduction

Aptamer binding to cells needs to be established as a proof of concept, prior to identification of the target in glioma cells. The SA43 and SA44 aptamers used here were adapted from GL43 and GL44 aptamer sequences detailed in the paper by Cerchia *et al* (Cerchia et al., 2009). GL43 and GL44 were generated by SELEX against U87MG cells and shown to be specific to glioma tissue (Cerchia et al., 2009). GL44 and GL43 were specifically chosen due to their low Kd (dissociation constant) which implies greater binding affinity to the target and hence greater specificity (Bisswanger, 2008).

It is the 3D structure of aptamers which bind to the target ligand with varying affinity (Pan and Clawson, 2009) and can be affected by van der Waals forces, hydrogen bonding and ionic interaction (Hermann and Patel, 2000; Long et al., 2008; Ruigrok et al., 2012). All aptamer interactions do not use those interactions but the affinity is affected by the size of the aptamer, temperature and physiological state of interaction. The larger the size of the aptamer, the greater is the number of 3D structures it can form and hence be more non-specific (Pan and Clawson, 2009). To increase specificity, a shorter aptamer sequence is desired.

Since the specific part of the aptamer sequence is the aptamer with the loop end rather than the attached primers, the GL43 and -44 aptamer sequences were truncated without the primers to generate two shortened aptamers to be 43 and 44 nucleotides long instead of another 40+ nucleotides attached as primers. SA43 and SA44 contain the DNA homolog of the unique GL43 and GL44 nucleotide sequences, but do not contain the primer sequences at the 3' and 5' ends, therefore "SA" denotes "shortened

aptamer". Cerchia *et al* also used truncated aptamers from GL44 and GL43 but shorter than 40 bases (Cerchia et al., 2009). SA56, another shortened aptamer from Cerchia *et al* was used which is an RNA aptamer. DNA and RNA aptamers are similar in function but vary in their stability (Zhu et al., 2015). RNA have a reactive hydroxyl group (-OH) which is susceptible to hydrolysis and degeneration of RNA. DNA on the other hand is relatively stable due to C-H bonding (Zhu et al., 2015). RNA is much smaller than DNA by about 10^3 to 10^6 times and more likely to cross the blood brain barrier (Germer et al., 2013), and is therefore perhaps more favourable to use as targeted therapy to the brain (Que-Gewirth and Sullenger, 2007). SA56 aptamer is a 43-nucleotide base aptamer and was used as a comparison for assessing RNA aptamer binding, similar to SA43 DNA aptamer.

SELEX was used to identify the aptamers. Positive selection was towards U87MG and counter-selection (or negative selection step) against T98G cell line by Cerchia *et al*. T98G cell line (Stein, 1979) originated from T98G glioblastoma cell line and is a polypoid variant (Coward and Harding, 2014). T98G cells are not capable of forming tumours in nude mice, and were therefore considered less tumourigenic and a suitable counter selection cell line by Cerchia *et al*. (2009).

The first aim of this chapter was to demonstrate aptamer binding affinity *in vitro* to glioma cell lines as determined by fluorescent confocal imaging using Cy3 as a fluorophore conjugated to the aptamers. Aptamer binding also needed to be assessed using biotin tagged aptamer (Starikov and Nilsson, 2002), as biotin would be the tag used for aptamer precipitation in downstream experiments (Viens et al., 2004; Lee et al., 2006). Since the second aim is to show translational clinical relevance, the affinity of SA43 and SA44 was also assessed in short term patient derived cultures (Farr-Jones et al., 1999; Furneaux et al., 2008).

To confirm selective binding of the shortened aptamers, control aptamers were also synthesised and consisted of random nucleotide sequences of equivalent composition of bases. The reason was to ensure that the aptamer binding was specific and no known negative control existed. Random control sequences should either bind to other targets or not bind at all. Spiegelmers {Eulberg, 2003 #2705} are biostable aptamers and essentially mirror image aptamers which take a hair pin bend. They are likely to reduce non-specific binding. The control aptamers used in the project were not spiegelmers, hence they should display differential binding and labelled SAneg1 and SAneg2 and their structures are discussed in chapter 5.3.

4.2 Confocal imaging of aptamer uptake

Live U87MG, 1321N1 and SVGp12 cell lines were incubated with SA44, SA43, SA56 RNA, SAneg1 and SAneg2. Cells were grown on coverslips and incubated with Cy3 tagged aptamer at physiological conditions in the dark. After a 90 minute incubation, the cells were washed and fixed with 4% PFA. They were then dehydrated and mounted on glass slides using DAPI and imaged using confocal microscopy. Aptamer binding was greater in U87MG and 1321N1 cell lines compared to the SVGp12 cell line (Figure 4.1, 4.2 and 4.3). The experiments represent n=3 with consistent results.

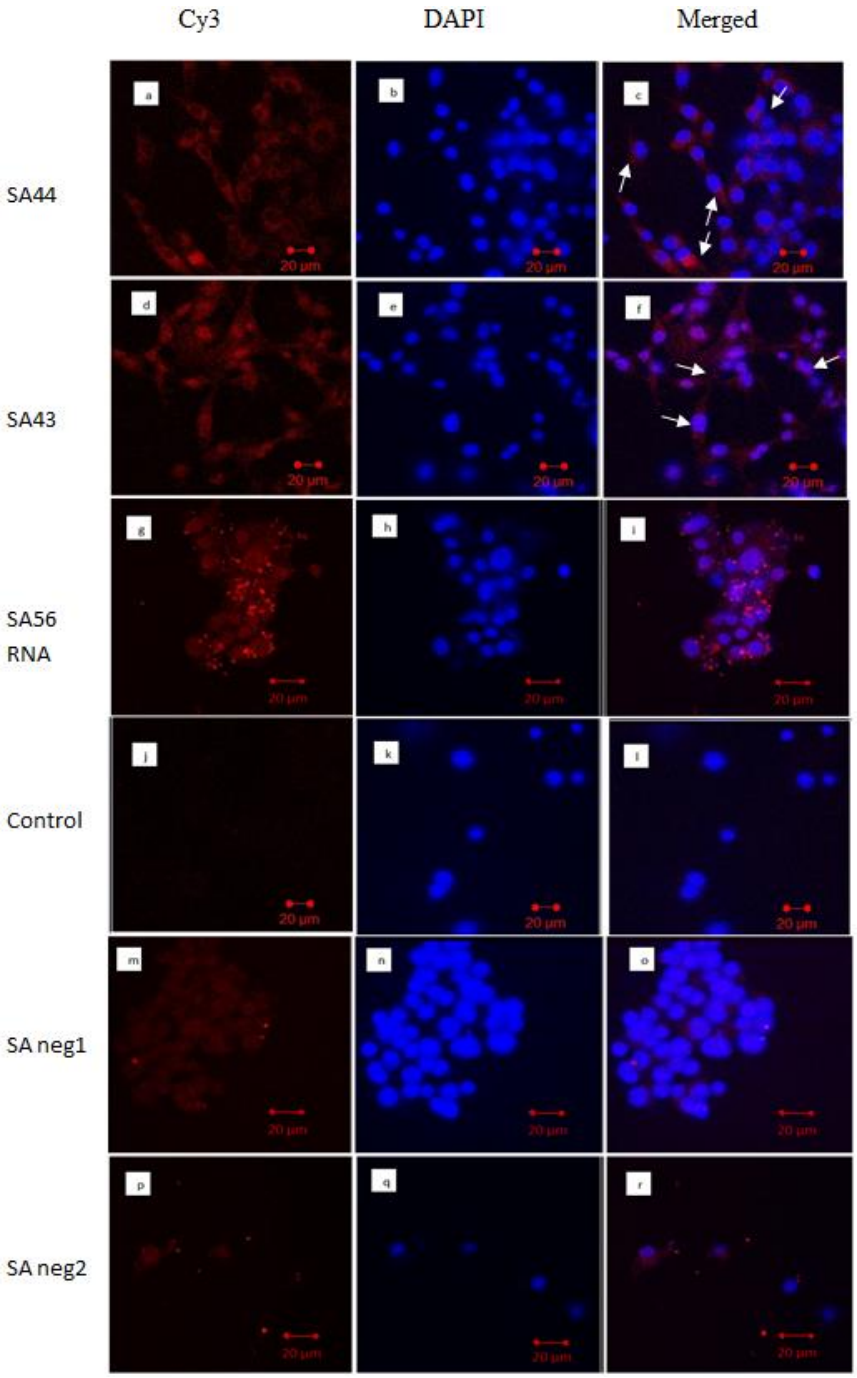

Figure 4.1 Confocal imaging of live U87MG cells with 100nM Cy3 tagged SA43, SA44 and SA56 RNA aptamers.

Aptamer binding was observed in the cytoplasm of U87MG cells after live incubation with each aptamer (A, D and G). Minimal aptamer uptake was observed with SANeg1 and SANeg2 (M and P) and no fluorescence was detected with no aptamer control (J). Cells were counterstained with the nuclear dye DAPI (B, E, H, K, N and Q). C, F, I, L, O and R show merged images of Cy3 and DAPI staining. Cells were viewed with a confocal microscope at 40x with an oil assisted lens. Scale bar = 20µm

Figure 4.1 shows images obtained using confocal microscopy with fluorescent tagged aptamers. Image (a) and (d) show extensive uptake of the Cy3 labelled aptamer SA44 and SA43 by the U87MG cell line respectively. The binding appears to be different compared to 1321N1 cell line (Figure 4.2) and a clear haloing of the nucleus can be seen (images (c) and (f) marked with arrow). The aptamer binding appears to be greater in the cytoplasm and likely on the surface membrane compared to the nucleus. Few cells show greater binding compared to others in the same image and could likely be a result of cells being in various stage of the growth cycle. Image (g) shows greater binding of SA 56 RNA aptamer to the U87MG cell line compared to 1321N1 (Figure 4.2). Image (j) shows the control without any fluorescence. Images (m) and (p) show a very faint signal with SANeg1 and SANeg2 aptamer when compared to 1321N1 (Figure 4.2) cell line. SANeg1 and SANeg2 were random sequence aptamers generated as a control for the project. There was differential biding in the SANeg1 and SANeg2 aptamers when compared to SA43 and SA44 aptamers and were thus carried forward for further experiments.

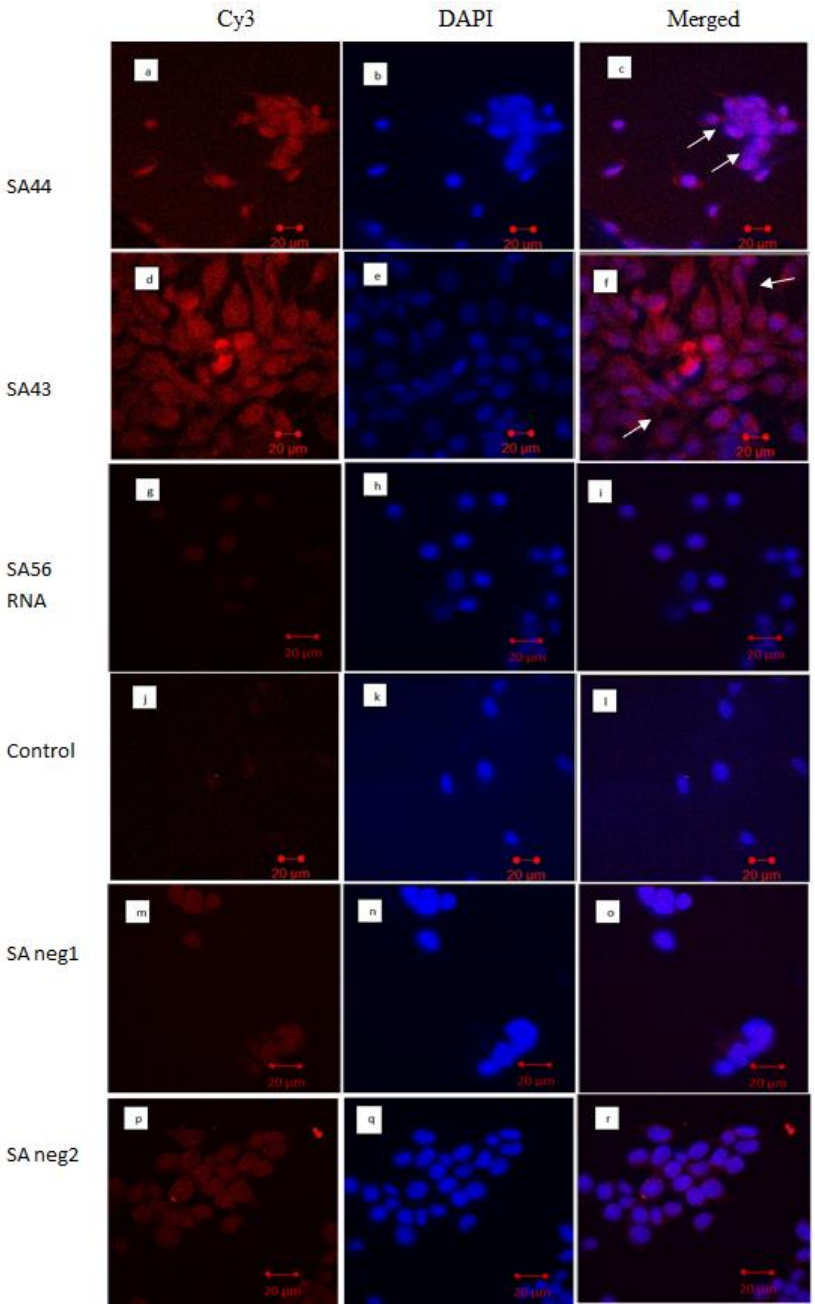

Figure 4.2 Confocal imaging of live 1321N1 cells incubated with 100nM Cy3 tagged SA43, SA44, SA56 RNA aptamers.

SA44 and SA43 was uptaken by 1321N1 cells and localised to the cytoplasm (arrows in A and D). Uptake SA56 RNA showed minimal uptake by the cells (G). The no aptamer control aptamer also showed minimum fluorescence (I) and both SA neg 1 and SA neg 2 showed reduced binding to 1321N1 cells (M and P). Cells were counterstained with the nuclear dye DAPI (B, E, H, K, N, Q). Images C, F, I, L, O and R showed merged Cy3 and DAPI images. Cells were viewed with a confocal microscope at 40x with an oil assisted lens. Scale bar = 20µm

Figure 4.2 shows images obtained using confocal microscopy Cy3 conjugated aptamers. Image a and d shows extensive uptake of the Cy3 labelled aptamer SA44 and SA43 DNA aptamer by the 1321N1 cell line, respectively. This is similar to U87MG cell line (Figure 4.1). The binding appears to be in the nucleus as well as the cytoplasm and appears more intense (red arrows). The binding is different to U87MG cell line where a haloing of the Cy3 signal could be seen in the merged images (Figure 4.1, images c and f). The binding is likely on the surface membrane as well. Few cells show greater binding compared to others, again signifying a variation in uptake possibly due to the growth phase of the cell. Image g shows SA56 RNA aptamer binding which is very minimal. The no aptamer control (j) showed minimal binding. Reduced binding was detected with SANeg1 and SANeg2 aptamer compared to SA43 and SA44. SANeg1 and SANeg2 were random sequence aptamers generated as a control for the project. There was differential biding in the SANeg1 and SANeg2 aptamers when compared to SA43 and SA44 aptamers and were thus carried forward for further experiments.

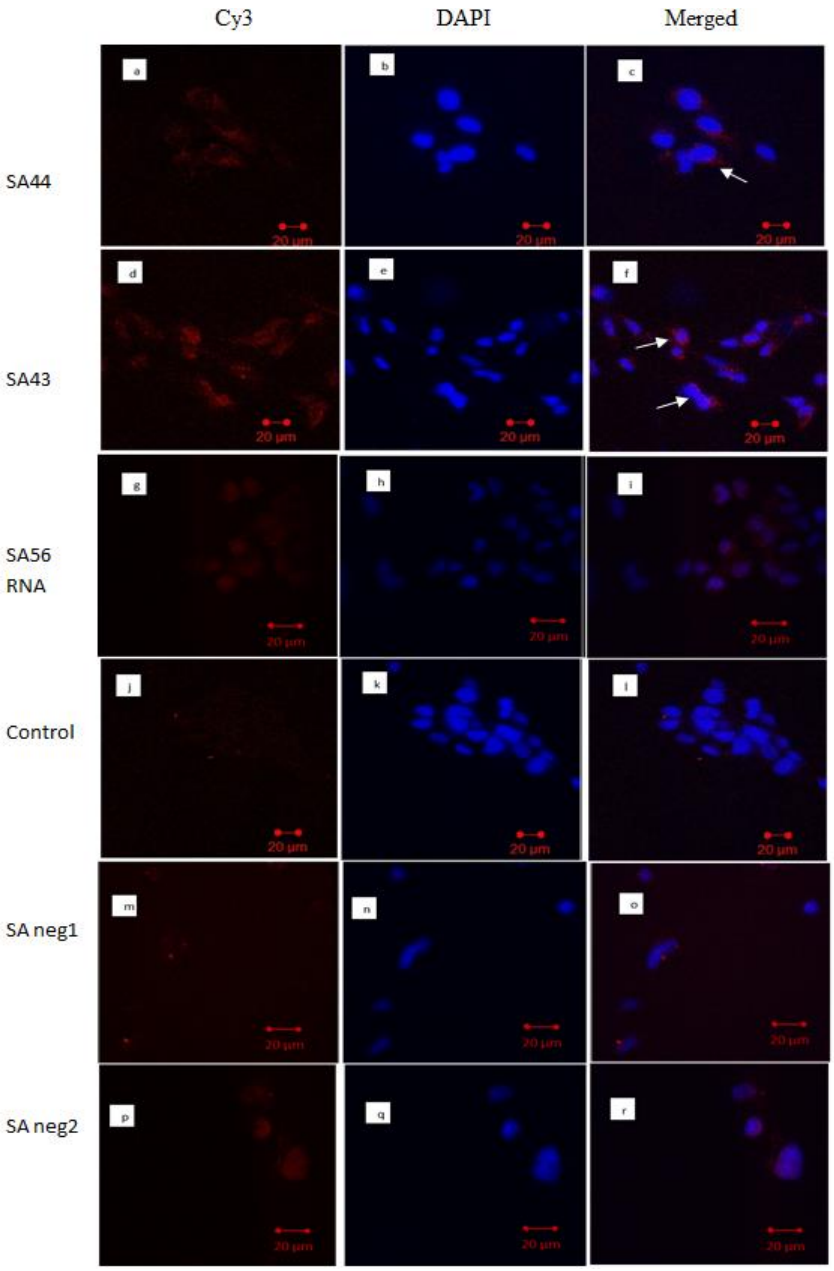

Figure 4.3 Confocal imaging of live SVGp12 cells incubated with 100nM of Cy3 conjugated aptamers.

Minimal uptake of SA44, SA43 and SA56 RNA was detected in SVGp12 cells (A, D and G). More uptake was observed with SA43 (D) than SA44 (A) and SA56 RNA (G). The no aptamer control showed no fluorescent staining (J) and SANeg1 and SA neg 2 showed minimum uptake by the cells (M and P). Cells were counterstained by the nuclear dye DAPI (B, E, H, K, N and Q). C, F, I, L, O, and F showed merged Cy3 and DAPI images. SA44 and SA43 appear to be localised in the cytoplasm and showed more intense binding when cells appeared be dividing (arrows C and F). Cells were viewed on a confocal microscope at 40x with an oil assisted lens. Scale bar =20µm

Figure 4.3 shows images obtained using confocal microscopy with fluorescent tagged aptamers. Image a and d show some uptake of the Cy3 labelled aptamer SA44 and SA43 by SVGp12. The uptake of SA43 aptamer in image (d) is greater than that of SA44 in image a. The binding to SVGp12 cells is markedly reduced compared to U87MG (Figure 4.1) and 1321N1 (Figure 4.2) cell lines. The aptamer binding appears to be present in the cytoplasm and minimally in the nucleus. This points to the fact that the nature of SVGp12 cells is different when compared to U87MG and 1321N1 cell lines with respect to the binding affinity of the aptamer sequences used in the experiments. The binding is seen greater in cells which are present in pairs of two and could be in division or in mitosis (Wadsworth, 2007) (red arrows in figure 4.3, (c) and (f)). The increased binding seen in dividing cells signifies binding of aptamer to over expressed targets during mitosis and cell division. This signifies likely greater targeting of dividing cells by the aptamer. No fluorescence can be seen in the control image (j) with no aptamer. Cy3 fluorescence can be seen in SAneg2 but not seen in SAneg1 except background non-specific staining. This, thus signifies aptamer binding to cells with SAneg2 but not with SAneg1.

4.3 Biotin-tagged aptamer staining

4.3.1 Biotin aptamer with commercial cell lines

U87MG, 1321N1 and SVGp12 cell lines showed consistent patterns of binding with Cy3 tagged aptamer, mainly SA44 and SA43. SA56, the RNA aptamer did show some binding to U87MG (figure 4.1, g) but not in other cell lines and not as significant binding compared to SA44 and SA43 (figure 4.1, 4.2, and 4.3). SA56 was not used further due to inconsistent results on further replicates and not selective to glioma cell lines. Cell lines U87MG and 1321N1 showed greater binding compared to SVGp12 to all the aptamers. SVGp12 cells were therefore used as the control cell line. SAneg1 and SAneg2 showed

some binding. SAneg1 appeared to bind to 1321N1 cell line but not to the other two cell lines and SAneg2 bound to U87MG more than SVGp12. SAneg1 and SAneg2 aptamers were utilised for further experiments since they were random novel aptamers. To enable aptamer target identification, the aptamers were tagged with biotin instead of Cy3 as biotin would be used in downstream precipitation experiments. The hypothesis was that replacement of Cy3 with biotin is not going to alter the binding structure of the aptamer (Ruigrok et al., 2012). This was initially attempted with live incubation with the biotin tagged aptamer (Chapter 2.8.1). Live incubation with biotinylated aptamer was not carried further as fixation of cells after incubation would cross link biotin as well, thus making detection of biotin difficult. Immunostaining techniques harbour the use of streptavidin-biotin affinity and endogenous biotin is blocked prior to DAB staining as standard to stop false positive result. The blocking of biotin would render the pre-reacted biotin-aptamer unavailable for binding. Therefore, the cells were incubated with biotinylated aptamer after fixation and permeabilisation (Chapter 2.8.4, Figure 4.4). The results below represent n=3, and showed consistency of results.

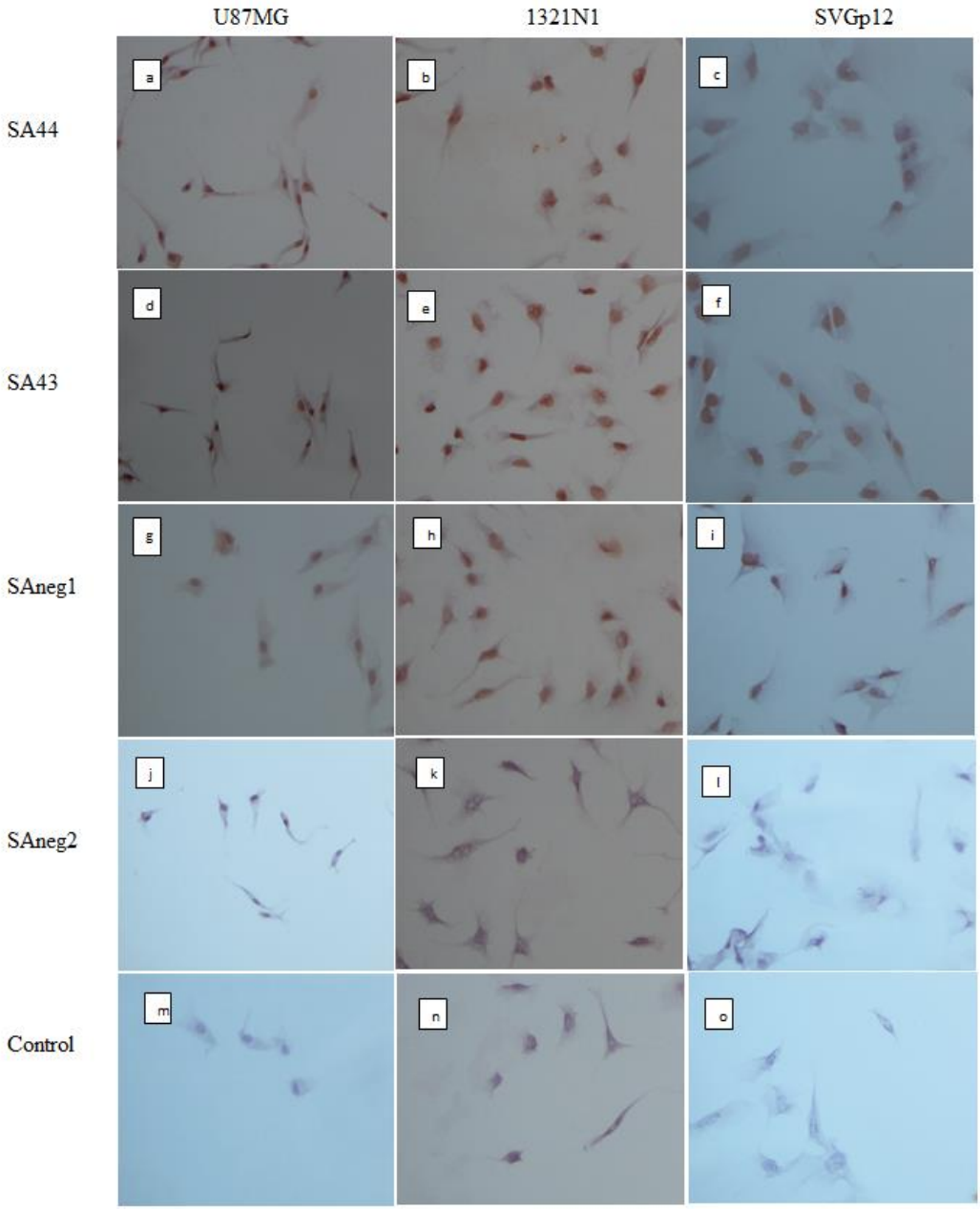

Figure 4.4 Staining of fixed cell lines U87MG, 1321N1 and SVGp12 with 100nM SA44, SA43, SAneg1 and SAneg2 aptamer.

SA44 showed binding to U87MG (A) and 1321N1 (B) cells but reduced binding to SVGp12 (C) cells. SA43 also showed binding to U87MG (D) and 1321N1 (E) cells and moderate levels of binding to SVGp12 (F) cells predominantly in the nucleus. SAneg1 showed some binding to all cell lines ((G, H and I) whereas SAneg2 showed minimal binding (J-L). As expected the no aptamer control showed no binding (M-O). Scale bar represents 50 µm.

Figure 4.4 showed SA43 and SA44 staining to glioma cells lines U87MG and 1321N1 and the control SVGp12 cell line. SA44 and SA43 bound to U87MG and 1321N1 cell lines as determined by the dark brown staining in the cytoplasm and around the nucleus (images a, b, d, e). SVGp12 also showed binding with SA44 and SA43 but mainly nuclear stain and not as strong as the glioma cell lines. There was minimal cytoplasmic staining in the SVGp12 cell lines (images c and f). Similarly, SAneg1 showed binding to U87MG and 1321N1 in the nuclear and cytoplasmic regions but reduced binding around the nuclear region of SVGp12. This suggests that SAneg1 appears to be reacting, similar to SA44 and SA43 aptamers and conforms to being a positive control to the aptamer staining itself. SAneg2 aptamer showed reduced staining across all three commercial cell lines (images j, k and l). In light of SA44, SA43 and SAneg1 aptamers, SAneg2 will be used as the negative control aptamer in downstream experiments. As expected, the control images (with no aptamer) do not show any staining (images m, n and o). SAneg2 images and control images show that the aptamer binding is selective to glioma cells.

4.3.2 Biotin aptamer with short term culture

In order to determine the translational potential of aptamers in the clinic, it was necessary to investigate aptamer binding to patient derived short term cultures. IN1528 and IN1612 were derived from grade IV glioma short term cultures created at the institute of neurology (Maleniak et al., 2001). The two short term cultures were characterised before use and confirmed as glial and human in origin. BTNW 914, BTNW 911 and BTNW 370 were short term cultures from patient tissue generated from patient tissue at the Royal Preston Hospital, Preston, England. These three cell lines have been characterised in Chapter 3 and utilised for biotinylated aptamer experiments.

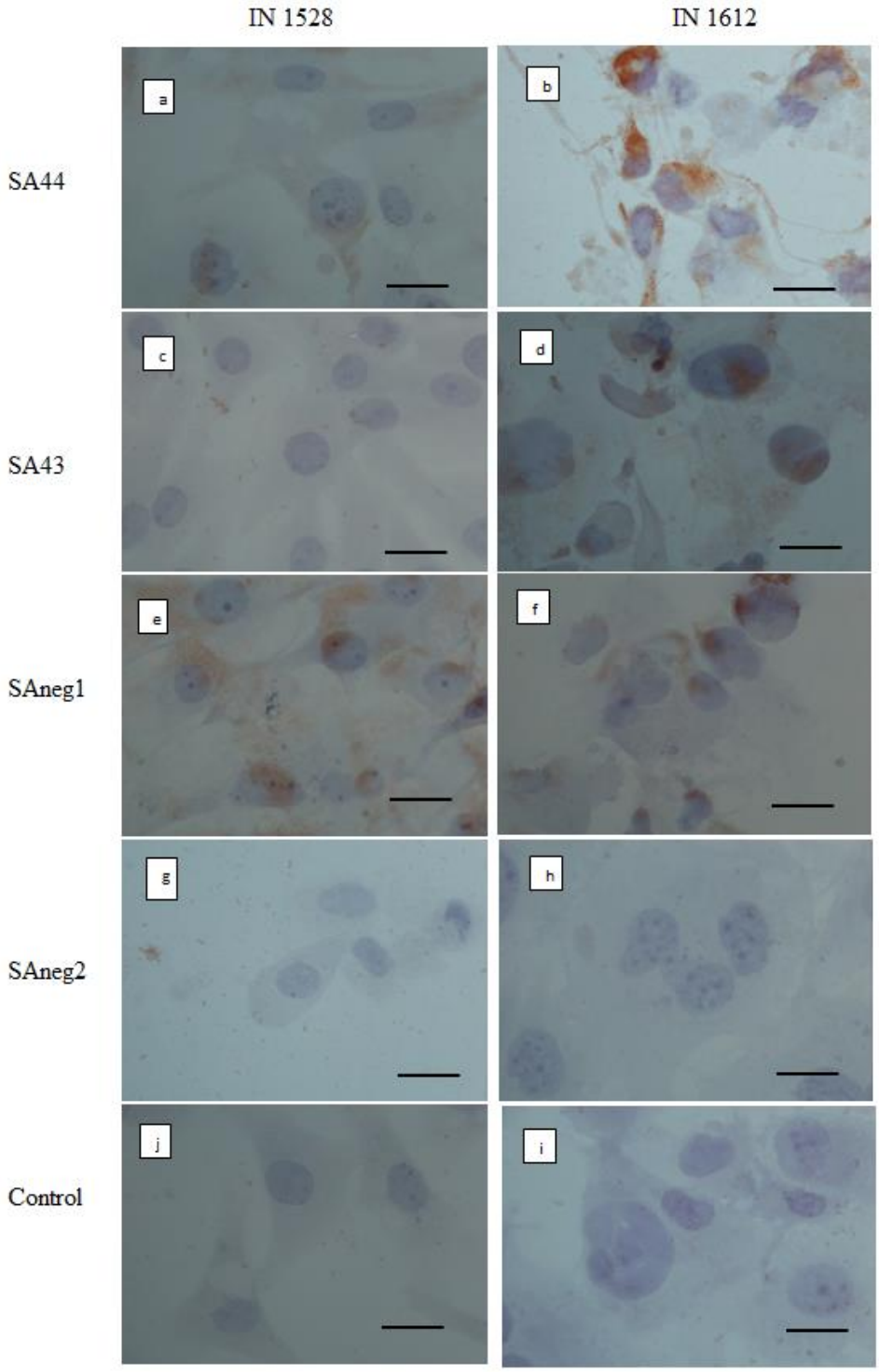

Figure 4.5 DAB staining of short term cultures IN 1528 and IN 1612

IN 1528 and IN1612 with SA44, SA43, SAneg1 and SAneg2 aptamer with control (no aptamer). Aptamer at 100nm concentration. Scale bar represents 20 µm. SA44, SA43 aptamer showed staining to cytoplasmic and nuclear regions to IN1612 (images b and d). SAneg1 showed perinuclear staining (images e and f). The control images (with no aptamer) did not show any staining (images i and j).

In Figure 4.5, SA44 bound to glioma short term cultures IN1528 and IN1612, derived from patient tissue. SA43 showed binding to IN1612 but not to IN1528. A heterogeneous pattern of binding was observed in the short term cultures than in the glioma cell lines, illustrating the heterogeneous nature of patient derived tissue and the selectivity of the aptamers to their target. SA44, SA43 aptamer showed strong staining to cytoplasmic and nuclear regions to IN1612 (images b and d). SAneg1 showed perinuclear staining (images e and f) and heterogeneous but much reduced compared to binding in cell lines (Figure 4.4). SAneg2 aptamer did not show any staining to the cells (images g and h) and is consistent with findings from the cell lines. The control images (with no aptamer) did not show any staining (images i and j). This confirmed the staining to be due to aptamer binding and specific. SAneg2 images and control images show that the aptamer binding is specific. As seen in fluorescent staining (Figure 4.1) with U87MG, cells appear to have a halo with cytoplasmic and likely surface binding.

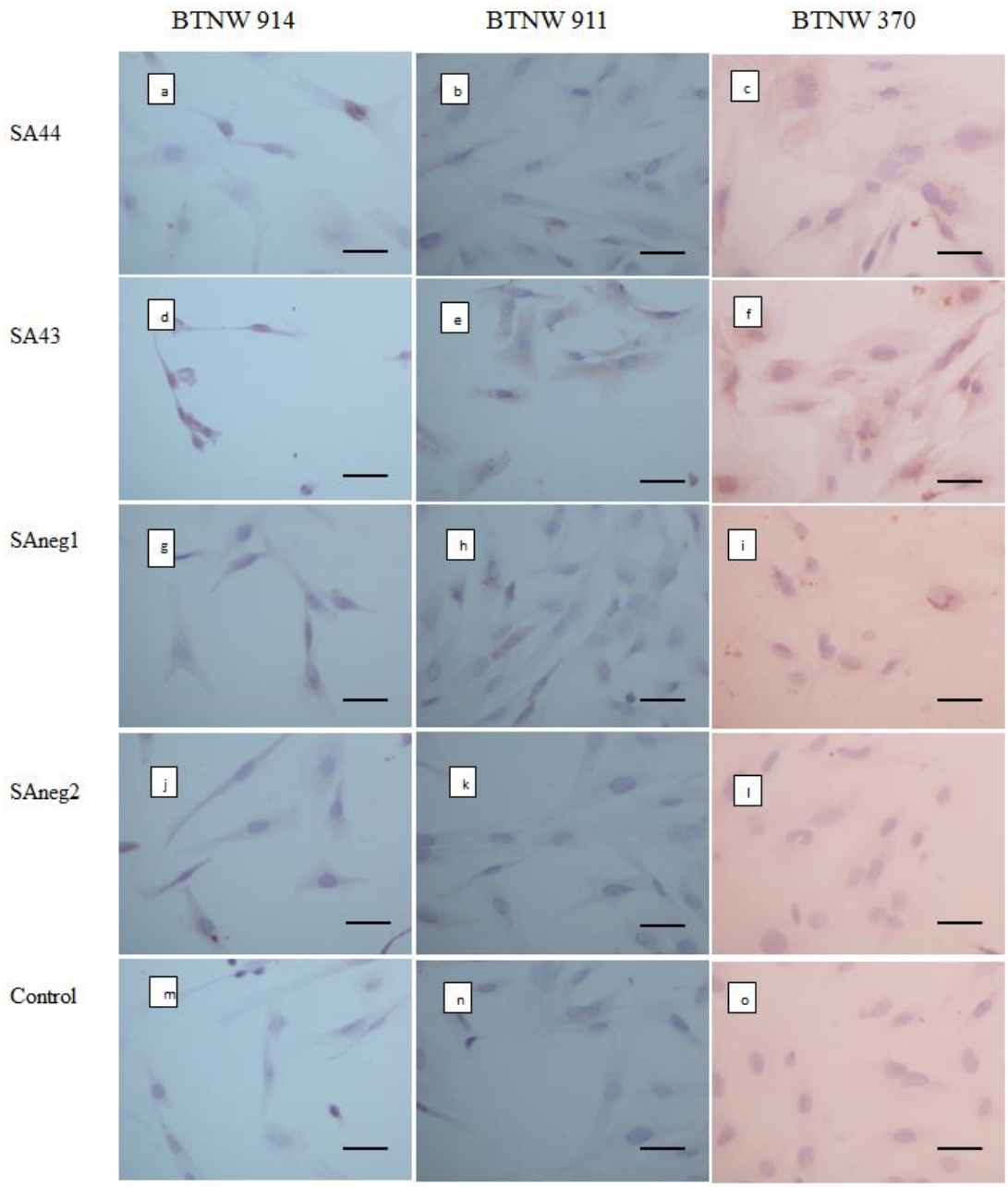

Figure 4.6 **DAB staining of short term cultures, BTNW**

BTNW 914 BTNW 911 and BTNW 370 with SA44, SA43, SAneg1 and SAneg2 aptamer with control (no aptamer). Aptamer at 100nm concentration. Scale bar represents 20 µm. SA44, SA43 aptamer bound to cytoplasmic and nuclear regions (images a, b, c, d, e and f). SAneg1 showed some staining (images g, h and i). SAneg2 aptamer did not show any staining to the cells (images j, k and l). The control images (with no aptamer) did not show any staining (images m, n and o). Hence the aptamer incubation is binding to cells and not non-specific.

In Figure 4.6, SA43 and SA44 bound to glioma short term cultures BTNW 914, BTNW 911 and BTNW 370, derived from patient tissue. A heterogeneous pattern of binding was observed in the short term cultures than in the glioma cell lines, and staining was markedly reduced in comparison to the cell lines, illustrating the heterogeneous nature of patient derived tissue and the selectivity of the aptamers to their target. SAneg1 showed some staining (images g, h and i) with mainly cytoplasmic and perinuclear appearance. SAneg2 aptamer did not show any staining to the cells (images j, k and l) and is consistent with findings from the cell lines. The control images did not show any staining (images m, n and o). This confirmed the staining to be due to aptamer binding and specific. SAneg2 images and control images show that the aptamer binding is specific.

4.4 Discussion

The aim of the chapter was to confirm the binding of SA43 and SA44 aptamers to glioma cell lines and patient derived tissue. The aim was also to assess the selectivity of the aptamers by including a glial cell line, SVGp12 as a non-cancerous control. The results show the SA43 and SA44 aptamers bound consistently and reproducibly to glioma cells, and that both Cy3 and biotin tagged aptamers can be utilised for targeting to glioma cells.

Aptamers identified by Cerchia *et al* were shortened in length since the primer increases the length of the aptamer which may impact on penetration through the BBB (Pan and Clawson, 2009). Aptamer binds to its targets using various binding forces like van der Waals and hydrogen bonding (Patel, 1997), together to conform to specific targets. The longer the aptamer, the greater chances of it binding or being 'sticky' to multiple molecules and reducing specificity. As aptamers are single stranded DNA or RNA, they

are able to contort into different 2D and 3D structures (Feigon et al., 1996; Lin and Patei, 1997; Patel, 1997). 2D structures are easier to predict using freely available online software such as M-Fold (Zuker, 2003). To reduce non-specificity, shorter aptamer sequences are better (Pan and Clawson, 2009). Since the active part of the aptamer is due to the conformation of the 3D structure, forming the 'loop' (Guo, 2010), the aptamer can be reduced in nucleotide number depending on what is hypothesised as the correct computational binding site (Cerchia et al., 2009; Nadal et al., 2013) . Further truncation can result in a more specific aptamer but can also affect the stability of the aptamer (Nadal et al., 2013). Aptamer folding was predicted using Mfold (Zuker, 2003) for the likely 2D structure and stem loop motifs typically observed in single stranded oligonucleotide folding. It was decided to utilise DNA aptamers in this research project due to improved stability compared to RNA aptamers, which may be of benefit for translation into clinical use if aptamers are utilised as novel therapeutics and/or drug targeting moieties (Zhu et al., 2015).

The aptamers were produced using SELEX against U87MG cells. The primers were merely attached to expand the population of the aptamer sequences by replication and in theory should not affect the final targeting potential of the aptamer. In contrast, Cerchia *et al* showed that incubation of truncated GL43 -44 aptamer with U87MG showed a time dependent reduction in detection of cyclin D1 detection and ERK phosphorylation, whereas in our studies, there was no biological activity of either SA43 or SA44 in U87MG cells (Aptekar et al., 2015) suggesting SA43 and SA44 DNA aptamers bind to a different target than the truncated RNA version.

Live cell incubation at 37°C showed that the aptamer was taken up readily by the glioma cell lines U87MG and 1321N1 compared to SVGp12. The aptamer appears to be present

mainly in the cytoplasm and perinuclear region as per the confocal imaging. There was fluorescence was also detected (indicating aptamer binding) in SVGp12 cells but is markedly reduced compared to the glioma cell lines. This could be likely due to the presence of similar target in the cells lines but over detection in the glioma cell lines. Confocal imaging at various depths did show aptamer binding around the cell membrane. The variation in the signal intensity also suggests that the aptamer target ligand is likely present on the cell surface as well and may well be an over detection of a cytoplasmic or nuclear structure.

The detection of aptamer binding to fixed cells was due to biotin-avidin interaction (Weber et al., 1989). Pre-incubation with the aptamer to live cells followed by cross-linking (fixing) to stabilize the cells would have made the biotin unavailable for detection. Also, the blocking of endogenous cellular biotin would also block the biotin conjugated to the aptamer, thereby invalidate any available biotin sites for avidin binding. Thereby, endogenous biotin was blocked after cell fixation prior to cell permeation and incubation of the biotin-conjugated aptamers. The hypothesis adapted was that the aptamers should continue to bind their target ligand via the non-covalent forces between aptamer and target irrespective of whether Cy3 or biotin was used as the tag (Starikov and Nilsson, 2002). This is similar to actual antigen-antibody interaction utilised in immunocytochemistry and supporting the use of aptamers as a direct replacement for antibodies. Later, the cells were incubated with biotinylated aptamer after fixation and permeabilisation (chapter 2.8.4) and showed consistent results of greater staining on the cancerous cell lines compared to SVGp12. Staining was found across the cellular matrix in the tumour cell lines whereas SVGp12 cell line showed faint, mainly peri-nuclear staining. No staining was seen in the control used with no aptamer.

Aptamer staining with both Cy3 and biotin showed binding in the cytoplasm and nuclear/peri-nuclear region. It was evidently seen more in the glioma cell lines compared to SVGp12. The binding appeared to be heterogeneous across the cells (Wadsworth, 2007). This could be because of varying detection of target molecule at various stages of the cell cycle.

Aptamer staining was then replicated to short term cultures. Gliomas, by nature, are a group of heterogeneous tumours and targeting is difficult due to the heterogeneity (Soeda et al., 2015). It was hence important to see the binding of the aptamers in patient tissue derived short-term cultures and assess the specificity. Significant binding of the SA43 and SA44 aptamers was also detected in the short-term cultures, but with greater heterogeneity than commercial glioma cell lines (compare Figure 4.6 with Figure 4.4). Two control aptamers, SAneg1 and SAneg2, which were of equivalent composition to the SA43 and SA44 aptamers randomly generated were used as a control aptamers. Biotin tagged SAneg1 bound to the commercial cell lines and short-term cultures but no binding was detected with SAneg2. This was replicable across the cell lines and further confirmed the fact that the binding of SA43 and SA44 appeared to be specific, towards a target rather than being pure DNA affinity. A parallel study looked at the application of these aptamers towards tissue diagnosis (Aptekar et al., 2015). The study showed that SAneg1 appeared to bind to majority of tissue sections including normal tissue whereas SAneg2 only bound to very few tissue sections. The binding properties could be used as a positive control with SAneg1 (not necessarily the relevant target) and negative control for SAneg2, hence their use in further experiments.

As a result of the experiments in this chapter, we were able to confirm consistent Cy3-aptamer staining to glioma cells. This was reproduced with biotin-conjugated SA43 and

SA44 aptamers thus proving that biotin is not interfering with the aptamer binding. The results were reproducible using short-term cultures, which are an important part of target detection, being patient derived. The aim of the project is to be able to apply the techniques towards patient specific targeted treatment and short-term cultures are a relevant step in the process. Presence of a negative (SAneg2) and possible positive control (SAneg1) proved the hypothesis of the current experiment and supported the next stages of research. Further pull-down and elution of the targets would throw more light on the nature of target proteins for the different aptamers in chapter 5 and chapter 6.

The next chapter details the protein extraction methodology and aptamer assisted precipitation of the target protein and its identification using mass spectroscopy. To identify the target, optimal protein extraction is essential. Since the aptamer binds to the target, the intention was to crosslink the aptamer to its target to maintain the binding during the target precipitation. The precipitate would then be identified using mass spectrometry and compared against known proteomic databases to identify and further confirm with other aptamers and cell lines.

Chapter 5

5 Optimisation of protein extraction, aptoprecipitation and proteomic analysis

5.1 Introduction

Conventional 3,3-Diaminobenzidine (DAB) staining and confocal imaging confirmed the selective uptake of SA43 and SA44 by U87MG and 1321N1 cell lines. It is not known, however, the identity of the target ligand to which the aptamers bind. In order to identify their respective targets, protein extraction and quantification experiments were carried out. Chromatin immunoprecipitation, or ChIP, uses streptavidin-biotin interaction to pulldown the antibody target ligand which can then be identified by mass spectrometry. ChIP methodology was adapted to use aptamer target interactions rather than antibody based interactions.

Optimal protein extraction is essential to confirm the binding targets. Harsh conditions for protein extractions, chemically or with heat can denature the epitope being investigated thereby compromising the ability to interpret the data obtained.

Two approaches for protein extraction from cultured cells were assessed using unfixed cells and fixed cells. Protein extraction using unfixed cells is well published with various existing techniques such as chemical (detergent) or mechanical (pestle and mortar) (Cilia et al., 2009; Lee, 2017). Protein extraction from fixed cells involved incubation of live cells with the aptamer followed by fixation using PFA, however has not been published before, so this was a novel approach to be tested. The concept being tested was to determine if crosslinking of the epitope to the aptamer resulted in the maintenance of the aptamer–target interaction. Protein extraction from fixed tissue as published utilises

heat and TCA extraction (Sadick et al., 2016; Sadick and Darling, 2017) but application with pre-reacted aptamer and effect on aptamer target binding is unknown.

Based on the results of Chapter 4, it was hypothesised that active aptamer uptake happens during live cell incubation, based on Cy3 staining (chapter 4.2). DAB staining with biotinylated aptamer showed consistent binding results and availability of target to aptamer despite cross linkage (chapter 4.3). Hence, the proof of concept was carried further and incubation with both live and fixed cells was performed with attempted protein extraction. Cells were fixed using 4% PFA and subjected to various lysis methods to achieve a target protein concentration of 2mg/ml for pulldown experiments. Protein was quantified using Bradford assay (Bradford, 1976; Ernst and Zor, 2010).

Unfixed cells were used for optimisation of protein quantification method using Bradford assay as a baseline. With live cells, there remained a concern of exposing the intracellular components to the aptamer on lysis. This might expose targets which the aptamer would not necessarily have access to in cells in their native form, and thus may generate false positive results.

Once adequate protein extraction was achieved, cells were subjected to aptamer incubation and streptavidin coated beads were used for protein pulldown assay, utilising streptavidin-biotin affinity for pull-down of targets.

Various buffers were used for protein interaction to keep aptamer epitope interaction as close to normal cellular physiology as possible (for example physiological buffered salts and physiological pH 7.4) and to reduce protein degradation. The protein extracted was compared to other techniques of protein extraction to confirm the optimal protein

content and quality of protein extraction. After developing the protocol, novel aptamers raised against glioma cell lines were used to verify the pulldown technique.

The epitopes were then identified by mass spectrometry analysis and target identification was confirmed by Western blot and siRNA in Chapter 6.

5.2 Protein extraction -

The results of the protein extraction method development are represented in the flowchart in Figure 5.1. Fixed and unfixed cells were used for the protein extraction and multiple buffers were tested for efficient extraction and compared using Bradford assay. Fixed cells, pre-reacted with the aptamer were used to crosslink the target to the aptamer. This would enable reduction in non-specific pulldown and also reduce the loss of the target during the downstream process of extraction. Unfixed cells were initially used to establish the protein extraction techniques and for protein gel electrophoresis. The unfixed cells became the important component of the project due to the difficulties face in protein extraction from fixed cells as detailed in the chapter. Due to the complexity of the optimal protein extraction technique, it is represented in a flowchart. The flowchart and the various combinations of reagents used in the development of the process are detailed in the next section and images. We will refer to the flowchart and justify how the final protein extraction protocol was optimised using various sections and images from the flowchart itself.

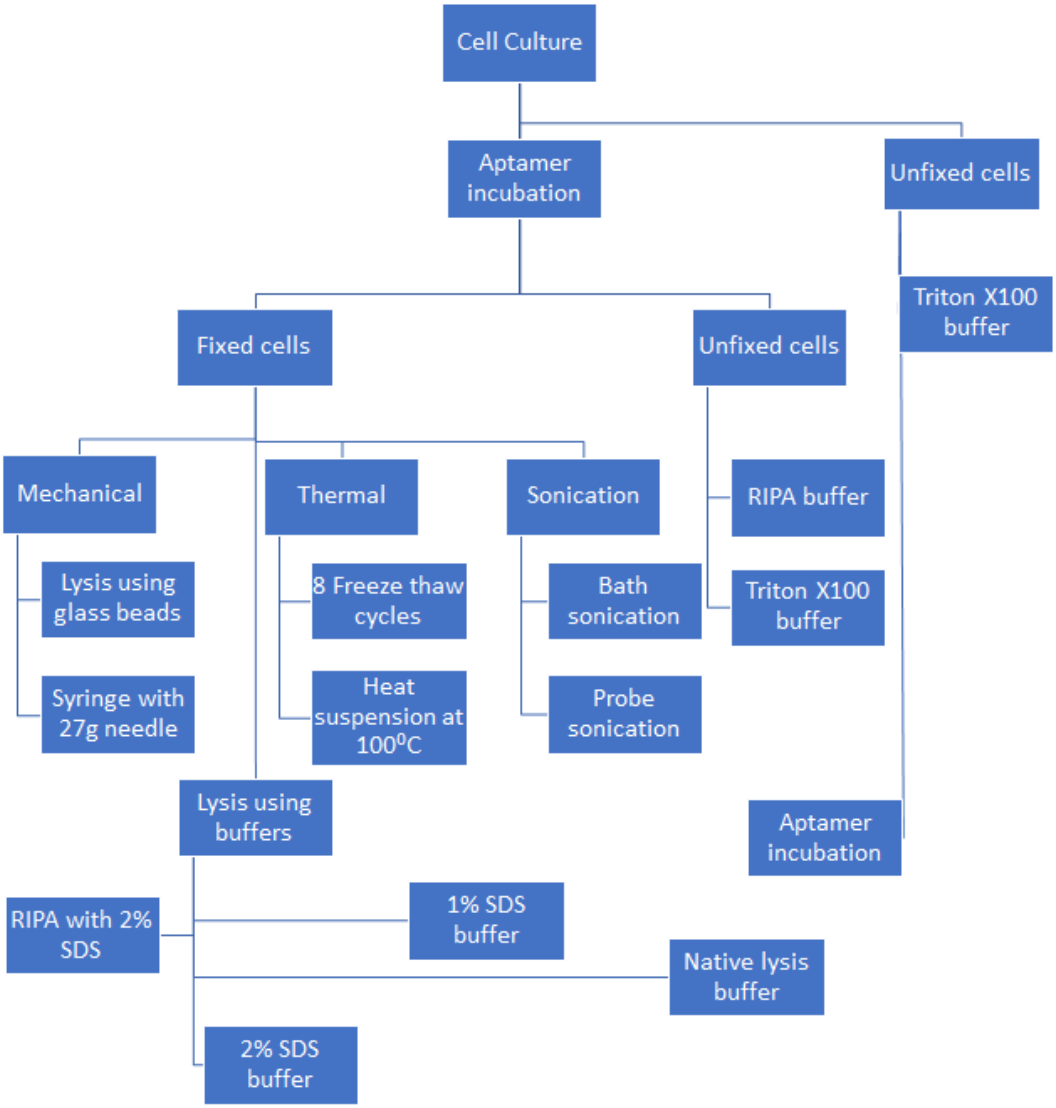

Figure 5.1 The process of protein extraction method development with cells.

Fixed and unfixed cell were used for protein extraction. After cell culture cells, were either incubated with aptamer or kept for lysis and incubation with aptamer (side arm). Cells which are pre-incubated with aptamer were either fixed or kept unfixed. Fixed cells, pre-incubated with aptamer were either placed directly into cell lysis buffers or subjected to mechanical, freeze-thaw and sonication methods for cell lysis before placing into lysis buffer(s). Unfixed cells were subjected to lysis by standard lysis buffers after aptamer incubation. Unfixed cells were then lysed first (side arm of the flowchart) and later incubated with aptamer in physiological buffers.

5.2.1 Protein extraction using fixed cells

Cells were first incubated with aptamer according to previous chapters and then fixed using PFA to be able to pull down the aptamer target epitope. Our collaborative research (Aptekar et al., 2015) has shown that the affinity of the aptamer for the target ligand is in the nM range with both SA43 and SA44 exhibiting dissociation constants (Kd) at 21.56 ± 4.6 nM and 21.11 ± 3.3 nM, respectively. Although our previous data showed the aptamers have high affinity for the target ligand, it is important to minimise disruption of the target-ligand interaction during the protein extraction stage. Cells were fixed using 4% PFA as in chapter 2.9.1. Post fixation, the cells were lysed using RIPA lysis buffer, RIPA lysis buffer with 2% SDS (sodium dodecyl sulphate) lysis buffer, 2% SDS lysis buffer, 1% lysis buffer and native lysis buffer (Figure 5.2). The protein extraction was tested using Bradford assay, by comparison of sample absorbance to absorbance of known BSA standards (Figure 5.3).

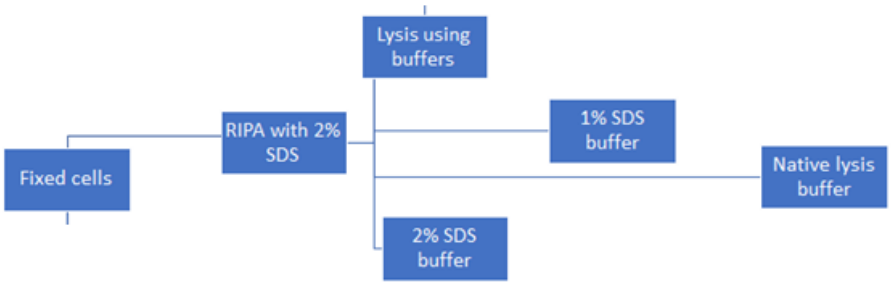

Figure 5.2 Fixed cell stage from protein extraction method development

Various lysis buffers as depicted in flowchart were used for protein extraction from fixed cells. Fixed cells, pre-incubated with aptamer were lysed with various buffers to optimise protein extraction.

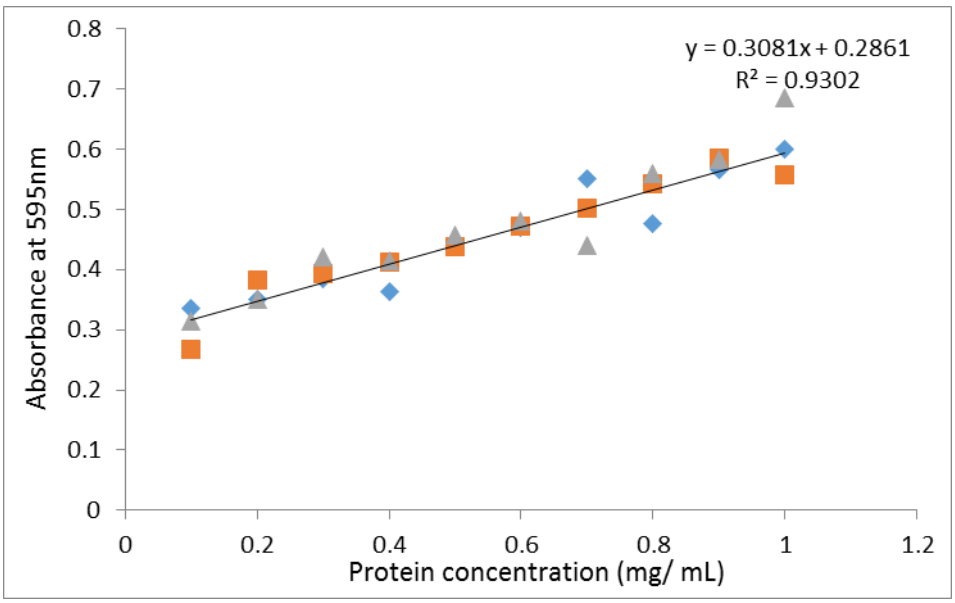

Figure 5.3 Typical standard curve for Bradford assay

Bradford assay showing absorbance of bovine serum albumin (BSA) standards run used for determination of protein concentration in extraction samples (n=3 repeats). Note the standard curve was performed at every experiement.

Fixed cell lysis with lysis buffers alone showed poor protein extraction with visible cell pellet left after lysis. Fixed cell lysis is difficult due to PFA cross-linkage in cell matrix (Ikeda et al., 1998; Sadick et al., 2016) and may require treatment with heat, chemical or physical measures.

5.2.2 Fixed cell protein extraction using mechanical methods

The fixed cells as described in section 2.9.1 were then subjected to protein extraction using mechanical methods (Figure 5.4). For uniformity of experiments, RIPA lysis buffer was used for other treatment methods of fixed cells as no difference was seen in the protein content extracted from other lysis buffer as in chapter 5.2.1 and RIPA has the lowest concentration of SDS at 0.1% and is least denaturing.

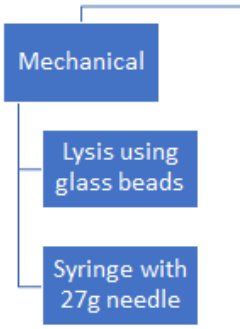

Figure 5.4 Mechanical methods for protein extraction from fixed U87MG.

Fixed U87MG cells were incubated with 100nm aptamer then fixed with 4% PFA. Fixed cells were then subjected to lysis using agitation of cells with glass beads in an Eppendorf tube. Alternatively, cells were lysed by aspiration with a syringe and 27g needle.

Cells were fixed and suspended in RIPA lysis buffer. They were then subjected to lysis using glass beads and 27G syringe methods (Thermofischerscientific, 2010). The proteins extracted were then run on gel electrophoresis as imaged in figure 5.8 along with other lysate methods, to compare protein content and quality.

5.2.3 Fixed cell protein extraction using thermal methods

The fixed cells as described in section 2.9.1 were then subjected to protein extraction using heat and freeze thaw cycles as different methods (Thermofischerscientific, 2010) and as detailed in chapter 2.9.1 (Figure 5.5). Protein was extracted from fixed U87MG cells after subjecting the cell pellets to heat at 95^{o}C for 2 hours. The proteins extracted were then run on gel as imaged in figure 5.6. Quality of protein content was considered high as depicted by distinct bands and lack of ‘smears’.

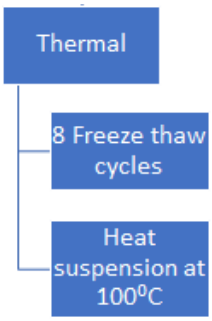

Figure 5.5 Thermal lysis methods on fixed U87MG cells.

U87MG cells were incubated with 100nM aptamer, fixed with 4%PFA then subjected to 8 freeze thaw cycles or heat suspension at 100˚C.

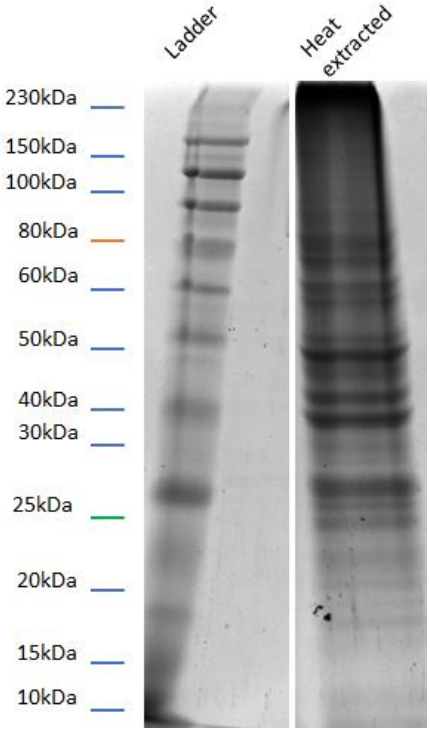

Figure 5.6 Heat extracted protein from fixed cells.

Protein lysate after thermal extraction from fixed U87MG cells. Distinct protein bands wer edetected which suggests high quality protein was extracted.

5.2.4 Fixed cell protein extraction using sonication methods

The fixed cells as created in chapter 2.9.1 were then subjected to protein extraction using bath sonication and probe sonication as different methods (Thermofischerscientific, 2010) and as detailed in chapter 2.9.1 (Figure 5.7). Visible

inspection of the cell pellet did not show any disintegration, and therefore this method was not processed further for Bradford assay or for polyacrylamide gel electrophoresis.

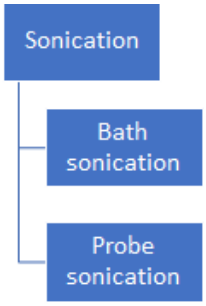

Figure 5.7 Bath and probe sonication on fixed U87MG cells.

U87MG cells were incubated with 100nM aptamer, fixed with 4% PFA and subjected to bath or probe sonification.

When using fixed cells, proteins were diluted 10x for Bradford assay, (figure 5.3), giving an average protein concentration of 400 – 500 µg/ml. This was seen across other methods with fixed cells. The proteins extracted were then run on a 10% polyacrlamide gel (figure 5.8) along with other lysate methods. Quality of protein was considered inadequate as few defined bands were detected in all of the lanes.

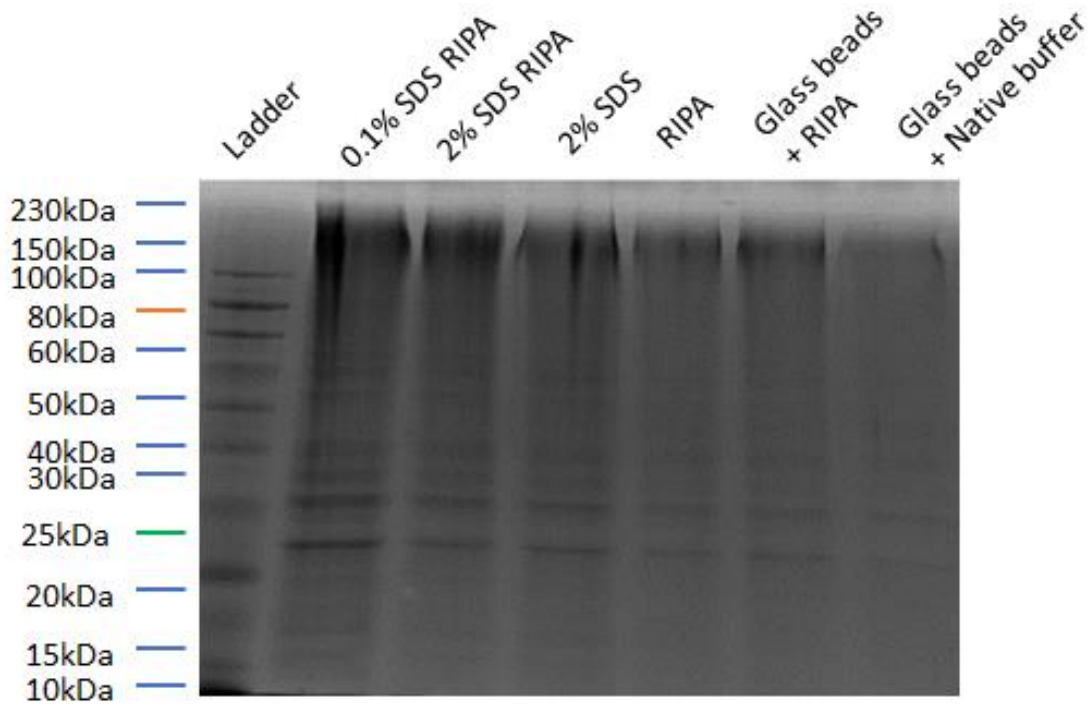

Figure 5.8 U87MG cells fixed with 4% PFA and subjected to various mechanical methods for protein extraction.

Lane 1 shows protein extraction using 0.1% SDS RIPA lysis buffer after freeze thaw cycles and appears to have the maximal concentration of protein compared to other lanes. Lane 2 is protein extraction using 2% SDS with RIPA lysis buffer, subjected to freeze thaw cycles. Lane 3 is 2% SDS only lysis buffer subjected to freeze thaw cycles. Lane 4 is RIPA lysis buffer with mechanical syringing of cells. Lane 5 and 6 are glass bead lysis in RIPA buffer and native lysis buffer respectively.

5.2.5 Unfixed cell protein extraction

U87MG cells were trysinised as in chapter 2.9.3 and lysed using RIPA lysis buffer and 0.1% Triton X100 lysis buffer as in figure 5.9. RIPA was used as it is a standard lysis buffer used in proteomics. RIPA is knonnw to be a good buffer for nuclear protein extraction. It does though denature the protein. Triton X100 does not denature the protein and is an equally good buffer like RIPA.

Figure 5.9 Buffer lysis of U87MG cells. U87MG cells were lysed with either RIPA lysis buffer or Triton x100 lysis buffer.

Bradford assay was performed for the cell lysates for various cell lines and table 5.1 details the results of protein extracted.

Table 5-1 Protein concentration extracted from unfixed U87MG cells n=3

Unfixed Cells	Protein concentration (Milligram of protein per ml of lysate)
U87MG	3.6
1321N1	5.35
SVGp12	4.21

Unfixed cells showed better protein extraction when compared to fixed cells. The extracted protein cell pellet also displayed visual clarity with no residual clumped sample in the Eppendorf tubes after lysis when compared to fixed cell lysis. Unfixed cells were lysed with RIPA and triton X100 as two steps of the flow chart as shown in Figure 5.9. Equivalent protein extraction was achieved from each as displayed above. The extracts from unfixed and fixed cells were also run on a gel to assess for quality of protein

separation (figure 5.10). There was cleaner appearance of bands on the unfixed protein separation lanes, pointing to better quality protein.

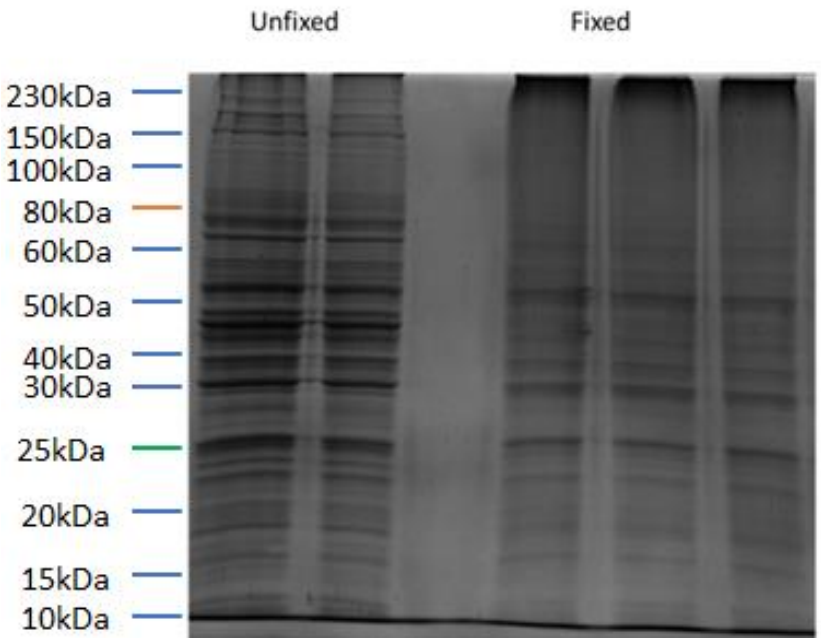

Figure 5.10 Protein extracts from unfixed and fixed U87MG cells

Distinct bands can be seen in the unfixed cell lysates compared to fixed cells (heat extracted) appeared with clear demarcation and greater in number. The gels are from the cell lysates and had equal loading protein content of 2.5mg/ml.

Final extraction protocol was utilised with triton X100 as it does not denature the protein and allows it to be reacted in its native form. The aptamer incubation in the unfixed cells would happen after lysis and it did raise the question of non-specific binding. In chapter 3 and chapter 4, clear internalisation of the aptamer was seen and supported binding likely on the surface as internalisation appeared to be an active process (Aptekar et al., 2015). Pre-reacting the aptamer to live cells and fixing, cross links the biotin attached to the aptamer as shown in chapter 4. Reversing this linkage with heat as in section 5.2.3 does give good protein content but aptamer-biotin link and target binding of the aptamer are not detected. Thus, aptamer incubation with unfixed cell lysate with triton X100 was adapted for assisted pull-down technique as in chapter 5.3.

5.3 Aptamer assisted pulldown of proteins

5.3.1 Method development

Chromatin immunoprecipitation or ChIP is a well established technique for biomarker discovery using antigen-antibody interaction (Aparicio et al., 2004; Viens et al., 2004). It employs the native attraction of streptavidin to biotin to enable the pulldown of target protein (Lee et al., 2006). Cell lysates with the target epitope or antigen are lysed after cross linking to pulldown the associated epitopes with the target antigen. The lysate is then incubated with biotin tagged antibody and then separated with column or beads (Dahl and Collas, 2008). The aim of the methodology is to extract the specific antigen and assess its expression in the lysate. ChiP protocol as per description was utilised as a guidance for the development of the aptamer assisted pull down.

After optimisation of protein extraction (section 5.2), cell lysates were incubated with biotin tagged aptamers and pulldown was attempted. Cells were lysed at 4^{o}C on a rotating platform, centrifuged and then incubated with the aptamer at the same temperature (chapter 2.11.4). Aptamer assisted precipitation was performed with the techniques as described in section 2.11.4.

Initially, magnetic streptavidin beads were used for extraction of pulldown. Gel electrophoresis of extraction, shown in figure 5.11, shows good pulldown of protein with magnetic beads from lysate but there were multiple protein bands pulled down with the magnetic beads indicating non-specific cross reactivity with the aptamer and/or magnetic beads with proteins had occurred (figure 5.11).

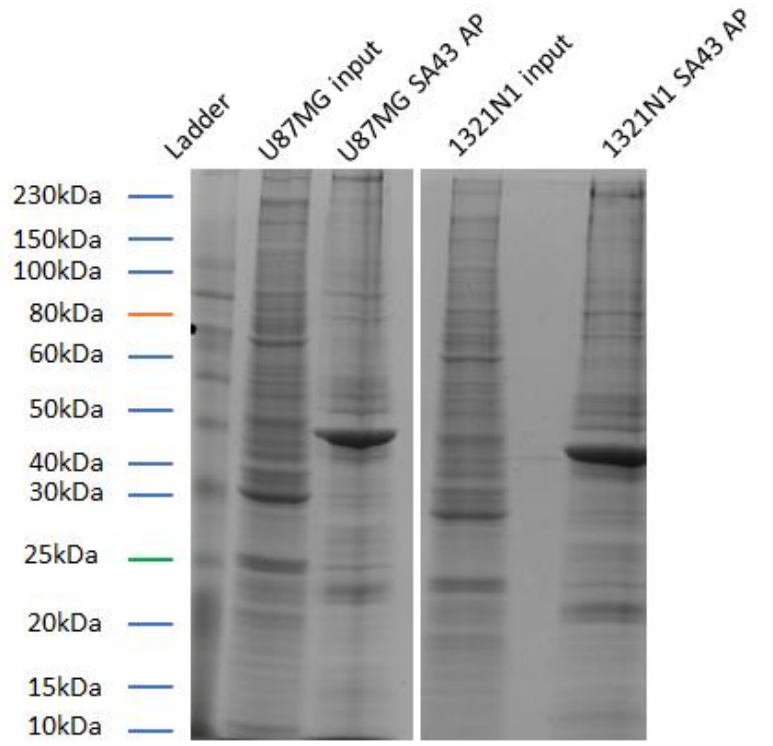

Figure 5.11 U87MG and 1321N1 cell lysate with aptamer assisted precipitation using SA43 aptamer.

U87MG SA43 AP and 1321N1 SA43 AP showing multiple bands of lower intensity compared to input lysates (all cell lysate) respectively. There is no specific pull-down of protein detected. The multiple bands in the AP lanes (aptamer assisted protein pulldown) suggest non-specific interaction with the aptamer and/or magnetic beads.

The multiple bands detected in the protein pulldown in the input (all cell lysate) and AP (just the aptamer bound protein) is likely due to non-specific binding. In addition, visual inspection showed that the protein and magnetic beads had clumped and therefore seemed to be promoting non-specific protein binding. Hence, streptavidin-agarose beads were then tested to assess whether they were superior to magnetic beads in reducing non-specific protein interaction. Multiple washing steps were included as in section 2.11.4 to reduce non-specific binding effects.

5.3.2 Aptamer assisted pull-down of targets - results

5.3.2.1 Cell line results

U87MG, 1321N1 and SVGp12 cell lines were lysed and incubated with the aptamers SA43 and SA44. The resultant aptoprecipitation results are shown in Figures 5.12-5.14.

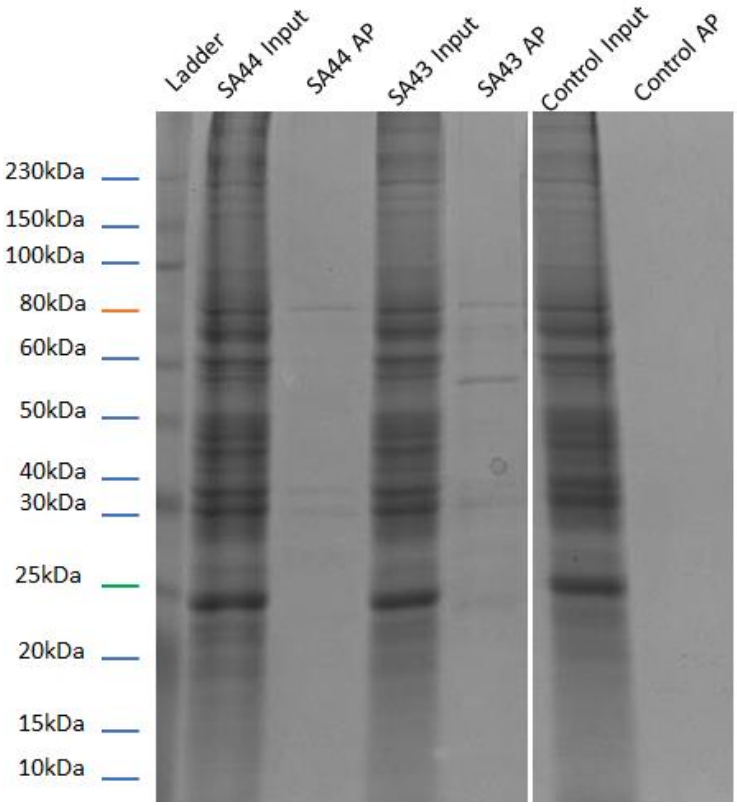

Figure 5.12 U87MG cell lysate with aptamer assisted precipitation using SA44 and SA43 aptamers.

U87MG cells were lysed and reacted with the aptamers SA44 and SA43 at 4^{o}C. The reacted lysate was then incubated with streptavidin beads at 4^{o}C and then washed for non-specific binding. The lysate bound to streptavidin beads was then eluted using laemmli buffer and run on 10% polyacrylamide gels and stained with Coomassie blue stain. These were then imaged using Geldoc™ imager (Bio-rad Laboratories Inc., Watford, UK) ™ imager (Bio-rad Laboratories Inc., Watford, UK) and showed specific bands in the SA44 AP and SA43 AP columns. The control AP is without aptamer and confirms absence of background binding to streptavidin beads. The image represents n=3

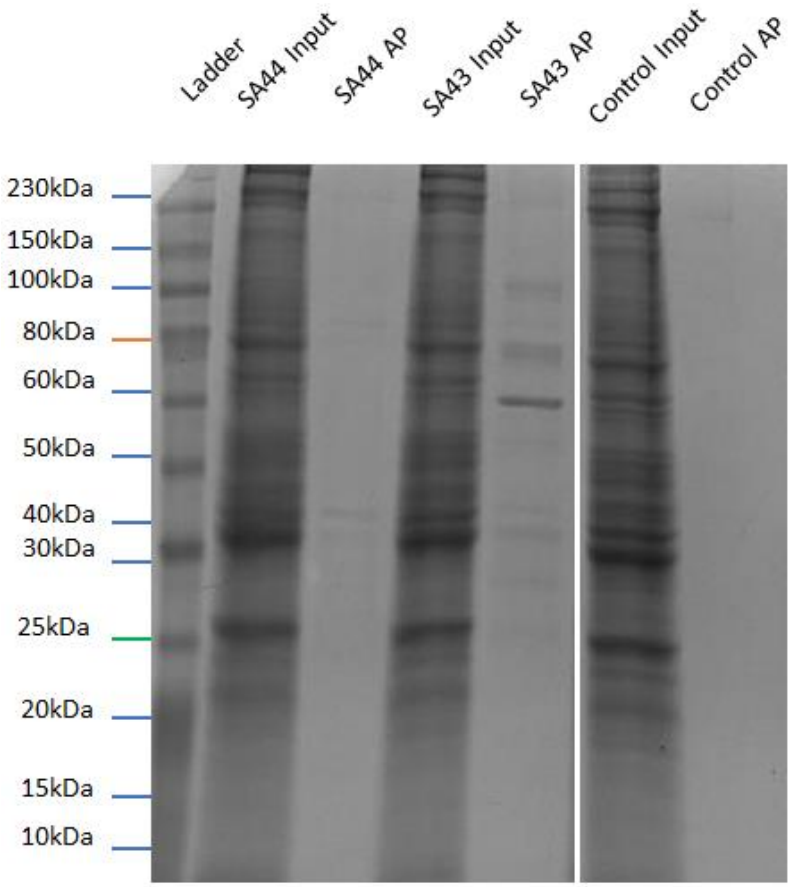

Figure 5.13 1321N1 cell lysate with aptamer assisted precipitation using SA44 and SA43 aptamers.

1321N1 cells were lysed and reacted with the aptamers SA44 and SA43 at 4^{o}C. The reacted lysate was then incubated with streptavidin beads at 4^{o}C and then washed for non-specific binding. The lysate bound to streptavidin beads was then eluted using laemmli buffer and run on 10% polyacrylamide gels and stained with Coomassie blue stain. These were then imaged using Geldoc™ imager (Bio-rad Laboratories Inc., Watford, UK) ™ imager (Bio-rad Laboratories Inc., Watford, UK) and showed specific bands in the SA44 AP and SA43 AP columns. The control AP is without aptamer and confirms absence of background binding to streptavidin beads. The image represents n=3.

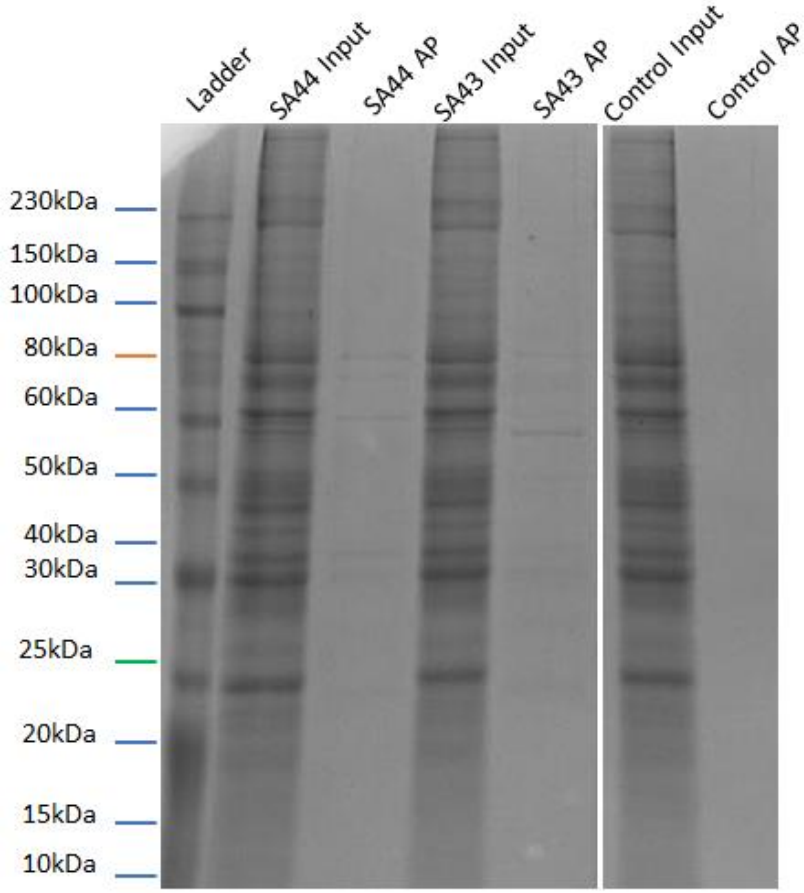

Figure 5.14 SVGp12 cell lysate with aptamer assisted precipitation using SA44 and SA43 aptamers.

SVGp12 cells were lysed and reacted with the aptamers SA44 and SA43 at 4^{o}C. The reacted lysate was then incubated with streptavidin beads at 4^{o}C and then washed for non-specific binding. The lysate bound to streptavidin beads was then eluted using laemmli buffer and run on 10% polyacrylamide gels and stained with Coomassie blue stain. These were then imaged using Geldoc™ imager (Bio-rad Laboratories Inc., Watford, UK) ™ imager (Bio-rad Laboratories Inc., Watford, UK) and showed specific bands in the SA44 AP and SA43 AP columns. The control AP is without aptamer and confirms absence of background binding to streptavidin beads. The image represents n=3

Consistent pull-down results were seen with all three cell lines U87MG, 1321N1 and SVGp12. The pulldowns were performed three times and further assessed using mass spectrometry analysis in section 5.4. The optimised method was then applied to short term cultures to assess the robustness of the protocol and confirm similarity in patient derived short term cultures.

5.3.2.2 Short term culture results

After the results of cell lines, short term cultures were expanded to enable experiments with optimal protein extraction and pull-down. Initial application was done with BTNW 911 and BTNW 914 short term cultures.

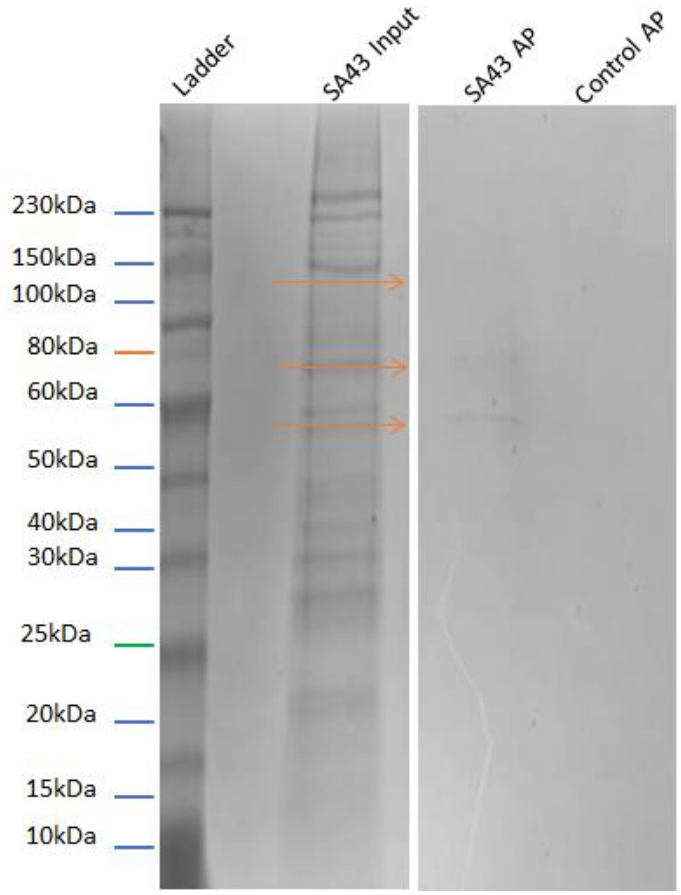

Figure 5.15 Short term culture BTNW 911 cell lysate reacted with SA43 aptamer.

SA43 AP is the protein sample eluted with apto-precipitation and run on gel. Faint bands can be seen in the SA43 AP lane, marked by the orange arrows. The control lane is clean which is the sample eluted off cell lysate reaction alone with streptavidin beads, hence no non-specific pulldown. Due to the nature of short term cultures, further repeats could not be carried out.

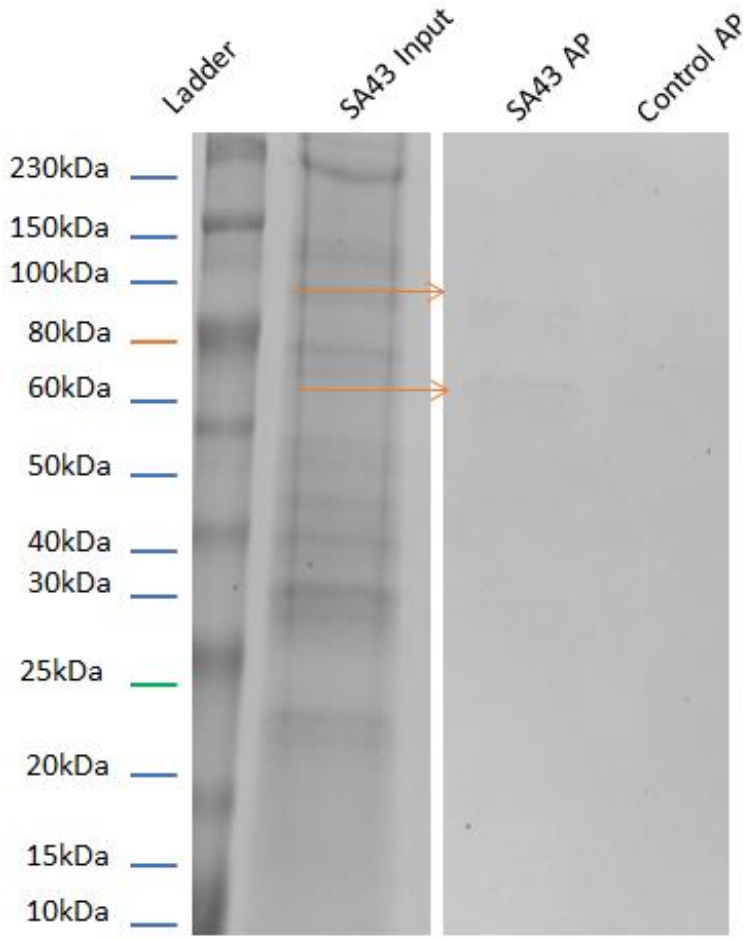

Figure 5.16 Short term culture BTNW 914 cell lysate reacted with SA43 aptamer.

SA43 input is the gel band for the cell lysate alone. SA43 AP is the protein sample eluted with apto-precipitation and run on gel. Faint bands can be seen in the SA43 AP lane, marked by the orange arrows. The control lane is clean which is the sample eluted off cell lysate reaction alone with streptavidin beads, hence no non-specific pulldown. The SA43 AP bands were seen in two experiments with the cell line. Due to the nature of short term cultures, further repeats could not be carried out. This supports that the aptamer is targeting and pulling down specifically.

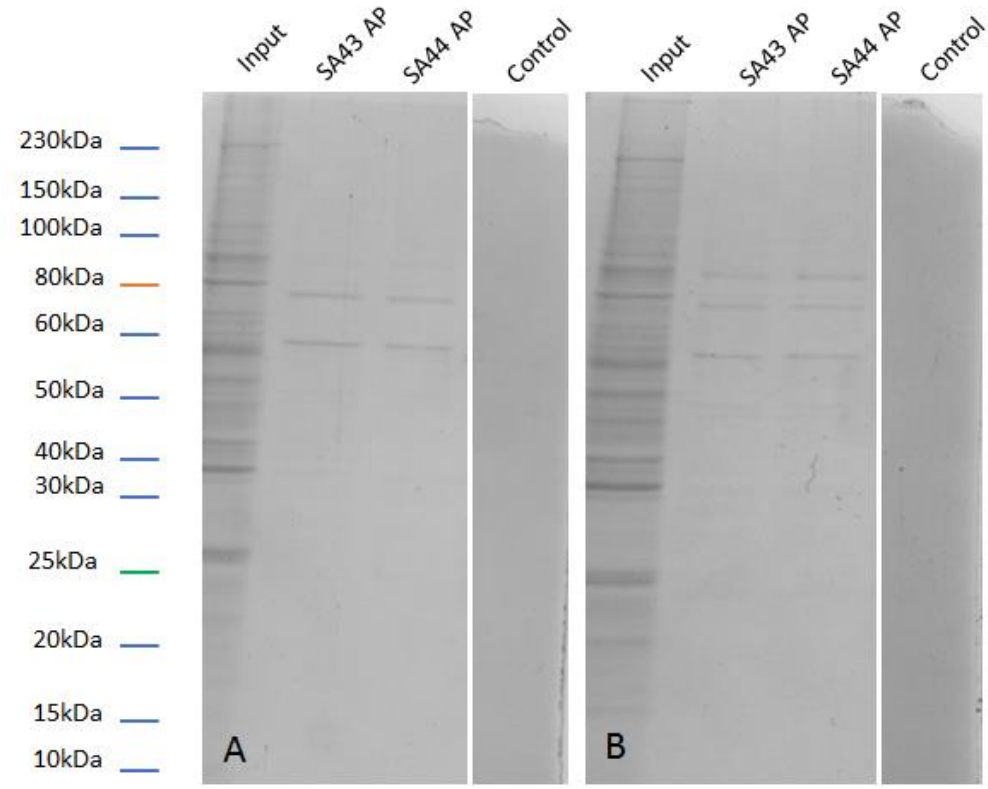

Figure 5.17 Short term culture W2045 (A) and W859 (B) cell lysate reacted with SA43 and SA44 aptamer.

SA43 AP and SA44 AP are the protein samples eluted with apto-precipitation and run on gel. Higher intensity bands was detected in the SA43 AP and SA44 AP lane. The control lane is clean which is the sample eluted off cell lysate reaction alone with streptavidin beads, hence no non-specific pulldown. The control lane is clean and no non-specific binding was detected. Due to the nature of short term cultures, single pull-down with the W2045 and W859 cell lines was done after optimisation of technique with commercial cell lines.

5.3.3 Novel aptamer assisted pull-down of proteins and structural comparison

The protocol developed using cell lines, for aptamer assisted pull down of proteins was applied to short term cultures, derived from glial tissue. This was seen in the section above and helped confirm the validity of the protocol and the aptamer interaction with

glial derived cell cultures. Further robustness of the protocol was planned with the use of novel aptamers generated in house at Uclan.

5.3.3.1 Novel TDM aptamer assisted pulldown with cell lines and short term cultures

A parallel project (Aptekar et al., 2015)looked at replication of aptamer generation using SELEX towards U87MG cell line as per Cerchia *et al* (Cerchia et al., 2009). Novel aptamers generated by SELEX were then used for DAB staining towards U87MG. Five of the aptamers generated showed good binding results in U87MG cell lines in a parallel project(Manangazira, 2013). Novel aptamers TDM2, TDM3, TDM7, TDM9 and TDM10 were used for pulldown of proteins with cell lysates and short term cultures. The images in Figures 5.18-5.20 show the pulldown results.

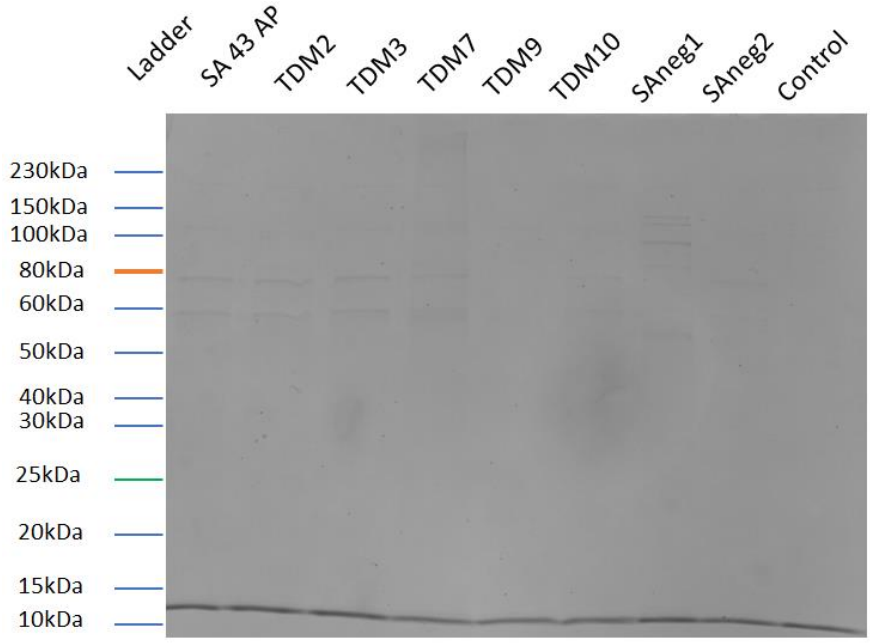

Figure 5.18 Aptamer assisted pulldown using SA and TDM aptamers with U87MG cell line.

Bands in the pulldown were detected in similar size range in SA43, TDM2, TDM3, TDM7 and TDM10. SANeg1 lane shows bands which are multiple in number and appear different to the other aptamer AP lanes. The control lane (no aptamer) was clear and confirms no non-specific binding.

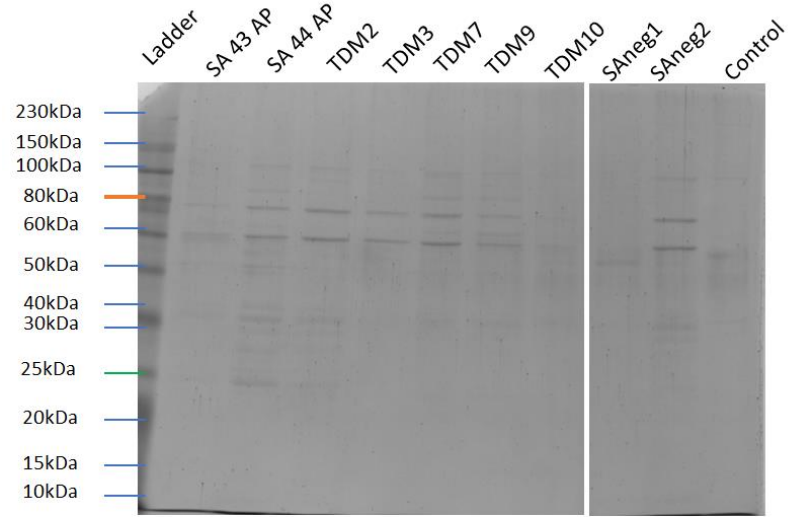

Figure 5.19 Aptamer assisted pulldown using SA and TDM aptamers with 1321N1 cell line.

Bands in the pulldown can be seen in similar range in SA43, TDM2, TDM3, TDM7 and TDM10. SANeg1 lane shows bands which are multiple in number and appear different to the other aptamer AP lane. The control lane (no aptamer) is clear and confirms no non-specific binding.

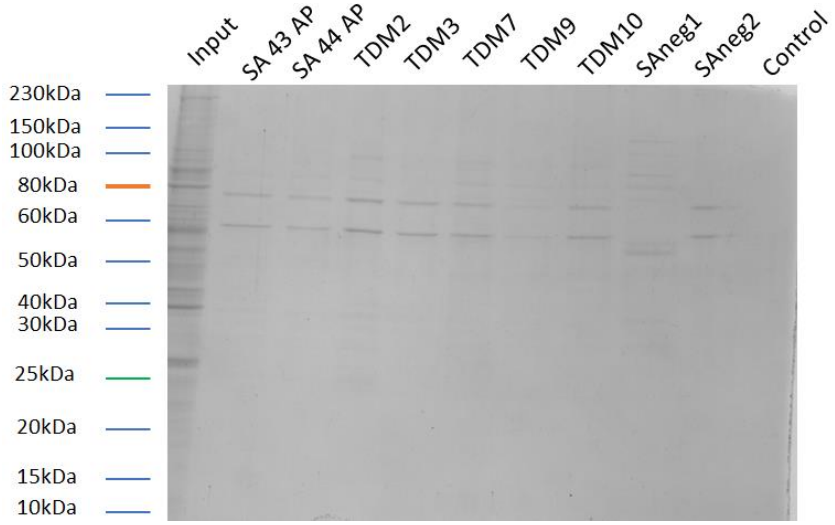

Figure 5.20 Aptamer assisted pulldown using SA and TDM aptamers with W2045 cell line.

Bands in the pulldown can be seen in similar range in SA43, TDM2, TDM3, TDM7 and TDM10. SANeg1 lane shows bands which are multiple in number and appear different to

the other aptamer AP lane. TDM9 shows faint bands. The control lane (no aptamer) is clear and confirms no non-specific binding.

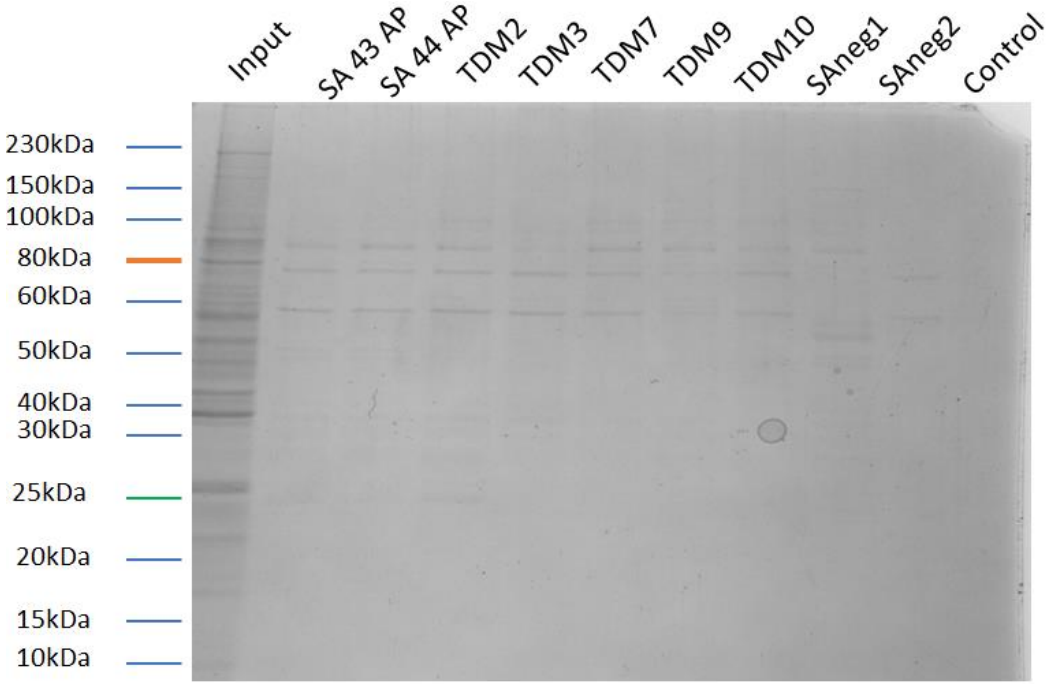

Figure 5.21 Aptamer assisted pulldown using SA and TDM aptamers with W859 cell line.

Bands in the pulldown) can be seen in similar range in SA43, TDM2, TDM3, TDM7 and TDM10. SANeg1 lane shows bands which are multiple in number and appear different to the other aptamer AP columns. TDM 9 shows faint bands but stronger presence compared to W2045. The control lane (no aptamer) is clear and confirms no non-specific binding.

The novel aptamer pulldown showed consistent bands seen between 60-100KDa and similar to pulldown with SA43 and SA44. There appeared to be less binding seen in TDM9 and TDM10 in the pulldowns as imaged. This was seen consistently across all the glial cell lines and short term cultures.

5.3.3.2 Aptamer computed structures using Mfold

Mfold (Zuker, 2003), a DNA and RNA folding web server was used to compare the structures of the SA aptamers and also the TDM aptamers used in the pulldown analysis

(Figures 5.22-5.30). Since the aptamers are single stranded DNA, they fold to form secondary structures and 'loops'. If a structure has greater number of predicted secondary structure, it is likely to be less specific. Though the final binding is due to a combination of hydrogen bonding and van der waals forces, the 'loop' in an aptamer is said to affect its affinity to binding targets (Feigon et al., 1996). 3D structure prediction of aptamers is also available in the form of SIMrna software and primarily predicting RNA structures (Genesilico, 2019).

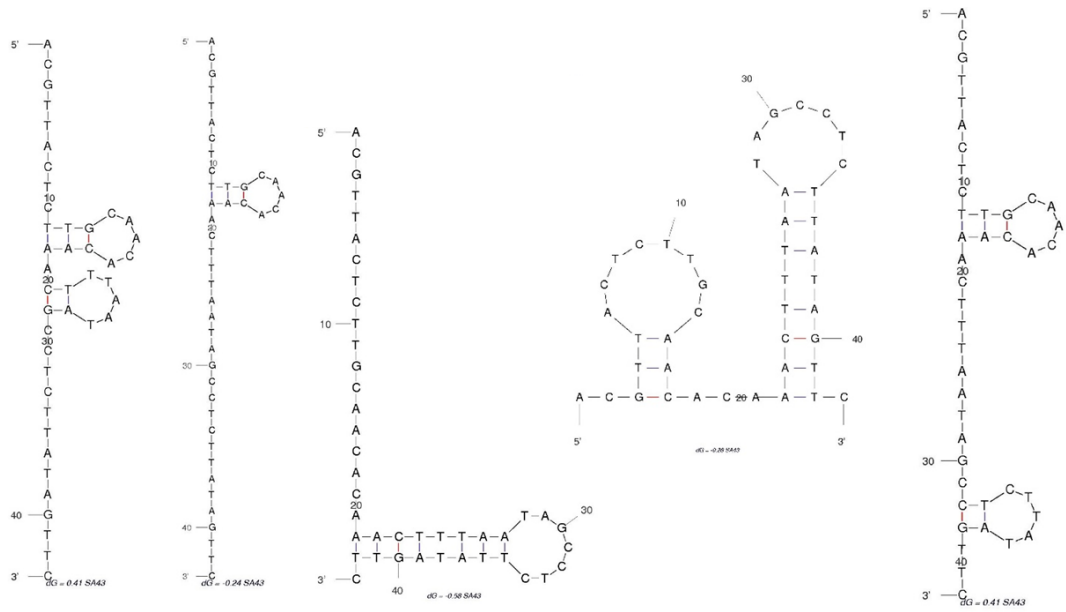

Figure 5.22 SA43 Mfold predicted structures

Five structures of the SA43 aptamer are predicted using Mfold software. The various predictions have differing dissociation and stability but not dissimilar to each other. The multiple structures does increase the chance of the aptamer being able to bind to various targets and not to one alone. Though the structures are 2D, the final 3D structure is what gives the aptamer ability to bind and target. Further analysis of the aptamer structure with SA44 showed that two of the predicted structures are similar as seen in figure 5.23.

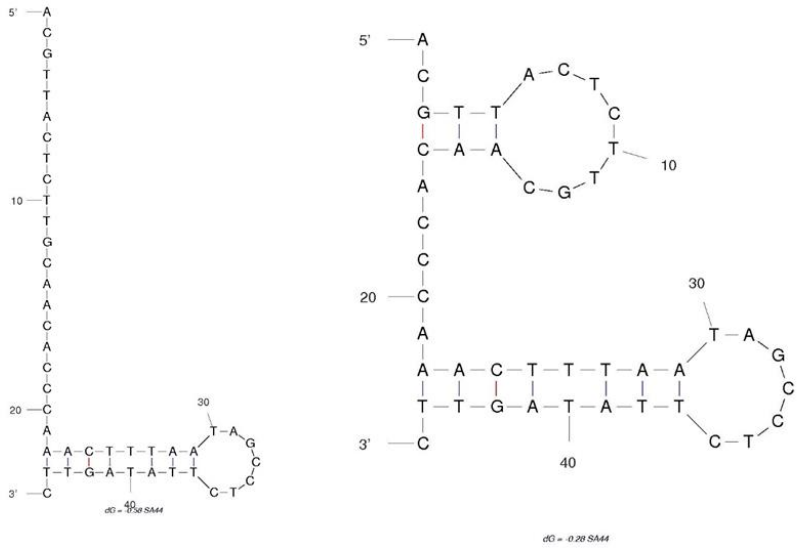

Figure 5.23 SA44 Mfold predicted structures

SA44 has two predicted 2D structures on mfold. Repeats of 'T-A-G-C-C-T' is seen in the loop part of the aptamer. This repeat is similar to two of the structures seen in the SA43 aptamer (figure 5.22 and figure 5.24 A and B). The loops are similar with similar repeats and hence the increased chances of binding to the same targets. SA44 though has only two predicted structures and the chances of the aptamer being more specific are higher. Despite the single nucleotide increase in the SA44 aptamer, both appear to bind to the same targets as per the protein gel electrophoresis. Final confirmation with the western blot and mass psectrometry will show if theybare identical in chapter 6.

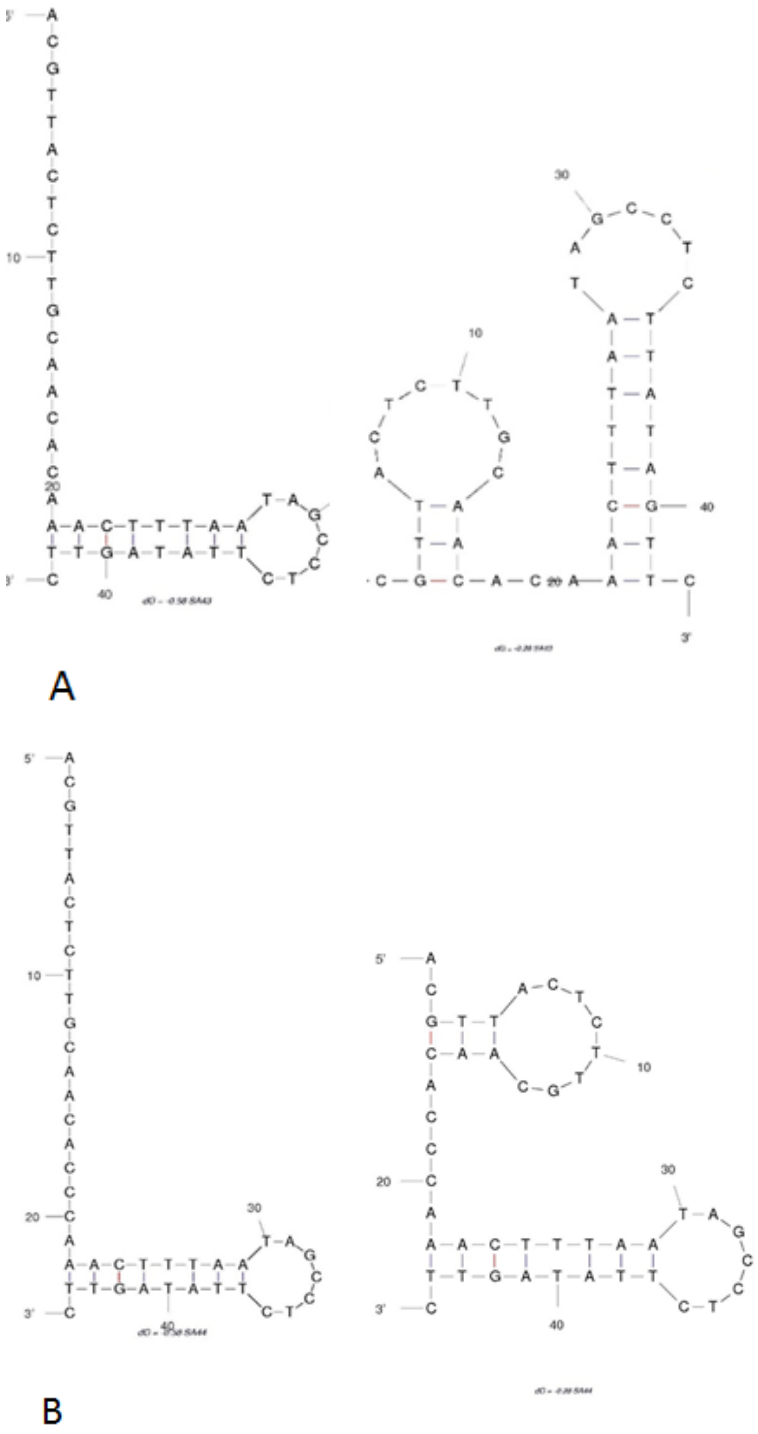

Figure 5.24 Comparison of aptamer structure e in SA43 (A) and SA44 (B)

'T-A-G-C-C-T' repeats seen in both SA43 (A) and SA44 (B) aptamer structures. The nucleotide stem in SA44 has one more nucleotide but eh rest of the sequence if the same.

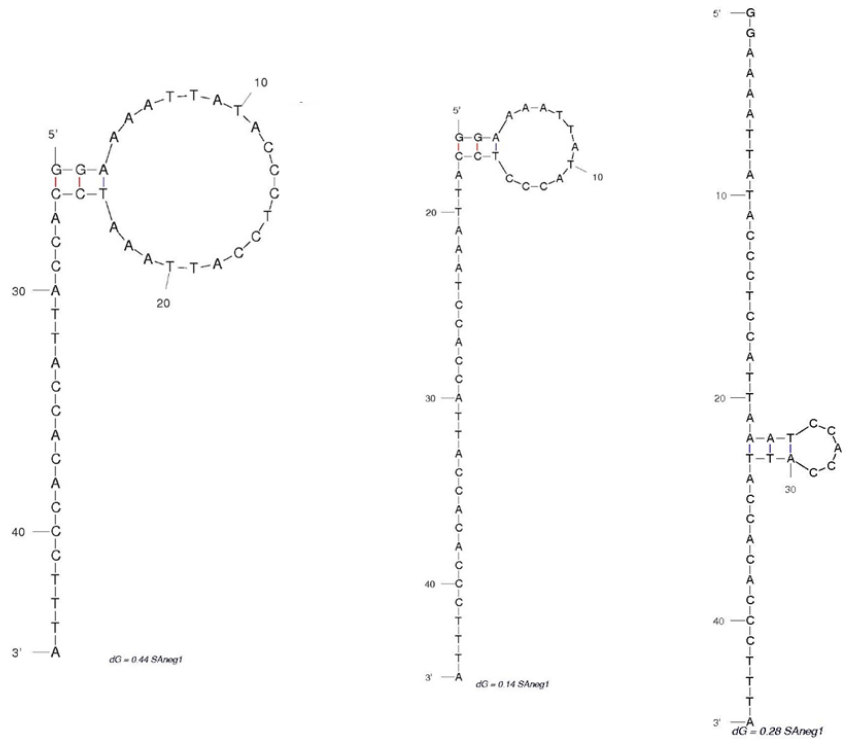

Figure 5.25 SANeg1 Mfold predicted structures

SANeg1 which was made inhouse has three predicted 2D structures, each with a single stem loop. The loops are not similar to the SA43 or SA44 aptamers.

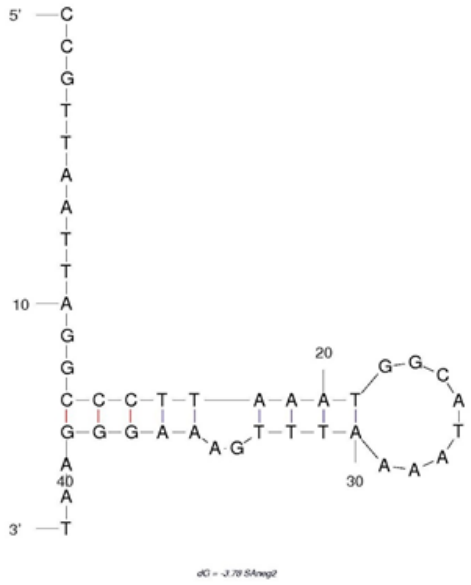

Figure 5.26 SANeg2 Mfold predicted structures

SANeg2 shows a single structure as predicted by Mfold consisting of a single stem loop. Due to the presence of a single structure, the aptamer is likely to be more specific to its target. The sequence does not share loops from SA43 or SA44.

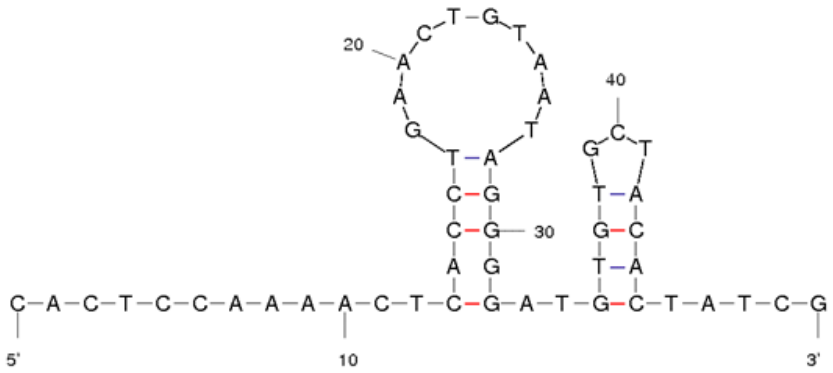

Figure 5.27 TDM2 Mfold predicted structures

TDM2, shows a single predicted structure on Mfold consisting of two stem loop structures. Due to the presence of a single structure, the aptamer is likely to be more specific to its target. The sequence does not share loops from SA43 or SA44.

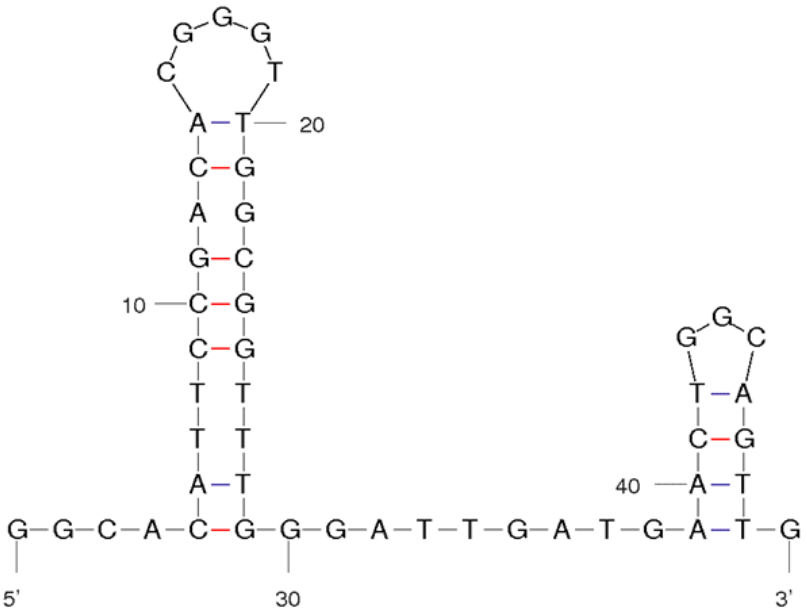

Figure 5.28 TDM3 Mfold predicted structures

TDM3 shows a single predicted structure on Mfold consisting of two stem loop structures. Due to the presence of a single structure, the aptamer is likely to be more specific to its target. The sequence does not share loops from SA43 or SA44.

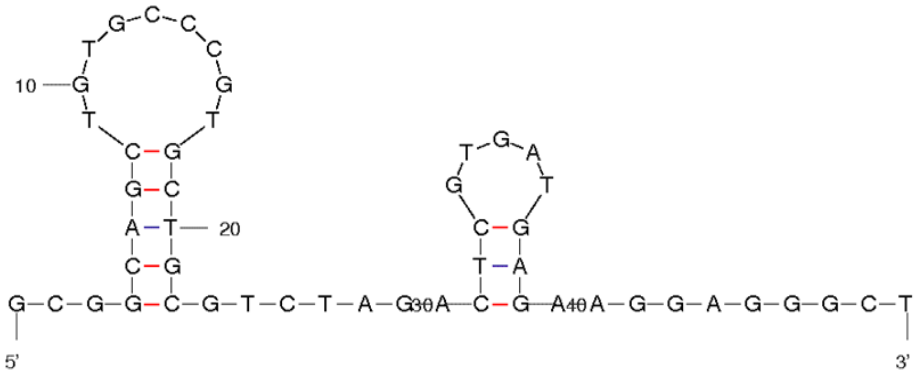

Figure 5.29 TDM7 Mfold predicted structures

TDM7 shows a single predicted structure on Mfold consisting of two stem loop structures. Due to the presence of a single structure, the aptamer is likely to be more specific to its target. The sequence does not share loops from SA43 or SA44.

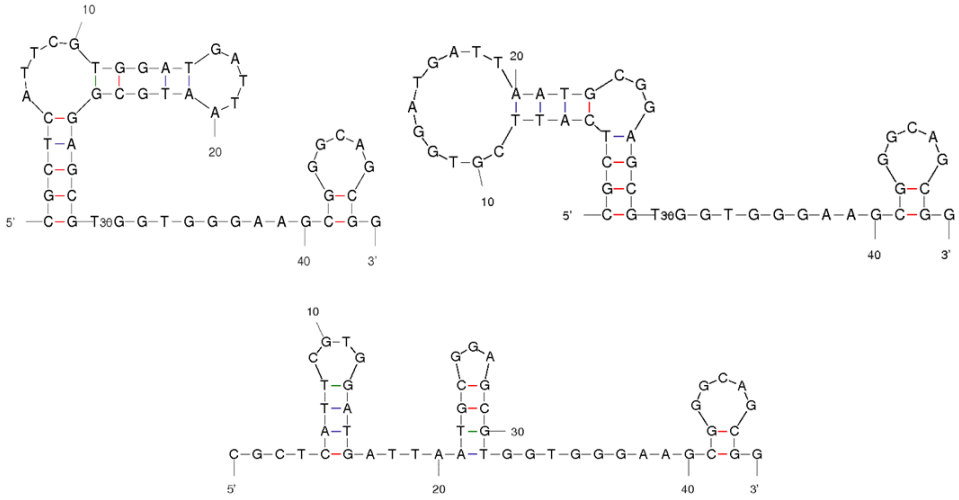

Figure 5.30 TDM9 Mfold predicted structures

TDM9 has three different predicted structures. The structures appear more complex with multiple loops present in each structure. The aptamer due to the various loops is likely to bind to different targets. The loops do not share nucleotide sequence with SA43 or SA44.

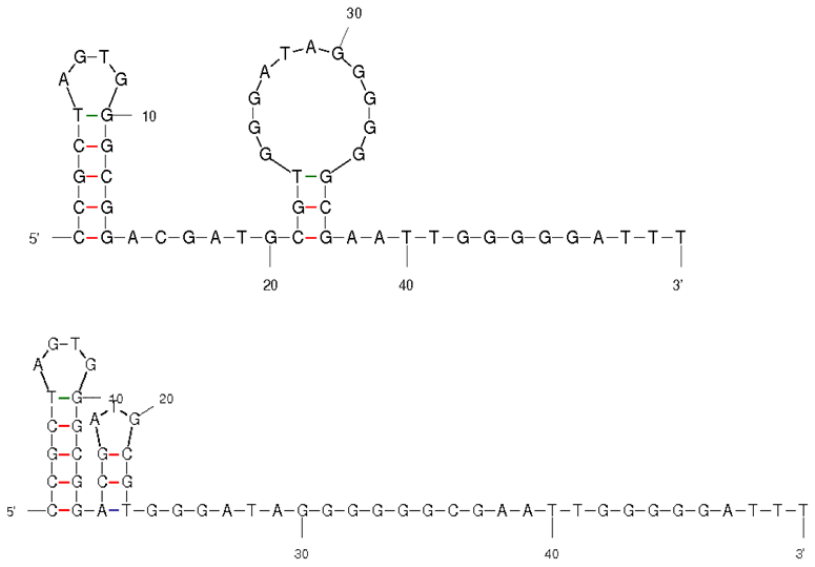

Figure 5.31 TDM10 Mfold predicted structures

TDM10 has two different predicted structures and each structure consists of two stem loops. The aptamer due to the various structures is likely to bind to different targets. The loops do not share nucleotide sequence with SA43 or SA44.

5.3.3.3 Structural comparison of aptamers

Common sequence in the loop structures is identified in the SA43 and SA44 aptamers as seen in figures 5.22, 5.23 and 5.24. The structures are predicted by Mfold based on ionic environment and temperature of folding. Typically, this is used for predicting RNA structures for mRNA binding. Binding is often associated with 'stem' and 'loop' structures, exposing critical sequences responsible for binding (Hofacker et al., 2002; Hofacker, 2004). When looking for the confirmation of the structure, it is likely one of the species is binding the target. This could be deduced by removal of bases and after loss for critical binding regions (Pan and Clawson, 2009) and described by 'crawling' method (Gopinath et al., 2017). The aptamer sequence is shortened to look for structural changes and when unchanged structurally can be used to look for similar

binding to target. In our research, the SA43 and SA44 aptamer showed similar sequences but the novel TDM aptamers had different stem and loops, thus implying the difficulty in predicting the final responsible sequence for target specificity. Since an aptamer binds with various binding affinities as detailed in section 1.5, the final target could be bound by multiple aptamers with different sequences but contain similar stem loop structures available for binding. Mathematical simulation of SELEX (Irvine et al., 1991; Levine and Nilsen-Hamilton, 2007) and the mathematical complexity of predicting aptamers towards multiple targets (Vant-Hull et al., 1998) does not take into account the stochastic effects of SELEX. It has also been shown that multiple target SELEX is likely not as useful as single target SELEX (Seo et al., 2010).

5.4 Proteomic analysis of pulldown proteins

Aptamer assisted pulldown of proteins from cell lines were sent for mass spectrometry proteomic analysis. The methodology was refined to ensure that aptamer bound proteins eluted from the streptavidin- agarose beads separated by gel electrophoresis were only present in the eluent (determined by corresponding clear lanes in the control gels). Initially, every protein band in the lane from the gel electrophoresis separation of aptamer assisted pulldown were excised and sent for proteomic analysis to identify the proteins. At later stages, only the consistent and most prominent bands were sent for replication of proteomic analysis to confirm results. Densitometry analysis of the aptamer pulldown was done on Geldoc™ imager (Bio-rad Laboratories Inc., Watford, UK) ™ imager (Bio-rad Laboratories Inc., Watford, UK) software with identified gel bands in the pulldown lanes. Mass spectrometry analysis of all the gel bands and blocks was performed at St Andrews University, Dundee.

5.4.1 Full proteomic analysis of aptamer assisted pulldown with SA43 aptamer in U87MG and 1321N1 cell lines

5.4.1.1 Pulldown from U87MG

Aptamer assisted pulldown with U87MG and 1321N1 cell lines were run on 10% polyacrylamide gels. These were then stained with Coomassie blue stain and imaged using Geldoc™ imager (Bio-rad Laboratories Inc., Watford, UK) ™ imager (Bio-rad Laboratories Inc., Watford, UK)™ imager (Bio-rad Laboratories Inc., Watford, UK) (figure 5.32).

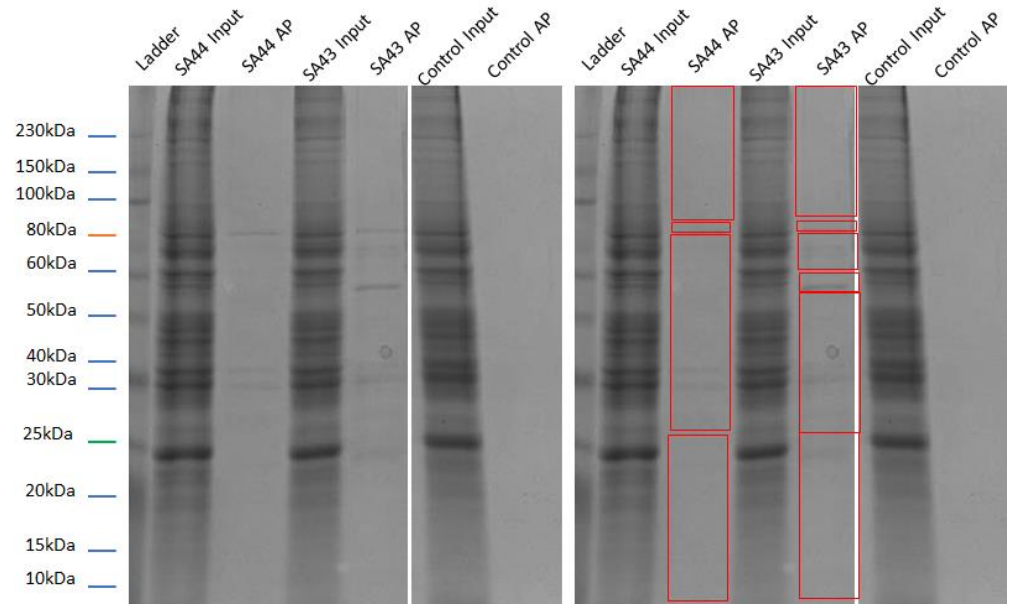

Figure 5.32 Aptamer assisted pulldown with SA44 and SA43 aptamers with U87MG cells.

The input lane shows the protein analysis of the cell lysate loaded onto the streptavidin-agarose beads, whereas the AP lane shows the protein analysis of eluent after aptamer assisted precipitation (AP). The two gel images are same and the second image on the right points to the specific identified bands and blocks sent for mass spectrometry. The control lane shows the same cell lysate that was loaded onto the agarose beads, but without any aptamers conjugated. The prominent bands and lane blocks, as indicated by red boxes, were sent for mass spectroscopy based proteomic analysis.

The aptamer pull-down columns were separated into segments and excised from the gels using sterile blades for each segment. The images in Figure 5.32 shows aptamer assisted pull-down of proteins in U87MG cell lines, using the SA43 and SA44 aptamers. Gel samples were prepared and digested with trypsin and peptides were analysed by LC-MS/MS mass spectrometry analysis (figure 5.33).

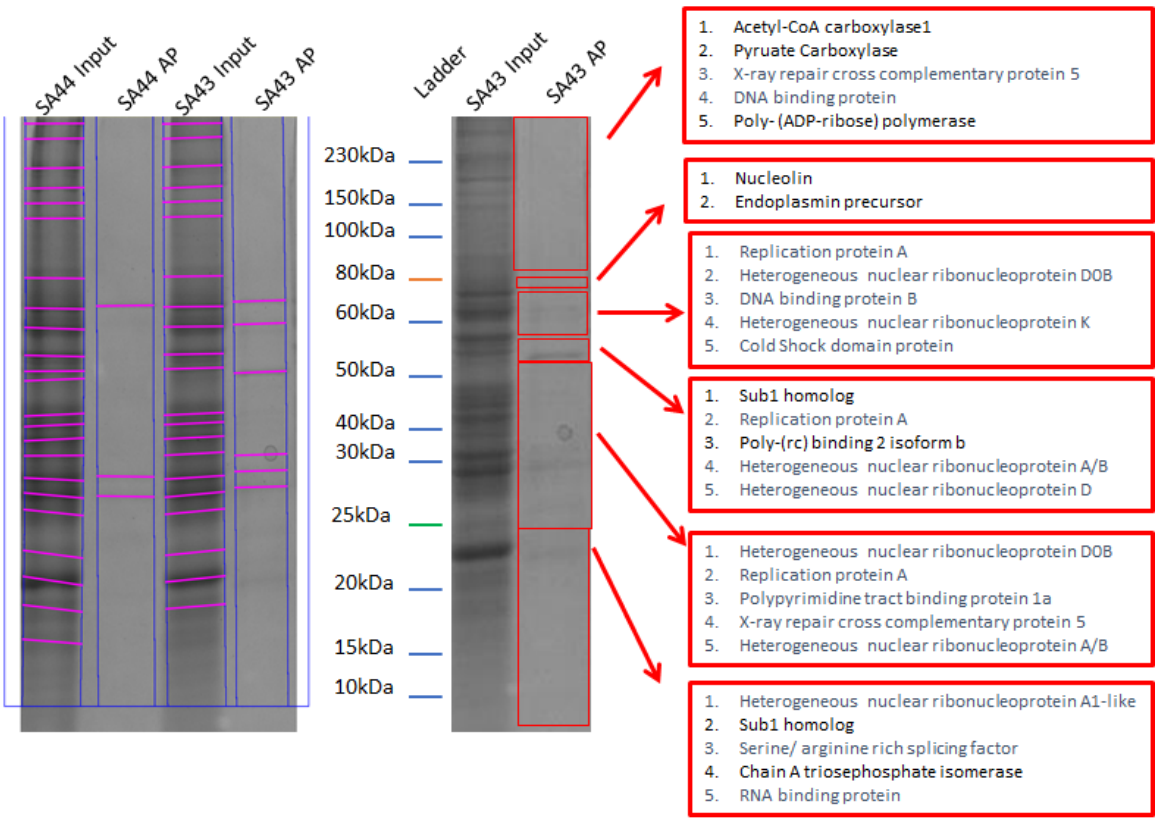

Figure 5.33 Densitometry and mass spectrometry analysis

Densitometry analysis of the SA44 and SA43 pulldown on Geldoc™ imager (Bio-rad Laboratories Inc., Watford, UK) ™ imager (Bio-rad Laboratories Inc., Watford, UK) software with identified gel bands in the pulldown lanes. Mass spectrometry analysis of the gel bands and the top 5 significant proteins hits for SA43 aptamer with U87MG cell line, performed at St Andrews University, Dundee. The terms in blue are all proteins with binding function. X-ray cross complementing (XRCC) protein 5 is Ku80 and Poly-(ADP-ribose) polymerase is PARP. X-ray cross complementing (XRCC) protein 6 is also known as Ku70.

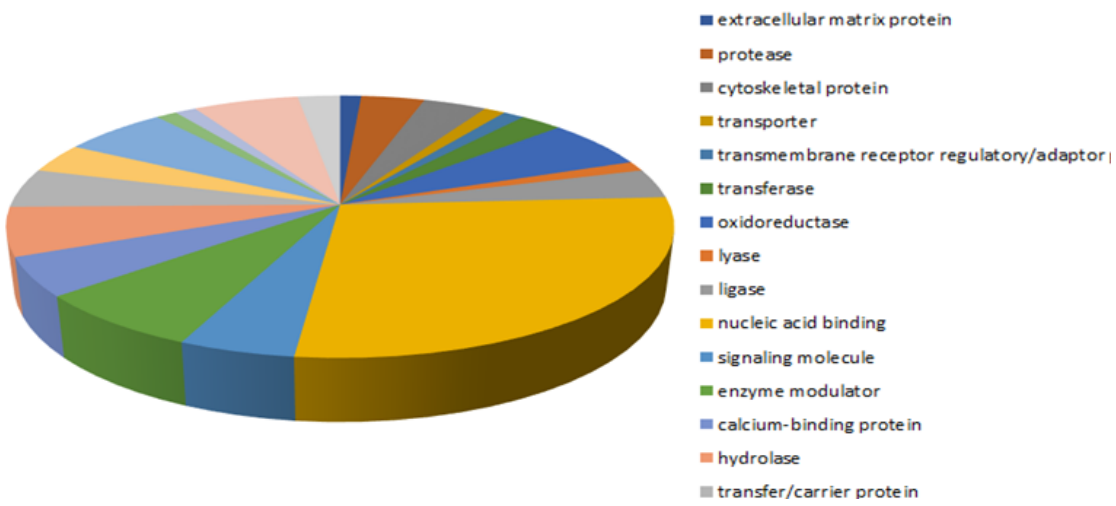

Figure 5.34 Protein analysis from SA43 aptamer and U87MG cell line.

Proteomic analysis from SA43 aptamer showed over a quarter of the binding is with nucleic acid binding proteins (orange sector) along with presence of cytoskeletal structure protein, transporters and transfer proteins amongst other hits.

The proteins were identified using Mascot software from matrix science with at least 2 peptides with 95% confidence and analysed using Panther protein classification software. The top five most abundant proteins identified for each gel fragment are shown in figure 5.33 with Panther analysis results (figure 5.34). Nucleic acid binding proteins were found to be in the highest content in the analysis (figure 5.34).

5.4.1.2 Pulldown from 1321N1

1321N1 cell line was also sent for mass spectroscopy analysis and the results were shown in Figures 5.35 for gel electrophoresis, Figure 5.36 for band excision and top five proteins identified and Figure 5.37 for Panther analysis. The sample were processed with the same protocol and stained using Coomassie blue.

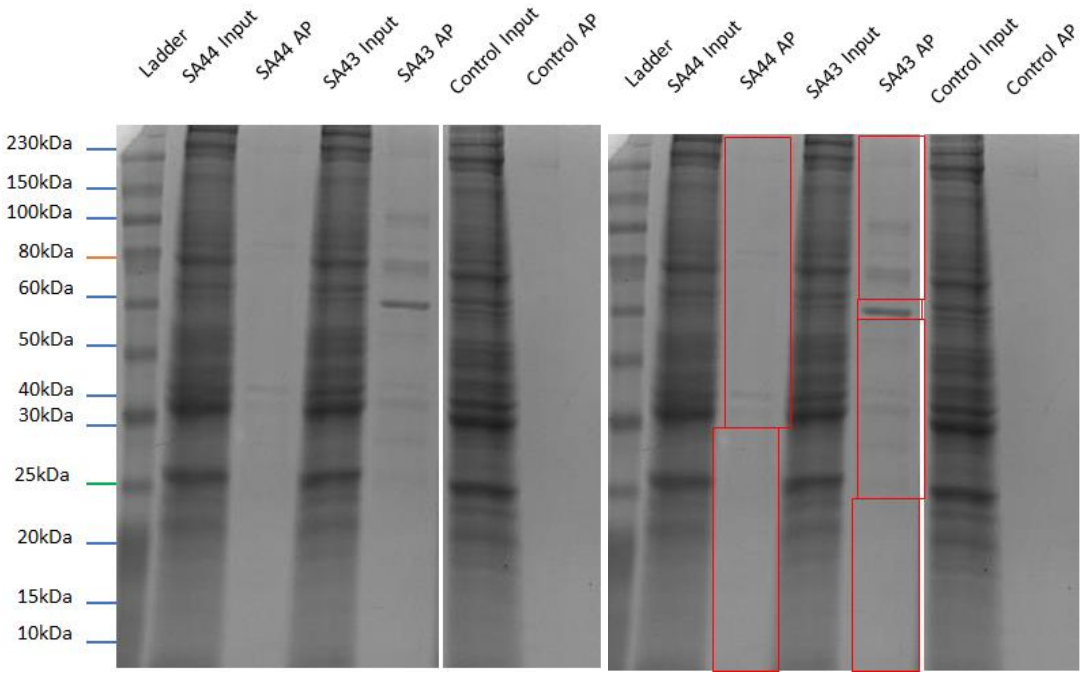

Figure 5.35 Aptamer assisted pulldown with SA44 and SA43 aptamers with 1321N1 cells.

The input lane shows the protein analysis of the cell lysate loaded onto the streptavidin-agarose beads, whereas the AP lane shows the protein analysis of eluent after aptamer assisted precipitation (AP) using SA43 and SA44 aptamer. The two gel images are same and the second image on the right points to the specific identified bands and blocks sent for mass spectrometry. The control lane shows the same cell lysate that was loaded onto the agarose beads, but without any aptamers conjugated. The prominent bands and lane blocks, as indicated by red boxes, were sent for mass spectroscopy based on Geldoc™ imager (Bio-rad Laboratories Inc., Watford, UK) ™ imager. The results of the mass spectrometry analysis are shown in image 5.36.

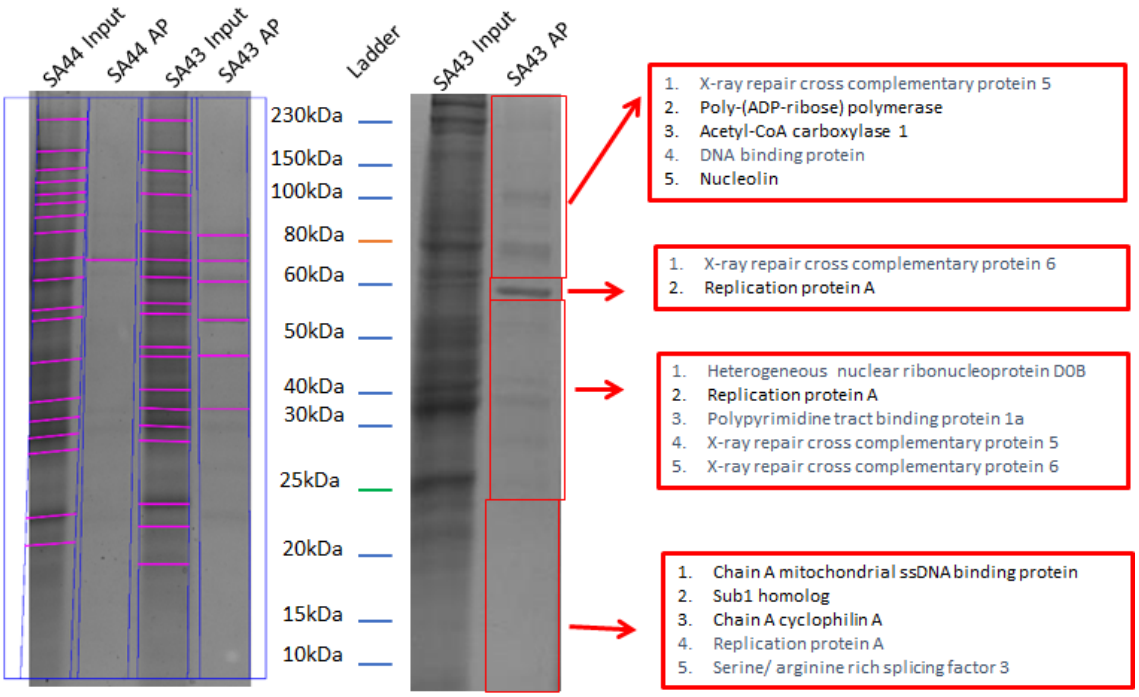

Figure 5.36 Densitometry analysis of SA43with 1321N1 cell line

SA43 and SA44 pulldown on Geldoc™ imager (Bio-rad Laboratories Inc., Watford, UK) ™ imager (Bio-rad Laboratories Inc., Watford, UK) software with identified gel bands in the pulldown lanes. Mass spectrometry analysis of the gel bands and the top 5 significant proteins hits for SA43 aptamer with 1321N1 cell line. The terms in blue are all proteins with binding function. XRCC 5 and XRCC 6 (Ku80 and ku70 respectively) and PARP were the significant hits in the pulldown as seen in the image above. Replication protein A was also seen along with nucleolin. Figure 5.37 shows the breakdown percentage of the proteins eluted with SA43 aptamer from figure 5.36.

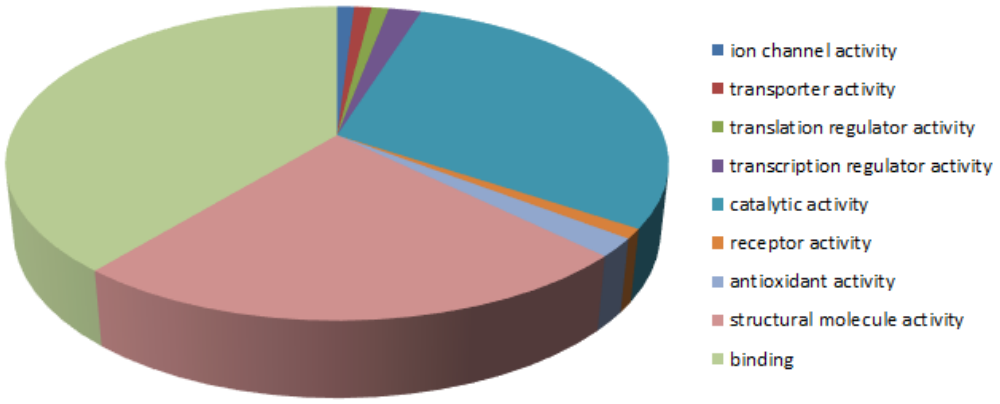

Figure 5.37 The splitting of the protein analysis from SA43 aptamer and 1321N1 cell line.

Over a quarter of the biding is with nucleic acid binding proteins (pink sector) along with presence of cytoskeletal structure protein, transporters and transfer proteins amongst other hits.

5.4.2 Analysis of pulldown results

5.4.2.1 Specific proteomic analysis of regions in U87MG cells

Subsequent pulldown was done with U87MG cells using SA43 and SA44 aptamers and sent for mass spectrometry analysis to confirm the targets of pulldown. Following method development and previous results, the analysis was limited to visualised protein bands of strong visibility and guided by the results of the first mass spectrometry analysis. Proteins of significance were found following repeat analysis of the same band from different aptamer-pulldowns, and were identified to be ku70 and ku80, as shown by the band between 60-80kDa in Figure 5.38. Ku70 and Ku80 and similar sized bands were detected on all subsequent gels involving SA43 and SA44 aptamers incubated with different glioma cells.

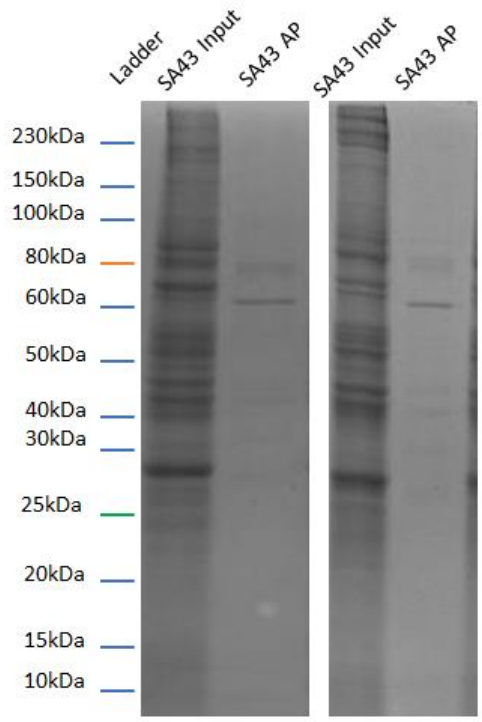

Figure 5.38 U87MG aptamer pulldown for mass spectrometry

Repeat aptamer assisted pulldown with SA43 and U87MG cell line twice showing consistent bands between 60 to 80kda. The bands were excised and sent for mass spectrometry analysis.

Further mass spectrometry analysis of the gel bands at 80kDa revealed XRCC5 (X-ray cross complementing protein 5), also known as Ku80 to be enriched along with the presence of cytokeratin fragments. Gel bands at the region of approximately 60kDa came back as XRCC6 (X-ray cross complementing protein 6, also known as Ku70) in both repeats of mass spectrometry analysis of pulldown and replication protein A with molecular weight of 70kDa.

5.4.2.2 Analysis of aptamer assisted pulldown in other cell lines

To further strengthen the robustness of the results and methodology of the technique, aptamer assisted pulldown using SA43 and SA44 aptamers was performed on other short term cultures derived from patient tissue. Cell lines BTNW 911 and BTNW 914

were used along with W859 and W2045 short term cultures, sourced from the University of Wolverhampton. The results of the gel electrophoresis separation of proteins eluted from the aptamer pull-down are shown below.

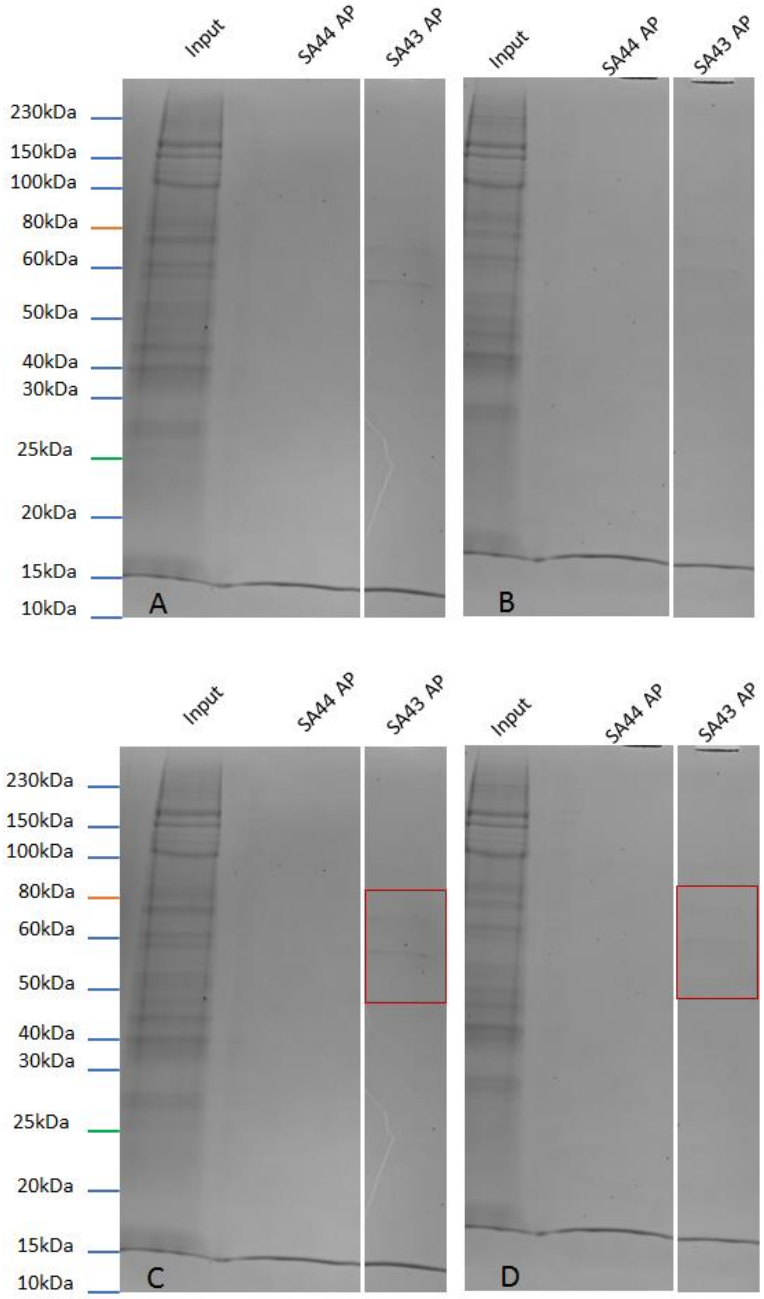

Figure 5.39 Aptamer assisted pulldown with BTNW short term cultures

Aptamer-assisted pulldown with SA44 and SA43 aptamer with BTNW 911 (image A) and BTNW 914 (image B). Images C and D show the gel blocks excised and sent for mass spectrometry analysis. A larger area was excised due to faint bands and possibility of crossover while cutting bands.

The analysis revealed presence of Ku70 and Ku80 in the gel blocks sent for both tissue derived cell lines along with presence of unidentified proteins on the mass spectrometry analysis. For the first time, poly ADP-ribose polymerase (PARP) was isolated as a significant hit along with ku80 in BTNW 911 and SA43 assisted pulldown. Due to the nature of short-term cultures and their growth characteristics, this experiment was performed twice and mass spectrometry was performed once.

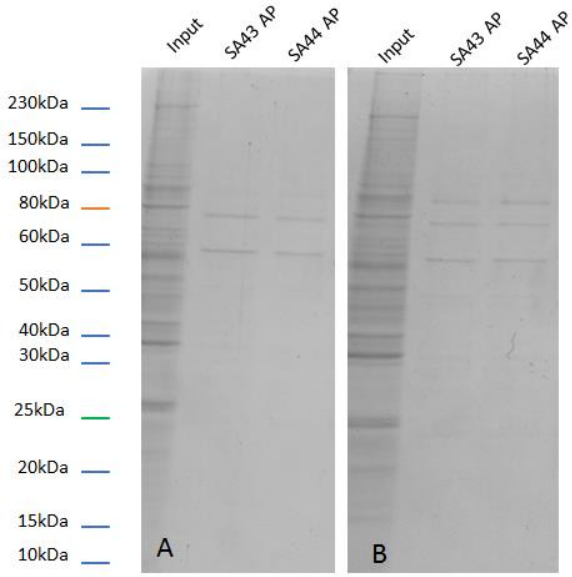

Figure 5.40 Aptamer assisted pulldown with Wolverhampton cell lines

Aptamer assisted pulldown with SA43 and SA44 and short term cultures W2045 (A) and W859 (B). Both pulldowns showed bands between 60-100kDa.

Due to the nature of short term cultures and growth curves, this was performed once and the proteomic analysis was not performed with SA43 and SA44 but other aptamers as seen in the next section with short term cultures W2045 and W859.

5.4.3 Analysis of aptamer assisted pulldown using novel aptamers

Novel aptamers with TDM prefix were generated in house by SELEX in a parallel project under similar conditions to the SA aptamer but with a different negative selection. The results from the TDM aptamers are detailed in the figures 5.41, 5.42 and 5.43.

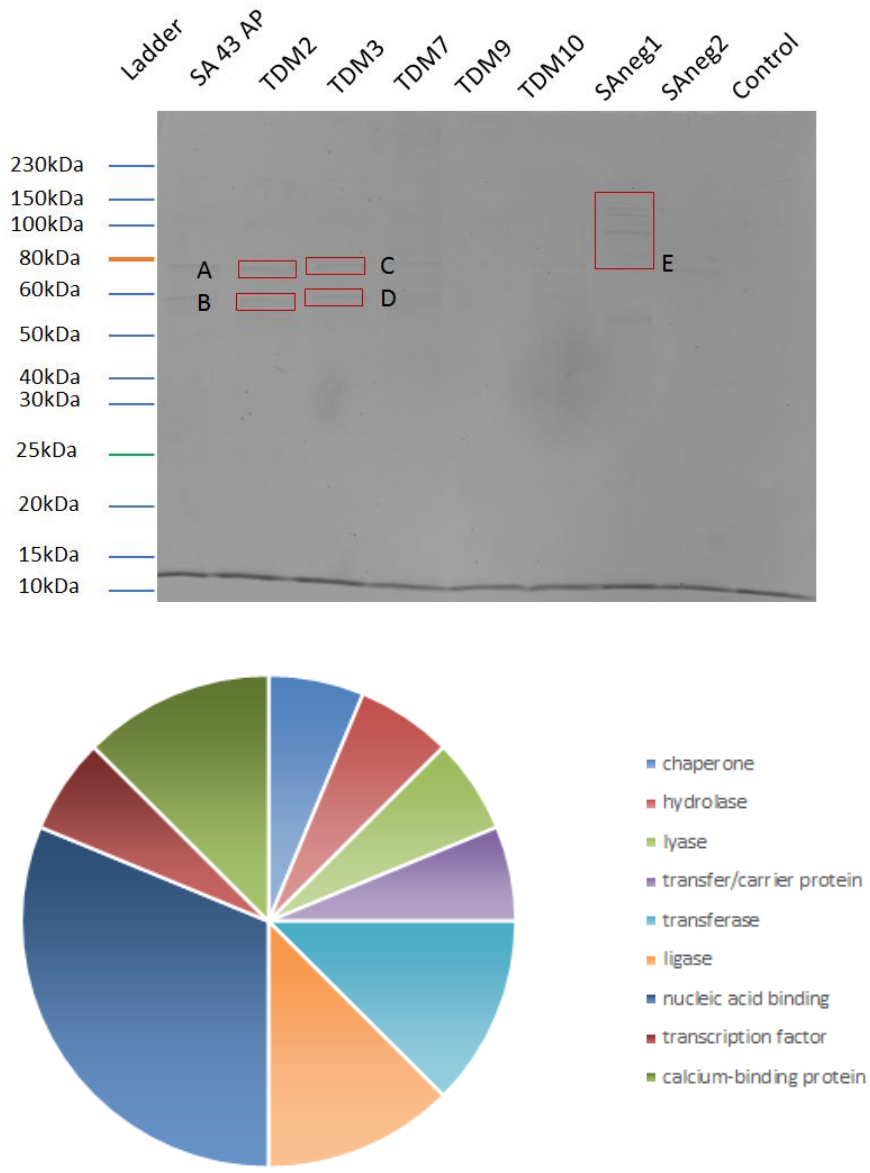

Figure 5.41 Aptamer-assisted pulldown using SA and TDM aptamers with U87MG cell line.

Block A to E as labelled were sent for mass spectrometry analysis. Gel bands A and C exclusively showed presence of ku80 along with contaminant cytokeratin of human origin on mass spectrometry analysis. Gel bands B showed Ku70 exclusively of human origin. Gel band D showed maximal presence of Ku70 and an isoform of Ku70. Pie chart showing the protein class distribution from SAneg1, block E. DNA helicase Q1 was also isolated, which is responsible for DNA repair. Gel block E showed highest signal of 100kDa coactivator or SND1 (staphylococcal nuclease domain containing protein 1), responsible for mRNA function. Vigilin, an RNA binding protein responsible for fat metabolism was the second most significant.

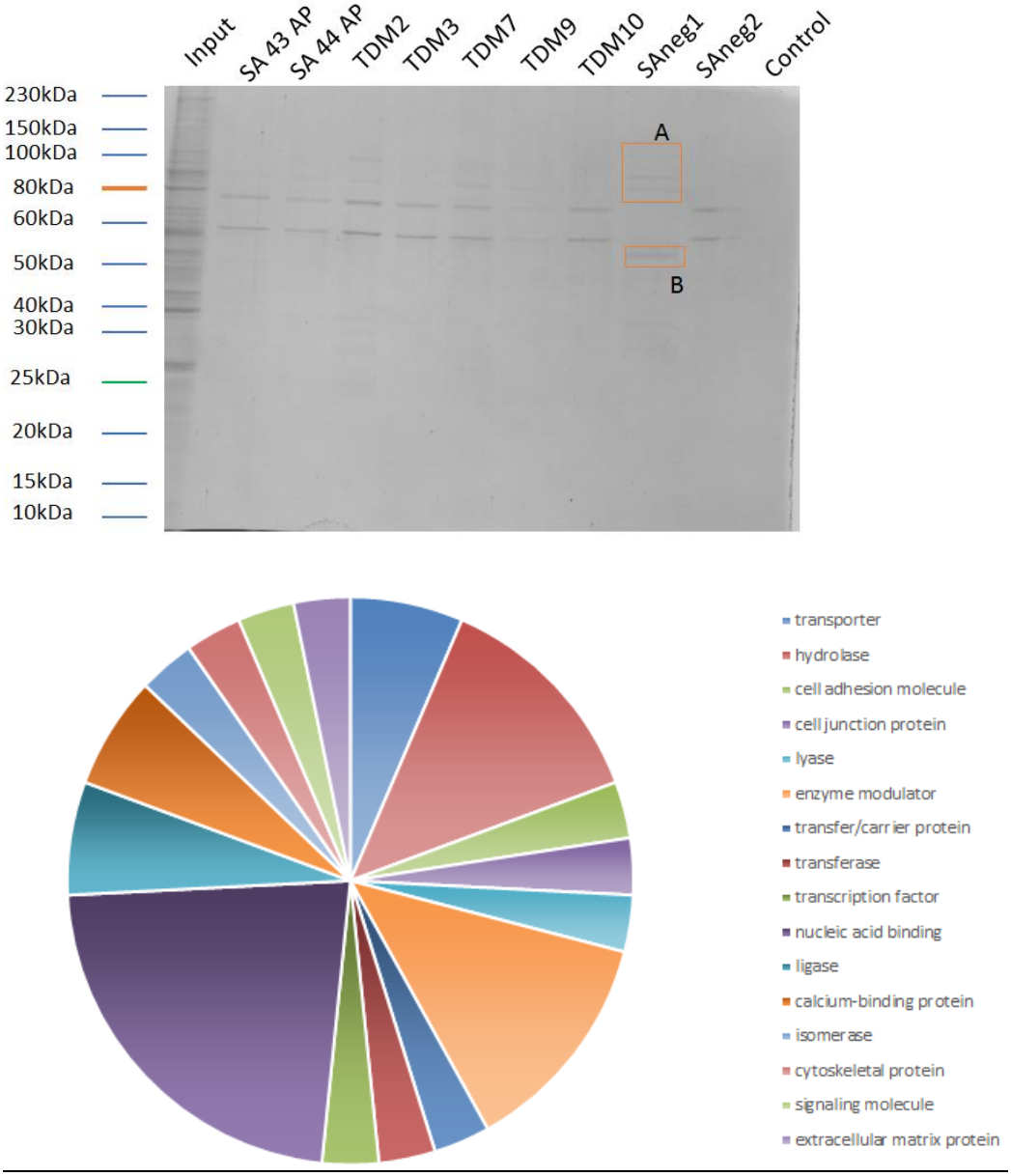

Figure 5.42 Aptamer assisted pulldown with W2045 short term culture.

SA43 and SA44 aptamers along with TDM aptamers were used for the pulldown. Red blocks marked as A and B were the gel segments sent for mass spectrometry analysis. Gel block A showed presence of vigilin and 100kDa coactivator with highest significant matches as seen with U87MG in figure 5.40. Pie chart showing the protein class distribution using panther analysis for SAneg1, block A. Other isolated proteins included transporter proteins and unnamed proteins of human origin. Gel band B showed heterogeneous nuclear ribonucleoprotein K as most significant, which is responsible for nuclear metabolism of mRNA.

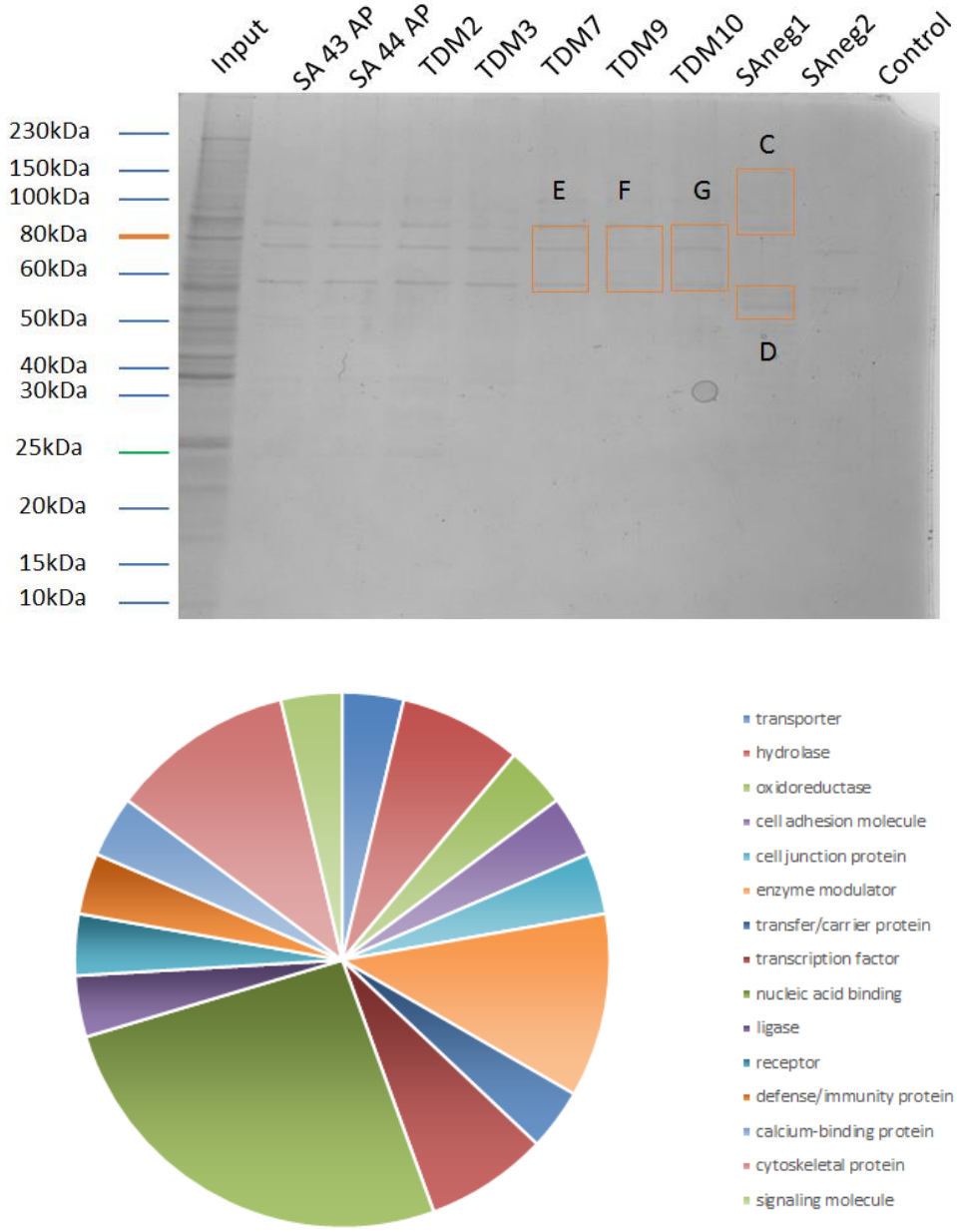

Figure 5.43 Aptamer assisted pulldown with W859 short term culture.

SA43 and SA44 aptamers along with TDM aptamers were used for the pulldown. Red blocks marked as C, D, E, F and G were the gel blocks sent for mass spectrometry analysis. Gel block E showed Ku70 and Ku80 as seen in earlier mass spectrometry analysis along with nucleolin, replication protein A and PARP as significant hits. Gel block F and G also showed ku70 and ku80 with replication protein A and PARP with less significance. Pie chart showing the protein class distribution using panther analysis for SAneg1, block C. Gel block C showed vigilin and 100kda coactivator as seen in figure 5.40 and figure 5.41. Gel block D again showed heterogeneous nuclear ribonucleoprotein K as most significant, similar to figure 5.41 in W2045 cell culture.

The TDM aptamers were generated towards U87MG cells and were included in the research project to further support and validate the results. The aptamer pulldown results from U87MG cell lines using selected TDM aptamers as shown in Figure 5.41 with blocks sent (Figure 5.18 without blocks marked of the same gel image) and from Wolverhampton cells in Figures 5.42 and 5.43, shows the similar pulldown results. TDM aptamers appear to bind to the same targets whereas the SANeg1 does not show binding to ku70 and ku80.

The mass spectrometry analysis of SANeg1 shows that it is consistently pulling a different subset of proteins and thus is a good and valid control with three repeats with different cell cultures.

5.5 Discussion

In chapter 4, we confirmed the binding affinity of the Cy3 tagged aptamers to glioma cell lines. Replacing biotin tag on the aptamers and incubation with fixed cells also showed good binding results. This reconfirmed the basis of the current chapter, to employ the biotin and streptavidin affinity and achieve a pulldown of the target epitope.

Before attempting pulldown, Optimal protein extraction from cells was required. The first step in working towards achieving a pulldown is to have consistent, good quality protein or target moiety. If the protein extraction varies, it can affect the development of the aptamer pulldown and give false positive results. The first attempts were made using fixed cells. The initial intention was to crosslink the reacted aptamer and hence reduce the chances of loss of the relevant target downstream from treatment, an adaptation directly from ChIP. Pre-reacting and crosslinking did not work due to varying degree of cross linking. Once crosslinked, aptamer linked biotin itself became

crosslinked and hence unavailable for binding to streptavidin. Biotin and streptavidin binding is the basis for DAB staining and ChIP. Reversal of crosslinking required harsh treatments and poor quality of protein as seen in the figures 5.7 and 5.8 when compared to unfixed cells. Though heat treatment of the reversal of crosslinking did show results (figure 5.10), the quality of bands on gel remained poorer than unfixed cells. It also left the aptamer in a non-physiological state due to the heat reversal of crosslinking. The poor protein content was also evident on Bradford assays and protein samples on gels as in figure 5.8 and 5.10. Protein extraction with unfixed cells is widely used for most mammalian research and has established protocols.

RIPA and triton X100 gave the most consistent results of protein extraction with least amount of stress to the cells in an unfixed state. RIPA and triton X100 gave comparable results of protein extraction with unfixed cells. After further review and analysis triton X100 was utilised for protein extraction due to be least interfering with protein assays and to keep the targets in its native state (Labeta et al., 1988). RIPA also has a good action for releasing greater nuclear content when compared to triton X100. Due to the presence of staining in chapter 4 in both cytoplasm and nucleus, it was felt that the likely target is expressed both in cytoplasm and nucleus. Though it was also known that the aptamer uptake is an active process, the likelihood of the target being cytoplasmic and on cell surface was greater. Hence, triton X100 was also chosen due to relative reduced nuclear content lysis in triton X100 compare to RIPA.

The pulldown method was the next step developed and utilised for aptamer assisted pulldown of proteins in section 5.3. Native Streptavidin-biotin affinity was adapter from ChIP (Aparicio et al., 2004) and utilised for developing the pull-down technique for aptamer assisted precipitation. Magnetic beads were first utilised due to assisted

sedimentation but due to excessive non-specific pull-down as in figure 5.11, streptavidin-agarose beads were utilised for further method development. After optimising washing steps, U87MG showed pull-down of specific bands as in figure 5.12 with SA43 and SA44. The method was repeated thrice to confirm repeatability and to eliminate non-specific pulldowns. After establishing the protocol with U87MG cell line, it was then applied for 1321N1 and SVGp12 cell lines to confirm the method robustness. Consistent repeat pull-down with U87MG, 1321N1 and SVGp12 cell lines confirmed optimisation of method and it was further expanded to test on short term cultures. The aptamer pulldown on all three cell lines U87MG, 1321N1 and SVGp12, all showed bands in similar molecular weight distribution between 100 to 60 kda. This was interesting to note as binding had been seen in SVGp12 cell line as well and it was not clear if the binding targets were same.

To further confirm the stability of the method, it was applied to short term cultures with exact same steps. Short term cultures BTNW911 and BTNW914 showed pull-down as in figure 5.15 and 5.16. Due to the nature of the short term cultures, repeat experiments could not be performed and target bands were faint. But the bands were also seen in the same distribution as the glioma cells lines, thus increasing the potential of the work. Wolverhampton cell lines W2045 and W859 were then used to test the aptamer and method and showed consistent pull-down at 60-100kDa (figure 5.17). the pulldown bands were verified later in chapter 5.4 with mass spectrometry and the targets confirmed to be Ku70 and ku80.

The aptamers used until now were sequences which had been truncated from Cerchia *et al*. Aptamer pull-down was the performed with novel aptamers and SANeg1 and SAneg2 aptamers with the cell lines and short term cultures to expand the results and

confirm the method development. The pull-down with SAneg1 showed bands at different molecular weight compared to the rest of the aptamers, SA and TDMs as seen in figures 5.18, 5.19 and 5.20. SAneg1 and all the other aptamer pulldown bands were then sent for mass spectroscopy to St Andrews university, Dundee for confirmation of targets as in section 5.4.

Aptamer structures were reviewed with Mfold (Zuker, 2003), open software for predicted aptamer structures. Aptamers due to being single stranded, bend and fold to form different structures and loops. The loops are formed in the aptamer and said to influence the binding to targets (Feigon et al., 1996). Hence, if the loops are similar, it is possible that the aptamers with two slightly different sequences can still bind to the same target. This is evident with the SA44 and SA443 aptamer which have a difference of only one nucleotide. The aptamers finally bind in a 3D structure under covalent bonding and van der waals forces. Common patterns were found in SA43 and SA44 as expected. SA43 aptamer could fold into five different 2D structures (figure 5.22) whereas SA44 only had two 2D structures (figure 5.23). The SA44 structures are identical to two of the SA43 structures and can explain the similarity in pulldown results. But SA43 is also the only aptamer which showed pulldown of PARP (section 5.4). It is hence likely that one of the other structure binds to PARP and the aptamer is in a state of different stoichiometry.

SANeg1 aptamer showed three different structures and did not show any similar loops like SA43 or SA44 aptamer (figure 5.24). SANeg2, TDM2, TDM3 and TDM7 instead showed only single predicted 2D structures of the aptamers and showed binding to the target. TDM9 and TDM10 aptamers have more than one predicted 2D structure and still showed binding to ku70 and ku80.The novel aptamers though do not share any loop

patterns but still showed similar pulldown and confirmed later with mass spectrometry. Despite having different structures, the targets pulled were similar though the aptamers with single predicted 2D structure had most abundant target as ku70 and ku80.

Mass spectrometry gives a report of target "hits" in the results. Interpretation of the data requires caution, as the true target ligands can be masked by other proteins and protein complexes that have been pulled with the target. The gel bands and blocks were sent for mass spectrometry and showed consistent presence of Ku70 and Ku80 with SA43, SA44, SAneg2 and TDM aptamers with all cell lines and short term cultures. The only aptamer which showed different bands in the pulldown and consistently, was SANeg1. The gel bands for SANeg1 were also sent for mass spectrometry and consistently showed pulldown of vigilin and 100kDa coactivator protein, with molecular weight of 140kDa and 100kDa, respectively. Despite the application of the same method and against all the cells lines used, SAneg1 pulldown was different every single time. This thus confirmed that the aptamer binding is specific in the glioma cell lines and short term cultures to the aptamers and novels aptamers except SANeg1. SANeg1 thus was a valid control.

The proteomic analysis also pulled down a lot of other proteins but ku70 and ku80 were amongst the highest in terms of presence and consistency. Ku70 and ku80 being DNA repair proteins were the most abundant and likely target for the aptamer. Poly ADP ribose or PARP was also detected in the pulldown with the SA43 aptamer. When the spectrometry analysis of the aptamers was compared against each other only SA43 appeared to pulldown PARP as well and seen in U87MG, 1321N1 and also BTNW 911 cell line. PARP are a family of enzymes that have the ability to transfer ADP-ribose to target proteins. PARP plays important roles in cellular processes including DNA repair in

homologous repair mechanisms (Morales et al., 2014) and likely involved in other cancer types (Fulton et al., 2017; Miller et al., 2019; Robson et al., 2019).

Replication protein A, a 70 kda subunit was also identified in some pulldowns. Replication protein A is involved in keeping the single stranded DNA straight and to prevent from forming loops and has also been identified as a potential target to developing therapies (Zou et al., 2006; Liu and Huang, 2016).

Multiple other proteins, nucleolin and cytokeratin structures were pulled down with SA43 and SA44 aptamers but were not significant due to not being reproducible in other pulldowns. TDM2 TDM3 and TDM7 mainly showed pulldown of ku70 and ku80 proteins and were more significant in producing consistent, specific pulldown when compared to SA43 and SA44.

Ku70 and Ku80 were the most consistent and abundant proteins detected on mass spectrometry with the aptamers except SANeg1. Further research into publications showed increased ku70 and ku80 expression in various cancers and the presence in DSB repair pathway via NHEJ. Hence, they became the main focus for confirmatory experiments. Confirmation of the results was needed and expanded in chapter 6 with western blotting and knockdown analysis for Ku70 and Ku80.

Chapter 6

6 Verification of aptamer assisted pulldown

6.1.1 Introduction

In the previous chapter, optimal protein extraction was developed using triton X100 for cell lysis which was then used for aptamer assisted pulldown of epitopes. These pull-downs were run on 10% SDS PAGE gels, and then sections of gel were excised and sent for mass spectroscopy analysis at St Andrews University, Dundee. Initial pull-downs had entire columns sent for mass spectrometry. At later stages, consistent bands at 70 – 80 Kda pointed towards the greater possibility of Ku70 and Ku80 proteins being the primary target of the aptamers.

Ku70 and Ku80 exist as a heterodimer protein in the cell nucleus. This is present during Non-homologous end joining (NHEJ) (Moore and Haber, 1996) or cell division. NHEJ is a form of DNA repair where homology of the DNA ends is not needed for division and repair (Moore and Haber, 1996). The Ku heterodimer is present normally in the cell nucleus. There is also supported evidence to suggest that due to over detection, these proteins are present in the cytoplasm of the cells and also expressed on the cell surface (Prabhakar et al., 1990; Dalziel et al., 1992; Persson et al., 2010).

Presence of these proteins on the cell surface would support the notion the Ku heterodimer as a potential therapeutic target for glioma. To move forward, it is essential to confirm the results of the pulldown and mass spectroscopy. The aim of this chapter is to confirm the aptamers targets as Ku70/80 heterodimer in glioma cell lines and short-term cultures.

6.1.2 Ku70 and Ku80 detection in Commercial cell lines

Mass spectroscopy analysis supported abundant presence and pulldown of Ku70 and Ku80 protein when compared to whole cell lysate. This prompted the first experiment to evaluate detection of Ku70 and Ku80 in commercial cell lines. Cell cultures were grown to 80% confluence in chamber slides and fixed with 4% PFA. They were then permeabilised and subjected to immunostaining with anti Ku70 and Ku80 antibodies. Two sets of immunostaining were performed; one set utilising anti Ku70 and Ku80 biotin tagged secondary antibody, and the other utilised an Alexa 488 anti Ku70 or Ku80 secondary antibody. A primary isotope control antibody was utilised for both the experiments.

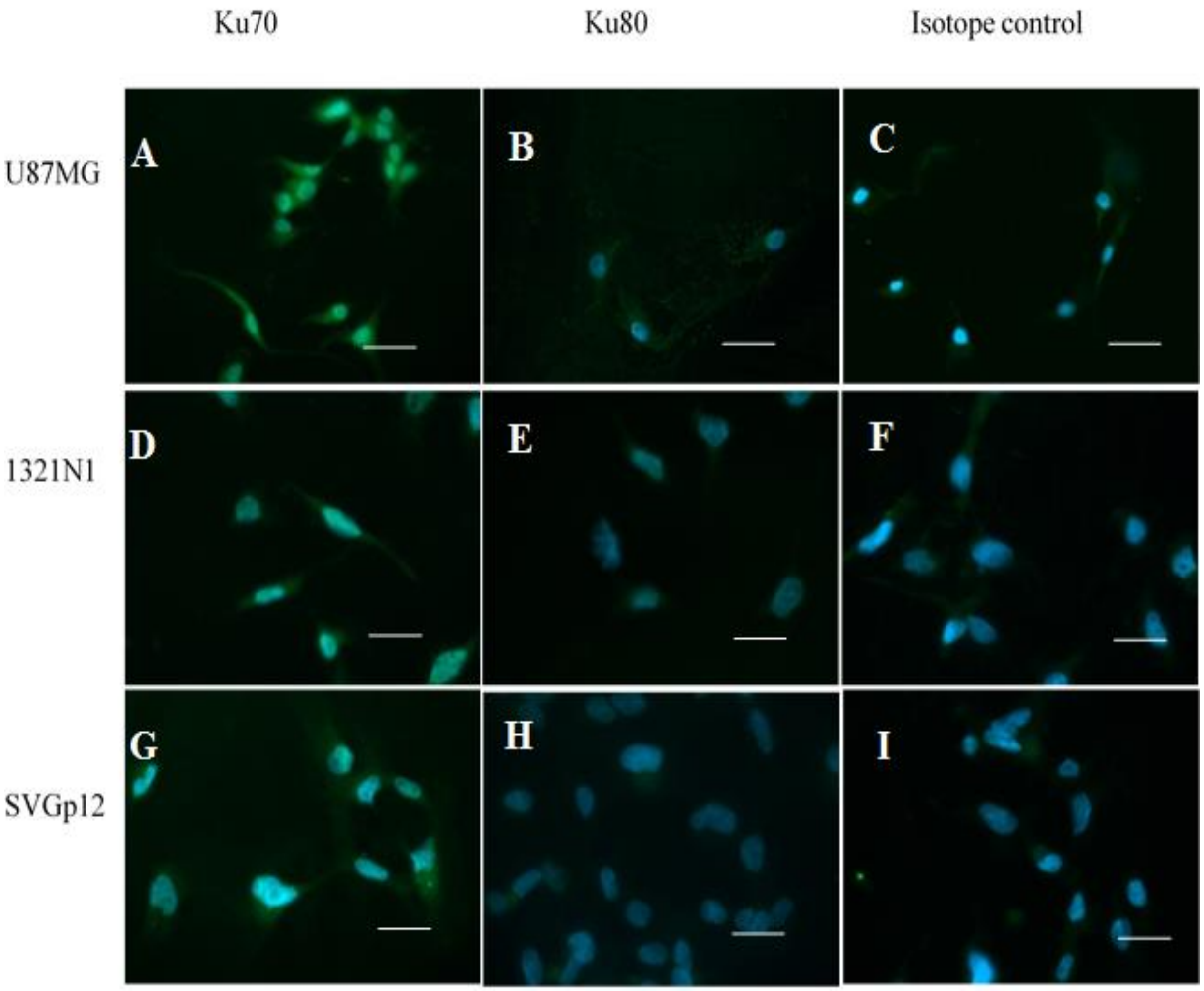

Figure 6.1 Ku70 and Ku80 detection in U87MG, 1321N1 and SVGp12 cell lines.

Ku70 detection is high in U87MG cells compared to 1321N1 and SVGp12 (A, D and G). Detection is seen in the nucleus and cytoplasm of all cell lines. Ku 80 detection is higher in U87MG and 1321N1 compared to SVGp12 (B, E and H) and is detected in the nucleus and cytoplasm of the cells. The scale bar represents 50µm.

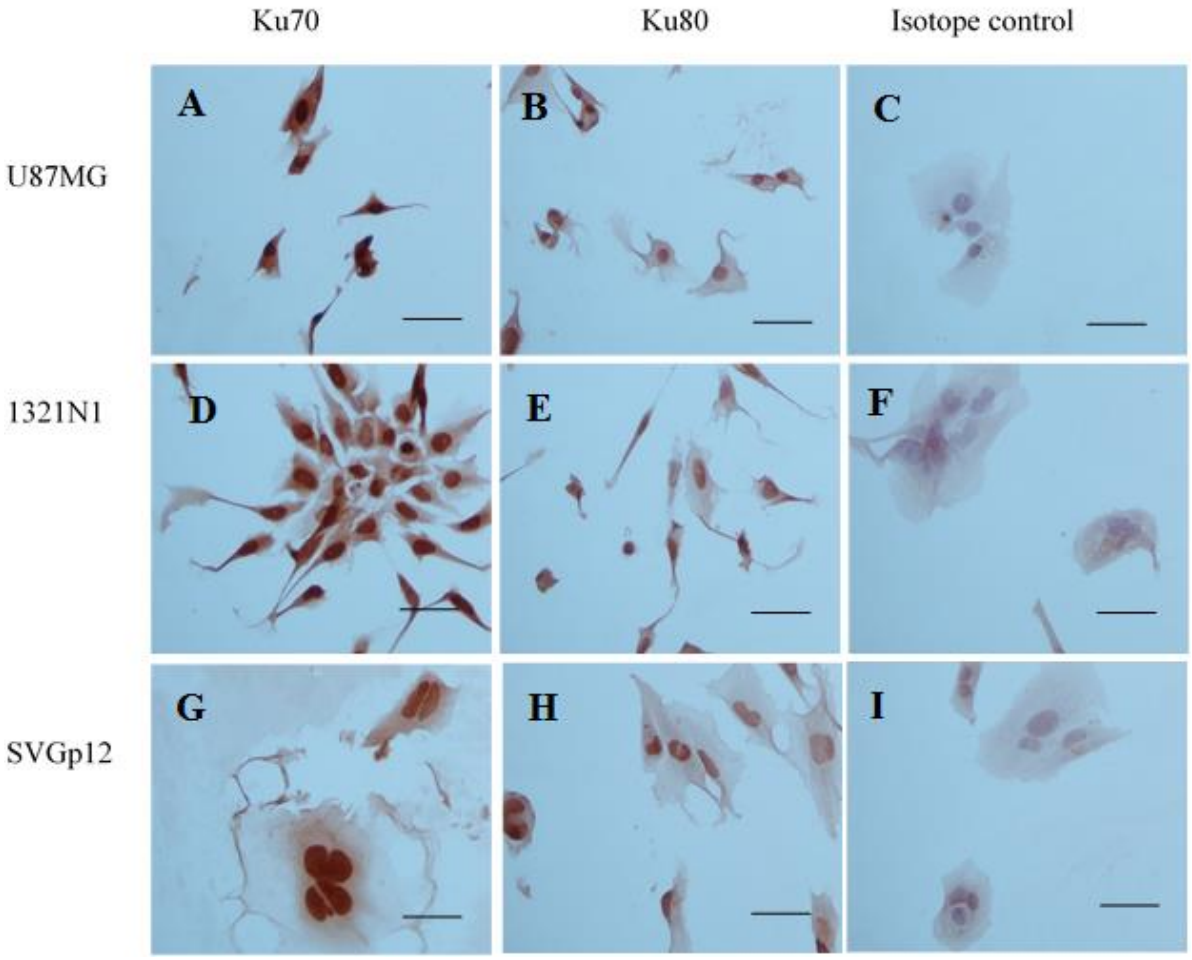

Figure 6.2 Ku70 and Ku80 detection in U87MG, 1321N1 and SVGp12.

Intense nuclear Ku70 staining was detected in all cell lines (A, D and G). U87MG also exhibited intense cytoplasmic staining (A). Cytoplasmic staining was also detected in 1321N1 and SVGp12 (D and G), although to a lesser extent than U87MG (A). Ku70 detection was detected in the nucleus and cytoplasm of all cell lines (B, E and H). C, F and I represent the isotype control. The scale bar represents 50µm.

6.2 Western blot analysis and densitometry

Antibody staining for Ku70 and Ku80 in glioma cell lines above showed significant presence of both proteins in the glioma cell lines. Further confirmation of the abundance of the Ku heterodimer was planned by performing western blot analysis and probing for the proteins. Densitometry analysis was done to assess the presence of the proteins in the pulldown and compared to the control aptamer and no aptamer (ref methods). Densitometry was also done from cellular lysate, without aptamer treatment to assess for total detection of Ku70 and Ku80 proteins.

6.3 Ku 70/80 detection in cell lines with aptamer

Aptamer pulldowns from various cell lines was done. The figures below show the percentage of pulldown seen in each of the columns confirming presence of Ku70 and Ku80. All experiments were performed at the same times and temperature conditions.

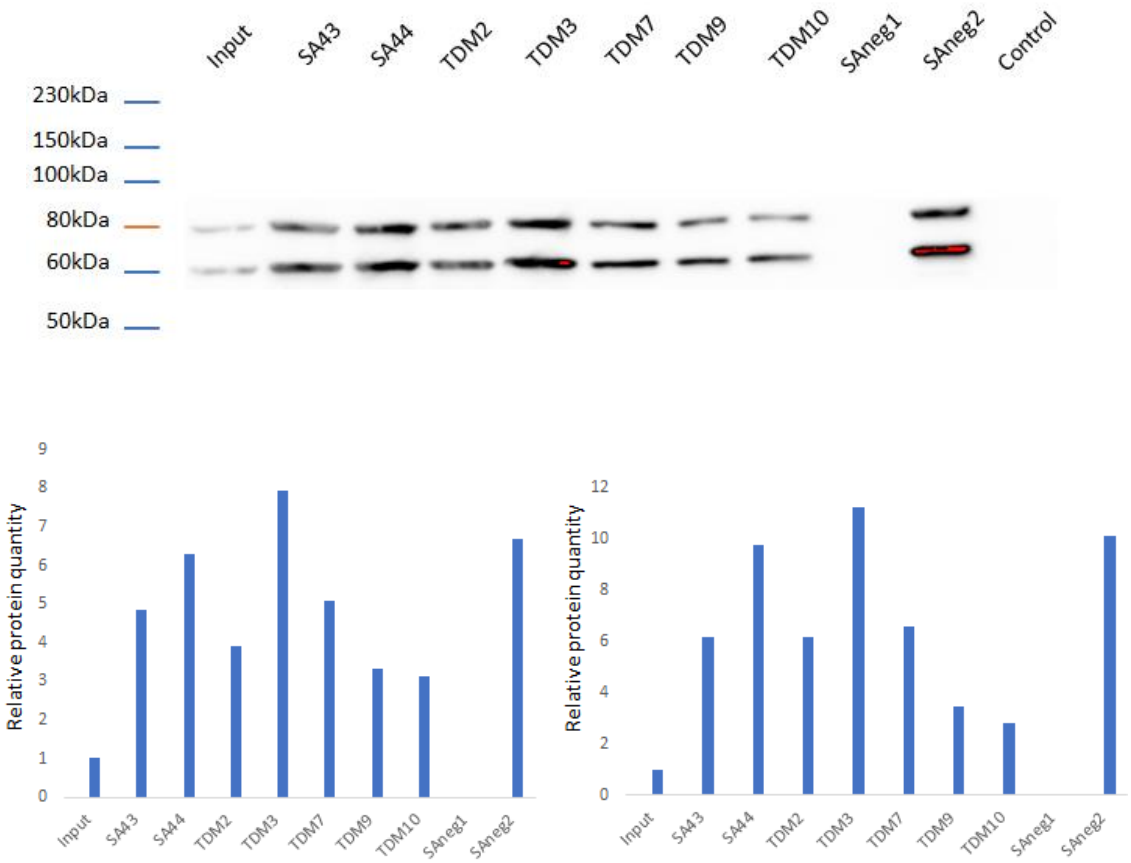

Figure 6.3 **U87MG cell lysate aptamer assisted precipitation and probing with Ku70 and Ku80 antibody**

The above figure shows blotting and probing of the aptamer pulldown with Ku70 and Ku80 antibody. There appears to be greater presence of Ku70 in the cell lysate as seen in the input column. Ku70 and Ku80 detection is seen in all columns except SAneg1 and control (no aptamer). This confirms that the pulldown is specific and detection of the proteins is present. Figure 6.3 showing densitometry analysis for Ku70 and Ku80 bands on U87MG probing. The densitometry analysis was done using Imagej software. The input from the cell lysate is the reference for each graph separately and as one. The pull-downs show greater detection of Ku70 and Ku80 except SANeg1 aptamer. (Ku70 graph on left and Ku80 on right)

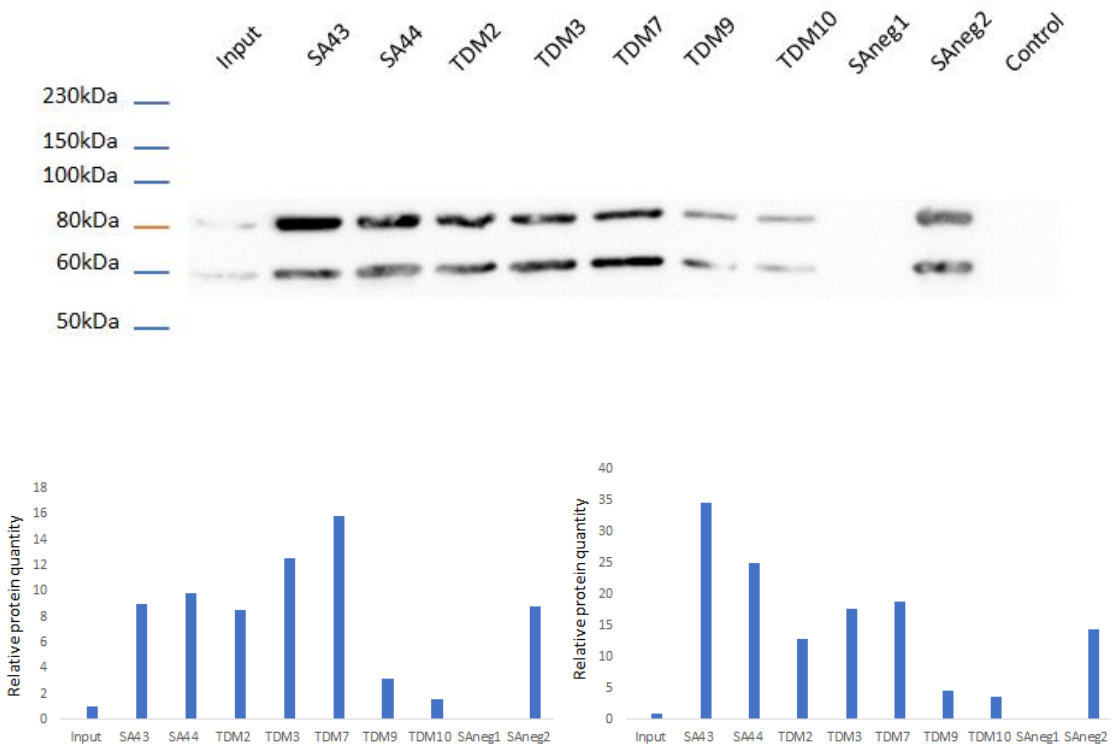

Figure 6.4 1321N1 **cell lysate aptamer assisted precipitation and probing with Ku70 and Ku80 antibody**

The above figure shows blotting and probing of the aptamer pulldown with Ku70 and Ku80 antibody. There appears to be greater presence of Ku70 in the cell lysate as seen in the input column. Ku70 and Ku80 detection is seen in all columns except SAneg1 and control (no aptamer). This confirms that the pulldown is specific and detection of the proteins is present. Figure showing densitometry analysis for Ku70 and Ku80 bands on 1321N1 probing. The densitometry analysis was done using Imagej software. The input from the cell lysate is the reference for each graph separately and as one. The pull-downs show greater detection of Ku70 and Ku80 except SANeg1 aptamer. TDM9 and TDM10 have the lowest relative detection in 1321N1 compared to input detection. (Ku70 graph on left and Ku80 on right)

6.4 Ku 70/80 detection in short term cultures with aptamer

Aptamer pulldowns from various short term cultures was done. The figures below show the percentage of pulldown seen in each of the columns confirming presence of Ku70 and Ku80. All experiments were performed at the same times and temperature conditions.

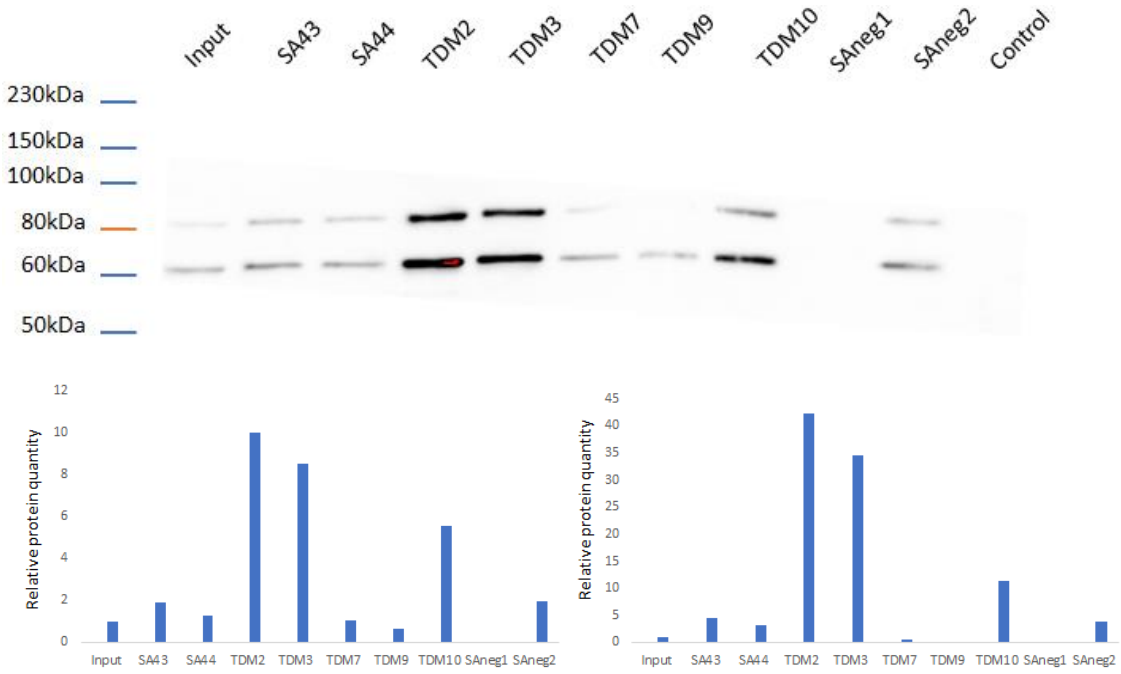

Figure 6.5 BTNW914 **cell lysate aptamer assisted precipitation and probing with Ku70 and Ku80 antibody**

The above figure shows blotting and probing of the aptamer pulldown with Ku70 and Ku80 antibody. There appears to be greater presence of Ku70 in the cell lysate as seen in the input column. This is much higher than the cell lines and in a ratio of 80:20. Ku70 and Ku80 detection is seen in all columns except SAneg1 and control (no aptamer). This confirms that the pulldown is specific and detection of the proteins is present. Figure showing densitometry analysis for Ku70 and Ku80 bands on BTNW914 probing. The densitometry analysis was done using Imagej software. The input from the cell lysate is the reference for each graph separately and as one. The pull-downs show greater detection of Ku70 and Ku80 except SANeg1 aptamer. TDM2 and TDM3 have the highest relative detection in BTNW914 compared to input detection. (Ku70 graph on left and Ku80 on right)

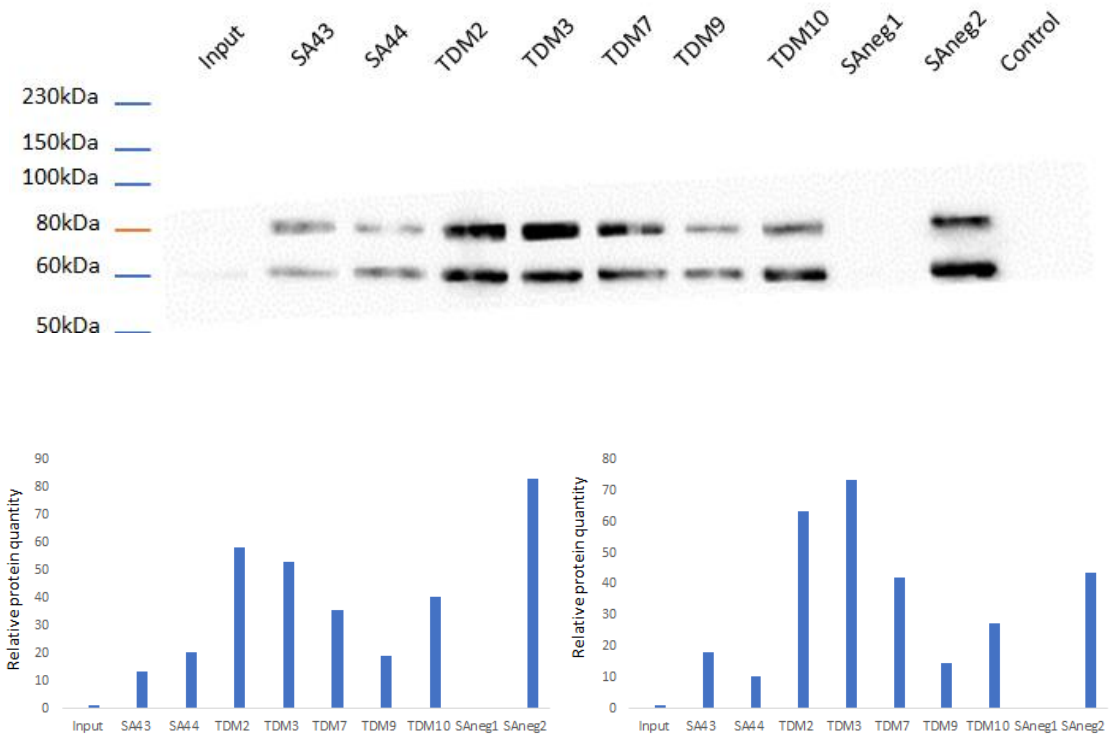

Figure 6.6 W2045 **cell lysate aptamer assisted precipitation and probing with Ku70 and Ku80 antibody**

The above figure shows blotting and probing of the aptamer pulldown with Ku70 and Ku80 antibody. There appears to be near equivalent presence of Ku70 in the cell lysate as Ku80, as seen in the input column. This is in variation to both the cell lines and also BTNW914. Ku70 and Ku80 detection is seen in all columns except SAneg1 and control (no aptamer). This confirms that the pulldown is specific and detection of the proteins is present. Figure showing densitometry analysis for Ku70 and Ku80 bands on W2045 probing. The densitometry analysis was done using Imagej software. The input from the cell lysate is the reference for each graph separately and as one. The pull-downs show greater detection of Ku70 and Ku80 except SANeg1 aptamer. The relative detection of Ku70 and Ku80 are the highest in W2045 when compared to other cell lysates. (Ku70 graph on left and Ku80 on right)

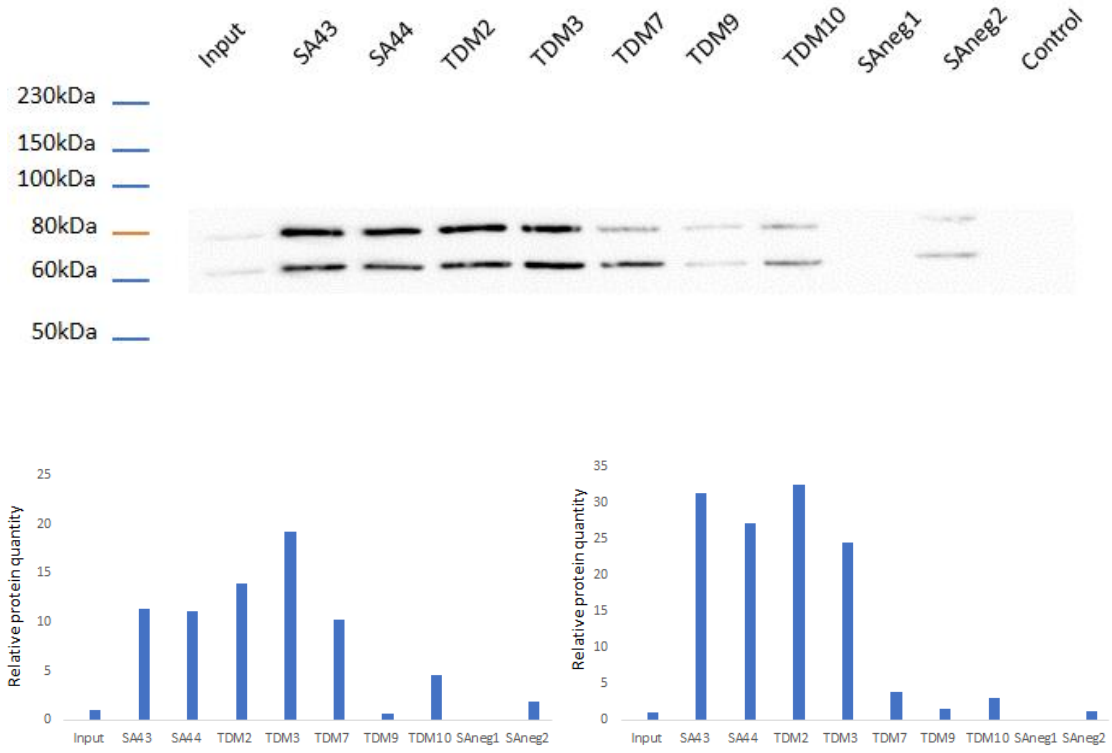

Figure 6.7 Aptamer pulldown followed by Ku70 and Ku80 antibody probing in W859 short term glioma cultures

The above figure shows blotting and probing of the aptamer pulldown with Ku70 and Ku80 antibody. The input lane shows presence of ku70 and ku80 in the cell lysate. Aptamer columns shows bands with Ku70 and Ku80 antibody probing. There appears to be greater detection of Ku70 in the aptamer assisted pulldown compared to the input column. Ku70 and Ku80 detection is seen in all columns except SAneg1 and control (no aptamer). Figure showing densitometry analysis for Ku70 and Ku80 bands on W859 probing. The densitometry analysis was done using Imagej software. The input from the cell lysate is the reference for each graph separately and as one. The pull-downs show greater detection of Ku70 and Ku80 except SANeg1 aptamer. TDM9 and TDM10 have the lowest relative detection in W859 compared to input detection. W859 also has high relative detection of protein, similar to W2045 cell lysate. (Ku70 graph on left and Ku80 on right)

Figures 6.3, 6.4, 6.5, 6.6 and 6.7 show consistent higher detection of Ku70 and Ku80 in the aptamer precipitation using SA43, SA44, TDM2, TDM3, TDM7 and SAneg2 aptamers. It is also seen in TDM9 and TDM 10 but at a lesser relative quantity. SAneg 1 does not shows any signal on densitometry analysis his is similar in detection in the input as U87MG and 1321N1 cell lines. This confirms that the pulldown is specific and pull-down of the proteins is present and specific.

6.5 Ku70/80 detection in cell lysate

Ku70 and ku80 was detected by mass spectrometry analysis and seen in pulldown with all the cell lines used. Due to the normal presence of ku70 and ku80 in cell nuclei, normal human astrocytes or NHA were incorporated to compare the presence of ku70 and ku80 in the NHA against the glial cell lines and short term cultures. Cell lysates of U87MG, 1321N1, SVGp12 and NHA were prepared as per the protocol for aptamer reaction. Aliquots of the lysates were then run on gel for western blotting and probed for Ku70 and Ku80 antibody to detect presence of the proteins in comparison to each other.

6.5.1 Densitometry analysis of cell lysate gel

Cell lysates of U87MG, 1321N1, SVGp12 and NHA as prepared above were run on gel at 0.3mg aliquots on Bradford assay. These were then compared on gel-doc and analysed using densitometry. Figure below shows the gel image of the lysates.

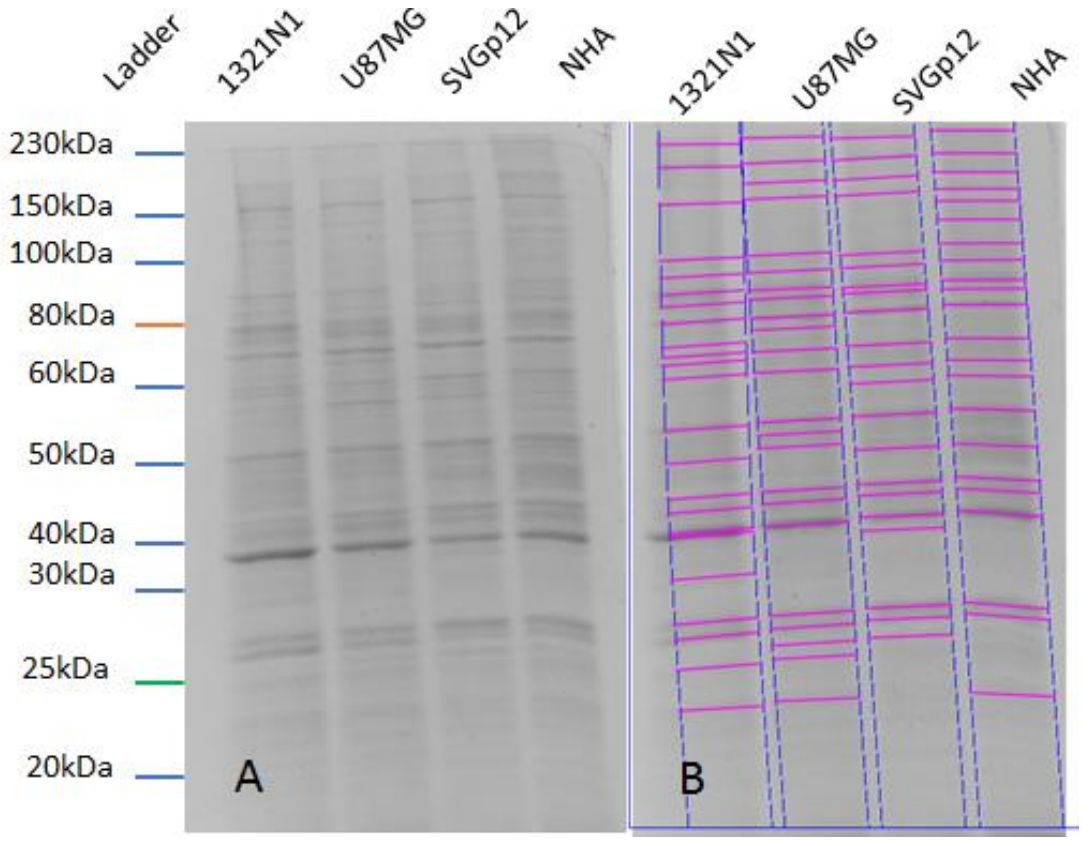

Figure 6.8 Gel run for cell lysates 1321N1, U87MG, SVGp12 and NHA

Cell lysates of 1321N1, U87MG, SVGp12 and NHA were run on a gel at 0.3mg/ml to look for protein band detection. The cell lysates show similar distribution of gel bands compared to each other as seen in A. Figure B shows the auto analysis using imagelab software for band detection.

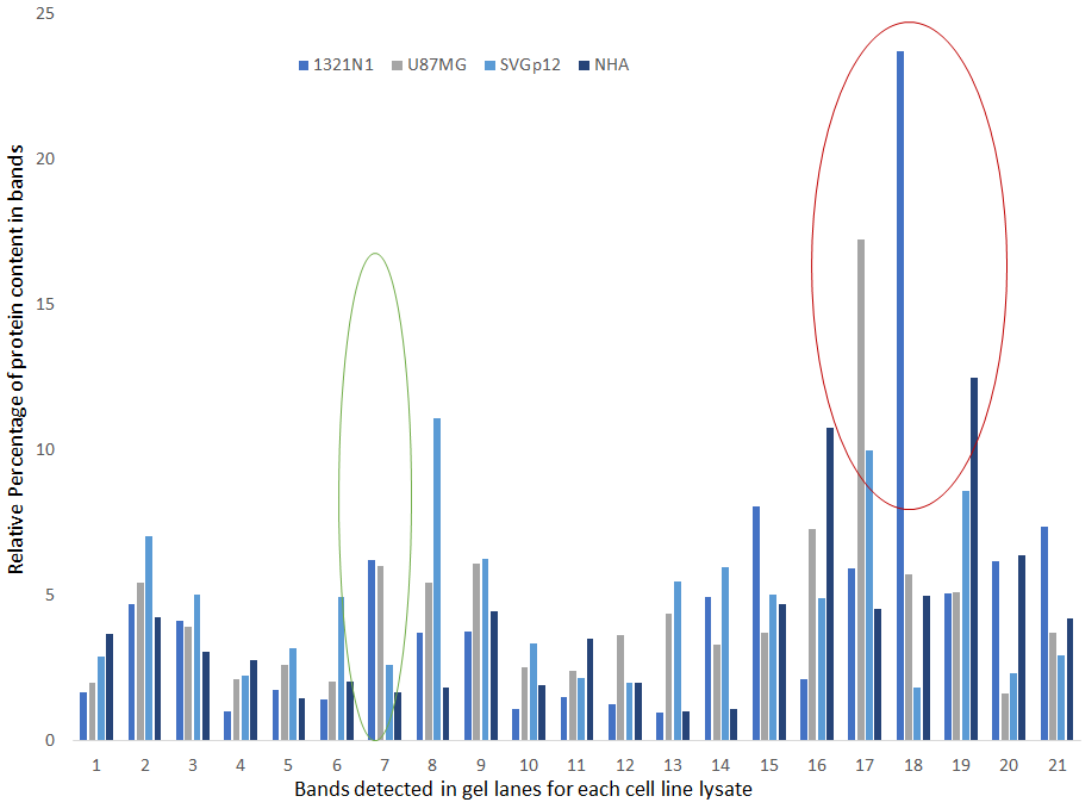

Figure 6.9 Percentage breakdown of bands on densitometry analysis in the four cell lysates from figure 6.8

The y axis is percentage of total protein content in the lane, relative to summation of measured density of all bands in the lane for specific cell lysate and x axis are the individual protein bands numbered 1-21 in each lane seen in figure 6.8. The green loop is around band 7 as seen in the figure 6.8 (B) of the gel and conforms to molecular weight around 60-80 KDa. Each bar corresponds to a different cell line and different lane within the gel. Densitometry analysis of the gel from figure 6.8 shows increased band detection in 1321, U87MG and SVGp12 at 60-80kda when compared to NHA. The higher percentage in 1321N1 and U87MG could be due to higher Ku protein content in the cells. This is less in the NHA column at band 7. Higher detection of smaller, molecular weight contents are seen further down the graph between 17-19 bands which are in close proximity in the gel. This also supports that despite other proteins and compounds in the cell, the aptamers do specifically pull-down Ku70 and Ku80.

Densitometry analysis showed increased detection around band 7 from top which is similar in columns of U87MG and 1321N1 and around 60-90kDa. At the same kDa, the bands in the SVGp12 and NHA are smaller, more so in NHA. This is also seen in the aptamer pulldown probing with Ku70 and Ku80.

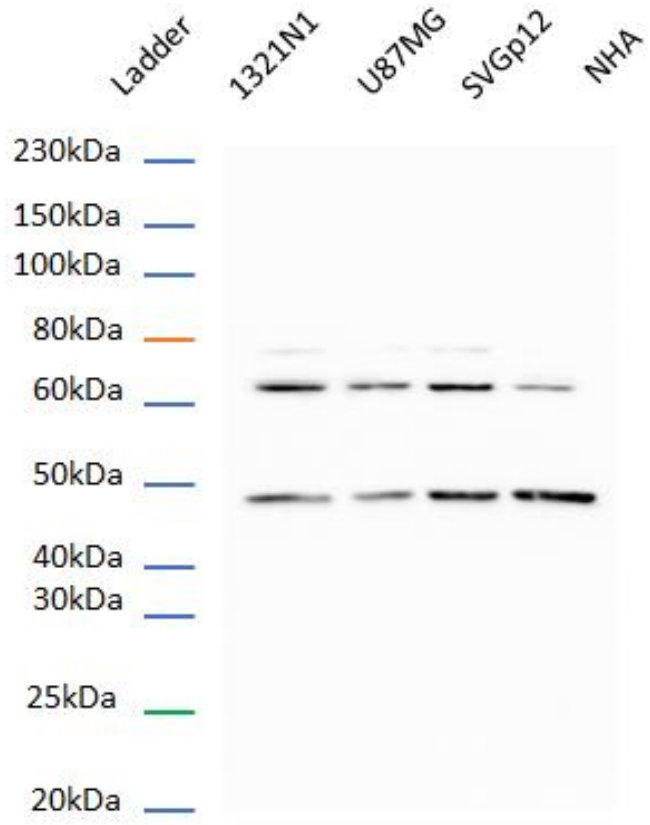

Figure 6.10 Ku70 and Ku80 antibody probing on the whole cell lysates from the image 6.8.

Whole cell lysate was probed for Ku70 and Ku80 relative expression in 1321N1, U87MG, SVGp12 and NHA cell lines. The top band in each column is for Ku80, the second from top is Ku70. The third lowest band is β actin to confirm protein presence. There is highest protein content in the NHA column but the lowest detection of Ku70 and Ku80 relative to the other cell lines.

6.6 Knockdown results of Ku70 and Ku80

To determine whether Ku70/80 proteins were the targets for both SA43 and SA44 aptamers, Ku70 and Ku80 proteins were knocked down by siRNA in U87MG cells, either individually or simultaneously, and biotin tagged SA43 and SA44 aptamers were incubated with the cells. The results show that compared to the wild type (no knock down) U87MG cells, there was reduced binding of both SA43 and SA44 aptamers in Ku70 knockdown U87MG cells, Ku80 U87MG cells, and no binding in Ku70/80 knockdown U87MG cells.

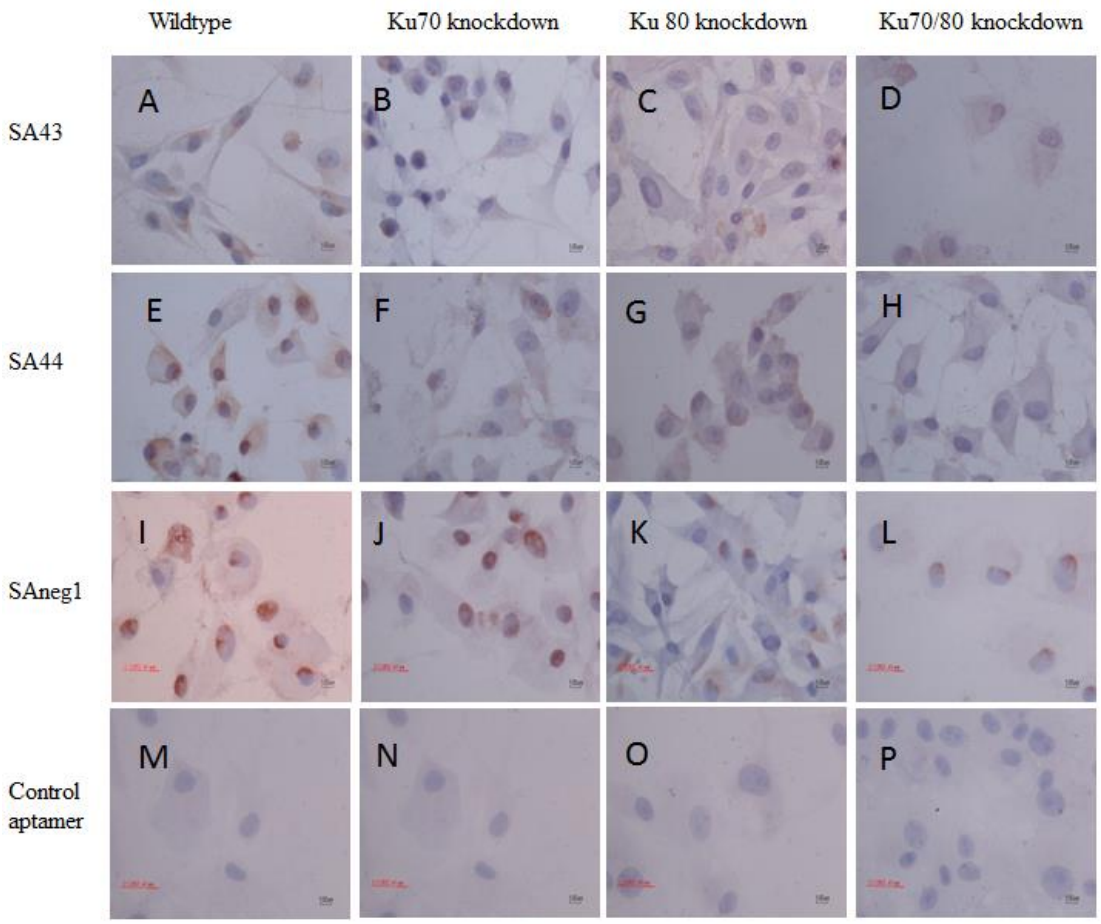

Figure 6.11 Aptamer staining after knock down by siRNA of Ku70 and Ku80 in U87MG cells.

In figure, A, E and I are aptamer staining with standard U87MG cells as positive control. M, N, O and P are negative controls with no aptamer addition in any of the cells with and without knockdown of Ku 70 or Ku80. Figure B, F and J have the effect of Ku70 knockdown on U87MG cells and then incubation with aptamers. There is reduced binding seen around the nucleus with SA43 and SA44 aptamer incubation in B and F respectively but binding seen in the cytoplasm. SAneg1 does how some nuclear binding but all three, B,f and J are reduced compared to the wildtype. In C, G and K, Ku80 has been knocked down and in comparison, there appears to be even lesser binding seen with all three aptamers, SA43, SA44 and SAneg1. In d, H and L, both Ku70 and Ku80 knockdown has been performed. There is again minimal cytoplasmic binding seen with SA43 aptamer and very little with SA44 and SAneg1. Cell morphology appears to be different in the combined Ku70 and Ku80 knockdown figures o D, H and L.

6.7 Discussion

In order to verify the aptamer target in glioma cell lines, aptamer assisted pulldown was performed in chapter 5. This showed protein bands between 60-100 KDa on the protein ladder. Excision of these bands followed by mass spectrometry analysis suggested the SA43 and SA44 aptamer were as Ku70 and Ku80 proteins. The aptamer assisted pulldown protocol was then applied to patient derived short term cultures, and mass spectrometry analysis revealed the target protein for SA43 and SA44 aptamer was also Ku70 and Ku80. Mass spectrometry can generate a number of target "hits" in the data report, therefore interpretation of the data requires caution, as the true target ligand might be masked by high levels of e.g. chaperone proteins or protein complexes that have been pulled down with the target. The aim of chapter six was to confirm the target ligand for SA43 and SA44 aptamers.

Publications have highlighted the increased detection of Ku70 and Ku80 in multiple tumours such as breast, colorectal, prostate and bladder (Prabhakar et al., 1990; Dalziel et al., 1992; Pucci et al., 2001; Mazzarelli et al., 2005; Chang et al., 2006; Alshareeda et al., 2013). PARP or Poly ADP ribose polymerase has recently been discussed in cancer research. It is also responsible for cell repair and is overexpressed in cancer cells. It is being researched for targeted therapy (Morales et al., 2014). PARP in our mass spectrometry analysis appears to bind in pull-downs to SA43 aptamer along with Ku70 and Ku80. This is exclusively seen with SA43 aptamer in U87MG and short term cultures. This is likely due to the multiple structures predicted for the aptamer and could well be used for targeting PARP as well. Olaparib is a PARP inhibitor with USFDA approval for use towards BRCA mutated ovarian cancer (Mirza et al., 2018). PARP plays an important role in DNA repair (Morales et al., 2014) and is also involved in other cancers like breast,

peritoneal and also glioma (Fulton et al., 2017; Miller et al., 2019; Robson et al., 2019). PARADIGM or Olapraib and radiotherapy for people with glioblastoma trial has looked at the use of olaparib in conjunction with temozolamide and radiotherapy. The trial is now evolved into PARADIGM 2 or looking at olaparib with radiotherapy alone and olaparib with radiotherapy and temozolamide combined. Dose changes in olaparib has been done to accommodate the hematological toxicity when combined with temozolamide. Patients are segregated according to their MGMT status and dose escalation in unmethylated patients can be done in the absence of temozolamide and minimal risk of hematological toxicity. OPARATIC trial (Olaparib with temozolamide for glioblastoma that has come back) has also looked at recurrent glioma (Halford et al., 2017).

Ku70 and Ku80 are DNA repair proteins involved in NHEJ for DSB repair and are over-expressed in a lot of cancers. Previous studies have shown the heterodimer to be present normally in cell nucleus, facilitating double stranded break (DSB) repair (Davis and Chen, 2013) via NHEJ and increased detection occurs after cell damage for DNA repair. DSB is a break in the DNA which results in both strands to be broken and repair is crucial to prevent aberrant repair, apoptosis or cancer genesis (Davis and Chen, 2013). DSB and NHEJ is upregulated in GBM (Annovazzi et al., 2015). Looking at the Kyoto encyclopaedia of genes and genomes or KEGG, NHEJ is seen with presence of Ku70 and Ku80 in glioma repair (KEGG). There is reported over detection in glioma but follow up studies have been scarce. In order to verify Ku70/80 as the target ligand for SA43 and SA44 aptamer, it was first necessary to confirm detection of Ku70 and Ku80 in the cells. Immunocytochemistry confirmed the nuclear and cytoplasmic detection of Ku70 and Ku80 in glioma cell lines and astrocyte control cell line. As expected, detection was high

in the glioma cell lines with detectable, but reduced detection, in the control astrocyte cell line.

The next step was to perform Western blot analysis on the protein extracts and precipitates. Cells were lysed and pulldown performed using aptamers SA43 and SA44. Novel TDM aptamers generated at UCLan were also used in the experiments, which were generated towards U87MG cells (Manangazira, 2013). 10 different aptamer sequences were generated after SELEX at Uclan against U87MG cell lines which were different to previously published aptamer sequences. Under graduate projects used the novel aptamers against glial cell lines and five sequences were shown to stain positively towards U87MG cell lines.

The five novel aptamers from the SELEX were utilised for pulldown with the same protocol. These aptamers were also used towards short term sequences to expand the cohort of samples and hence, increased the statistical significance of the results. Novel aptamer used in the study were generated using SELEX and developed with positive selection towards U87MG cell line. The fact that the novel aptamers also pulldown the same targets supports the validity of the pulldown technique. This also indicates that the different aptamer sequences can bind to the same target.

Chapter 7

7 Discussion and future direction

7.1 Current situation and basis of research

The aim of the research project was to identify the targets of aptamers in glioma. The current treatment management for glioma harbours on surgery followed by concomitant chemo and radiotherapy as per the Stupp protocol (Stupp et al., 2005). The heterogeneity of glioma (Kleihues et al., 2002) and the lack of clear tumour margins (Neira et al., 2017) makes curing glioma a big challenge. This is seen in the slow improvement in the meaningful survival of GBM patients over the last 50 years (McKinney, 2004; Krex et al., 2007). Poor response to chemotherapy agents when compared to other tumours, is majorly due to the poor penetration of the BBB (Deeken and Löscher, 2007). Small sized molecules can penetrate the BBB (Geldenhuys et al., 2015) and are usually lipid molecules (Banks, 2009). Aptamers, being only single stranded DNA or RNA and non-immunogenic, could cross the BBB. The usual molecular size of substances crossing the BBB are between 400-600Da but molecules up to 78kDa in the form of cytokine induced neutrophil chemoattractant-1 are known to pass through transmembrane diffusion (Banks, 2010).

Published aptamer sequences by Cerchia et al, (2009) specific to glioma, were selected. These sequences were truncated to make them more specific and shorter to assess for better targeting (Macdonald et al., 2016). To confirm that the aptamers are specific to glioma, staining with fluorescent tagged aptamers was performed (Chapter 3). Firstly, confocal imaging with live aptamer incubation, followed by biotinylated aptamer was performed on fixed cells. The biotinylated aptamers were used to enable pulldown of target epitope attached to the aptamer using streptavidin affinity to biotin. A parallel

project (Aptekar et al., 2015) looked at confirming live aptamer uptake using Cy3 tagged aptamer and performing FACS analysis (Aptekar et al., 2015). This confirmed the findings seen in the confocal imaging of aptamer uptake and internalisation of the aptamer. According to the parallel study, the internalisation of the aptamer was an active process as no uptake was seen at 4^{o}C. This would imply that a surface 'target' is likely to exist which helps the aptamer to bind and internalise. There was also no change seen in aptamer uptake before and after trypsinisation, thus likely preserving the surface 'target' despite trypsinisation. It is also likely that the aptamers are being internalised by a 'pathway' and could be one of the already known pathways (EGFR pathway) identified to be dysregulated in cancer genomics studies (Creixell et al., 2015).

The technique for aptamer assisted pulldown of targets was refined and consistent results were achieved with clear protein separation bands seen by gel electrophoresis. These proteins were then cut from gels and sent for mass spectrometry analysis, initially as whole columns (chapter 5). Mass spectrometry analysis of the whole column confirmed repeatable identification of Ku proteins (chapter 5). Mass spectrometry thus showed identification of Ku proteins in glioma cells and an over detection intracellularly, compared to non-cancerous SVGp12 cells, as widely seen in this thesis in microscopy experiments and confirmed with pulldown techniques.

If Ku70 and Ku80 are expressed on the surface of U87MG cells then it is likely that the novel aptamers generated using SELEX at UcLan are also selectively binding to the Ku proteins as these aptamers were generated under similar physiological conditions to the Cerchia aptamers (GL43, -44 and -56) (Manangazira, 2013). The technique used for generating the novel aptamers, used U87MG cells for positive selection and introduced a negative selection against SVGp12 cells (which was not done by Cerchia et al. (2009).

Two random aptamers, SAneg1 and SAneg2 were also generated as an isoform of the specific aptamers to create control aptamers. These acted as positive and negative controls as seen in the immunostaining experiments as determined in Chapter 4. If the aptamers were specific to Ku proteins as seen largely in the results, they will enable distinguishing cancerous cells from non-cancerous and could enable targeted therapy (Fischer et al., 2001). Other cancers are known to over-express Ku proteins such as colorectal (Beggs et al., 2012), cervical (Beskow et al., 2009), leukaemia (Pei et al., 2013), breast (Alshareeda et al., 2013), prostate (Al-Ubaidi et al., 2013) and bladder cancer (Stronati et al., 2001) amongst other cancer tissues (Pucci et al., 2001). The over detection of Ku proteins in these cancers could also be targeted (Pucci et al., 2001).

7.2 Aptamer assisted pulldown and applications

For the purpose of identification of targets, a novel technique was developed. Aptamer assisted pulldown was designed using known techniques of protein extraction and modifying ChIP technology (Aparicio et al., 2004; Xu et al., 2010; Ye et al., 2012). ChIP techniques showed a way forward on how to enable pulldown using biotin-streptavidin affinity (Weber et al., 1989). Streptavidin is a protein purified from Streptomyces avidinii, a bacterium (Weber et al., 1989). Streptavidin and biotin (Vitamin B7 or C_{10} H_{16} O_3 N_2 S) have a very high affinity with a dissociation constant of 10^{-14} mol/l and is the strongest non-covalent interaction in nature (Chivers et al., 2011). The bond is also extremely resistant to organic solvents and extremes of temperature and pH. The bond can break without denaturing streptavidin by heating to 70^{o}C in water (Holmberg et al., 2005). The final protocol was developed for the aptamer pulldown and can theoretically be applied to other cell extractions. The two factors which can affect pulldown with cells lines is the location of the target epitope and interference with triton X100 (Pchelintsev

et al., 2016). The protocol uses cell lysis with triton X100, a non-denaturing agent at very low concentration. This was modified from earlier usage to preserve protein function and specificity to the aptamer by preserving the protein target in its native form. Triton X100 at this concentration does not interfere with proteomic assessment. If the target epitope is primarily located on the cell surface, sub-fractionation or differential lysis could be performed and aptamer incubated with separate fractions.

7.3 Confirmation of targets Ku70 and Ku80

Ku70 and Ku80 exist as a heterodimer in the DNA repair pathway for NHEJ repair (Mazzarelli et al., 2005; Alshareeda et al., 2013). We know from various publications of DNA repair proteins being overexpressed in various cancers (Moll et al., 1999; Fischer et al., 2001; Pucci et al., 2001; Bouchaert et al., 2012). Ku70 and Ku80 has also been shown to be present on the surface of cells (Prabhakar et al., 1990). The explanation for over detection is the attempt of the cell to repair itself. Similarly, the presence of Ku proteins in the cytoplasm and surface is due to diffusion and abundance of the protein. Mass spectroscopic analysis of the pulldown from the commercial cell lines and short term cultures pointed to over detection of Ku repair proteins which were being targeted by the aptamer (chapter 5). To confirm the results, we first looked at presence of Ku protein in normal cells as published in literature. Ku protein, though produced in the nucleus for Double stranded break or DSB repair through NHEJ, is present in the cytoplasm of healthy cells compared to senescent cells (Seluanov et al., 2007). This was seen with reduced detection seen in DAB staining of SVGp12 and very minimal in NHA cells. It was also confirmed with cell lysate detection seen in chapter 6 of NHA. We already know its over-detection in various cancerous cells (Pucci et al., 2001).

We then confirmed our mass spectroscopy results by probing for Ku proteins. This was done using immunocytochemistry using anti Ku antibodies. This showed consistent results of presence of Ku70, much more than Ku80 in the various glial cell lines (chapter 6).

The next step was to perform the aptamer pulldown and confirmation using Western blot analysis. This was also to show the total detection of Ku proteins in the cell lines and specificity of the aptamers when compared to the whole cell lysate. The selectivity of the aptamers was further highlighted by the fact the control aptamer did not pull-down Ku protein and no binding detected on the Western blots.

Further confirmation was done with knockdown of Ku proteins in cells. To confirm the targeting of Ku heterodimer and variation in binding, mRNA knockdown was performed in U87MG cells and short term cultures (Gold et al., 2012). After the knockdown, clear differentiation in the staining was seen with lesser nuclear staining compared to cytoplasmic in U87MG. This serves as a clear example and is likely due to the abundance of Ku protein in the cytoplasm, but the primary effect of the knockdown is seen in the nuclear region and hence reduced staining.

7.4 Ku70 and Ku80 in cell lines and short-term cultures

The commercial lines used in the project mainly harboured on U87MG cells, which originated from a 44yr old female patient in Uppsala, Sweden (Allen et al., 2016). The cell line, in a recent publication has been shown to be different from the original U87MG cell line and also has a Y chromosome and likely contaminated over the course of the years, although it is still confirmed as a glioma cell line. There is no mention in literature of proteomic detection of Ku in U87MG or the likely alterations done to create the cell

line (Wang et al., 2016). EGFRvIII has been widely reported in U87MG and GBM but was not pulled down by the aptamers. DNA repair mechanisms in GBM by Erasimus et al (Erasimus et al., 2016) found presence of Ku70/80 along with XRCC1 and XRCC4 and PARP1 presence in repair mechanisms in glioma. This conforms with our results, especially with SA43 and TDM aptamers for PARP1 and Ku together (Chapter 5).

We then looked at 1321N1 cell line, a human astrocytoma cell line isolated in 1972 (England, 2016). It is a sub clone of the cell line 1181N1 which in turn was isolated from the parent line U-118 MG. There are no publications present on the actual cloning of the cell line and its exact origin. There is no reference to DNA repair protein detection in publications with regards to 1321N1 cell line or of Ku or XRCC.

When we looked at SVGp12, the cell line originated by transfecting plasmids of JC virus into foetal brain cells (Wroblewska et al., 1980). Studies into JC virus and polyoma virus shows over detection of Ku proteins in infected cells. It also points to dispersion of Ku from its nuclear position to cytoplasmic displacement seen in the infected cells (Reston, 1987). This supports the fact that we found detection Ku protein in SVGp12 cell line and aptamer binding in the cytoplasmic region of SVGp12. SVGp12 cell line might not have been the best control cell line in hindsight but did lead to explain why we were seeing staining in the initial stages of the project. This was especially so since SVGp12 cells were used as a negative SELEX round in the production of TDM aptamers. Studies have pointed to over detection on Ku proteins on cell surface (Prabhakar et al., 1990) and also increased surface detection in hypoxic conditions (Muller et al., 2005). There is also a thought that the protein is not primarily a nuclear in location but secreted by plasma membrane transporter (Nickel, 2003; Muller et al., 2005). There is also evidence to suggest that Ku is involved in pro-survival and pro-invasive processes (Nagase and

Woessner, 1999; Monferran et al., 2004a; Monferran et al., 2004b; Muller et al., 2005). It is also possible that the binding is to an isoform of Ku which is over-expressed in cancerous cells. It can also be postulated that Ku detection on surface of SVGp12 is not present or much reduced compared to other glioma cell lines and has thus served to be a viable negative selection in SELEX.

7.5 Potential future experiments for clinical application

A move for a quicker diagnosis in cancer is needed to enable earlier diagnosis and treatment. The final aim being application of aptamers for glioma therapy and diagnosis. For this purpose, greater efforts are being directed towards diagnosis from blood and blood markers. Spectroscopy along with microfluidics with biosensors are being employed and this is exactly where aptamers can come into play (Liu et al., 2013).

Due to the over detection of Ku proteins seen in glioma, there is a chance of spillage of this into the blood stream. In glioma, the blood brain barrier is disrupted and hence theoretically, it is possible for detection of biomarkers in blood. An experiment to analyse the same can be done by taking blood samples from healthy patients and those having confirmed diagnosis of glioma, before and after surgery. The blood/serum/plasma can then be blotted on blotting paper and probed with Ku70/ Ku80 antibodies for Ku proteins. At the same time, aptamer probing can also be done on a parallel dot blot. As a further confirmation, tumour sample from the patient can be lysed and assessed for Ku protein over detection. This will give a result in three forms and can be applied for future research and clinical applications. This though is not specific to glioma and is likely to pick other cancers as well.

Recent publications in spectrometry have given strong results to suggest diagnosis with serum spectra of up to 90% specificity for glioma (Hands et al., 2016). This is though performed without knowing the elements resulting in this spectral change. The results of this technology can be more robust with concomitant analysis of the serum and could likely be Ku proteins.

7.6 AP with patient tissue

Current research has been done with commercial cell lines and short term cultures derived from patient tissue. Both these have cell cultures are in a way not a true representation of the patient glioma tissue. Glioma's being heterogeneous in nature are made up of various heteromorphic cells and express various proteins (Jung et al., 2011). Not much has been mentioned or discussed about the over detection of Ku proteins in literature. It is possible that other cancerous cells which are more proliferative in the living tissue than in the cultured confines of the lab are present. With this situation hence, performing aptamer assisted precipitation from patient tissue would be an ideal further research direction. Aptamer probing on tissue sections has already been performed in the parallel study by Aptekar *et al* (Aptekar et al., 2015). This shows the presence of certain proteins being targeted by the aptamer and can be used for tissue diagnosis. These targets as confirmed by the current research project shows them as Ku70 and Ku80. Another precursor could be SELEX with fresh patient tissue. It has already been shown that specific aptamers can be generated by single round of SELEX with tissue section. This could be utilised towards fresh tissue and will likely provide greater affinity due to removal of tissue processing steps which can lead to loss of biomarkers.

7.7 Crossing the blood brain barrier

Aptamers are single stranded DNA and RNA oligonucleotides. Human nucleotides are 0.6nm in length and average 50 nucleotides in length, the whole length of the aptamer is approximately 30nm, not taking into account the folding and binding of the aptamer. This equates to roughly 15,382Da. The tight junctions of the BBB allow only molecules smaller than 500Da weight by passive diffusion (Banks, 2009). Considering this, it is unlikely the aptamers are able to passively diffuse through the BBB. In order to generate aptamers which are able to pass the BBB, either by active transport or facilitated diffusion or other mechanisms, studies have applied in vitro SELEX to identify aptamers that cross the BBB (Kumar, 2015). A parallel study/PhD has evaluated SA43 and found to cross a valid human BBB model (Kumar, 2015). Ongoing animal studies have also shown the aptamer being localised to the tumour though extracranially at present. It supports the likelihood of the aptamer being administered systemically and being able to target the tumour.

7.8 Clinical application of results

Aptamers have been hailed as replacement for antibodies (Bunka and Stockley, 2006). They are non-immunogenic, small, do not need to be kept at cold temperature when not suspended and can be emailed as a sequence for local production. Multiple publications have cited the possibility of aptamers replacing roles of antibodies in diagnosis, treatment and development of new treatment modalities (Brody and Gold, 2000; Blank and Blind, 2005; Bunka and Stockley, 2006; Berezovski et al., 2008; Bouchard et al., 2010; Bunka et al., 2010).

The current aptamer research into SA43 can be utilised towards diagnosis for glioma as already shown by Aptekar *et al*. Clinical application in patient treatment can be done by

using the aptamer conjugated with a fluorescent dye or a near infra-red dye to enable surgical excision. Aptamer conjugated with chemotherapy can be used as a targeted chemotherapy with less toxicity to the patient and greater compliance. Whether the targeting is via systemic administration or by direct infusion techniques/ convection (Debinski and Tatter, 2009, 2010; Chapdelaine et al., 2015).

Another use can be towards use as a screening tool (Bunka et al., 2010). Since ku is over expressed and can be detected in blood stream, it can be used as a screening tool for a population. Though not as specific as expected at the beginning of the project, it could serve as a generic test for cancer screening after further research.

Tumour diagnosis is labour intensive and can take weeks since the first concern due to a neurological sign or decline. Current two-month cancer pathways for delivering cancer treatment in the NHS have been under stress and not being met in certain locations. Quicker screening and diagnosis of glioma can certainly affect survival rates and a drive towards achieving this goal is ongoing. Blood testing using spectrometry has shown the proof of concept. It is likely that Ku is over expressed in patient serum and could also be used for early diagnosis.

7.9 Recurrent tumour SELEX, AP and probing with aptamer

Recurrent glioma is more difficult to treat. It is resistant to standard chemotherapy and usually second line of treatment with PCV and other anti-cancer drugs are used. These have greater side effects and tumour response is very variable. AP with recurrent tumour could enable targeting and create patient specific treatment. Automated SELEX from patient tissue at recurrence and generating new novel aptamers can be used for targeting, either via tissue directly or primary tumour cell cultures from patient. It can

also result in greater understanding of recurrent tumour pathology. By performing AP for target protein, the process can give an indication on the change in tumour detection or repair mechanism away from NHEJ.

7.10 Summary

In Summary, the aim to develop a novel method for performing pulldown using aptamers was achieved. The published glioma specific aptamers were tested against cell lines and short term cultures and the novel protocol was used with various aptamers including novel aptamers generated using SELEX. Data analysis showed and confirmed the target to be DNA repair proteins ku70 and ku80. PARP was also found in certain pulldown with SA43 aptamer only. The protocol can be used for developing targeted therapy in glioma and possibly other cancers using aptamers for patient specific treatment.

APPENDICES

Appendix 1 Cell lines and media used

Cell lines	Description	Culture medium (Lonza, UK)	Media constituents
1321N1	Astrocytoma grade 2	Dulbecco's Modified Eagle Medium (DMEM), 10 % FBS and L-glutamine (2 mM)	1 mM sodium bicarbonate 1.0 g/l glucose 25 mM Hepes 0.0011 g/l phenol red
U87MG	Glioblastoma grade 4	Eagle's Minimum Essential Medium (EMEM), 10% FBS, L-glutamine (2 mM), Sodium pyruvate (5 mM) and NEAA (5 mM)	2.2 g/l sodium bicarbonate 4.5 g/l glucose 10 mM Hepes 0.0053 g/l phenol red
SVGp12	Foetal astrocyte	Eagle's Minimum Essential Medium (EMEM), 10% FBS, L-glutamine (2 mM), Sodium pyruvate (5 mM) and NEAA (5 mM)	2.2 g/l sodium bicarbonate 4.5 g/l glucose 10 mM Hepes 0.0053 g/l phenol red

Appendix 2 reagents used in cell culture

Reagent	Storage	Constituents	Supplier
Fetal Bovine serum (FBS)	-20°C	Heat inactivated FBS	Lonza, UK
L-glutamine	-20°C	200 mM L-glutamine	Lonza, UK
Non essential Amino acids	2-8°C	100x non essential amino acid	Lonza, UK
Phosphate Buffer saline (PBS)	Room temperature	8 g/l NaCl, 0.2 g/l KCl, 1.44 g/l Na2PO4 0.24 g/l KH2PO4, pH 7.4	Fischer scientific, UK
Trypsin	-20°C	0.5 g Porcine trypsin	Lonza, UK
Dimethyl-sulfoxide (DMSO)	Room temperature	99.5% dimethyl sulfoxide 0.81% sodium chloride	Lonza, UK
Trypan Blue	Room temperature	0.81% (w/v) sodium chloride 0.06% (w/v) potassium phosphate dibasic	Sigma, UK

Appendix 3

Western blotting preparation

10 % SDS PAGE gel recipe

Recipe for casting resolving and stacking gel for SDS-PAGE.

Materials	10% Resolving Gel (for two gels)	4% Stacking Gel (for two gels)
dH_2O	4.7 mL	4.5 mL
1.5M Tris Buffer (pH 8.8)	2.6 mL	-
1M Tris Buffer (pH 6.8)	-	0.76 mL
10% SDS	100 µl	60 µl
40% Acrylamide	2.5 mL	0.6 mL
10% APS (freshly made only)	100 µl	60 µl
TEMED (added prior to pouring gel)	10 µl	6 µl
Total Volume	10 mL	6 mL

	Buffer	Recipe
1	Triton X100 buffer	0.1% Triton X100 303 g Trisbase (FW 121.1)
2	Sample loading buffer	4% SDS 10% 2-mercaptoehtanol 20% glycerol 0.004% bromophenol blue 0.125 M Tris HCl
3	Electrophoresis buffer (10X)	303 g Trisbase (FW 121.1) 1440 g glycine (FW 75.07) 100 g SDS
4	Transfer buffer (10X)	303 g Trisbase, 1440 g glycine
5	Wash buffer (10X)	24.23 g Trizma HCl 80.06 g NaCl 800 ml distilled water. pH to 7.6
6	Blocking buffer	Wash buffer + 5 % milk powder
7	Stripping buffer	15 g glycine 1 g SDS 10 ml Tween 20 800ml with ultrapure water Adjust pH to 2.2

Appendix 4

Attached publication

Agnihotri, S., K.E. Burrell, A. Wolf, S. Jalali, C. Hawkins, J.T. Rutka, and G. Zadeh. 2013. Glioblastoma, a brief review of history, molecular genetics, animal models and novel therapeutic strategies. *Arch Immunol Ther Exp*. 61:25-41.

Al-Ubaidi, F.L., N. Schultz, O. Loseva, L. Egevad, T. Granfors, and T. Helleday. 2013. Castration therapy results in decreased Ku70 levels in prostate cancer. *Clin Cancer Res*. 19:1547-1556.

Allen, M., M. Bjerke, H. Edlund, S. Nelander, and B. Westermark. 2016. Origin of the U87MG glioma cell line: Good news and bad news. *Sci Transl Med*. 8:354re353.

Alshareeda, A.T., O.H. Negm, N. Albarakati, A.R. Green, C. Nolan, R. Sultana, S. Madhusudan, A. Benhasouna, P. Tighe, I.O. Ellis, and E.A. Rakha. 2013. Clinicopathological significance of KU70/KU80, a key DNA damage repair protein in breast cancer. *Breast Cancer Res Treat*. 139:301-310.

Annovazzi, L., V. Caldera, M. Mellai, C. Riganti, L. Battaglia, D. Chirio, A. Melcarne, and D. Schiffer. 2015. The DNA damage/repair cascade in glioblastoma cell lines after chemotherapeutic agent treatment. *Int J Oncol*. 46:2299-2308.

Aparicio, O., J.V. Geisberg, and K. Struhl. 2004. Chromatin immunoprecipitation for determining the association of proteins with specific genomic sequences in vivo. *Curr Protoc Cell Biol*. 17:7.

Aptekar, S., M. Arora, C.L. Lawrence, R.W. Lea, K. Ashton, T. Dawson, J.E. Alder, and L. Shaw. 2015. Selective Targeting to Glioma with Nucleic Acid Aptamers. *PLoS One*. 10:e0134957.

Baba, S., S.Y. Cho, Z. Ye, L. Cheng, J.M. Engles, and R.L. Wahl. 2007. How reproducible is bioluminescent imaging of tumor cell growth? Single time point versus the dynamic measurement approach. *Mol Imaging*. 6:315-322.

Baird, N.J., and A.R. Ferre-D'Amare. 2013. Modulation of quaternary structure and enhancement of ligand binding by the K-turn of tandem glycine riboswitches. *Rna*. 19:167-176.

Banan, R., and C. Hartmann. 2017. The new WHO 2016 classification of brain tumors-what neurosurgeons need to know. *Acta Neurochir (Wien)*. 159:403-418.

Banks, W.A. 2009. Characteristics of compounds that cross the blood-brain barrier. *BMC Neurol*. 9 Suppl 1:S3.

Banks, W.A. 2010. Blood-brain barrier as a regulatory interface. *Forum Nutr*. 63:102-110.

Bayrac, A.T., K. Sefah, P. Parekh, C. Bayrac, B. Gulbakan, H.A. Oktem, and W. Tan. 2011. In vitro Selection of DNA Aptamers to Glioblastoma Multiforme. *ACS Chem Neurosci*. 2:175-181.

Beggs, A.D., E. Domingo, M. McGregor, M. Presz, E. Johnstone, R. Midgley, D. Kerr, D. Oukrif, M. Novelli, M. Abulafi, S.V. Hodgson, W. Fadhil, M. Ilyas, and I.P. Tomlinson. 2012. Loss of expression of the double strand break repair protein ATM is associated with worse prognosis in colorectal cancer and loss of Ku70 expression is associated with CIN. *Oncotarget*. 3:1348-1355.

Behin, A., K. Hoang-Xuan, A.F. Carpentier, and J.-Y. Delattre. 2003. Primary brain tumours in adults. *The Lancet*. 361:323-331.

Benson, L. 2018. Tumor Treating Fields Technology: Alternating Electric Field Therapy for the Treatment of Solid Tumors. *Semin Oncol Nurs*. 34:137-150.

Berezovski, M.V., M. Lechmann, M.U. Musheev, T.W. Mak, and S.N. Krylov. 2008. Aptamer-facilitated biomarker discovery (AptaBiD). *J Am Chem Soc*. 130:9137-9143.

Bergström, T.F., A. Josefsson, H.A. Erlich, and U. Gyllensten. 1998. Recent origin of HLA-DRB1 alleles and implications for human evolution. *Nature Genetics*. 18:237.

Bernstein, J.J., and C.A. Woodard. 1995. Glioblastoma cells do not intravasate into blood vessels. *Neurosurgery*. 36:124-132.

Beskow, C., J. Skikuniene, A. Holgersson, B. Nilsson, R. Lewensohn, L. Kanter, and K. Viktorsson. 2009. Radioresistant cervical cancer shows upregulation of the NHEJ proteins DNA-PKcs, Ku70 and Ku86. *Br J Cancer*. 101:816-821.

Bisswanger, H. 2008. Enzyme kinetics : principles and methods. 2nd. rev. and updated.ed. Wiley-VCH, Weinheim (Federal Republic of Germany). xviii, 301 p. pp.

Blank, M., and M. Blind. 2005. Aptamers as tools for target validation. *Curr Opin Chem Biol*. 9:336-342.

Bock, L.C., L.C. Griffin, J.A. Latham, E.H. Vermaas, and J.J. Toole. 1992. Selection of single-stranded DNA molecules that bind and inhibit human thrombin. *Nature*. 355:564-566.

Bouchaert, P., S. Guerif, C. Debiais, J. Irani, and G. Fromont. 2012. DNA-PKcs expression predicts response to radiotherapy in prostate cancer. *Int J Radiat Oncol Biol Phys*. 84:1179-1185.

Bouchard, P.R., R.M. Hutabarat, and K.M. Thompson. 2010. Discovery and development of therapeutic aptamers. *Annu Rev Pharmacol Toxicol*. 50:237-257.

Bradford, M.M. 1976. A rapid and sensitive method for the quantitation of microgram quantities of protein utilizing the principle of protein-dye binding. *Anal Biochem*. 72:248-254.

Bready, D., and D.G. Placantonakis. 2019. Molecular Pathogenesis of Low-Grade Glioma. *Neurosurg Clin N Am*. 30:17-25.

Brehar, F.M., R.M. Gorgan[1], and M. Lisievici. 2012. Image-guided stereotactic biopsy of infiltrative, multicentric and deep-seated supratentorial cerebral gliomas.

Brody, E.N., and L. Gold. 2000. Aptamers as therapeutic and diagnostic agents. *Reviews in Molecular Biotechnology*. 74:5-13.

Bunka, D.H.J., O. Platonova, and P.G. Stockley. 2010. Development of aptamer therapeutics. *Current Opinion in Pharmacology*. 10:557-562.

Bunka, D.H.J., and P.G. Stockley. 2006. Aptamers come of age – at last. *Nat Rev Micro*. 4:588-596.

Capes-Davis, A., G. Theodosopoulos, I. Atkin, H.G. Drexler, A. Kohara, R.A. MacLeod, J.R. Masters, Y. Nakamura, Y.A. Reid, R.R. Reddel, and R.I. Freshney. 2010. Check your cultures! A list of cross-contaminated or misidentified cell lines. *Int J Cancer*. 127:1-8.

Cerchia, L., and V. de Franciscis. 2010. Targeting cancer cells with nucleic acid aptamers. *Trends Biotechnol*. 28:517-525.

Cerchia, L., F. Duconge, C. Pestourie, J. Boulay, Y. Aissouni, K. Gombert, B. Tavitian, V. de Franciscis, and D. Libri. 2005. Neutralizing aptamers from whole-cell SELEX inhibit the RET receptor tyrosine kinase. *PLoS Biol*. 3:22.

Cerchia, L., C.L. Esposito, A.H. Jacobs, B. Tavitian, and V. de Franciscis. 2009. Differential SELEX in human glioma cell lines. *PLoS One*. 4:e7971.

Cerchia, L., J. Hamm, D. Libri, B. Tavitian, and V. de Franciscis. 2002. Nucleic acid aptamers in cancer medicine. *FEBS Lett*. 528:12-16.

Chakraborty, B., Z. Jiang, Y. Li, and H.-Z. Yu. 2009. Rational design and performance testing of aptamer-based electrochemical biosensors for adenosine. *Journal of Electroanalytical Chemistry*. 635:75-82.

Chamberlain, M. 2011. Evolving strategies: future treatment of glioblastoma. *Expert Rev Neurother*. 11:519-532.

Chang, H., Y. Ding, P. Wang, Q. Wang, Y. Lin, and B. Li. 2018. Cutaneous Metastases of the Glioma. *J Craniofac Surg*. 29:e94-e96.

Chang, H.W., S.Y. Kim, S.L. Yi, S.H. Son, Y. Song do, S.Y. Moon, J.H. Kim, E.K. Choi, S.D. Ahn, S.S. Shin, K.K. Lee, and S.W. Lee. 2006. Expression of Ku80 correlates with sensitivities to radiation in cancer cell lines of the head and neck. *Oral Oncol*. 42:979-986.

Chapdelaine, I., C.L. de Roij van Zuijdewijn, I.M. Mostovaya, R. Levesque, A. Davenport, P.J. Blankestijn, C. Wanner, M.J. Nube, M.P. Grooteman, C. Basile, F. Locatelli, F. Maduell, S. Mitra, C. Ronco, R. Shroff, and J. Tattersall. 2015. Optimization of the convection volume in online post-dilution haemodiafiltration: practical and technical issues. *Clin Kidney J*. 8:191-198.

Chen, J.-W., X.-P. Liu, K.-J. Feng, Y. Liang, J.-H. Jiang, G.-L. Shen, and R.-Q. Yu. 2008. Detection of adenosine using surface-enhanced Raman scattering based on structure-switching signaling aptamer. *Biosensors and Bioelectronics*. 24:66-71.

Chester, K. 2004. Engineering antibodies for clinical applications in cancer. *Tumour. Biol.* 25:91-98.

Chivers, C.E., A.L. Koner, E.D. Lowe, and M. Howarth. 2011. How the biotin-streptavidin interaction was made even stronger: investigation via crystallography and a chimaeric tetramer. *Biochem J*. 435:55-63.

Chowdhary, S.A., T. Ryken, and H.B. Newton. 2015. Survival outcomes and safety of carmustine wafers in the treatment of high-grade gliomas: a meta-analysis. *Journal of Neuro-Oncology*. 122:367-382.

Cibiel, A., C. Pestourie, and F. Ducongé. 2012. In vivo uses of aptamers selected against cell surface biomarkers for therapy and molecular imaging. *Biochimie*. 94:1595-1606.

Cilia, M., T. Fish, X. Yang, M. McLaughlin, T.W. Thannhauser, and S. Gray. 2009. A comparison of protein extraction methods suitable for gel-based proteomic studies of aphid proteins. *Journal of biomolecular techniques : JBT*. 20:201-215.

Coward, J., and A. Harding. 2014. Size Does Matter: Why Polyploid Tumor Cells are Critical Drug Targets in the War on Cancer. *Front Oncol*. 4.

Creixell, P., J. Reimand, S. Haider, G. Wu, T. Shibata, M. Vazquez, V. Mustonen, A. Gonzalez-Perez, J. Pearson, C. Sander, B.J. Raphael, D.S. Marks, B.F.F. Ouellette, A. Valencia, G.D. Bader, P.C. Boutros, J.M. Stuart, R. Linding, N. Lopez-Bigas, and L.D. Stein. 2015. Pathway and network analysis of cancer genomes. *Nat Methods*. 12:615-621.

CRUK. 2011. Brain, other CNS and intracranial tumours statistics. *In*.

CRUK. 2018. brain and other cns and intracranial tumours and mortality. *In*.

CRUK. 2019. brain, other CNS and intracranial tumours incidence statistics. *In*.

Cullen, B.R., and W.C. Greene. 1989. Regulatory pathways governing HIV-1 replication. *Cell*. 58:423-426.

Da Ros, M., V. De Gregorio, A.L. Iorio, L. Giunti, M. Guidi, M. de Martino, L. Genitori, and I. Sardi. 2018. Glioblastoma Chemoresistance: The Double Play by Microenvironment and Blood-Brain Barrier. *International journal of molecular sciences*. 19:2879.

Dahl, J.A., and P. Collas. 2008. A rapid micro chromatin immunoprecipitation assay (microChIP). *Nat Protoc*. 3:1032-1045.

Dalziel, R.G., S.C. Mendelson, and J.P. Quinn. 1992. The nuclear autoimmune antigen Ku is also present on the cell surface. *Autoimmunity*. 13:265-267.

Dang C, G.T., Surbone A, et al 2003. Growth Curve Analysis. In: Kufe DW, Pollock RE, Weichselbaum RR. *In*.

Davis, A.J., and D.J. Chen. 2013. DNA double strand break repair via non-homologous end-joining. *Translational cancer research*. 2:130-143.

Debinski, W., and S.B. Tatter. 2009. Convection-enhanced delivery for the treatment of brain tumors. *Expert Rev Neurother*. 9:1519-1527.

Debinski, W., and S.B. Tatter. 2010. Convection-enhanced delivery to achieve widespread distribution of viral vectors: Predicting clinical implementation. *Curr Opin Mol Ther*. 12:647-653.

Deeken, J.F., and W. Löscher. 2007. The Blood-Brain Barrier and Cancer: Transporters, Treatment, and Trojan Horses. *Clinical Cancer Research*. 13:1663-1674.

Degefa, T.H., and J. Kwak. 2008. Label-free aptasensor for platelet-derived growth factor (PDGF) protein. *Analytica Chimica Acta*. 613:163-168.

Duffau, H. 2018. Diffuse low-grade glioma, oncological outcome and quality of life: a surgical perspective. *Curr Opin Oncol*. 30:383-389.

Ellenbogen, A., Sehkar. 2012. Principles of Neurological Surgery. *In*.

Ellington, A.D., and J.W. Szostak. 1990. In vitro selection of RNA molecules that bind specific ligands. *Nature*. 346:818-822.

England, P.H. 2016. ECACC catalogue 86030402. *In*.

Erasimus, H., M. Gobin, S. Niclou, and E. Van Dyck. 2016. DNA repair mechanisms and their clinical impact in glioblastoma. *Mutat Res Rev Mutat Res*. 769:19-35.

Ernst, O., and T. Zor. 2010. Linearization of the bradford protein assay. *Journal of visualized experiments : JoVE*.1918.

Eyvazzadeh, N., A. Neshasteh-Riz, and S. Mahdavi. 2015. DNA Damage of Glioblastoma Multiform Cells Induced by Beta Radiation of Iodine-131 in The Presence or Absence of Topotecan: A Picogreen and Colonogenic Assay. 99-110 pp.

Fabian, D., M.D.P. Guillermo Prieto Eibl, I. Alnahhas, N. Sebastian, P. Giglio, V. Puduvalli, J. Gonzalez, and J.D. Palmer. 2019a. Treatment of Glioblastoma (GBM) with the Addition of Tumor-Treating Fields (TTF): A Review. *Cancers (Basel)*. 11.

Fabian, D., M.D.P. Guillermo Prieto Eibl, I. Alnahhas, N. Sebastian, P. Giglio, V. Puduvalli, J. Gonzalez, and J.D. Palmer. 2019b. Treatment of Glioblastoma (GBM) with the Addition of Tumor-Treating Fields (TTF): A Review. *Cancers*. 11:174.

Farr-Jones, M.A., I.F. Parney, and K.C. Petruk. 1999. Improved Technique for Establishing Short Term Human Brain Tumor Cultures. *Journal of Neuro-Oncology*. 43:1-10.

Feigon, J., T. Dieckmann, and F.W. Smith. 1996. Aptamer structures from A to ζ. *Chemistry & Biology*. 3:611-617.

Feng, K., C. Sun, Y. Kang, J. Chen, J.-H. Jiang, G.-L. Shen, and R.-Q. Yu. 2008. Label-free electrochemical detection of nanomolar adenosine based on target-induced aptamer displacement. *Electrochemistry Communications*. 10:531-535.

Filley, A.C., M. Henriquez, and M. Dey. 2017. Recurrent glioma clinical trial, CheckMate-143: the game is not over yet. *Oncotarget*. 8:91779-91794.

Fina, L., H. Molgaard, D. Robertson, N. Bradley, P. Monaghan, D. Delia, D. Sutherland, M. Baker, and M. Greaves. 1990. Expression of the CD34 gene in vascular endothelial cells. *Blood*. 75:2417-2426.

Fischer, U., D. Hemmer, D. Heckel, A. Michel, W. Feiden, W.I. Steudel, T. Hulsebos, and E. Meese. 2001. KUB3 amplification and overexpression in human gliomas. *Glia*. 36:1-10.

Forst, D.A., B.V. Nahed, J.S. Loeffler, and T.T. Batchelor. 2014. Low-grade gliomas. *The Oncologist*. 19:403-413.

Fortin, D. 2012. The blood-brain barrier: its influence in the treatment of brain tumors metastases. *Curr Cancer Drug Targets*. 12:247-259.

Freshney. 2005. Basic Principles of Cell Culture. *In* Culture of Cells for Tissue Engineering.

Freshney. 2006. Basic Principles of Cell Culture. *In* Culture of Cells for Tissue Engineering.

Fulton, B., S.C. Short, A. James, S. Nowicki, C. McBain, S. Jefferies, C. Kelly, J. Stobo, A. Morris, A. Williamson, and A.J. Chalmers. 2017. PARADIGM-2: Two parallel phase I studies of olaparib and radiotherapy or olaparib and radiotherapy plus temozolomide in patients with newly diagnosed glioblastoma, with treatment stratified by MGMT status. *Clin Transl Radiat Oncol*. 8:12-16.

Furneaux, C.E., E.S. Marshall, K. Yeoh, S.J. Monteith, P.J. Mews, C.A. Sansur, R.J. Oskouian, K.J. Sharples, and B.C. Baguley. 2008. Cell cycle times of short-term cultures of brain cancers as predictors of survival. *British Journal of Cancer*. 99:1678-1683.

Gazdar, A.F., B. Gao, and J.D. Minna. 2010. Lung cancer cell lines: Useless artifacts or invaluable tools for medical science? *Lung cancer (Amsterdam, Netherlands)*. 68:309-318.

Geldenhuys, W., D. Wehrung, A. Groshev, A. Hirani, and V. Sutariya. 2015. Brain-targeted delivery of doxorubicin using glutathione-coated nanoparticles for brain cancers. *Pharm Dev Technol*. 20:497-506.

Genesilico. 2019. SimRNA RNA 3D predictor. *In*.

Germer, K., M. Leonard, and X. Zhang. 2013. RNA aptamers and their therapeutic and diagnostic applications. *Int J Biochem Mol Biol*. 4:27-40.

Gillet, J.-P., A.M. Calcagno, S. Varma, M. Marino, L.J. Green, M.I. Vora, C. Patel, J.N. Orina, T.A. Eliseeva, V. Singal, R. Padmanabhan, B. Davidson, R. Ganapathi, A.K. Sood, B.R. Rueda, S.V. Ambudkar, and M.M. Gottesman. 2011. Redefining the relevance of established cancer cell lines to the study of mechanisms of clinical anti-cancer drug resistance. *Proceedings of the National Academy of Sciences of the United States of America*. 108:18708-18713.

Gold, L., N. Janjic, T. Jarvis, D. Schneider, J.J. Walker, S.K. Wilcox, and D. Zichi. 2012. Aptamers and the RNA world, past and present. *Cold Spring Harb Perspect Biol*. 4.

Goodden, J., B. Pizer, B. Pettorini, D. Williams, J. Blair, M. Didi, N. Thorp, and C. Mallucci. 2014. The role of surgery in optic pathway/hypothalamic gliomas in children. *J Neurosurg Pediatr*. 13:1-12.

Gopinath, S.C.B., T. Lakshmipriya, M.K. Md Arshad, C.H. Voon, T. Adam, U. Hashim, H. Singh, and S.V. Chinni. 2017. Shortening full-length aptamer by crawling base deletion – Assisted by Mfold web server application. *Journal of the Association of Arab Universities for Basic and Applied Sciences*. 23:37-42.

Goyal, R., S.K. Mathur, S. Gupta, R. Goyal, S. Kumar, A. Batra, S. Hasija, and R. Sen. 2015. Immunohistochemical expression of glial fibrillary acidic protein and CAM5.2 in glial tumors and their role in differentiating glial tumors from metastatic tumors of central nervous system. *Journal of Neurosciences in Rural Practice*. 6:499-503.

Green, L.S., D. Jellinek, C. Bell, L.A. Beebe, B.D. Feistner, S.C. Gill, F.M. Jucker, and N. Janjic. 1995. Nuclease-resistant nucleic acid ligands to vascular permeability factor/vascular endothelial growth factor. *Chem Biol*. 2:683-695.

Greenberg. 2014. Handbook of Neurosurery. *In*.

Guo, L., H. Zhang, and B. Chen. 2017. Nivolumab as Programmed Death-1 (PD-1) Inhibitor for Targeted Immunotherapy in Tumor. *Journal of Cancer*. 8:410-416.

Guo, P. 2010. The emerging field of RNA nanotechnology. *Nat Nanotechnol*. 5:833-842.

Hadjipanayis, C.G., G. Widhalm, and W. Stummer. 2015. What is the Surgical Benefit of Utilizing 5-Aminolevulinic Acid for Fluorescence-Guided Surgery of Malignant Gliomas? *Neurosurgery*. 77:663-673.

Halford, S.E.R., G. Cruickshank, L. Dunn, S. Erridge, L. Godfrey, C. Herbert, S. Jefferies, J.S. Lopez, C. McBain, M. Pittman, R. Sleigh, C. Watts, M.F. Webster-Smith, and A.J. Chalmers. 2017. Results of the OPARATIC trial: A phase I dose escalation study of olaparib in combination with temozolomide (TMZ) in patients with relapsed glioblastoma (GBM). *Journal of Clinical Oncology*. 35:2022-2022.

Hands, J.R., G. Clemens, R. Stables, K. Ashton, A. Brodbelt, C. Davis, T.P. Dawson, M.D. Jenkinson, R.W. Lea, C. Walker, and M.J. Baker. 2016. Brain tumour differentiation: rapid stratified serum diagnostics via attenuated total reflection Fourier-transform infrared spectroscopy. *J Neurooncol*. 127:463-472.

Hartmann, J., and S.E. Croteau. 2016. 2017 Clinical trials update: Innovations in hemophilia therapy. *Am J Hematol*. 91:1252-1260.

Hentschel, S.J., and R. Sawaya. 2003. Optimizing outcomes with maximal surgical resection of malignant gliomas. *Cancer Control*. 10:109-114.

Hermann, T., and D.J. Patel. 2000. Adaptive recognition by nucleic acid aptamers. *Science*. 287:820-825.

Hicke, B.J., C. Marion, Y.F. Chang, T. Gould, C.K. Lynott, D. Parma, P.G. Schmidt, and S. Warren. 2001. Tenascin-C aptamers are generated using tumor cells and purified protein. *J Biol Chem*. 276:48644-48654.

Hicke, B.J., A.W. Stephens, T. Gould, Y.F. Chang, C.K. Lynott, J. Heil, S. Borkowski, C.S. Hilger, G. Cook, S. Warren, and P.G. Schmidt. 2006. Tumor targeting by an aptamer. *J Nucl Med*. 47:668-678.

Hofacker, I.L. 2004. RNA secondary structure analysis using the Vienna RNA package. *Curr Protoc Bioinformatics*. Chapter 12:Unit 12 12.

Hofacker, I.L., M. Fekete, and P.F. Stadler. 2002. Secondary structure prediction for aligned RNA sequences. *J Mol Biol*. 319:1059-1066.

Holland, E.C. 2000. Glioblastoma multiforme: the terminator. *Proc Natl Acad Sci U S A*. 97:6242-6244.

Holmberg, A., A. Blomstergren, O. Nord, M. Lukacs, J. Lundeberg, and M. Uhlen. 2005. The biotin-streptavidin interaction can be reversibly broken using water at elevated temperatures. *Electrophoresis*. 26:501-510.

Hottinger, A.F., P. Pacheco, and R. Stupp. 2016. Tumor treating fields: a novel treatment modality and its use in brain tumors. *Neuro-Oncology*. 18:1338-1349.

Huh, Y.S., and D. Erickson. 2010. Aptamer based surface enhanced Raman scattering detection of vasopressin using multilayer nanotube arrays. *Biosensors and Bioelectronics*. 25:1240-1243.

Huizenga, D.E., and J.W. Szostak. 1995. A DNA Aptamer That Binds Adenosine and ATP. *Biochemistry*. 34:656-665.

Huse, J.T., and E.C. Holland. 2010. Targeting brain cancer: advances in the molecular pathology of malignant glioma and medulloblastoma. *Nat Rev Cancer*. 10:319-331.

Ikeda, K., T. Monden, T. Kanoh, M. Tsujie, H. Izawa, A. Haba, T. Ohnishi, M. Sekimoto, N. Tomita, H. Shiozaki, and M. Monden. 1998. Extraction and analysis of diagnostically useful proteins from formalin-fixed, paraffin-embedded tissue sections. *J Histochem Cytochem*. 46:397-403.

Irvine, D., C. Tuerk, and L. Gold. 1991. SELEXION. Systematic evolution of ligands by exponential enrichment with integrated optimization by non-linear analysis. *J Mol Biol*. 222:739-761.

Iwamoto, F.M., and H.A. Fine. 2010. Bevacizumab for Malignant Gliomas. *Archives of Neurology*. 67:285-288.

Jayasena, S.D. 1999. Aptamers: an emerging class of molecules that rival antibodies in diagnostics. *Clin Chem*. 45:1628-1650.

Jellinek, D., L.S. Green, C. Bell, C.K. Lynott, N. Gill, C. Vargeese, G. Kirschenheuter, D.P. McGee, P. Abesinghe, W.A. Pieken, and et al. 1995. Potent 2'-amino-2'-deoxypyrimidine RNA inhibitors of basic fibroblast growth factor. *Biochemistry*. 34:11363-11372.

Jenkinson M, K., K. M. . 2017. Brain tumour research in the UK: current and future challenges.

Jung, C.S., A.W. Unterberg, and C. Hartmann. 2011. Diagnostic markers for glioblastoma. *Histol Histopathol*. 26:1327-1341.

Kaur, G., and J.M. Dufour. 2012. Cell lines: Valuable tools or useless artifacts. *Spermatogenesis*. 2:1-5.

KEGG. 2019.

Kleihues, P., D.N. LOUIS, B.W. SCHEITHAUER, L.B. RORKE, G. REIFENBERGER, P.C. BURGER, and W.K. CAVENEE. 2002. The WHO Classification of Tumors of the Nervous System. *Journal of Neuropathology & Experimental Neurology*. 61:215-225.

Klussman, S. 2005. The Aptamer Handbook. *In*.

Korshoej, A.R., J.C.H. Sorensen, G. von Oettingen, F.R. Poulsen, and A. Thielscher. 2019. Optimization of tumor treating fields using singular value decomposition and minimization of field anisotropy. *Phys Med Biol*. 64:04NT03.

Krex, D., B. Klink, C. Hartmann, A. von Deimling, T. Pietsch, M. Simon, M. Sabel, J.P. Steinbach, O. Heese, G. Reifenberger, M. Weller, G. Schackert, and f.t.G.G. Network. 2007. Long-term survival with glioblastoma multiforme. *Brain*. 130:2596-2606.

Krishnamoorthy, S.K., V. Relias, S. Sebastian, V. Jayaraman, and M.W. Saif. 2015. Management of regorafenib-related toxicities: a review. *Therap Adv Gastroenterol*. 8:285-297.

Kumar, S.A. 2015. Developing a physiologically relevant blood brain barrier model for the study of drug disposition in glioma. Uclan,

Labeta, M.O., N. Fernandez, and H. Festenstein. 1988. Solubilisation effect of Nonidet P-40, triton X-100 and CHAPS in the detection of MHC-like glycoproteins. *J Immunol Methods*. 112:133-138.

Lanese, A., E. Franceschi, and A.A. Brandes. 2018. The Risk Assessment in Low-Grade Gliomas: An Analysis of the European Organization for Research and Treatment of Cancer (EORTC) and the Radiation Therapy Oncology Group (RTOG) criteria. *Oncology and Therapy*. 6:105-108.

Lee, C.H. 2017. A Simple Outline of Methods for Protein Isolation and Purification. *Endocrinology and metabolism (Seoul, Korea)*. 32:18-22.

Lee, T.I., S.E. Johnstone, and R.A. Young. 2006. Chromatin immunoprecipitation and microarray-based analysis of protein location. *Nat Protoc*. 1:729-748.

Lerga, T.M., and C.K. O'Sullivan. 2008. Rapid determination of total hardness in water using fluorescent molecular aptamer beacon. *Analytica Chimica Acta*. 610:105-111.

Levine, H.A., and M. Nilsen-Hamilton. 2007. A mathematical analysis of SELEX. *Comput Biol Chem*. 31:11-35.

Li, B., Y. Wang, H. Wei, and S. Dong. 2008. Amplified electrochemical aptasensor taking AuNPs based sandwich sensing platform as a model. *Biosensors and Bioelectronics*. 23:965-970.

Lin, C.H., and D.J. Patei. 1997. Structural basis of DNA folding and recognition in an AMP-DNA aptamer complex: distinct architectures but common recognition motifs for DNA and RNA aptamers complexed to AMP. *Chemistry & Biology*. 4:817-832.

Lin, G., E. Finger, and J.C. Gutierrez-Ramos. 1995. Expression of CD34 in endothelial cells, hematopoietic progenitors and nervous cells in fetal and adult mouse tissues. *Eur J Immunol*. 25:1508-1516.

Liu, R., Z. Mao, D.L. Matthews, C.S. Li, J.W. Chan, and N. Satake. 2013. Novel single-cell functional analysis of red blood cells using laser tweezers Raman spectroscopy: application for sickle cell disease. *Exp Hematol*. 41:656-661 e651.

Liu, T., and J. Huang. 2016. Replication protein A and more: single-stranded DNA-binding proteins in eukaryotic cells. *Acta Biochimica et Biophysica Sinica*. 48:665-670.

Livnah, O., E.A. Bayer, M. Wilchek, and J.L. Sussman. 1993. Three-dimensional structures of avidin and the avidin-biotin complex. *Proc Natl Acad Sci U S A*. 90:5076-5080.

Lombardi, G., A. Pambuku, L. Bellu, M. Farina, A. Della Puppa, L. Denaro, and V. Zagonel. 2017. Effectiveness of antiangiogenic drugs in glioblastoma patients: A systematic review and meta-analysis of randomized clinical trials. *Crit Rev Oncol Hematol*. 111:94-102.

Lombardi, G., G.L.D. Salvo, R. Ruda, E. Franceschi, M. Eoli, M. Faedi, A. Pace, I. Lolli, S. Rizzato, D. Germano, F. Pasqualetti, M. Farina, G. Magni, L. Bellu, A. Pambuku, E. Bergo, S. Indraccolo, M.P. Gardiman, R. Soffietti, and V. Zagonel. 2018. Updated results of REGOMA: A randomized, multicenter, controlled open-label phase II clinical trial evaluating regorafenib in relapsed glioblastoma (GBM) patients (PTS). *Journal of Clinical Oncology*. 36:2047-2047.

Long, S.B., M.B. Long, R.R. White, and B.A. Sullenger. 2008. Crystal structure of an RNA aptamer bound to thrombin. *Rna*. 14:2504-2512.

Louis, D.N., H. Ohgaki, O.D. Wiestler, W.K. Cavenee, P.C. Burger, A. Jouvet, B.W. Scheithauer, and P. Kleihues. 2007. The 2007 WHO classification of tumours of the central nervous system. *Acta Neuropathol*. 114:97-109.

Louis, D.N., A. Perry, G. Reifenberger, A. von Deimling, D. Figarella-Branger, W.K. Cavenee, H. Ohgaki, O.D. Wiestler, P. Kleihues, and D.W. Ellison. 2016. The 2016 World Health Organization Classification of Tumors of the Central Nervous System: a summary. *Acta Neuropathol*. 131:803-820.

Lu, Y., X. Li, L. Zhang, P. Yu, L. Su, and L. Mao. 2008. Aptamer-Based Electrochemical Sensors with Aptamer−Complementary DNA Oligonucleotides as Probe. *Analytical Chemistry*. 80:1883-1890.

Lukk, M., M. Kapushesky, J. Nikkilä, H. Parkinson, A. Goncalves, W. Huber, E. Ukkonen, and A. Brazma. 2010. A global map of human gene expression. *Nature biotechnology*. 28:322-324.

Macdonald, J., P. Houghton, D. Xiang, W. Duan, and S. Shigdar. 2016. Truncation and Mutation of a Transferrin Receptor Aptamer Enhances Binding Affinity. *Nucleic Acid Ther*. 26:348-354.

Machado, C.M.L., A. Schenka, J. Vassallo, W.M.S.C. Tamashiro, E.M. Gonçalves, S.C. Genari, and L. Verinaud. 2005. Morphological characterization of a human glioma cell l ine. *Cancer Cell International*. 5:13-13.

Maleniak, T.C., J.L. Darling, P.R. Lowenstein, and M.G. Castro. 2001. Adenovirus-mediated expression of HSV1-TK or Fas ligand induces cell death in primary human glioma-derived cell cultures that are resistant to the chemotherapeutic agent CCNU. *Cancer Gene Therapy*. 8:589.

Manangazira, D. 2013. The generation of novel aptamers for glioma and their pharmacokinetic profile in vitro Uclan,

Marciniak, R.A., B.J. Calnan, A.D. Frankel, and P.A. Sharp. 1990. HIV-1 Tat protein trans-activates transcription in vitro. *Cell*. 63:791-802.

Markovic, O., and N. Markovic. 1998. Cell cross-contamination in cell cultures: The silent and neglected danger. *In Vitro Cellular & Developmental Biology - Animal*. 34:1-8.

Mayer, G. 2009. The chemical biology of aptamers. *Angew Chem Int Ed Engl*. 48:2672-2689.

Mazzarelli, P., P. Parrella, D. Seripa, E. Signori, G. Perrone, C. Rabitti, D. Borzomati, A. Gabbrielli, M.G. Matera, C. Gravina, M. Caricato, M.L. Poeta, M. Rinaldi, S. Valeri, R. Coppola, and V.M. Fazio. 2005. DNA end binding activity and Ku70/80 heterodimer expression in human colorectal tumor. *World J Gastroenterol*. 11:6694-6700.

McGirt, M.J., K.D. Than, J.D. Weingart, K.L. Chaichana, F.J. Attenello, A. Olivi, J. Laterra, L.R. Kleinberg, S.A. Grossman, H. Brem, and A. Quiñones-Hinojosa. 2009. Gliadel (BCNU) wafer plus concomitant temozolomide therapy after primary resection of glioblastoma multiforme. *Journal of neurosurgery*. 110:583-588.

McKinney, P.A. 2004. Brain tumours: incidence, survival, and aetiology. *Journal of Neurology, Neurosurgery & Psychiatry*. 75:ii12-ii17.

McMahon, G. 2000. VEGF Receptor Signaling in Tumor Angiogenesis. *The Oncologist*. 5:3-10.

Miller, R.E., S.M. Crusz, and J.A. Ledermann. 2019. Olaparib maintenance for first-line treatment of ovarian cancer: will SOLO1 reset the standard of care? *Future Oncol*. 15:1845-1853.

Mirza, M.R., S. Pignata, and J.A. Ledermann. 2018. Latest clinical evidence and further development of PARP inhibitors in ovarian cancer. *Annals of Oncology*. 29:1366-1376.

Mitra, A., L. Mishra, and S. Li. 2013. Technologies for deriving primary tumor cells for use in personalized cancer therapy. *Trends Biotechnol*. 31:347-354.

Moll, U., R. Lau, M.A. Sypes, M.M. Gupta, and C.W. Anderson. 1999. DNA-PK, the DNA-activated protein kinase, is differentially expressed in normal and malignant human tissues. *Oncogene*. 18:3114-3126.

Monferran, S., C. Muller, L. Mourey, P. Frit, and B. Salles. 2004a. The Membrane-associated form of the DNA repair protein Ku is involved in cell adhesion to fibronectin. *J Mol Biol*. 337:503-511.

Monferran, S., J. Paupert, S. Dauvillier, B. Salles, and C. Muller. 2004b. The membrane form of the DNA repair protein Ku interacts at the cell surface with metalloproteinase 9. *EMBO J*. 23:3758-3768.

Moore, J.K., and J.E. Haber. 1996. Cell cycle and genetic requirements of two pathways of nonhomologous end-joining repair of double-strand breaks in Saccharomyces cerevisiae. *Mol Cell Biol*. 16:2164-2173.

Morales, J., L. Li, F.J. Fattah, Y. Dong, E.A. Bey, M. Patel, J. Gao, and D.A. Boothman. 2014. Review of poly (ADP-ribose) polymerase (PARP) mechanisms of action and rationale for targeting in cancer and other diseases. *Critical reviews in eukaryotic gene expression*. 24:15-28.

Mourad, P.D., L. Farrell, L.D. Stamps, M.R. Chicoine, and D.L. Silbergeld. 2005. Why are systemic glioblastoma metastases rare? Systemic and cerebral growth of mouse glioblastoma. *Surgical Neurology*. 63:511-519.

Muller, C., J. Paupert, S. Monferran, and B. Salles. 2005. The double life of the Ku protein: facing the DNA breaks and the extracellular environment. *Cell Cycle*. 4:438-441.

Nabors, L.B., K.L. Fink, T. Mikkelsen, D. Grujicic, R. Tarnawski, D.H. Nam, M. Mazurkiewicz, M. Salacz, L. Ashby, V. Zagonel, R. Depenni, J.R. Perry, C. Hicking, M. Picard, M.E. Hegi, B. Lhermitte, and D.A. Reardon. 2015. Two cilengitide regimens in combination with standard treatment for patients with newly diagnosed glioblastoma and unmethylated MGMT gene promoter: results of the open-label, controlled, randomized phase II CORE study. *Neuro Oncol*. 17:708-717.

Nadal, P., M. Svobodova, T. Mairal, and C.K. O'Sullivan. 2013. Probing high-affinity 11-mer DNA aptamer against Lup an 1 (β-conglutin). *Analytical and Bioanalytical Chemistry*. 405:9343-9349.

Nagase, H., and J.F. Woessner, Jr. 1999. Matrix metalloproteinases. *J Biol Chem*. 274:21491-21494.

Nardone, R.M. 2007. Eradication of cross-contaminated cell lines: A call for action. *Cell Biology and Toxicology*. 23:367-372.

Neira, J.A., T.H. Ung, J.S. Sims, H.R. Malone, D.S. Chow, J.L. Samanamud, G.J. Zanazzi, X. Guo, S.G. Bowden, B. Zhao, S.A. Sheth, G.M. McKhann, 2nd, M.B. Sisti, P. Canoll, R.S. D'Amico, and J.N. Bruce. 2017. Aggressive resection at the infiltrative margins of glioblastoma facilitated by intraoperative fluorescein guidance. *J Neurosurg*. 127:111-122.

Nelson, A.J., R. Zakaria, M.D. Jenkinson, and A.R. Brodbelt. 2019. Extent of resection predicts risk of progression in adult pilocytic astrocytoma. *Br J Neurosurg*. 33:343-347.

Neuros.net. 2014. brain tumours in general. *In*.

Ng, E.W., D.T. Shima, P. Calias, E.T. Cunningham, Jr., D.R. Guyer, and A.P. Adamis. 2006. Pegaptanib, a targeted anti-VEGF aptamer for ocular vascular disease. *Nat Rev Drug Discov*. 5:123-132.

Ng, H.K., C.C. Tse, and S.T. Lo. 1987. Meningiomas and arachnoid cells: an immunohistochemical study of epithelial markers. *Pathology*. 19:253-257.

NICE. 2019. NICE Brain tumour recommendations. *In*.

NICE.org.uk. 2018. Brain tumours (primary) and brain metastases in adults. *In*.

Nickel, W. 2003. The mystery of nonclassical protein secretion. A current view on cargo proteins and potential export routes. *Eur J Biochem*. 270:2109-2119.

NOXXON. 2015. NOX-E36. *In*.

Ohgaki, H., and P. Kleihues. 2007. Genetic pathways to primary and secondary glioblastoma. *Am J Pathol*. 170:1445-1453.

Omar, A.I. 2014. Tumor treating field therapy in combination with bevacizumab for the treatment of recurrent glioblastoma. *J Vis Exp*.e51638.

Osborne, S.E., I. Matsumura, and A.D. Ellington. 1997. Aptamers as therapeutic and diagnostic reagents: problems and prospects. *Curr Opin Chem Biol*. 1:5-9.

Osborne, S.E., J. Völker, S.Y. Stevens, K.J. Breslauer, and G.D. Glick. 1996. Design, Synthesis, and Analysis of Disulfide Cross-Linked DNA Duplexes. *Journal of the American Chemical Society*. 118:11993-12003.

Pan, W., and G.A. Clawson. 2009. The shorter the better: reducing fixed primer regions of oligonucleotide libraries for aptamer selection. *Molecules*. 14:1353-1369.

Park, J.H., N. Jung, S.J. Kang, H.S. Kim, E. Kim, H.J. Lee, H.R. Jung, M. Choe, and Y.J. Shim. 2019. Survival and Prognosis of Patients with Pilocytic Astrocytoma: A Single-Center Study. *Brain Tumor Res Treat*. 7:92-97.

Patel, D.J. 1997. Structural analysis of nucleic acid aptamers. *Curr Opin Chem Biol*. 1:32-46.

Pchelintsev, N.A., P.D. Adams, and D.M. Nelson. 2016. Critical Parameters for Efficient Sonication and Improved Chromatin Immunoprecipitation of High Molecular Weight Proteins. *PloS one*. 11:e0148023.

Pei, J.S., Y.M. Lee, H.H. Lo, Y.N. Hsu, S.S. Lin, and D.T. Bau. 2013. Association of X-ray repair cross-complementing-6 genotypes with childhood leukemia. *Anticancer Res*. 33:5395-5399.

Persson, O., L.G. Salford, J. Fransson, B. Widegren, C.A. Borrebaeck, and B. Holmqvist. 2010. Distribution, cellular localization, and therapeutic potential of the tumor-associated antigen Ku70/80 in glioblastoma multiforme. *J Neurooncol*. 97:207-215.

Pestourie, C., L. Cerchia, K. Gombert, Y. Aissouni, J. Boulay, V. De Franciscis, D. Libri, B. Tavitian, and F. Duconge. 2006. Comparison of different strategies to select aptamers against a transmembrane protein target. *Oligonucleotides*. 16:323-335.

Phillips, J.A., D. Lopez-Colon, Z. Zhu, Y. Xu, and W. Tan. 2008. Applications of aptamers in cancer cell biology. *Analytica Chimica Acta*. 621:101-108.

Prabhakar, B.S., G.P. Allaway, J. Srinivasappa, and A.L. Notkins. 1990. Cell surface expression of the 70-kD component of Ku, a DNA-binding nuclear autoantigen. *J Clin Invest*. 86:1301-1305.

Pu, Y., Z. Zhu, H. Liu, J. Zhang, J. Liu, and W. Tan. 2010. Using aptamers to visualize and capture cancer cells. *Analytical and bioanalytical chemistry*. 397:3225-3233.

Pucci, S., P. Mazzarelli, C. Rabitti, M. Giai, M. Gallucci, G. Flammia, A. Alcini, V. Altomare, and V.M. Fazio. 2001. Tumor specific modulation of KU70/80 DNA binding activity in breast and bladder human tumor biopsies. *Oncogene*. 20:739-747.

Purves D, A.G., Fitzpatrick D, et al., editors. ; 2001. Neuroglial Cells. 2001. Neuroscience. 2nd edition. Sunderland (MA): Sinauer Associates. *In*.

Que-Gewirth, N.S., and B.A. Sullenger. 2007. Gene therapy progress and prospects: RNA aptamers. *Gene Ther*. 14:283-291.

Rampling, R., A. James, and V. Papanastassiou. 2004. The present and future management of malignant brain tumours: surgery, radiotherapy, chemotherapy. *Journal of Neurology, Neurosurgery & Psychiatry*. 75:ii24-ii30.

Reston, E.O.M. 1987. Immortal line of Human fetal glial cells. *In*, United states.

Robson, M.E., N. Tung, P. Conte, S.A. Im, E. Senkus, B. Xu, N. Masuda, S. Delaloge, W. Li, A. Armstrong, W. Wu, C. Goessl, S. Runswick, and S.M. Domchek. 2019. OlympiAD final overall survival and tolerability results: Olaparib versus chemotherapy treatment of physician's choice in patients with a germline BRCA mutation and HER2-negative metastatic breast cancer. *Ann Oncol*. 30:558-566.

Rotta, J.M., D.B. Rodrigues, J.M. Diniz, B.M. Abreu, F. Kamimura, U.O. Sousa, R.V. Botelho, and M.F. Oliveira. 2018. Analysis of survival in patients with brain metastases treated surgically: Impact of age, gender, oncologic status, chemotherapy, radiotherapy, number and localization of lesions, and primary cancer site. *Rev Assoc Med Bras (1992)*. 64:717-722.

Ruckman, J., L.S. Green, J. Beeson, S. Waugh, W.L. Gillette, D.D. Henninger, L. Claesson-Welsh, and N. Janjic. 1998. 2'-Fluoropyrimidine RNA-based aptamers to the 165-amino acid form of vascular endothelial growth factor (VEGF165). Inhibition of receptor binding and VEGF-induced vascular permeability through interactions requiring the exon 7-encoded domain. *J Biol Chem*. 273:20556-20567.

Ruigrok, V.J., M. Levisson, J. Hekelaar, H. Smidt, B.W. Dijkstra, and J. van der Oost. 2012. Characterization of aptamer-protein complexes by X-ray crystallography and alternative approaches. *Int J Mol Sci*. 13:10537-10552.

Sadick, J.S., M.E. Boutin, D. Hoffman-Kim, and E.M. Darling. 2016. Protein characterization of intracellular target-sorted, formalin-fixed cell subpopulations. *Scientific Reports*. 6:33999-33999.

Sadick, J.S., and E.M. Darling. 2017. Processing fixed and stored adipose-derived stem cells for quantitative protein array assays. *Biotechniques*. 63:275-280.

Sampson, J.H., L.E. Crotty, S. Lee, G.E. Archer, D.M. Ashley, C.J. Wikstrand, L.P. Hale, C. Small, G. Dranoff, A.H. Friedman, H.S. Friedman, and D.D. Bigner. 2000. Unarmed, tumor-specific monoclonal antibody effectively treats brain tumors. *Proceedings of the National Academy of Sciences*. 97:7503-7508.

Sampson, T. 2003. Aptamers and SELEX: the technology. *World Patent Information*. 25:123-129.

Sanai, N., and M.S. Berger. 2008. Glioma extent of resection and its impact on patient outcome. *Neurosurgery*. 62:753-764.

Schrama, D. 2004. Shift from systemic to site-specific memory by tumor-targeted IL-2. *J. Immunol.* 172:5843-5850.

Schüling, T., A. Eilers, T. Scheper, and J. Walter. 2018. Aptamer-based lateral flow assays. 78-102 pp.

Seluanov, A., J. Danek, N. Hause, and V. Gorbunova. 2007. Changes in the level and distribution of Ku proteins during cellular senescence. *DNA Repair (Amst)*. 6:1740-1748.

Sennino, B. 2010. Two is better than one: benefits of VEGF and PDGF inhibition in ovarian cancer. *Cancer Biol Ther*. 9:183-185.

Seo, Y.J., S. Chen, M. Nilsen-Hamilton, and H.A. Levine. 2010. A mathematical analysis of multiple-target SELEX. *Bull Math Biol*. 72:1623-1665.

Sharma, S.K., K.D. Bagshawe, and R.H. Begent. 2005. Advances in antibody-directed enzyme prodrug therapy. *Curr. Opin. Investig. Drugs*. 6:611-615.

Shigdar, s. 2010. Aptamer Therapeutics: The 21st Century's magic Bullet of nanomedicine.

Sidney, L.E., M.J. Branch, S.E. Dunphy, H.S. Dua, and A. Hopkinson. 2014. Concise Review: Evidence for CD34 as a Common Marker for Diverse Progenitors. *Stem Cells (Dayton, Ohio)*. 32:1380-1389.

Soeda, A., A. Hara, T. Kunisada, S.-i. Yoshimura, T. Iwama, and D.M. Park. 2015. The Evidence of Glioblastoma Heterogeneity. *Scientific Reports*. 5:7979.

Spencer, V.A., J.-M. Sun, L. Li, and J.R. Davie. 2003. Chromatin immunoprecipitation: a tool for studying histone acetylation and transcription factor binding. *Methods*. 31:67-75.

Srisawat, C. 2014.

Starikov, E.B., and L. Nilsson. 2002. Structural basis of biotin–RNA aptamer binding: a theoretical study. *Chemical Physics Letters*. 363:39-44.

Stein, G.H. 1979. T98G: an anchorage-independent human tumor cell line that exhibits stationary phase G1 arrest in vitro. *J Cell Physiol*. 99:43-54.

Stoltenburg, R., C. Reinemann, and B. Strehlitz. 2007. SELEX—A (r)evolutionary method to generate high-affinity nucleic acid ligands. *Biomolecular Engineering*. 24:381-403.

Stronati, L., G. Gensabella, C. Lamberti, P. Barattini, D. Frasca, C. Tanzarella, S. Giacobini, M.G. Toscano, C. Santacroce, and D.T. Danesi. 2001. Expression and DNA binding activity of the Ku heterodimer in bladder carcinoma. *Cancer*. 92:2484-2492.

Stummer, W., T. Beck, W. Beyer, J.H. Mehrkens, A. Obermeier, N. Etminan, H. Stepp, J.C. Tonn, R. Baumgartner, J. Herms, and F.W. Kreth. 2008. Long-sustaining response in a patient with non-resectable, distant recurrence of glioblastoma multiforme treated by interstitial photodynamic therapy using 5-ALA: case report. *J Neurooncol*. 87:103-109.

Stummer, W., U. Nestler, F. Stockhammer, D. Krex, B.C. Kern, H.M. Mehdorn, G.H. Vince, and U. Pichlmeier. 2011. Favorable outcome in the elderly cohort treated by concomitant temozolomide radiochemotherapy in a multicentric phase II safety study of 5-ALA. *J Neurooncol*. 103:361-370.

Stupp, R., W.P. Mason, M.J. van den Bent, M. Weller, B. Fisher, M.J. Taphoorn, K. Belanger, A.A. Brandes, C. Marosi, U. Bogdahn, J. Curschmann, R.C. Janzer, S.K. Ludwin, T. Gorlia, A. Allgeier, D. Lacombe, J.G. Cairncross, E. Eisenhauer, and R.O. Mirimanoff. 2005. Radiotherapy plus concomitant and adjuvant temozolomide for glioblastoma. *N Engl J Med*. 352:987-996.

Sundaram, P., H. Kurniawan, M.E. Byrne, and J. Wower. 2013. Therapeutic RNA aptamers in clinical trials. *European Journal of Pharmaceutical Sciences*. 48:259-271.

Takano, S. 2012. Glioblastoma angiogenesis: VEGF resistance solutions and new strategies based on molecular mechanisms of tumor vessel formation. *Brain Tumor Pathol*. 29:73-86.

Thermofischerscientific. 2010. Traditional methods of cell lysis. *In*.

Tombelli, S., M. Minunni, and M. Mascini. 2005. Analytical applications of aptamers. *Biosensors and Bioelectronics*. 20:2424-2434.

Tombelli, S., M. Minunni, and M. Mascini. 2007. Aptamers-based assays for diagnostics, environmental and food analysis. *Biomolecular Engineering*. 24:191-200.

Tuerk, C., and L. Gold. 1990. Systematic evolution of ligands by exponential enrichment: RNA ligands to bacteriophage T4 DNA polymerase. *Science*. 249:505-510.

Utsuki, S., H. Oka, C. Kijima, Y. Miyajima, H. Hagiwara, and K. Fujii. 2011. Utility of intraoperative fluorescent diagnosis of residual hemangioblastoma using 5-aminolevulinic acid. *Neurology India*. 59:612-615.

Vant-Hull, B., A. Payano-Baez, R.H. Davis, and L. Gold. 1998. The mathematics of SELEX against complex targets. *J Mol Biol*. 278:579-597.

Viens, A., U. Mechold, H. Lehrmann, A. Harel-Bellan, and V. Ogryzko. 2004. Use of protein biotinylation in vivo for chromatin immunoprecipitation. *Analytical Biochemistry*. 325:68-76.

Wadsworth, P. 2007. Studying Mitosis in Cultured Mammalian Cells. *Cold Spring Harbor Protocols*. 2007:pdb.prot4674.

Wang, G.Q., and L.X. Chen. 2009. Aptameric SERS sensor for Hg2+ analysis using silver nanoparticles. *Chinese Chemical Letters*. 20:1475-1477.

Wang, J., F. Wang, and S. Dong. 2009. Methylene blue as an indicator for sensitive electrochemical detection of adenosine based on aptamer switch. *Journal of Electroanalytical Chemistry*. 626:1-5.

Wang, Y., J. Fang, J. Nie, L. Dai, W. Hu, J. Zhang, X. Ma, J. Han, X. Chen, G. Tian, D. Wu, S. Han, and J. Long. 2016. [Timing of Brain Radiation Therapy Impacts Outcomes in Patients with Non-small Cell Lung Cancer Who Develop Brain Metastases]. *Zhongguo Fei Ai Za Zhi*. 19:508-514.

Warren, K.E. 2018. Beyond the Blood:Brain Barrier: The Importance of Central Nervous System (CNS) Pharmacokinetics for the Treatment of CNS Tumors, Including Diffuse Intrinsic Pontine Glioma. *Frontiers in Oncology*. 8.

Weber, P., D. Ohlendorf, J. Wendoloski, and F. Salemme. 1989. Structural origins of high-affinity biotin binding to streptavidin. *Science*. 243:85-88.

Weiss, S., D. Proske, M. Neumann, M.H. Groschup, H.A. Kretzschmar, M. Famulok, and E.L. Winnacker. 1997. RNA aptamers specifically interact with the prion protein PrP. *J Virol*. 71:8790-8797.

Wenger, K.J., M. Wagner, S.-J. You, K. Franz, P.N. Harter, M.C. Burger, M. Voss, M.W. Ronellenfitsch, E. Fokas, J.P. Steinbach, and O. Bähr. 2017. Bevacizumab as a last-line treatment for glioblastoma following failure of radiotherapy, temozolomide and lomustine. *Oncology letters*. 14:1141-1146.

Wesseling, P., and D. Capper. 2018. WHO 2016 Classification of gliomas. *Neuropathol Appl Neurobiol*. 44:139-150.

Westphal, M., D.C. Hilt, E. Bortey, P. Delavault, R. Olivares, P.C. Warnke, I.R. Whittle, J. Jaaskelainen, and Z. Ram. 2003. A phase 3 trial of local chemotherapy with biodegradable carmustine (BCNU) wafers (Gliadel wafers) in patients with primary malignant glioma. *Neuro Oncol*. 5:79-88.

Whittle, I.R. 2004. The dilemma of low grade glioma. *Journal of Neurology, Neurosurgery & Psychiatry*. 75:ii31-ii36.

Wroblewska, Z., M. Wellish, and D. Gilden. 1980. Growth of JC virus in adult human brain cell cultures. *Arch Virol*. 65:141-148.

Xu, Y., X. Yang, and E. Wang. 2010. Review: Aptamers in microfluidic chips. *Analytica Chimica Acta*. 683:12-20.

Yan, A.C., and M. Levy. 2009. Aptamers and aptamer targeted delivery. *RNA Biol*. 6:316-320.

Yang, L., X. Zhang, M. Ye, J. Jiang, R. Yang, T. Fu, Y. Chen, K. Wang, C. Liu, and W. Tan. 2011. Aptamer-conjugated nanomaterials and their applications. *Advanced Drug Delivery Reviews*. 63:1361-1370.

Yang, Y., D. Yang, H.J. Schluesener, and Z. Zhang. 2007. Advances in SELEX and application of aptamers in the central nervous system. *Biomolecular Engineering*. 24:583-592.

Ye, M., J. Hu, M. Peng, J. Liu, H. Liu, X. Zhao, and W. Tan. 2012. Generating Aptamers by Cell-SELEX for Applications in Molecular Medicine. *Int J Mol Sci*. 13:3341-3353.

Zhang, Y., D. Bottinelli, F. Lisacek, J. Luban, C. Strambio-De-Castillia, E. Varesio, and G. Hopfgartner. 2015. Optimization of human dendritic cell sample preparation for mass spectrometry-based proteomic studies. *Anal Biochem*. 484:40-50.

Zhu, Q., G. Liu, and M. Kai. 2015. DNA Aptamers in the Diagnosis and Treatment of Human Diseases. *Molecules*. 20:20979-20997.

Zou, Y., Y. Liu, X. Wu, and S.M. Shell. 2006. Functions of human replication protein A (RPA): from DNA replication to DNA damage and stress responses. *J Cell Physiol*. 208:267-273.

Zuker, M. 2003. Mfold web server for nucleic acid folding and hybridization prediction. *Nucleic Acids Res*. 31:3406-3415.

Zulch, K.J. 1980. Principles of the new World Health Organization (WHO) classification of brain tumors. *Neuroradiology*. 19:59-66.

Zulch, K.J. 1981. Historical development of the classification of brain tumours and the new proposal of the World Health Organization (WHO). *Neurosurg Rev*. 4:123-127.

Zulch, K.J., and H.D. Mennel. 1977. New aspects of brain tumor research. *J Neurol*. 214:241-250.